SYNTHESIS, STRUCTURE OF OXOMOLYBDENUM (VI), (V) AND (IV)-DITHIOLENE COMPLEXES: ALKYLATION AND OTHER PERTINENT REACTIONS IN RELEVANCE TO MOLYBDENUM-COFACTOR IN MOLYBDOENZYMES

A Thesis Submitted
in Partial Fulfilment of the Requirement
for the Degree of

DOCTOR OF PHILOSOPHY

by

RABINDRANATH MAITI

to the

DEPARTMENT OF CHEMISTRY
INDIAN INSTITUTE OF TECHNOLOGY, KANPUR

MARCH, 1996

Dedicated to
My Parents

STATEMENT

I hereby declare that the matter embodied in this thesis "Synthesis, Structure of Oxomolybdenum (VI), (V) and (IV)-dithiolene Complexes: Alkylation and Other Pertinent Reactions in Relevance to Molybdenum-co factor in Molybdoenzymes", is the result of investigations carried out by me in the Department of Chemistry, Indian Institute of Technology, Kanpur, India, under the supervision of Professor S. Sarkar.

In keeping with the general practice of reporting scientific observations, due acknowledgement has been made wherever the work described is based on the findings of other investigators.

Kanpur:
March, 1996.

RnMaiti
Rabindranath Maiti

CERTIFICATE

Certified that the work, "Synthesis, Structure of Oxomolybdenum (VI), (V) and (IV)-dithiolene Complexes: Alkylation and Other Pertinent Reactions in Relevance to Molybdenum-cofactor in Molybdoenzymes", presented in this thesis has been carried out by Mr. Rabindranath Maiti, under my supervision and the same has not been submitted elsewhere for a degree.

(S. Sarkar)

Thesis Supervisor

Department of Chemistry

I.I.T. Kanpur

Kanpur:
March, 1996.

DEPARTMENT OF CHEMISTRY

INDIAN INSTITUTE OF TECHNOLOGY KANPUR, INDIA

CERTIFICATE OF COURSE WORK

This is to certify that Mr. Rabindranath Maiti has satisfactorily completed all the courses required for the Ph.D. program. The courses include:

chm 605 Principles of Organic Chemistry

chm 624 Modern Physical Methods in Chemistry

chm 625 Principles of Physical Chemistry

chm 645 Principles of Inorganic Chemistry

chm 646 Bio-inorganic Chemistry

chm 651 Crystal and Molecular Structure by Single crystal X-ray Diffraction.

chm 800 General Seminar

chm 801 Special Seminar

chm 900 Post Graduate Research

Mr. Rabindranath Maiti was admitted to the candidacy of the Ph.D. degree in October 1991 after he successfully completed the written and oral qualifying examinations.

(S. K. Dogra)
Head
Department of Chemistry
Indian Institute of Technology
Kanpur - 208016

(Convenor)(P. Guptabhaya)
Department of Postgraduate
Committee, Department of
Chemistry, I.I.T. Kanpur.

ACKNOWLEDGEMENTS

It is great pleasure, I record my deep sense of gratitude to Professor Sabyasachi Sarkar, my thesis supervisor, for suggesting this research problem and for guiding me throughout the course of this research work.

I feel extremely grateful to Mrs. Sarkar for her patience, tolerance and hospitality during my discussions with professor Sarkar at their apartment.

I am grateful to Prof. P. K. Bharadwaj and Prof. A. Mukherjee (Jadavpur University), for their kind help in solving the structure of the synthesized compounds.

I am grateful to Prof. R. N. Mukherjee for his kind help and discussions related to my work.

I am thankful to Dr. P. K. Chaudhury and Dr. S. K. Das for their help in kinetic study of my thesis work.

I am also thankful to my labmates Khukudi, Subrata da, Ujjawal, and Kaushik for their pleasant association and help.

I offer my sincere thanks to all the faculty members and the students of the department for their cooperation.

I thank my friends Tapan, Raghu, Gagan, Apurba, Tapan Khan, Sanchita, Jayaraj, Venkat, Madhav, Manoj,and Debnath for their helpful and remembering company throughout my stay at I.I.T.

I thank to Ahmed and Kanaujia for their help in my work.

Last but not the least, I take the opportunity to acknowledge my parents, my sisters and my close relatives for their love patience and encouragement throughout my career .

Rabindranath Maiti.

CONTENTS

SYNOPSIS

The thesis entitled, "Synthesis, Structure of Oxomolybdenum (VI), (V) and (IV)-dithiolene Complexes: Alkylation and Other Pertinent Reactions in Relevance to Molybdenum-cofactor in Molybdoenzymes", consists of five chapters.

In chapter 1, a brief introduction highlighting important background information relevance to the inorganic and biochemistry of molybdenum in pterin containing molybdoenzymes has been provided. Based on this theme a general account on, (i) classification of molybdoenzymes, (ii) the presence of universal molybdenum-cofactor (Moco) in oxomolybdoenzymes, (iii) coordination around molybdenum in these Moco and (iv) synthetic analogue reactions to mimic enzymatic reactions have been presented.

Chapter 2 of this thesis presents the scope of the present work. This is based upon background information available in the literature on the work on oxomolybdoenzymes and on synthetic analogue model complexes as introduced in chapter 1. The important contribution for the elucidation of the structural aspect of Moco was based on degradative and derivatization of the isolated Moco due to the absence of any X-ray structural analysis. Another important aspect of Moco is its reported instability and stability in the fully oxidized and fully reduced state respectively under anaerobic condition. The intermediate EPR active pentavalent state has been reported to interact with thiols. In view of these, dithiolene coordinated oxomolybdenum species have been subjected to similar reactions to understand the detailed chemistry of these reactions. Interestingly, the corresponding tungstoenzyme,

aldehyde ferredoxin oxidoreductase (AOR), which has been structurally characterized has been subjected to similar alkylation reaction and comparative model reactions are carried out for the understanding of these important reactions in the most precise manner.

Chapter 3 describes the experimental procedures and the details involved in the present work which has been subdivided into two sections. Section 3.1, contains the details of the materials and methods of analysis and work up manipulations of the newly prepared compounds and the relevant particulars of different instruments and equipments used for characterization of these complexes. The section 3.2 describes the physicochemical and structural investigations of the synthesized complexes. The analyses include IR, electronic and FAB mass spectroscopic studies, magnetics, cyclic voltammetric measurements and single crystal X-ray diffraction studies.

Chapter 4 presents the results and discussion of the functional analogue and other pertinent reactions carried out with the synthesized complexes which is divided into five parts.

Section 4.1 describes the synthetic aspect of the newly prepared complexes. The chemistry and reactivities of these complexes have been compared with those of Moco.

Section 4.2 describes the reductase type of synthetic analogue reaction similar to trimethylamine N-oxide (TMANO) reductase. *E.coli* utilizes this enzyme which does not show nitrate reductase activity due to the deficiency in the structural gene for the activity. The synthesized complex $[Mo^{IV}O(mnt)_2]^{2-}$ mimics the activity of TMANO reductase. TMANO in aqueous solution remains in equilibrium as:

$$(CH_3)_3NO + H_2O \rightleftharpoons (CH_3)_3NOH^+ + OH^- \quad \text{---------- (1)}$$

and the reported anaerobic respiration coupled with oxidative phosphorylation suggest the influence of proton in such reaction. In fact, the kinetic behavior of the native enzyme has been reported to be strongly pH dependent. Based on these, the pH dependent kinetics of the oxygen atom transfer reaction :

$$\underset{(E)}{[Mo^{IV}O(mnt)_2]^{2-}} + \underset{(S)}{Me_3NO} \xrightarrow{H^+} \underset{(P)}{[Mo^{VI}O_2(mnt)_2]^{2-}} + Me_3NH^+ \quad \text{---------- (2)}$$

has been carried out which followed substrate saturation behavior. The observed rate (k_{obs}) for the reaction (2) was found to be in agreement with the expression (equation 3) derived under quasiequlibrium condition of the reaction scheme (1)

$$k_{obs} = \frac{[S_o]\left[k_2 + \frac{k_2''}{k'}[H^+] + \frac{k_2}{K'K''}[H^+]^2 \right]}{\left[\frac{K_s(K + [H^+]}{K} + [S_o]\left(1 + \frac{1}{K'}[H^+] + \frac{1}{K'K''}[H^+]^2\right)\right]} \quad \text{----------(3)}$$

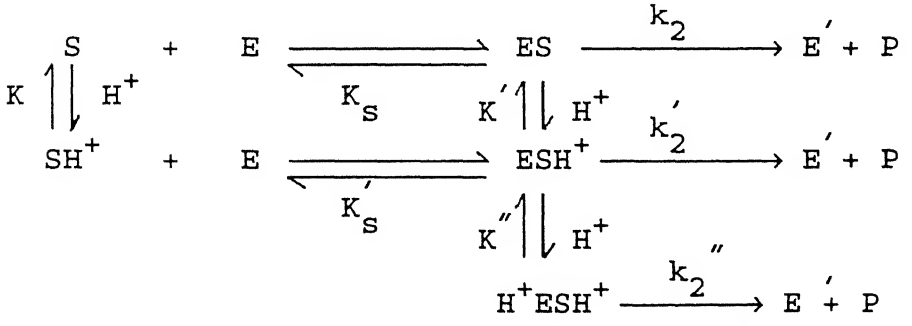

Scheme 1

The dissociation constant (M) and rate constants (s^{-1}) values obtained are: $K_s = 5.00 \times 10^{-3}$; $K_s' = 1.63 \times 10^{-3}$; $K = 3.04 \times 10^{-7}$; $K' = 9.93 \times 10^{-6}$; $K'' = 1.00 \times 10^{-4}$ and $k_2 = 5.43 \times 10^{-4}$; $k_2' = 1.20 \times 10^{-2}$; $k_2'' = 9.99 \times 10^{-2}$. $[S_o]$ = total concentration of TMANO.

The unusual form of TMANO like Me_3N^+-O^- which in hydrated

form remains as $[Me_3NOH]^+OH^-$ clearly suggest that the cationic species is also relevant for substrate activity. In the synthetic analogue chemistry described here $[PyH]_2[Mo^{IV}O(mnt)_2]$ has been shown to remain as hydrogen bonded like M=O---H^+ in the solid state. The corresponding $[Et_3NH]_2[Mo^{IV}O(mnt)_2]$ salt is soluble in CH_2Cl_2 displaying different electronic spectral feature compared to that of $[Et_4N]_2[MoO(mnt)_2]$. The ready oxotransfer reaction in CH_2Cl_2 with the protonated salt of the complex ion with TMANO and phase transfer reaction in CH_2Cl_2-H_2O using different acids involving $[Et_4N]_2[MoO(mnt)_2]$ and TMANO and finally the reaction using $[Me_3NOH][BPh_4]$ and $[Et_4N]_2[MoO(mnt)_2]$ in acid free acetone strongly mimics the role of hydrophobic site of TMANO reductase for anaerobic respiration of bacteria like *E.coli.*

Section 4.3 describes the reduction of $[Bu_4N]_2[Mo^{VI}O_2(mnt)_2]$ by thiophenol. Thiols are physiologically potent electron donor by the reaction: 2 Cys.SH $\rightleftharpoons$ Cys.SS.Cys + 2 H^+ + 2e^- -------(4) and the reduction of Mo(VI) to Mo(IV) by thiol is an appropriate simulation of biological reduction. The reaction between $[Mo^{VI}O_2(mnt)_2]^{2-}$ and PhSH is followed by electronic spectroscopy and cyclic voltammetry. On mixing these, the reaction slowly proceed to yield $[Mo^{VI}O(SPh)_2(mnt)_2]^{2-}$ before the electron transfer reaction. The above species finally responded reductive elimination with the change of oxidation state of Mo(VI) to Mo(IV) yielding $[Mo^{IV}O(mnt)_2]^{2-}$ and PhSSPh. The entire course of the reaction has been presumed to take place as :

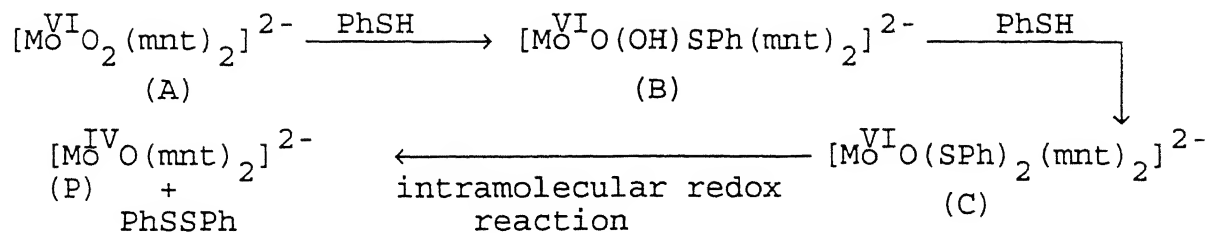

Scheme 2.

The identification of the intermediate $[Mo^{VI}O(OH)(SPh)(mnt)_2]^{2-}$ has been made by cyclic voltammetry where the respective cathodic peak potentials for $[Mo^{VI}O_2(mnt)_2]^{2-}$(A), $[Mo^{VI}O(OH)(SPh)(mnt)_2]^{2-}$(B) and $[Mo^{VI}O(SPh)_2(mnt)_2]^{2-}$(C) have been identified at -1.13 V, -1.06V and -0.99V *vs* Ag/AgCl respectively in CH_3CN (6.3% water). The kinetics of this reaction has been analyzed as :

$$A \xrightarrow{k_1} B \xrightarrow{k_2} C \xrightarrow{k_3} P \text{ (P = Product)}$$

In the presence of excess of thiophenol the electronic spectrum showed the change of $[Mo^{VI}O_2(mnt)_2]^{2-}$ to $[Mo^{VI}O(OH)(SPh)(mnt)_2]^{2-}$ which slowly changed to $[Mo^{VI}O(SPh)_2(mnt)_2]^{2-}$ with an isosbestic point at 610 nm. within 10 min. of the initial reaction where virtually no reduction occurred.Thus monitoring the change in the absorption of the reaction mixture at 610 nm. the kinetics has been performed for which the expression used is :

$$OD = \varepsilon_1 C_A^{\,o} e^{-k_1 t} + \varepsilon_2 C_A^{\,o} k_1 \left(e^{-k_1 t} - e^{-k_2 t} \right) / (k_2 - k_1)$$
$$+ \varepsilon_3 C_A^{\,o} k_1 k_2 \left[\{ e^{-k_1 t} / (k_2 - k_1)(k_3 - k_1) \} - \{ e^{-k_2 t} / (k_2 - k_1)(k_3 - k_2) \} \right.$$
$$\left. + \{ e^{-k_3 t} / (k_3 - k_1)(k_3 - k_2) \} \right]$$
$$+ \varepsilon_4 C_A^{\,o} \left[1 - \{ k_2 k_3 e^{-k_1 t} / (k_2 - k_1)(k_3 - k_1) \} + \{ k_1 k_3 e^{-k_2 t} / (k_2 - k_1) \right.$$
$$\left. (k_3 - k_2) \} - \{ k_1 k_2 e^{-k_3 t} / (k_3 - k_1)(k_3 - k_2) \} \right] \text{ -------- (5)}$$

The experiments were performed in pure CH_3CN as well as in CH_3CN with 6.3% water. Using nonlinear least-square regression analysis the kinetic parameters obtained are :(rates are in CH_3CN, (s^{-1})), $k_1 = 2.82(\ 6) \times 10^{-1}$, $k_2 = 6.09(\ 5) \times 10^{-2}$ and $k_3 = 1.66(\ 8) \times 10^{-3}$;

(in aqueous CH_3CN, s^{-1}) k_1= 2.91(4)x10^{-1}, k_2= 6.15(3)x10^{-2} and k_3= 3.41(6)x10^{-3}.

The section 4.4 describes the alkylation reactions involving iodoacetamide and methyliodide using synthetic analogue complexes which were compared with the alkylation reactions of Moco and Wco involving iodoacetamide. The results suggest that such reactions do not necessarily involved in the release of reactive sulfhydryl groups of the ligated dithiolenes. It was also demonstrated that only half of the stoichiometric amount of Mo / W was released as free polymetalate (M = Mo / W) and the major portion of the ligated dithiolene in the starting complex was found to be distributed in the formation of stable $[M(mnt)_3]^{2-}$ and $[Mo_2O_4(mnt)_2]^{2-}$ which were not susceptible to such alkylation reactions. The free mnt in the form of alkylated derivative like cam-mnt (cam = CH_2CONH_2) or Me_2mnt was found to be around 50% based on the mnt available in starting molybdenum complexes and only 25% from that of the corresponding tungsten complexes. The alkylation reactions involve several yet unresolved redox and other reactions and finally the important product distribution may be written as :

$$24\ [MoO(mnt)_2]^{2-} \xrightarrow{RI/\ H_2O} 2\ [Mo_6O_{19}]^{2-} + 3\ [Mo_2O_4(mnt)_2]^{2-} + 6\ [Mo(mnt)_3]^{2-} + 24\ R_2mnt + 26\ R_4NI + ----. \quad -------(6)$$

$$12\ [WO_2(mnt)_2]^{2-} \xrightarrow{RI/\ H_2O} [W_6O_{19}]^{2-} + 6\ [W(mnt)_3]^{2-} + 6\ R_2mnt + 10\ R_4NI + -----. \quad -------(7)$$

These reactions strongly suggest the ineffectiveness of the reported alkylation reactions of these cofactors in elucidating their compositions with respect to the ratio between MPT ligand /

respective metal (M= Mo / W).

The section 4.5 describes the chemistry of monodithiolene coordinated molybdenum complexes characterized as dimeric species like $[Mo_2O_4(mnt)_2]^{2-}$. The well known chemistry like

$$[Mo_2O_4]^{2+} \xrightarrow{HX} [Mo_2O_3X_2]^{2+} + H_2O \text{ ----------(8)}$$

has been exploited to synthesize a series of complexes of the general formula $[Mo_2O_3X_2(mnt)_2]^{2-}$ (X = Cl,Br,SPh and ClC_6H_5S). The reverse of the reaction (8) like hydrolysis of $\{Mo_2O_3\}^{4+}$ core to produce $\{Mo_2O_4\}^{2+}$ is also known in the literature. In solution these complexes, in the presence of trace amount of water, displayed interesting reactions. It has been demonstrated by detail EPR and electronic spectral studies that the overall reaction followed as shown in Scheme 3 :

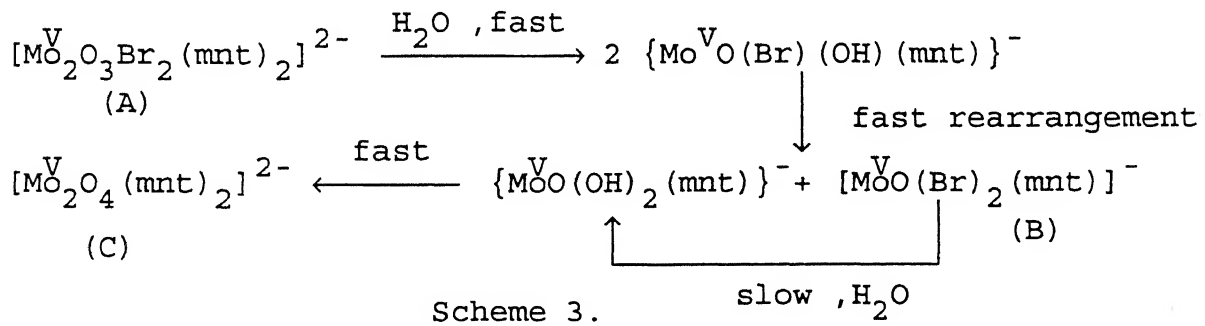

Scheme 3.

Identification of the species $[Mo^{V}O(Br)_2(mnt)]^-$ by time dependent EPR spectroscopy has been made which displayed characteristic superhyperfine interaction of two equivalent Br nuclei. The absence of any other EPR signal in the detailed time dependent EPR investigation supported the entire course of the reaction as (Scheme 3). The hydrolytic scheme thus may be represented as :

$$A \xrightarrow{k_1} B \xrightarrow{k_2} C \text{ ----------(9)}$$

The kinetics of this reaction (9) has been followed by monitoring the change in optical density at two different wavelengths and the final expression to evaluate kinetic parameters used as :

$$OD = \varepsilon_1 C_A^{\circ} e^{-k_1 t} + \varepsilon_2 C_A^{\circ} k_1 (e^{-k_1 t} - e^{-k_2 t}) / (k_2 - k_1) + \varepsilon_3 C_A^{\circ} + \{\varepsilon_3 C_A^{\circ} (k_2 e^{-k_1 t} - k_1 e^{-k_2 t})\} / (k_2 - k_1) \quad \text{------(10)}$$

By nonlinear least-square regression analysis the values obtained are, (at wavelength 478 nm., s^{-1}) k_1= 3.043(4)x10^{-2} and k_2= 7.798(5)x10^{-5}; (at wavelength 585 nm.,s^{-1}) k_1= 2.416(7)x10^{-2} and k_2= 8.919(6)x 10^{-5}.The corresponding thiophenolato complex, $[Mo_2O_3(SPh)_2(mnt)_2]^{2-}$, being sparingly soluble in CH_2Cl_2 restricted similar studies as done for the bromo complex. However, in the presence of excess PhSH this compound in CH_2Cl_2 slowly dissolved and from EPR spectroscopy the presence of two EPR active species could be identified. The species with <g> = 1.992 is suggested to be due to $[M^{V}OO(SPh)_2(mnt)]^{-}$ and for $[M^{V}OO(SPh)_3(mnt)]^{2-}$, the <g> value at 1.982 is assigned. The relevance of these EPR active species with those of the isolated reduced Moco in the presence of thiophenol under one electron oxidation has been highlighted.

In the oxotransfer reactions the real reduction potential values of the complexes and of different substrates do not display any driving potential difference expected for any reaction to occur. Based on the reported redox potentials of different molybdoenzymes and substrates and oxotransfer reactions of model complexes it is suggested that the cause of atom transfer reactions may not be predictable by using the electron transfer concept and reduction potential values measured by cyclic voltammetry for model compounds or by spectroscopic coupled to potentiometry using mediator dye for native enzymes. Thus an enzymatic oxotransfer reaction primarily demands the formation of

a substrate bound new molybdenum species (Michaelis complex). The intrinsic instability of this new species dictates further reaction.

CHAPTER 1

INTRODUCTION

Despite relatively low terrestrial abundance of molybdenum its concentration in natural water is maximum compared to other transition metals[1]. Molybdenum commonly available in its group valency (+VI) in the form of $[MoO_4]^{2-}$ ion. It can accommodate two electrons oxidation state changes like $Mo^{VI} \longrightarrow Mo^{IV}$ in either a single two electrons step or in two closely coupled one electron steps. Molybdenum has another important property in its $[MoO_4]^{2-}$ anion. Under slightly acidic condition protonation of the Mo=O group occurs resulting in the formation of polymolybdate anions wherein several intermediate pH dependent species exist. This protonation enhances the coordination of molybdenum from four to six with the involvement of hydroxyl ion[2]. Thus the involvement of molybdenum in biology specially in oxomolybdoenzymes is related to these properties wherein being tetrahedral structure of $[MoO_4]^{2-}$, it can be available in water, which can be readily transported to the biological systems similar to isostructural PO_4^{3-} and SO_4^{2-} anions. It is now known that the molybdenum containing enzymes are involved in the metabolism and energy generation in organisms involving key role in the nitrogen, sulfur, carbon and arsenic cycles. The reduction of bound form of $N^{V} \longrightarrow N^{III}$, $S^{IV} \longrightarrow S^{II}$ or oxidation of $S^{IV} \longrightarrow S^{VI}$, $As^{III} \longrightarrow As^{V}$, $C\text{-}H \longrightarrow C\text{-}OH$, $CO \longrightarrow CO_2$ are involved in one step two electrons transfer processes. As molybdenum can respond to similar one step

two electrons transfer redox process its association in such cycles is understood. Furthermore the involvement of alternative successive one electrontransfer processes for molybdenum makes it a suitable element for the ready regeneration in its original redox state . The facile proton coupled electron transfer reactions make the use of molybdenum more suitable in biological redox transformation .

With the exception of the molybdoenzyme, nitrogenase, the other class of molybdoenzymes appear to catalyze general reaction:

$$X + H_2O \rightleftharpoons XO + 2H^+ + 2e^- \quad \text{--------(1.1)}$$

For the forward reaction of reaction 1.1 the involved enzymes are oxidase type and for the catalytic reverse reaction the enzymes are termed as reductase type. Generally this class of molybdoenzymes are actually oxidoreductase type. Thus for example, sulfite oxidase is actually named as sulfite fericytochrome-c oxidoreductase[3]. The overall reaction catalyzed by enzyme is :

$$SO_3^{2-} + H_2O + 2 \text{ cytochrome } c^{3+} \longrightarrow SO_4^{2-} + 2H^+ + 2 \text{ cytochrome } c^{2+} \quad \text{----------(1.2)}$$

reaction 1.2 takes place in two segments that is the reaction comprised of oxotransfer reaction from the molybdoenzymes to the substrate SO_3^{2-} causing oxidation of $SO_3^{2-} \longrightarrow SO_4^{2-}$ and thus the reduced molybdenum center of the enzyme is step wisely oxidized by cytochrome-c involving two successive one electron oxidation process. Interestingly cytochrome-c does not directly interact with the molybdenum center of the enzyme rather it works via a cytochrome-b_5 type heme center which is another prosthetic group present in the sulfite oxidase.The present knowledge

suggests that the reduced molybdenum center incorporates one oxygen atom from water which essentially coordinates to the vacant site of the reduced molybdenum site after oxotransfer reaction.

The involvement of proton coupled electron transfer may be viewed in this regeneration of the oxidized enzyme as :

$$\{Mo^{IV}O(H_2O)\} \xrightarrow{-e^-,-H^+} \{Mo^{V}O(OH)\} \xrightarrow{-e^-,-H^+} [\ Mo^{VI}\ O_2]$$

Scheme 1.1

It is reasonably probable from the model studies and also from single turn over experiments[4] on related xanthine oxidase that direct oxotransfer from the oxidized molybdenum center to the substrate is likely for sulfite oxidase. Similarly for a reductase class of enzyme like DMSO reductase the forward reaction involves the reduction of the substrate DMSO by oxotransfer to DMS the reduced form of DMSO. For this enzyme, isotopic work has established such direct oxygen atom transfer reaction[5]. Interestingly, DMSO reductase may be obtained in several forms and in some cases this enzyme contained only molybdenum containing cofactor without the association of any other form of redox active prosthetic groups[6]. This means that this type of enzyme is involved directly with the reducing substrates to generate back the active reduced enzyme. This regeneration may happens to be a direct two electron transfer or involving step wise one electron transfer by suitable reducing substrate . These reductions may be proton coupled or not depending on the nature of the reductant present.

All these oxomolybdoenzymes involved apparent oxotransfer

chemistry . However the actual mechanism of action of this oxotransfer reaction may be different . For this reason these enzymes are sometimes termed as molybdenum hydroxylases[7], oxotransferases[4], oxotype molybdoenzymes[8] and pterin containing molybdoenzymes[9]. When mechanistic details are not properly known and all these molybdoenzymes contain a 6-substituted pterin ,it is better to refer these enzymes as ptrin containing molybdoenzymes. There are several such enzymes known. These are tabulated in Table 1.1. All these enzymes contain a common molybdenum cofactor(Mo-co) as suggested by Pateman *et al.*[10] This cofactor was later shown to contain a pterin [11]. All these enzymes are now known to contain some form of this pterin called molybdopterin. Representative of these are shown in Figure 1.1. Unlike most of the known cofactors in biology Mo-co is not isolable using normal procedures. The cofactor activity is extremely labile in the presence of air. For the structural characterization of Mo-co elegant derivatization and spectroscopic analysis done by Rajagopalan and coworkers[11,12] led to the elucidation of structure of Moco. The worth noting features of this cofactor are: (a) the presence of a pterin moiety, (b) the side chain of the pterin contains a dithiolene group ,(c) the presence of a phosphoester group and (d) the coordination to molybdenum via dithiol moiety to give a dithiolene coordination . The entire ligand without molybdenum is termed as molybdopterin which as well as the molybdenum cofactor are anionic in nature . Molybdenum cofactor deficient *nit-1* mutants of *Neurospora crassa*[13] provide apoproteins for the reconstitution of nitrate reductase, using Mo-co from different sourceswhich is schematically shown in Scheme 1.2 .

Table 1.1 PTERIN-CONTAINING MOLYBDOENZYME

No.	Site (a)	Enzyme	Source	MW (KDa) Subunit (b)	Composition	Substrat Product (c)
1.	S	Sulfite oxidase	Mammalian livers	110, α_2	2Mo, 2Cyt$_b$	SO_3^{2-}/SO_4^{2-}
2.	S	Sulfite oxidase	*T.novellus*	40, M	Mo, heme Fe	SO_3^{2-}/SO_4^{2-}
3.	S	DMSO reductase	*R.sphaeroides* *R.capsulatus*	82, M	1Mo	Me_2SO / Me_2S
4.	S	Biotin-*S*-oxide reductase	Bacteria	----	-----	-----
5.	N	Nitrate - reductase	Plants,fungi, algae, bacteria	228 (fungal)	2Mo, 2Cyt$_b$, 2FAD	NO_3^-/ NO_2^-
6.	N	Trimethylamine *N*-oxide reductase	*E.coli*	200, M	2Mo, 1Fe, 1.5Zn	Me_3NO / Me_3N
7.	C	Xanthine - oxidase	Cow's milk, mammalian livers, kidney	275, α_2	2Mo, $4Fe_2S_2$, 2FAD	Xn/ XnO
8.	C	Xanthine - dehydrogenase	Chicken liver, bacteria	300, α_2	------	Xn/ XnO
9.	C	Aldehyde - oxidase	Rabbit liver	280, α_2	2Mo, $4Fe_2S_2$, 2FAD	RH/ RHO
10.	C	Formate - dehydrogenase	Plants, fungi, yeast, bacteria	105-263	Mo, Se, Fe_nS_n	HCO_2^- / HCO_3^-
11.	C	Carbon - monoxide dehydrogenase	Bacteria	230-300	2Mo, $4Fe_2S_2$, 2FAD, 2Se	CO/ CO_2
12.	As	Arsinite oxidase	Bacteria	---	Mo, Fe_xS_y	AsO_3^{3-} / AsO_4^{3-}

[a] Enzymes are grouped according to the type of atom in the substrate that undergoes oxidation / reduction.

[b] M, monomer.

[c] The products and reactants of general($X + H_2O \rightleftharpoons XO + 2H^+ + 2e^-$) are quoted.

[d] Xn, xanthine or other purin substrates; XnO, uric acid or other purin products.

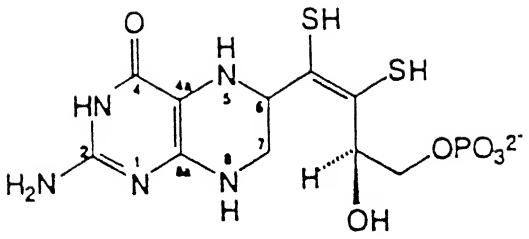

(a)

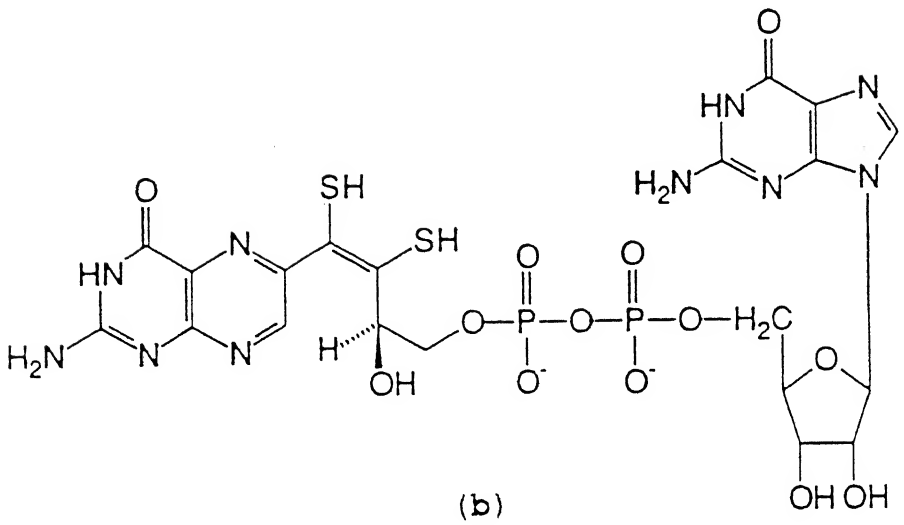

(b)

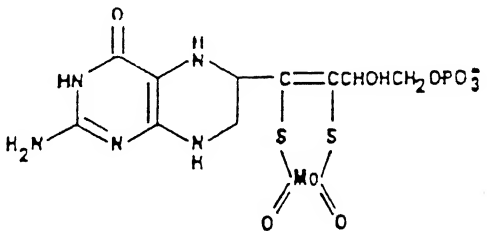

(c)

Fig. 1.1 (a) Molybdopterin (**MPT**), (b) Bactopterin (**MGD**) and (c) Molybdenum cofactor (**Mo-co**).

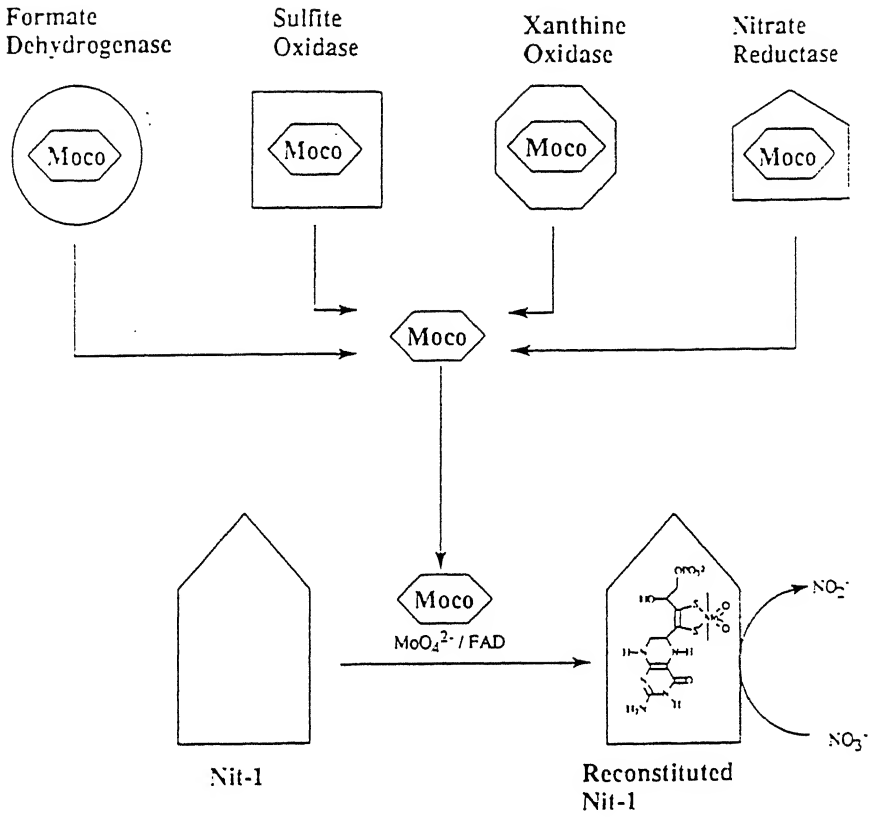

cheme 1.2 A schematic representation of the reconstitution of the poprotein from *Nit-1* with molybdenum cofactor from a variety of ources.

COORDINATION AROUND MOLYBDENUM ATOM IN THESE ENZYME:

No X-ray structural data are yet available for any of these enzymes reported in Table 1.1. However X-ray crystal structure of the related pterin containing tungsten enzyme aldehydeferridoxin oxidoreductase (AOR) is recently known.[14] Interestingly, the structure of the tungsten cofactor present in this enzyme definitely shows the presence of two molybdopterin ligation, contrary to the expected one molybdopterin ligation as thought to be present in molybdoenzymes . Most of the precrystallographic structural information came from the Extended X-ray Absorption Fine Structure (EXAFS) and by EPR spectroscopy involving the unstable Mo(V) intermediate oxidation state of these enzymes.

EXAFS STUDIES:

Structural information about the first coordination sphere of molybdenum in molybdoenzymes has come from Mo_k edge EXAFS studies. The best studied enzymes by EXAFS are xanthine oxidase , xanthine dehydrogenase and sulfite oxidase . The suggested structure of the reduced and oxidized form of these enzyme are shown in Figure 1.2. EXAFS studies clearly suggest the distinction between xanthine oxidase / dehydrogenase and sulfite oxidase . In the oxidized state of these enzymes the clear existence of $Mo^{VI}OS$ moiety in xanthine oxidase /dehydrogenase distinctly differs from that of sulfite oxidase where a dioxo molybdenum group exists. In the reduced state of all these enzymes only one terminal oxo group is retained[15]. It is interesting to note that all these enzymes in

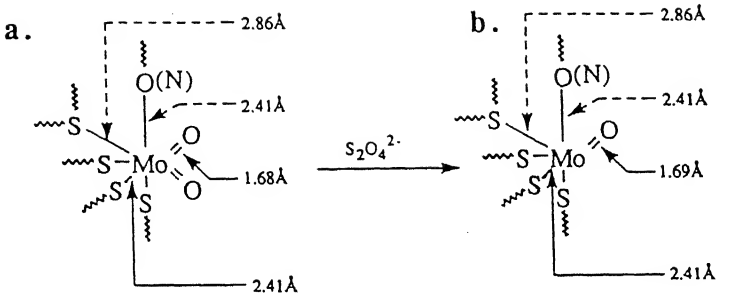

The coordination geometry around the molybdenum centers as suggested by a combination of EXAFS and EPR studies for sulfite oxidase: **a.** oxidized form; **b.** reduced form.

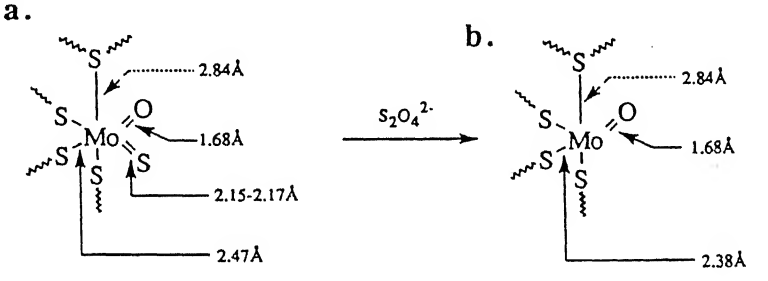

The coordination geometry around the molybdenum centers as suggested by a combination of EXAFS and EPR studies for xanthine oxidase: **a.** oxidized form; **b.** reduced form

Fig. 1.2

the reduced or in the oxidized form suggested to be attached with at least three sulfur atoms similar to thiolate type . In sulfite oxidase the possible presence of either a nitrogen or/ and oxygen and of another sulfur atom at a relatively longer distance are less definite. Interestingly tungsten EXAFS studies on AOR enzyme showned very similar donor atom coordination around tungsten to that of molybdenum in sulfite oxidase.[16] Surprisingly the X-ray structure of the tungsten enzyme definitely shows the presence of two molybdopterin ligation comprising four W-S thiolate ligation. Furthermore this X-ray structure revealed the absence of any covalent linkage of the tungsten cofactor (W-co) to the apoprotein. Interpretation of EXAFS data has also been found to be inconsistent with the molybdoenzyme, nitrogenase, in relation to its X-ray structure.[17]

EPR SPECTROSCOPY:

This technique is more relevant to the enzymes containing $Mo^{VI}OS$ moiety in the oxidized state . This is because of the fact that this class of enzyme like xanthine oxidase contains four redox active centers . The electron transfer in the substrate oxidation is very quickly equillibrated amongst all the redox centers by virtue of close redox potential values.[18] Bray and coworkers have extensively used this technique to understand the mechanism of electron transfer in these enzymes.[19] As back as 1966 it was reported that $[MoO_4]^{2-}$ reacts with dithiols to produce EPR signals very similar to those of xanthine oxidase.[20] The oxomolybdo-dithiol complexes since now been isolated[21], reveals of the four Mo-S ligation in these complexes, thus once more raising

the possibility of two molybdopterin ligations around molybdenum in these enzymes.

The unstable Mo(V) state of sulfite oxidase is sensitive to pH and to anions present in the medium.[22] Phosphate, sulfate or chloride are effective inhibitors of sulfite oxidase.[23] The interaction of these anions with the molybdenum center can be directly observed by EPR spectroscopy . Combination of EXAFS and EPR data under high chloride and low chloride concentration[24] for sulfite oxidase suggest the possible minimal structure in the Mo^{VI},Mo^{V}& Mo^{IV}oxidation states of the enzyme as shown in Figure 1.3.

OTHER STUDIES :

Electronic Spectroscopy: The presence of other prosthetic groups like flavin, heme or iron-sulfur proteins in pterin containing molybdoenzymes made it difficult to observe electronic spectral feature of molybdopterin part specially in the reduced state. The strong absorption of these prosthetic groups in the oxidized or in the reduced state made the spectral characterization of this molybdenum center difficult. However, DMSO reductase from*R. Spheroids*, from *Specialis Denitrificants*[6] and from *R. Capsulatants*[6] have been shown to contain only Moco and a single polypeptide chain.[25] For this, electronic spectroscopy has been used to probe the molybdenum center.[6]

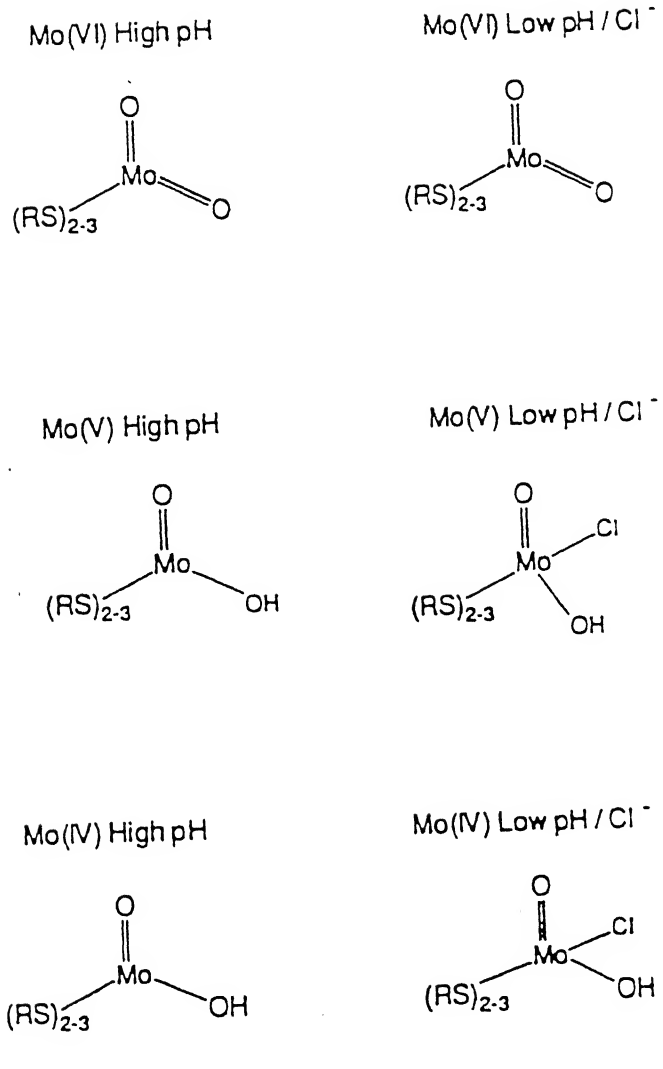

Fig. 1.3 Minimal structures for the high and low-pH species in the Mo(VI), Mo(V) and Mo(IV) oxidation states of sulfite oxidase, based upon EXAFS and EPR results.

Raman spectroscopy: The oxidised and reduced form of DMSO reductase from *R.Spheroids* has been subjected to resonance Raman spectroscopic studies using ^{34}S isotopic shift technique . A vibration at 335 cm^{-1} has been assigned as Mo-S(dithiolene) vibration . For the reduced form the same vibration is assigned to appear at 385 cm^{-1}.[26] This enzyme has been shown to contain a molybdopterin guanine dinucleotide.[25] Though no EXAFS or other structural studies of this enzyme is known yet the possibility for the Mo-S thiol coordination other than molybdopterin ligation is there. The presence of dithiolene as well as thiolate coordination can be distinguished at least with isotopic enriched study. The reported Mo-S(dithiolene) vibration at 349 cm^{-1} for a model $[Mo^{IV}O]$ complex[27] suggest that in DMSO reductase Mo-S interaction is much stronger than that of the model complex.

MOLYBDENUM COFACTOR

Since the early studies of Pateman and coworkers[10] followed by Nason *et al* [28], the existence of a common molybdenum cofactor (Moco) is known for most of the molybdoenzymes .The isolation and characterization of this Moco is extensively pursued by Rajagopalan and coworkers[11,29] and Bray *et al*.[30] It was found that Mo-co is extremely unstable to lose the molybdenum once it is released from protein . However Hawkes and Bray[30] reported that the cofactor isolated from xanthine oxidase or sulfite oxidase is stable under anaerobic condition in the presence of sodium dithionite even in aqueous solution for a day at $4^{o}C$. It has been further demonstrated that this cofactor on electrochemical

oxidation in the presence of thiophenol displayed EPR signal characteristic of Mo(V) with little loss of cofactor activity.[30] However the structure of the intact Moco or that of any molybdoenzyme known to date is on the basis of a series of degradation and spectroscopic investigation by Rajagopalan and coworkers.[11,29] They have proposed the structure of the organic component present in the Mo-co and named this organic moiety as molybdopterin. Subsequent work on the biosynthesis of molybdopterin suggested a molybdopterin precursor which on oxidation yielded a pterin derivative known as compound Z. All these work is summarized in Scheme 1.3.

Interestingly several bacterial proteins yielded the organic component of Mo-co not identical to molybdopterin. These organic moieties named as bactopterin[31] have been shown to be molybdopterin dinucleotide . Variation of nuclic bases like guanine, adenine, cytosine and hypoxanthene are known.[32] All of the pterin containing Mo-co responded positively in the *nit-1* assay because the crude extract also contain the enzymes which produce molybdopterin by cleaving off the dinucleotide fragments. Representative bactopterin is shown in Figure 1.1.

Quantitation of molybdopterin in sulfite oxidase has been done by phosphate analysis knowing well that a molybdopterin contains a phosphoester linkage . As for active Mo-co, the linkage of phosphoester is essential for activity hence analysis of phosphate is taken as the equivalent of the molybdopterin attached to molybdenum in sulfite oxidase . Against subunit activity of sulfite oxidase the analysed phosphate was reported to be 1:1 from native enzyme or from the trichloroacetic acid pellet of native

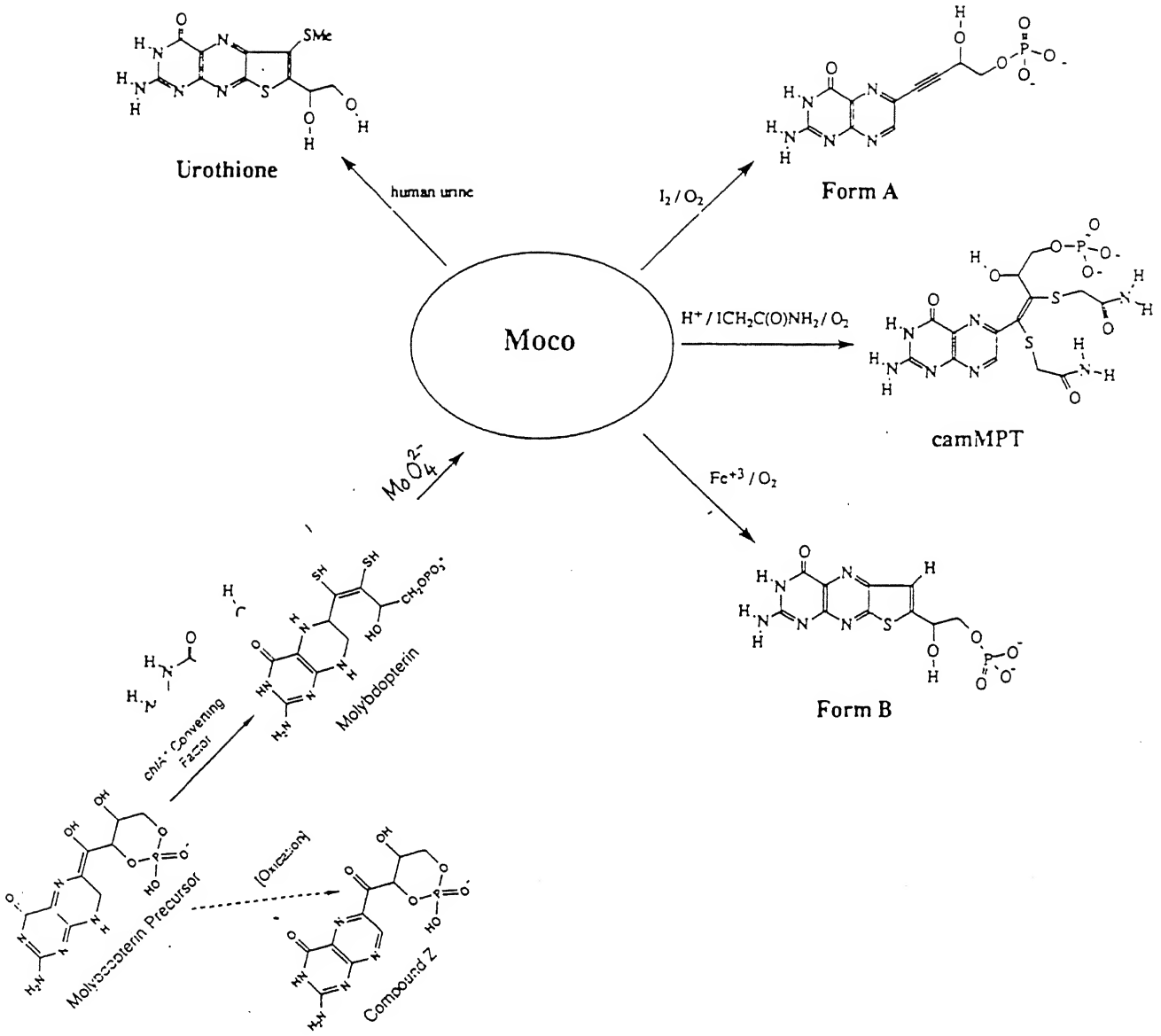

Scheme 1.3 The known form of molybdopterin derivatives including Form A, B and Z, a di(carboxamidomethyl) derivative (camMPT) and Urothione.

enzyme.[11] Interestingly it is reported that under the conditions used trichloroacetic acid does not affect the subunit activity and the protein can be precipitated in the presence of it . It has also been reported that oxidation of enzyme specially with iodine resulted in the degradation of the molybdopterin ligand with the formation of the'Form A' (see Scheme 1.3). However this degradation is reported to be not quantitative in nature . After this degradation the rest of the enzyme can be precipitated out by trichloroacetic acid . This trichloroacetic acid pellet showed phosphate concentration almost half to the molybdenum present as measured by subunit activity. Thus considering intact molybdopterin ligation for enzymatic activity the phosphate : subunit activity ratio should have been reverse, that is the part of the phosphate which did not come out in the form of 'Form A' should have been left in the protein and as suggested by Rajagopalan and coworkers this left out'Form A' is having a strong covalent attachment with the denatured protein. This part of the phosphate may not be accountable for the subunit activity of the enzyme. However absolute phosphate assay will definitely include this part of phosphate thereby the phosphate : subunit activity should have been greater than one . This analysis thus suggested that the conditions used in the phosphate assay is problematic in nature. The reported stability of the reduced Moco under anaerobic condition even in aqueous solution in the presence of dithionite[30] strongly suggest the stability of $\{Mo^{IV}O\}$ moiety even in absence of the proposed anchoring protein ligand. Considering the coordination chemistry of $\{Mo^{IV}O\}$, the existence of a stable $\{O=Mo^{IV}\text{——}(S)_2(\text{diothiolene})\}$ in aqueous medium in the absence of

any recognised ligand other than water is highly unlikely . This coordinately unsaturated moiety can readily lead to polymerization of the monomeric molybdenum center. Another important observation to question the stoicheometry of Mo-co came from the X-ray structure of tungsten cofactor aldehyde ferredoxin oxidoreductase[14]. In this tungsten cofactor the presence of two molybdopterin ligation is not surprising based on the known chemistry of molybdenum[33] as well as of tungsten itself.[34] This chemistry is thus reflection of group property of molybdenum and tungsten where both show parallel chemistry.

For the identification of the nature of the organic moiety that is the molybdopterin , the method used was alkylation reaction by iodoacetamide . This reaction exploits the well known chemistry of iodoacetamide to react with sulfhydryl group.Interestingly , for sulfite oxidase the yield of the released organic moiety di-(carboxamidomethyl)molybdopterin (camMPT) was reported to agree with the proposed one molybdopterin ligation to molybdenum in Moco of sulfite oxidase . Extension of this work to AOR enzyme however resulted poor yield of camMPT . Though for both these enzymes the universal protein denaturant SDS was used[25,35] the poor yield for the AOR has been thought to be due to the partial release of the cofactor under denaturing condition used and / or the existence of a more complicated pterin system was presumed. The X-ray structural studies of AOR clearly demonstrated the absence of any covalent linkage between tungsten cofactor and apoprotein and the presence of only hydrogen bonding between the cofactor and apoprotein . Considering the presence of covalent linkage between Moco and apoprotein in sulfite oxidase

the denaturation to release the free cofactor from sulfite oxidase would be more difficult compared to that from AOR. Secondly the established stoichiometry of the presence of two molybdopterins per tungsten in AOR[14] should have yielded more, if not double, the amount of camMPT compare to that from sulfite oxidase. The identical nature of camMPT from both the species using spectroscopy once more strongly suggest that though this alkylation reaction extensively contributed to understand the organic component of the cofactor but failed to establish the exact stoichiometry of molybdopterin ligands attached to the respective metal.

MODEL STUDIES

By definition a model system represents the simplified description of system a to assist prediction of the structural information of the original one. Although tungsten containing aldehyde ferredoxin oxidoreductase (AOR) enzyme has been structurally characterised by X-ray, but the structure of no other molybdoenzyme of this class is known till today. The presence of a dissociable common molybdenum cofactor in these molybdoenzymes thus may permit to model this cofactor.Thus for designing a model for this cofactor two important factors are to be kept in mind. Firstly the synthesized complexes should have very similar donor atom ligation around molybdenum to the cofactor which would be reflected by the resemblance of spectral and other physiochemical properties of the model compound to those of the cofactor. Three dimensional structural information of these model compounds may

then be used to predict the geometry around molybdenum in the cofactor for which similar structural information is not yet known. This part of the model may be called as structural analogue to molybdenum cofactor. Secondly an even more important criterion for model compound lies in its ability to function similarly in relation to the native enzyme. This functional model may not demonstrate exactly identical activity of the molybdoenzyme. This is because of the fact that in these model enzymes the catalytic cycles are not completed by its own but here only one half cycle can be completed. In native enzymes the two halves of the catalytic cycles are governed by two different redox centers, one is the molybdenum center and another is the other redox centers attached to the apoprotein near to molybdenum center whereas in model systems only molybdenum is present and regeneration of the resting molybdenum center for a full catalytic cycle is not possible except for the model of DMSO reductase.

Based on the above limitations and essential qualifications of a model compound, several contributions have been made which are briefly outlined below.

COMPLEXES CONTAINING MoO_2(VI) MOIETY.

Simple oxohalo complexes of the type MoO_2X_2 (X = halides) have long been known. Derivatives like $MoO_2Cl_2L_2$ (L = CH_3COCH_3, DMF, DMSO, Ph_3PO, Ph_3AsO, PyO)[36] have been prepared by direct reaction of MoO_2Cl_2 and L. These complexes are good starting materials for the complexes like $MoO_2(acac)_2$, $MoO_2(oxine)_2$. The complex anion $[MoO_2Cl_4]^{2-}$ is stable in HCl solution of molybdate(VI).[37] MoO_2(β-diketonate)$_2$ complexes are alternatively

prepared by acidification of aqueous MoO_4^{2-} and β-diketone solution.[38] Complexes of the type $MoO_2(R_2dtc)_2$ (R = CH_3, C_2H_5) were prepared by Malatesta[39] using approate ligand with MoO_4^{2-} in water followed by acidification . Improved methods were devised for these complexes.[40] The reactions of monomeric $MoO_2(R_2dtc)_2$ with phosphines[40c,41] lead to oxotransfer reaction according to equation;

$$[Mo^{VI}O_2(R_2dtc)_2 + PPh_3 \longrightarrow [Mo^{IV}O(R_2dtc)_2] + PPh_3{=}O \quad \text{----(1.3)}$$

Here the course of the reaction follows the dimer monomer conversion path. Thus half of the compound $MoO_2(R_2dtc)_2$ when reduced to $MoO(R_2dtc)_2$ the other half gets reacted with it leading to the following comproportionation reaction:

$$[MoO_2(R_2dtc)_2] + [MoO(R_2dtc)_2] \rightleftharpoons [Mo_2O_3(R_2dtc)_2] \quad \text{----(1.4)}$$

This important reaction of dioxomolybdenum complex led to correlate electron or oxotransfer capability of synthesized complexes in relevance to oxomolybdoenzymes. The surge in the syntheses of complexes containing MoO_2(VI) core stem from unusual reactivity of this core. The diverse interests related to structural varities, donor atom dependence, electrochemical behavior and correlation of these in relevance to oxotransfer capability have been undertaken. This resulted in the designing of the multi donor sites ligands to hold the MoO_2(VI) moiety to prevent unwanted dimerization in the oxotransfer reactions by posing steric crowding.

Remembering the donor sites in the active site of molybdoenzymes the ligands having combinations of S/N/O donor

atoms were chosen. The complexes $[MoO_2(R)\text{-}cysOMe)_2$ and $[MoO_2((S)\text{-}PenOMe)_2]$ (Cys = cysteine ,Pen = Penisilimine) are readily synthesized by reacting MoO_4^{2-} with the hydrochloride of the ligand in water.[42] A series of complexes of the type $MoO_2(L\text{-}L)_2$ (L-L = tox, 8-mercaptoquinoline, mee, N,N'-dimethyl-N,N'-bis(2-mercaptoethyl) ethylenediamine, mpe, sap, salisaldehyde o-hydroxyanil) have been reported.[43] Some of these complexes have been studied for the reaction like dehydrogenation of hydrazo-benzene to azobenzene.[44] A dioxo complex $MoO_2[CH_3NHCH_2C(CH_3)_2S]_2$, with interesting structure has been reported.[45] Holm and coworkers have reported the analogue reaction system of the molybdenum oxotransferases using $[MoO_2(tBuL\text{-}NS)_2]$ (tBuL-NS = bis (4-*tert*-butylphenyl)-2-pyridylmethanethiolate).[46] Amongst anionic complexes of MoO_2(VI) core, $[Et_4N]_2[MoO_2(bdt)_2]$ (bdt= benzene dithiolate)[47], $[NH_4]_2[MoO_2(O_2CCSPh_2)_2]$[48] and very recently an interesting compound $[Bu_4N]_2[MoO_2(mnt)_2]$ (mnt= 1,2-dicyanoethyl-enedithiolate)[33a] has been reported, which oxidizes HSO_3^- to SO_4^{2-} following the enzymatic saturation kinetic behavior.

Amongst tridentate Schiff's base ligands with O,N,S donor atoms the 5-H-$sspH_2$ ligand has been shown to coordinate to MoO_2(VI) core as dianionic tridentate ligand with a solvent molecule like DMF is present (5-H-$sspH_2$= 2-salicylideneamino benzenethiolato(2-)).[49] Several derivatives of tridentate schiff's bases like ssp, sap and sae have been made with MoO_2(VI) moiety.[50]A mixed ligand complex, $[MoO_2(pdmt)(tmso)]$ is also known.[51] Oxo transfer reaction has been demonstrated using the MoO_2(VI) complexes with Schiff's base ligands like S-benzyl3-(5-R-2-hydro- xyphenyl) mehthylene dithiocarbaazate and

S-methyl3-(2-hydroxyphenyl) methylene dithiocarbazate.[52]

The ligand, hydrotris(3,5-dimethylpyrazolyl)borate forms complexes like $[MoO_2X(HB(3,5\text{-}Me_2pz)_3)]$ which possesses a frame work to impose *facial* coordination.[53] These compounds have an exchangable monodentate anionic ligand and to synthesize the complex $[HB(Me_2pz)_3][MoO_2(S_2P(OEt)_2]$ monodentate dithiophosphate ligand has been used.[54] The complex $MoO_2(LNS_2)$ (LNS_2= 2,6-bis(2,2-diphenyl-2-sulfidoethyl)pyridine(2-)) and the oxo version with respect to this ligand, $MoO_2(LNO_2)(DMSO)$ have been synthesized.[55] A MoO_2^{2+} complex with *threo*-α,α-di-*tert*-butyl-2,6pyridinedimethanol, has also been reported.[56] Several complexes with tetradentate pseudomacrocylic ligands have been designed to make the complex with MoO_2(VI) moiety.[57] The protonated forms of these ligands are presented in Figure 1.4. Some of the representative model complexes are shown in Figure 1.5.

COMPLEXES CONTAINING MoO(IV) MOIETY.

MoO(IV) complexes are relatively rare in comparison to dioxo Mo(VI) complexes. Considering the model aspect, only few of such complexes have been reported. The synthesis of $[MoO(R_2dtc)_2]$ is probably the first and best studied complex of all. It was synthesized by reacting Na_2MoO_4 and R_2dtc^- in the presence of excess of sodium dithionate in aqueous medium[58] or by reacting $MoO_2(R_2dtc)_2$ with PhSH.[59] The synthesis of $[MoO(mnt)_2]^{2-}$ has long been reported.[60] Though this compound is very much similar to $MoO(R_2dtc)_2$ with regard to donor atom and specially containing direct dithiolene linkage in relevance to molybdenum cofactor yet no attempt has been made to test its reactivity. The compound like

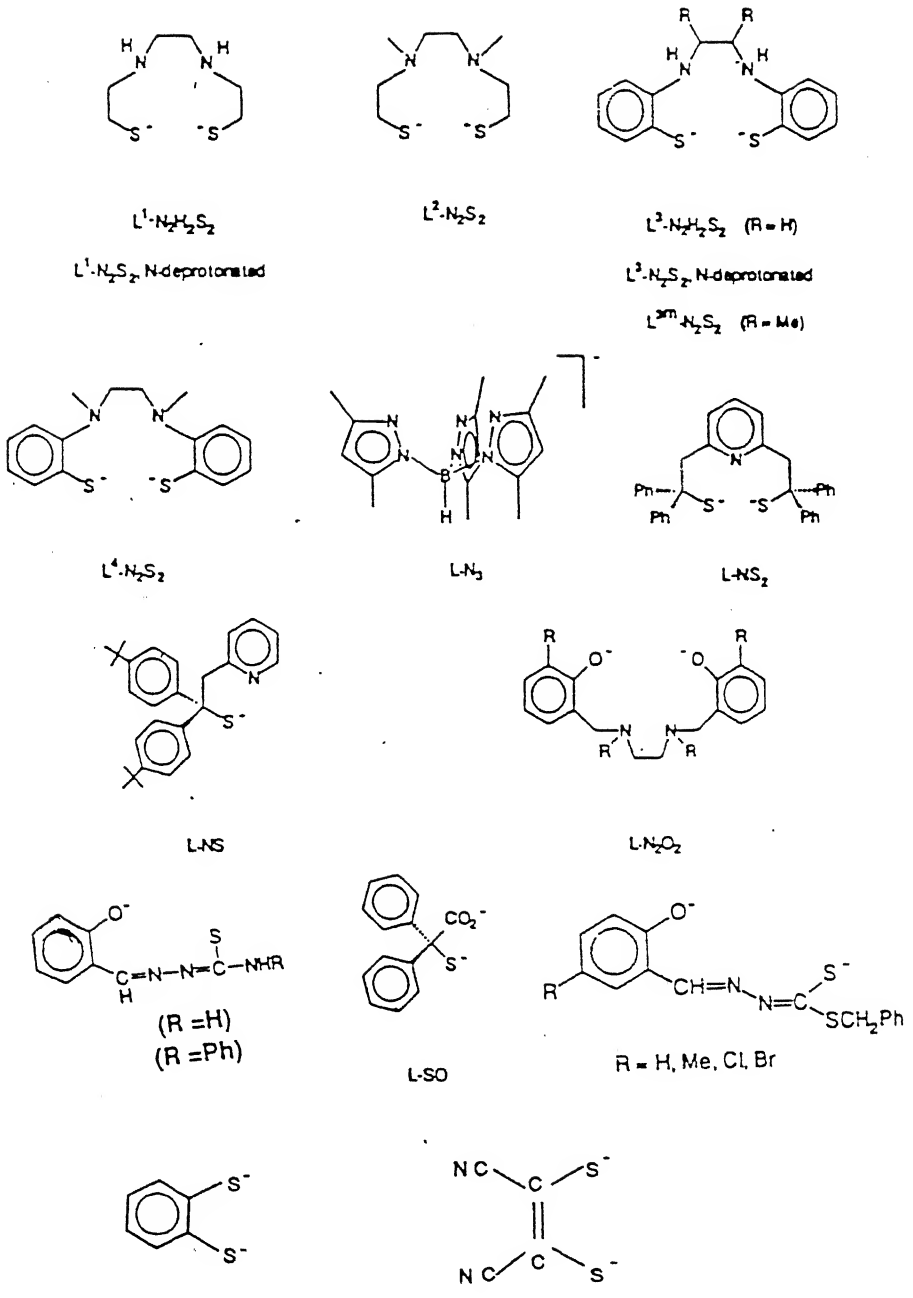

Fig. 1.4 Some of the representative ligands used in model studies.

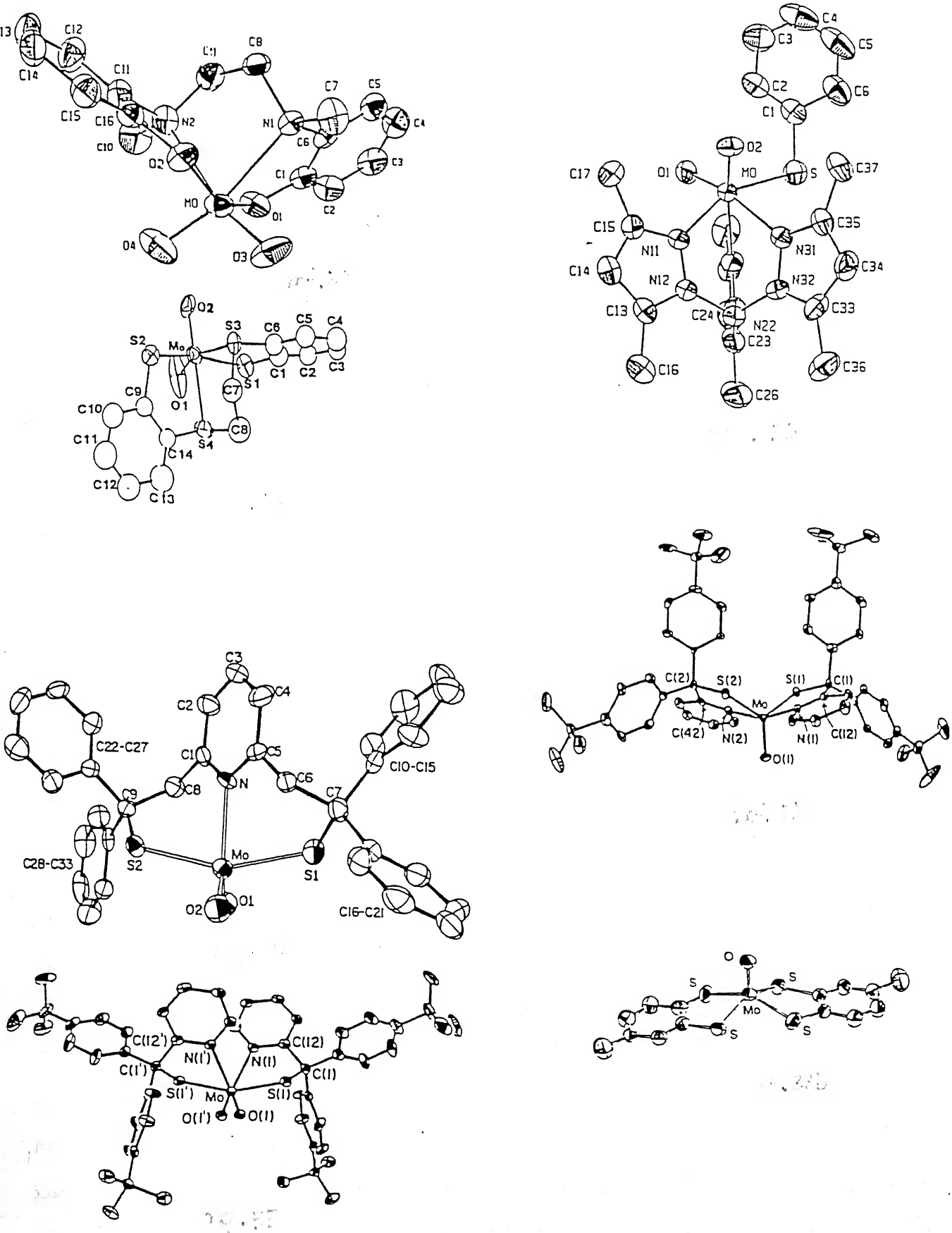

Fig. 1.5 Some of the representative model complexes. (See Ref. 9)

$MoO(LNS_2)(DMF)$ has been synthesized by the reaction between $MoO_2(LNS_2)$ and PPh_3 in DMF medium.[55] Similarly $MoO(dttd)(PPh_2Et)$ is reported.[57d] The reported complex $MoO_2(tBuL\text{-}NS)_2$ reacts with one equivalent of the strongly basic Et_3P to form corresponding tetravalent monoxo complex $MoO(tBuL\text{-}NS)_2$.[46] The complex like $[Et_4N]_2[MoO(S_2C_2(COPh)_2)_2]$ and $[Et_4N]_2[MoO(S_2C_2(COOMe)_2)_2]$ have also been reported.[61] Other MoO(IV) complexes reported are $[Et_4N]_2[MoO(bdt)_2]$[33b] and $[Et_4N]_2[MoO(mnt)_2]$[33a], and their reactivities are studied.

COMPLEXES CONTAINING $\{MoO(OH)\}^{2+}$ MOIETY.

Synthesis of complexes containing above core has not yet been reported. A long known TPP complex with $\{trans\text{-}MoO(OH)\}^{2+}$ moiety is reported[62] (TPP = dianion of *meso*-tetraphenyl porphyrin). It is even more difficult to stabilize similar core using SH^- instead of OH^- in relevance to xanthine oxidase. The presence of these moieties have been accounted for during the catalytic cycle as transient species in native enzymes. Even from the knowledge of enzymatic systems the instability of these cores suggest that the efficiency of the system to flip from MoO_2(VI) or MoOS(VI) to MoO(IV) and the reverse required for the regeneration stage of the relevant (reductase or oxidase type) enzyme is mostly done by one electron donor or acceptor. This accounts for two successive one electron transfer processes which must proceed *via* pentavalent molybdenum in either way. This oxidation state is thus not relevant for actual substrate's reduction or oxidation except for xanthine oxidase class of enzymes where internal redistribution of electron density occurs. For most of the other enzymes this

oxidation state is passage for achieving the next oxidation state in both ways and especially for the regeneration stage which should be faster and thus a transient Mo(V) species is seen by EPR.[23] It is important to note that from $\{MoO\}^{2+}$ core in enzymeatic reaction, $\{MoO_2\}^{2+}$ core is achieved by aquation with successive deprotonation. Thus in some elegant experiments demonstrations have been made by electrochemically generated MoO(V) species either from MoO_2(VI) or MoO(IV) species wherein ^1H superhyperfine coupled EPR spectra were observed.[63] However it is reported that isolated Moco in Mo(V) state did not show any proton superhyperfine splitting in its EPR spectrum.[30c]

BIOLOGICALLY IRRELEVANT $\{Mo_2O_3\}^{+4}$ AND $\{Mo_2O_4\}^{+2}$ MOIETY.

Dinucler complexes are common in the Mo(V) state with μ-oxo and di-μ-oxo bridges. In case of $Mo_2O_3^{+4}$ core there are mainly three types of possible arrangements of the two terminal oxo groups with respect to Mo-O-Mo bridging axis and are called *syn* type, *anti* type and linear type. The compounds are generally of dark colored and diamagnetic.These complexes have been reviewed by Steifel.[64] The $Mo_2O_3(R_2dtc)_4$ complexes were first prepared by Malatesta[39] using SO_2 or $S_2O_4^{2-}$ as the reducing agent to reduce $MoO_2(R_2dtc)_2$ complexes. The complexes $Mo_2O_3(S_2P(OR))_4$[40] and $Mo_2O_3L_4$ with L=O-ethylcysteine, O-methylcysteine and N-methylsalicylaldimine[42] have been reported. Donald and Bair have synthesized the $Mo_2O_3(dtc)_2(THF)_2I_2$ by iodine oxidation of $Mo_2(dtc)_4$.[65] The Mo_2O_3 complexes having hydrotrispyrazolyl borate $(HB(pz)_3)^-$ ligand are reported extensively. The complex $[HB(pz)_3Mo_2O_3Cl_2$ is synthesized and structurally characterized[66],

it is isolated as two geometrical isomers called C_2-dimer and C_i-dimer depending on the crystallographically imposed C_2 axis and center of inversion respectively.Recently C.G.Young *et al* have structurally characterised the complex $Mo_2O_3(SPh)_2(HB(pz)_3)_2$[67], synthesized the complex by stirring $MoO_2(SPh)(HB(pz)_3)$ with PPh_3 in toluene but the reported yield is very poor. The complex like $Mo_2O_3L_3$ a new triply bridged system is also reported (L= thioglycolic acid).[68] In all these complexes the O=Mo-O-Mo=O unit is structurally of *trans* planer arrangement that means two oxo groups are in *anti* position. There are also examples for the *cis* arrangements like $Mo_2O_3L_4$ (L= dipropyl dithiocarbamate)[69] and $Mo_2O_3(S_2CPh)_4$.[70] The compound containing linear O=Mo-O-Mo=O unit is also reported.[71] A series of Schiff's base complexes of the type $Mo_2O_3L_2(solv)_2$ where L = 2-salicylidineamino-phenolate(2-),(sap); or 2-salicyld- eneamino-benzene thiolate(2-),(ssp); and solv = solvent, have been reported.[72] These compounds are synthesized following the comproportion concept in the oxotransfer reactions between MoO_2^{2+} species and Ph_2EtP in DMF. The complexes having N_2S_2 or NS donor like $Mo_2O_3(C_5H_4NS)_4$[73] and $Mo_2O_3L_2$ where LH_2= N,N′-dimethyl-N,N′-bis(2-marcaptoehtyl)-ethylenediamine are known.[57b]

By carrying out preparation in slightly acidic solutions, a large number of $Mo_2O_4^{2+}$ core containing complexes have been isolated. In number of cases the di-μ-oxo species has been prepared by the hydrolysis of $Mo_2O_3^{4+}$ species. A large number of compounds having $Mo_2O_4^{2+}$moiety are known.[64] A series of thiobenzoate complexes of the type $Mo_2O_4L_2(Py)_2$ and $Na_2Mo_2O_4L_4$ have been reported.[74] The $Mo_2O_4^{2+}$complexes containing N_2S_2 donor

ligands like (sap), (ssp) are reported, the compounds are insoluble in most of the common organic solvents.[57b] Enemark *et al* have synthesized a new varity of $[Mo_2O_4L_2]^{2+}$ complexes having two isomers (L= 1,5,9-triazacyclododecane). Oxidative decarbonylation of $LMo(CO)_3$ in $HClO_4$ with dioxygen produced the two isomers, purple *anti*-$[L_2Mo_2O_4](ClO_4)_2.2H_2O$ and yellow *syn*-$[L_2Mo_2O_4](ClO_4)_2.H_2O$, the compounds are structurally characterized.[75] The complex $Mo_2O_4(HB(pz)_3)_2$ as the major product obtained from the reaction between $KHB(pz)_3$ and $[MoOCl_5]^{2-}$ in aqueous HCl solution(pH~ 2).The complex is easily converted to $Mo_2O_3^{4+}$ core by reacting with HCl.[66] Sarkar and coworkers have reported and structurally characterized complexes of the type $Mo_2O_4X_2L_2$ (where X= Cl, Br; L= dipyrazolylmethane).[76] They have synthesized these complexes in high yield by the reaction between Mo(II)-π-allyl complexes and the said ligand in CH_2Cl_2 medium under dioxygen. In all these complexes the molybdenum is hexacoordinated. There are some examples of penta- coordinated complex also, Boyd *et al.* have structurally characterized the complexes like $[Mo_2O_4(SPh)_4]^{2-}$, $[Mo_2O_4(S(CH_2)_3S)_2]$ and the similar $[Mo_2O_4(SCH_2(CHOH)_2CH_2S)_2]$; by adding Me_4NOH to a 1 M HCl-MeOH solution of $[Mo_2O_4(H_2O)_6]^{2+}$ and thiophenol, the yield of these compounds are very poor.[7]

CHAPTER 2

SCOPE OF THE INVESTIGATION

Molybdenum enzymes other than nitrogenase possess a pterin containing unique molybdenum cofactor (Mo-co). Enzymes containing Moco include oxydases , reductases and dehydrogenases and are found in bacteria , plants and animals including human.

The molybdenum in Mo-co is shown to be associated with the pterin cofactor via a 1,2-enedithiolate linkage of the α and β carbons of the pterin side chain. At the other end of the carbon of dithiolene a phosphate ester is linked. The minimum coordination number of molybdenum around in Moco is postulated to be four (shown in Figure 2.1).

For the oxidase type of enzymes the presence of $\{Mo^{VI}O_2\}$ or $\{Mo^{VI}OS\}$ moiety is proposed. The oxo group attached to molybdenum is involved in oxotransfer reaction. From the molybdenum EXAFS analysis of oxidase type enzymes the coordination geometry around molybdenum center is shown to be comprised of two oxo groups at 1.68 Å which are within the range of Mo-O bond distances for all crystallographically characterized *cis* dioxo molybdenum complexes. Three sulfur atoms at a distance of 2.41 Å are assigned to thiolate ligands . Less definitive suggestions are made with the possible presence of either a nitrogen or an oxygen atom at a Mo-N(O) distance of 2.19 Å and a sulfuratom at 2.86 Å .

On reduction of sulfite oxidase one of the oxo ligands at 1.68 Å is replaced by a Mo-O(N) bond of 2.04 Å which is suggested

to be a OH^- or H_2O ligand.[8,24a,78] The proposed structure of the reduced and oxidised form of sulfite oxidase are shown in Figure 1.2.

The proposed structure of Moco in sulfite oxidase or in xanthine oxidase contains one molybdopterin ligation . This ratio between molybdenum and molybdopterin ligand as 1:1 has been directly inferred by the quantitative analysis of sulfite oxidase. The methodology used in the analysis is to detemine the ratio between the subunit activity of sulfite oxidase : phosphate analysis. It has been shown that all phosphate present there is covalently attached to molybdopterin.[11]

Interestingly in the same study it is demonstrated that trichloroacetic acid pellet of the native enzyme does not lose enzymatic activity and from this pellet the ratio between found phosphate : subunit activity is also 1:1 . However after the release of "form A" (*vide supra*) the trichloroacetic acid pellet showed appreciable activity of sulfite oxidase and from this pellet the phosphate analysis per subunit activity obtained only 0.55:1 . This part of the reported quantitative analysis is shown in table 2.1 . From the above results it may be inferred that phosphate analysis is at a lower side of the expected value.[11]

The EXAFS results showed the presence of distinctly three Mo-thiol ligation . It is presumed that the third molybdenum thiol ligation may arise from the protein through a cysteinyl ligation . At this stage the reported X-ray structure of tungsten containing aldehyde ferridoxin oxidoreductase (AOR) showed definitely two molybdopterins ligation to tungsten center.[14] Interestingly EXAFS studies on AOR demonstrated very similar donor atoms around the

tungsten to that of molybdenum in sulfite oxidase.[16] Furthermore, the X-ray structure of AOR enzyme disproved that the cofactor is covalently linked to apoprotein.[14] Recently it was demonstrated that $[Mo^{VI}O_2(mnt)_2]^{2-}$ quantitatively reduces bisulfite to sulfate following saturation kinetics behaviour.[33a]

Based on the above results the following work may be attempted to resolve the issue :

1. Stabilization of a mononuclear oxo molybdenum species with one dithiolene ligation wherein the other donor atom may be nitrogen , oxygen or sulfur .

2. In the alkylation reaction of the *insitu* released Moco from enzyme led to the isolation of alkylated molybdopterin . In these reactions it is presumed that hydrolytic instability of the released Moco resulted the formation of reactive sulfhydryl groups which in turn is alkylated . In these reactions the fate of the molybdenum is presumed to be molybdate as the hydrolytic by-product . Similar alkylation reaction using synthesized complexes like $[Mo^{VI}O_2(mnt)_2]^{2-}$ and $[Mo^{IV}O(mnt)_2]^{2-}$ would be helpful in the understanding of the said alkylation reaction .

3. If in molybdoenzymes the Moco is not covalently linked to the apoprotein then it should be hydrogen bonded to the protein . The anionic nature of the Moco strongly suggest that a protonated amine residue of the apoprotein may serve as the cation to hold Moco. Attempts can be made to use some of the basic amino acids for this purpose . It would be further interesting to see if the protonated chiral amino acid can impose enantiomerization of the isolated complex .

4. In sulfite oxidase the forward oxidation reaction is now

known to be a two electron reduction process whereby Mo^{VI} is directly reduced to Mo^{IV} . In regeneration of the oxidised form successive two one electron oxidation occurs with the incorporation of one oxo group from a coordinated water with the successive release of one proton in each step . This suggest that EPR active species $\{Mo^{V}O(OH)\}$, is not involved in the substrate oxidation process . Interestingly EPR studies at this stage in the enzymatic reaction yields maximum 50% EPR active species, it is presumed that the electron transfer in the chain Mo^{IV}- Mo^{V}- Mo^{VI} is pretty fast. It has been shown by Bray and coworkers[30c] that isolated reduced cofactor from sulfite oxidase under proper electrochemical oxidation in the presence of excess of thiols yielded EPR signals of Mo(V) in high intensity where besides, MPT ligation thiolate coordination is suggested. Similar study using model mono dithiolene complexes under excess thiophenol would lead to a better understanding of the interaction of thiophenol with the protein free reduced Mo-co .

5. In the saturation kinetics behaviour of the model complex, $[Mo^{VI}O_2(mnt)_2]^{2-}$, with bisulfite, the chemistry of the substrate bound molybdenum complex which is similar to enzyme substrate (Michaelis) complex is less understood. Oxidation by $[Mo^{VI}O_2(mnt)_2]^{2-}$ to other biologically important substrate like thiophenol may be attempted to understand the possibility of stepwise one electron redox reaction with the involvement of $\{Mo^{V}O\}$ and $PhS^{\cdot}$ radical intermediate or the direct involvement of a two electron redox reaction which is equivalent to reductive elemination of a hepta-coordinated Mo^{VI} species. This hepta-coordinated species may be formed by the reaction between two

equivalents of PhSH with one equivalent of $[Mo^{VI}O_2(mnt)_2]^{2-}$ moiety to generate unstable $[Mo^{VI}O(PhS)_2(mnt)_2]^{2-}$ species .

6. The above reaction is important in another aspect where the reductase class of molybdoenzymes after the desired forward reaction is regenerated back to Mo^{IV} species to complete the catalytic cycle . Recently it has been proposed by Nakamura and coworkers that complexes like $[Mo^{IV}O(bdt)_2]^{2-}$ may or may not respond to saturation kinetics behavior using trimethylamine-N-oxide (TMANO) as the substrate.[33c] This reaction as demonstrated by them involves two interesting features; first the enzymatic saturation kinetics behavior is susceptible to the substituent groups present in the used different derivatives of bdt as ligand, secondly it is proposed that the substrate TMANO is first attached to *trans* position of the oxo group in the complex which responds to *trans-cis* isomerization to lead the oxo transfer reaction. It would be interesting to check the reactivity between $[MoO(mnt)_2]^{2-}$ and TMANO in relevance to TMANO reductase as well as in relation to the studies made by Nakamura and coworkers.[33c]

For all the known oxomolybdoenzymes the substrate TMANO is unique because of its of very polar $\overset{+}{N}$-$\bar{O}$ bond. TMANO reductase involves a coupled phosphorylation reaction wherein proton transfer steps are involved.[79] TMANO in aqueous medium is basic in nature because of the possible aquation,

$$Me_3NO + H_2O \rightleftharpoons Me_3NOH^+ + OH^- \quad \text{---------(2.1)}$$

The reported pH dependent activity of TMANO reductase and the involvement of protomotive force for phosphorylation strongly suggest the possibility of the existence of Me_3NOH^+ form of TMANO as the alternative substrate. This form in the form of a ion-pair

should be lypophilic and thus would be easier to pass across the membrane .

Thus a proton dependent kinectic study would be interesting. Furthermore in *E.coli.* other inducible enzymes like DMSO reductase is closely related to TMANO reductase. It would be interesting to check if the model complex demonstrate DMSO reductase activity also.

7. In oxotransfer reaction of molybdoenzymes irrespective of reductase or oxidase type the important end products are either $\{MoO_2\}^{2+}$ or $\{MoO\}^{2+}$ moiety . The imvolvement of these enzymatic reactions via Michaelis type complexation undoubtedly suggest the involvement of inner sphere mechanism . In most of the cases the electron (atom) transfer reactions take place after the formation of enzyme substrate complexation . From inorganic chemistry point of view if the molybdoenzyme is considered to be a molybdenum complex then in the enzyme-substrate complex, where the substrate is attached to molybdenum directly or through an attached atom to molybdenum in the resting state , the coordination enviornment around molybdenum is bound to be changed compared to that of the resting state . Thus the measured redox potential of molybdenum in the resting state of the molybdoenzyme would no way reflect any thermodynamical property of the changed molybdenum species present in the form of the enzyme-substrate complex . This argument is also valid for unbound substrate and enzyme bound substrate .

The Mo^{VI} / Mo^{V} and Mo^{V} / Mo^{IV} redox couples of DMSO reductase were reported to be in the range of +0.065V to -0.15V *vs* NHE in the pH range of 5-9.[80] Whereas DMSO, the substrate for this enzyme is electrochemically stable over a large range of potential from

far positive to far negative values and infact is used as a solvent for electrochemical studies . Thus it would be helpful to verify the predictability of measured redox potential values for different molybdoenzymes and for functionaly competent model complexes using only electron transfer concept.[34b]

CHAPTER 3

SYNTHESIS & CHARACTERIZATION

3.1 EXPERIMENTAL SECTION:

3.1.1 Materials. The materials which have been used for the syntheses, reactivities and characterizations of the compounds in this work are obtained likewise:

$[Bu_4N]Br$, $[Et_4N]Br$, trimethylamine N-oxide, thiophenol and bipyridyl are purchased from Aldrich; $NaHSO_3$, citric acid, KH_2PO_4, $[Ph_4P]Br$, and oxalic acid from Merck; molybdic acid from Thomas Baker and Co.; $Na_2MoO_4.2H_2O$ from John Baker Inc; NaCN from May and Baker Ltd.; sodium diethyldithiocarbamate, ammonium diethyldithiophosphate from BDH chemicals Ltd.; ammonium citrate, (L+)lysinium monohydrochloride from LOBA-CHIEME Co.; HCl and HBr from s.d. fiNE-cHEM Ltd.; hydrazene hydrochloride from REIDEL (Germany). The chemicals were used as purchased. All solvents were reagent grade, purified and dried by standard methods. Doubled distilled water was used to make buffer and for other uses. Anaerobic syntheses, when necessary, were carried out in argon atmosphere.

3.1.2 Physical Measurements: Elemental analyses for C,H,N were determined with a EA 1108-Elemental Analyzer. Sulfur was estimated gravimetrically as $BaSO_4$ (*vide infra*). Infrared spectra were recorded as KBr pellets on Perkin Elmer 577 and as CsI pellet on

Perkin Elmer 783 IR spectrophotometers. UV-Visible electronic spectra were measured in different solvents by a Shimadzu 160 UV-Visible spectrophotometer. Negative ion (FAB^-) mass spectra were recorded on a Jeol SX 102/DA-6000 Mass spectrometer/Data system using argon (6 KV, 10 mA) as FAB gas. The accelerating voltage was 10 KV and spectra were recorded at room temperature using m-nitrobenzyl alcohol as the matrix. EPR spectra were recorded with a Varian E-109 spectrometer. Samples were prepared under argon and transferred to EPR cell by gas tight syrings. EPR parameters were obtained from the measured spectra by inspection using DPPH as standard.

Cyclic voltammetric measurements were made with CV27 BAS Bioanalytical Systems using 10^{-3} M solutions of the compounds by glassy carbon working electrode, Ag/AgCl reference electrode, platinum auxilliary electrode and either $[Bu_4N]ClO_4$ or $[Et_4N]ClO_4$ as supporting electrolyte.

X-ray structure and determination: Diffraction quality crystals were obtained different methods as described elsewhere (*vide infra*). A single crystal for each complex was sealed in a glass capillary under argon atmosphere for the X-ray measurements. The measurements were performed at 25^oC on a Enraf-Nonius CAD4 diffractometer equipped with a Mo X-ray source and a graphite monochromator. Intensity data for all crystals were obtained with the use of a θ-2θ step scan technique. For each data set collected, three standard reflcetions were monitored (periodically) after every 97 reflections and showed no significant decay during data collection. Lattice parameters were obtained from a least square analysis of 25 machine centered

reflections with $20^{o} < 2\theta < 30^{o}$. The data were collected for Lorentz and polarization effects, and absorption corrections were applied. The basic crystallographic parameters of the compounds were listed in the tables (*vide infra*).

The structures were solved by either direct method using XTAL 3.2 package, refined on F by full matrix least-square calculations or by Patterson technique followed by fourier syntheses and refined on F^2 through full-matrix least-square calculations using SHELXS 86 and SHELXS 93 to refine the structures ; Molecular Graphics was used to draw the ORTEP diagrams. All non-hydrogen atoms were refined anisotropically and hydrogens were isotropically ; all hydrogens were placed on the calculated positions with a assumed C-H distance of 0.95 Å. A PC-486 / PDP 11/45 computer was used for all calculations . The complete tables of calculated hydrogen atom positions, bond distances and angles, positional and thermal parameters were given for all compounds.

Kinetic measurement:

All kinetic measurements were carried out by the spectrophotometric method by the use of a Simadzu 160 spectrophotometer provided with a piezoelectric thermostating device for the regulation of temperature. In a typical experiment a stock solution was taken in the cell of path length 1 cm. fitted with a serum cap and placed in the cell compartment; after thermal equilibrium the reactant was added to the cell solution by calibrated syringe and the cell contents were quickly mixed. The progress of the reaction was monitored by the decay of absorbance of a particular peak with time. Three kinetic run were made for

each reaction. All computations for data analysis were performed with NAG subroutine programs on a Hewlett-Packard(HP 9000) computer.

Procedure for the gravimetric estimation of sulfur:

About 0.3 g of the sulfur containing complex was oxidized with an excess of alkaline bromine water. the excess bromine was evaporated off by warming the solution slowly on a water bath. To the resulting solution hydrochloric acid was added slowly and the liberated bromine was again evaporated off by boiling the solution. The solution was then filtered and the sulfate in the filtrate was estimated gravimetrically as $BaSO_4$ by standard method.[81]

3.1.3 Synthesis :

Preparation of the ligand, 1,2-dicyanoethylene dithiolate, disodium salt (Na_2mnt) :

The ligand, Na_2mnt,was prepared by the procedure[82] published by Steifel *et al.* Sodium cyanide (10 g) was suspended in 50 ml of DMF, 15 ml of CS_2 was added dropwise to the suspension with vigorous stirring and constant cooling. When CS_2 addition was over the cooling was discontinued and the stirring was continued for another hr. The resulting dark brown mass was then dissolved in 200 ml of $CHCl_3$ and filtered. The $CHCl_3$ solution was then refluxed for 6hrs.during which time the yellow product precipitated out. The solution was filtered hot. The yellow product was then washed with $CHCl_3$ and dried under vaccum. Yield 7g.

The compound showed characteristic bands at 2190 and 1440

cm^{-1} in the IR spectrum which are for the ν(CN) and ν(C=C) vibrations respectively.[82]

1. Synthesis of $[Bu_4N]_2[Mo^{VI}O_2(mnt)_2]$:[33a]

2 mmol of $Na_2MoO_4.2H_2O$ (0.485 g) and 4 mmol of Na_2mnt (0.745 g) were taken in 40 ml of citric acid-phosphate buffer (pH ~ 6) at 10^oC . 5 mmol of Bu_4NBr (1.6 g) was added when a red-brown oily mass was formed. The oily mass was solidified at room temperature on standing. The red-brown solid was filtered and washed with cold water, isopropanol and finally with diethyl ether then dried in vacuo.This product was recrystallized from CH_3CN, isopropanol and diethyl ether. Yield 1.1 g (61% based on $Na_2MoO_4.2H_2O$).

Anal. Calcd. (found): 53.78 (53.71); H, 8.12 (8.31); N, 9.40 (9.51); S, 14.35 (14.42).

2. Synthesis of $[Ph_4P]_2[Mo^{VI}O_2(mnt)_2],2H_2O$:

1 mmol of $[Bu_4N]_2[Mo^{VI}O_2(mnt)_2]$ (0.890 g) was dissolved in 10 ml CH_3CN then 2.2 mmol of Ph_4PBr (0.945 g) was added to it , the solution was kept for 1 hr at room temperature .To this solution 15 ml of isopropanol and 10 ml of diethyl ether were added to cause turbidity and allow to stand at 20^oC. After 2 days red crystals were separated out which were collected by filtration and dried under vacuo .

Yield 0.975 g (90 % based on the starting compound) .

Anal. Calcd. (found): C, 59.90 (59.81); H, 3.95 (4.08); N, 4.98 (4.86); S, 11.40 (11.51).

3. synthesis of $[Et_4N]_2[Mo^{VI}O_2(mnt)_2]$ using oxalic acid :

2 mmol of $Na_2MoO_4.2H_2O$ (0.485 g) and 2 mmol of oxalic acid (0.180 g) were taken in 50 ml of distilled water and the mixture was cooled to 10^oC . 4 mmol of Na_2mnt (0.745 g) dissolved in 10 ml cold methanol was added whereby the color of the solution turned red brown. 5 mmol of Et_4NBr (1.050 g) dissolved in 10 ml methanol was added into this solution with slow stirring and the mixture was kept at 10^oC for 2-3 hrs. Beautiful needle shaped crystalline compound was separated out which was filtered, washed with cold water and vaccum dried. Yield 0.670 g (50 % based on the $Na_2MoO_4.2H_2O$) .

Anal. Calcd. (found): C, 34.14 (34.20); H, 6.03 (6.12); N, 12.56 (12.63); S, 19.15 (19.21).

4. Reaction of $[Bu_4N]_2[Mo^{IV}O(mnt)_2]$ with trimethylamine N-oxide; synthesis of $[Bu_4N]_2[Mo^{VI}O_2(mnt)_2]$:

1 mmol of $[Bu_4N]_2[Mo^{IV}O(mnt)_2]$ (0.876 g) was dissolved in 6 ml of acetone, the effective pH of the solution was adjusted to ~ 6 by the addition of glacial acetic acid. 1 mmol of trimethylamine N-oxide was dissolved in minimum volume (1 ml) of acetone was added to the above solution containing $[Bu_4N]_2[Mo^{IV}O(mnt)_2]$ whereby the color of the solution immediately changed to deep red brown. The solution was kept for 15min. to complete the reaction.Addition 0f 15 ml of diethylether into it and on standing overnight in a fridge red crystalline compound was separated out which was isolated by filtration and dried under vacuum .Yield 0.800 g (89% based on the starting complex).

From analysis and from spectroscopic data the compound was

confirmed as that from method 1.

5. Synthesis of $[Bu_4N]_2[Mo^{IV}O(mnt)_2]$:

This compound was synthesized earlier.[33a] The alternative methods are as follows :

Method A 2 mmol of molybdic acid (0.360 g) , 4 mmol of Na_2mnt (0.745 g) and 2mmol of $NaHSO_3$ (0.208 g) were taken in 100 ml of distilled water . The mixture was warmed upto 60°C in a water bath to get a clear brown-green solution . Addition of 5 mmol of Bu_4NBr (1.6 g) to this solution caused the precipitation of a dirty-green solid , which was filtered washed with water ,isopropanol and ether . This solid was recrystallized from CH_3CN , isopropanol and diethyl ether . Yield 1.1 g (65% based on the used $Na_2MoO_4.2H_2O$) .

Anal. Calcd. (found): C, 54.76 (54.70); H, 8.27 (8.32); N, 9.58 (9.66); S, 14.62 (14.60).

Method B By the reaction between $[Mo^{VI}O_2(mnt)_2]^{2-}$ and PhSH :

A solution of 1 mmol of $[Bu_4N]_2[Mo^{VI}O_2(mnt)_2]$ (0.890 g) in 10 ml CH_3CN was treated with 5 mmol of PhSH (0.50 ml) . The solution was kept for overnight at room temperature , the starting red-brown colored solution changed to green-brown over this period of time .Addition of 10 ml isopropanol and 10 ml diethyl ether caused the precipitation of a dirty-green solid. Analysis of the solid proved that it is $[Bu_4N]_2[Mo^{IV}O(mnt)_2]$ .Yield 0.785 g (90% based on the starting compound).

IR and UV-vis are identical to that obtained from method A.

6. Synthesis of $[PyH]_2[Mo^{IV}O(mnt)_2]$:

This complex was reported earlier.[33a] An improved method of the synthesis is given below.

5 mmol of molybdic acid (0.90g), 10 mmol of Na_2mnt (1.85g) and 11.5 mmol of $NaHSO_3$ (1.20g) were taken in 15 ml of distilled water. The mixture was heated upto 60°C when a clear green-brown solution was obtained. A freshly prepared solution of pyridinium acetate was added dropwise into the solution whereby a microcrystalline compound was precipitated out. This on standing for 2-3 hrs in fridge yielded this green crystalline compound in high yield. The compound was filtered washed with cold water and dried under vacuo. Yield 1.85 g (60 % based on the molybdic acid used).

Anal. Calcd. (found): C, 39.12 (39.10); H, 2.19 (2.25); N, 15.21 (15.30); S, 23.21 (23.14).

7. Synthesis of $[BipyH]_2[Mo^{IV}O(mnt)_2]$:

1 mmol of $[PyH]_2[Mo^{IV}O(mnt)_2]$ was dessolved in 10 ml of MeOH and 2 mmol of Bipy (0.31 g) was added to it and stirred for 10 min. A brown microcrystalline product precipitated out. Which was filtered,washed with ether andsucked dry . yield 92 % based on starting compound .

Anal. Calcd. (found): C, 47.58 (47.63); H, 2.56 (2.60); N, 15.85 (15.90); S, 18.15 (18.05).

8. Synthesis of $[(C_2H_5)_3NH]_2[Mo^{IV}O(mnt)_2]$:

The same method was adopted as for the synthesis of $[PyH]_2[Mo^{IV}O(mnt)_2]$, only in place of pyridine triethylammine was used. Yield 1.9g. (60% based on starting compound).

Anal. Calcd. (found): C,40.26 (40.20); H, 5.40 (5.52); N, 14.08 (14.15); S, 21.50 (21.40).

9. Synthesis of $[Lysinium]_2[Mo^{IV}O(mnt)_2]$:

The lysinium salt was obtained in the same way as for the preparation of $[PyH]_2[Mo^{IV}O(mnt)_2]$, only difference is that in place of pyridine L(+) lysinium monohydrochloride was used as cation . The crude product was recrystallized from water on standing the solution in a desiccator containing KOH pellets .Yield 1.0 g (40 %, based on the molybdic acid used).

Anal. Calcd. (found): C, 47.58 (47.63); H, 2.56 (2.60); N, 15.85 (15.90); S, 18.15 (18.05).

3.1.4 ALKYLATION REACTION OF $[Bu_4N]_2[Mo^{VI}O_2(mnt)_2]$:

(a) Using Iodoacetamide:

200 mg (0.22 mmol) of $[Bu_4N]_2[Mo^{VI}O_2(mnt)_2]$ was dissolved in 5 ml degassed CH_3CN containing 5% water, 800 mg (4.32 mmol, an excess amount) of iodoacetamide was added to the solution and stirred to dissolve the amount completely and the mixture was kept for overnight at room temparature. 2-3 ml of distilled water and 5 ml of isopropanol were added into it, to cause the precipitation of a light yellow microcrystalline compound (A) which was filtered and dried under vacuum. From the filtrate the organic solvents

were evaporated to precipitate a mixture from which the aqueous part was filtered out and washed with water. The aqueous part and the filtrate was evaporated in vacuo (mnt derv.).The yellow-green mass left in the reaction flask was dissolved in minimum amount of CH_3CN and by fractional crystallization using isopropanol and water three different products (B, C and D) were obtained. While the aqueous part was evaporated to dryness,the residue left was washed with CH_2Cl_2 to remove excess iodoacetamide and the pale yellow residue left (mnt derv.) was dried under vacuum.

The analysis of the products:

For (A) Anal. Calcd. (found): C, 28.16 (28.40); H, 5.32 (5.51); N, 2.05 (1.96); IR (KBr pellet, cm^{-1}) νMo-O, 950(s), 808(sh), 795(br,s).

For (B) Anal. Calcd. (found): C, 47.05 (47.21); H, 7.10 (7.40); N, 8.23 (8.35); S, 12.56 (12.70); IR (CsI pellet, cm^{-1}), νMo-O, 977(vs), 965(w), νMo-O_b, 730(s), 470(m), νMo-S, 360(s); Uv-vis. (MeCN), 357 nm. (10660); FAB^- (3-NBA), 537 (P^-), 778(P^- + Bu_4N^+).

For (C) Anal. Calcd. (found): C, 54.76 (54.88); H, 8.27 (8.30); N, 9.58 (9.66); S, 14.62 (14.77); IR (CsI pellet, cm^{-1}), νMo-O, 928(vs), νMo-S, 335(s); UV-vis (MeCN), 363(10055), 395(sh), 491(187), 602(110).

For (D) The analytical and spectroscopic data are identical to that of the reported $[Bu_4N]_2[Mo(mnt)_3]$ compound.[83]

For (mnt derv.) Anal. Calcd. (found): C, 37.48 (37.63); H, 3.14 (3.22); N, 21.85 (21.65); mp. 178°C; IR (KBr pellet, cm^{-1}), νN-H 3400(s), 3300(s), 3195(s), νCN 2200(vs), νCO 1650(vs), νC=C 1490(s); NMR (d-acetone), δ 4.03(s,4H), 6.73(br.s,2H), 7.20(br.s,2H).

The compounds are characterized as:

(A) = $[Bu_4N]_2[Mo_6O_{19}]$ (D) = $[Bu_4N]_2[Mo^{IV}(mnt)_3]$

(B) = $[Bu_4N]_2[Mo_2{}^{V}O_4(mnt)_2]$ (mnt derv.) = $[C_2H_4ON]_2mnt$

(C) = $[Bu_4N]_2[Mo^{IV}O(mnt)_2]$,

Percentage of yields were shown in Table 4.3.2.

(b) Using Methyliodide :

200 mg of $[Bu_4N]_2[Mo^{VI}O_2(mnt)_2]$ was dissolved in 5 ml degassed CH_3CN containing 5% water. An excess of (~ 1.2 ml) CH_3I was added to the solution with constant stirring at room temperature. Within 10 min the red color of the solution changed to yellow-orange which on standing for 36 hrs at 30°C in waterbath changed to yellow. The excess of CH_3I was removed by vacuum suction, 5 ml of isopropanol and 2-3 ml of distilled water were added to the solution and kept for an hour at room temperature . An yellow microcrystalline product (A) was precipitated out which was filtered and dried under vacuo. From the filtrate the organic solvents were evaporated out, the sticky yellow-green mass left in the reaction flask was then triturated with CCl_4(~ 5-7 ml), the light yellow CCl_4solution was filtered and evaporated to dryness in vacuo and the residue obtained was kept for analysis (mnt derv.). The residue left after CCl_4 extraction was dissolved in minimum amount of CH_3CN and by fractional crystallization using isopropanol and water two different compounds (B) and (D)were isolated.

Analyses of the products (A), (B) and (D) are identical to that of the products (A), (B) and (D) obtained from the reaction with iodoacetamide.

For (mnt derv.) Anal. Calcd. (found): C, 42.31 (42.18); H, 3.56 (3.85); N, 16.45 (16.60); mp. 99°C IR (KBr pellet, cm^{-1}), νCN 2210(vs), νC=C 1420(s), NMR (d-acetone), δ 2.73(s).

So the compounds are:

(A) = $[Bu_4N]_2[Mo_6O_{19}]$, (D) = $[Bu_4N]_2[Mo^{IV}(mnt)_3]$.

(B) = $[Bu_4N]_2[Mo_2{}^{V}O_4(mnt)_2]$, (mnt derv.) = $[CH_3]_2$mnt

Percentage of yields are listed in table 4.3.2.

ALKYLATION REACTION OF $[Bu_4N][Mo^{IV}O(mnt)_2]$:

(a) Using Iodoacetamide :

200 mg (~ 0.23 mmol) of $[Bu_4N]_2[Mo^{IV}O(mnt)_2]$ was dissolved in 5 ml degassed CH_3CN containing 5% water and an excess amount of iodoacetamide 800 mg (4.23 mmol) was added to it and kept for 60 hrs at 30°C. The starting green-brown solution gradually turned greenish-yellow over this period of time. 2-3 ml of water and 5 ml of isopropanol were added into it and kept for an hour. When a yellow micro- crystalline product (A) precipitated out, which was filtered and dried under vacuum. From the filtrate the organic solvents were evaporated by vacuum to precipitate a mixture from which the aqueous part was filtered out and washed with water. The aqueous part and the filtrate was evaporated in vacuo. The yellow-green precipitate left after the organic solvent evaporation was dissolved in minimum volume of CH_3CN and by fractional crystallization using isopropanol and water, two products (B) and (D) were obtained.While the aqueous part was evaporated to dryness, the excess iodoacetamide was removed by washing with CH_2Cl_2 and light yellow residue left (mnt derv.) was kept for analysis.

The analytical and spectroscopic data for the products (A, B, D and mnt derv.) are identical to that of the products (A, B, D and mnt derv.) obtained from method (a) in the above reaction.

(A) = $[Bu_4N]_2[Mo_6O_{19}]$, (B) = $[Bu_4N]_2[Mo_2^{V}O_4(mnt)_2]$,

(D) = $[Bu_4N]_2[Mo^{IV}(mnt)_3]$, (mnt derv.) = $[C_2H_4ON]_2mnt$

Percentage of products are listed in table 4.3.2.

(b) Using Methyliodide :

0.200 g of $[Bu_4N]_2[M\overset{IV}{o}O(mnt)_2]$ (~ 0.23 mmol) was dissolved in 5 ml of degassed CH_3CN containing 5% water. An excess amount of CH_3I (~ 1.2 ml) was added to the solution dropwise with constant stirring and was kept for 60 hrs. at $30^{o}C$. The starting green-brown solution turned greenish-yellow during this time . About 2-3 ml of water and 5 ml of isopropanol were added into it and on standing, a yellow microcrystalline compound (A) was precipitated out which was filtered and dried. From the filtrate the solvents were evaporated out and the residue left in the flask was triturated with CCl_4, the light yellow solution obtained was evaporated to yield the mnt derivative which was analysed. The residue left in the flask after CCl_4 extraction was dissolved in minimum volume of CH_3CN and by fractional crystallization using isopropanol and water two products (B and D) were obtained. Analytical and spectroscopic data for the compounds were same as those of compounds obtained from the method (b) of the above reaction.

So the compounds are:

(A) = $[Bu_4N]_2[Mo_6O_{19}]$, (B) = $[Bu_4N]_2[Mo_2^{V}O_4(mnt)_2]$,

(D) = $[Bu_4N]_2[Mo^{IV}(mnt)_3]$, (mnt derv.) = $[CH_3]_2mnt$.

Percentage of yield were listed in table 4.3.2.

Data from similar alkylation reactions using $[W^{IV}O(mnt)_2]^{2-}$ and $[W^{VI}O_2(mnt)_2]^{2-}$ were also listed for comparison.[84]

DIRECT SYNTHESIS OF $[Bu_4N]_2[Mo_2^{V}O_4(mnt)_2]$ FROM HEPTAMOLYBDATE :

4.2 mmol (5.0 g) of ammonium heptamolybdate was taken in 30 ml of 4N HCl , stirred well to dissolve it . 10 g of hydrazine hydrochloride was added and the solution was digested at 80°C in a waterbath for 6hrs. Whereby the color of the solution became dark brown. The solution was then cooled and kept as a stoc solution for further experiments .

10 ml of this solution (containing 9.4 mmol of molybdenum) was taken in a conical flask and the pH of the solution was adjusted to about 5.5 by addition of a 25 % sodium acetate solution with constant stirring . 10.8 mmol of Bu_4NBr (3.5g) dissolved in water 10 mmol of Na_2mnt (1.80g) dissolved in water separately were added simultaneously into the molybdenum containing solution with stirring. The stirring was continued for several hours whereby a fluffy bright yellow precipitate was formed. The precipitate was filtered, washed with water and dried. This was recrystallized from CH_3CN, isopropanol and water. Yield 80% (based on the starting complex).

Anal. Calcd. (found): C, 47.05 (47.21); H, 7.10 (7.40); N, 8.23 (8.35); S, 12.56 (12.70); IR (CsI pellet, cm^{-1}), νMo-O, 977(vs), 965(w), $\nu Mo\text{-}O_b$, 730(s), 470(m), νMo-S, 360(s); Uv-vis. (MeCN), 357 nm. (10660); FAB^- (3-NBA), 537 (P^-), 778(P^- + Bu_4N^+).

3.1.5 REACTION OF $[Bu_4N]_2[Mo^V_2O_4(mnt)_2]$ WITH HBr, HCl, PhSH AND C_6H_4ClS

1. Reaction with HBr, synthesis of $[Bu_4N]_2[Mo^V_2O_3(Br)_2(mnt)_2]$:

1 mmol of $[Bu_4N]_2[Mo_2O_4(mnt)_2]$ (1.02g) was dissolved in minimum volume (~3ml) of dry acetone, 10 ml of dry MeOH was added to it . 1ml concentrated HBr was added dropwise with constant stirring in cold. The starting yellow solution became blue-violet and finally deep blue violet microcrystalline product was precipitated out. The reaction mixture was allowed to stand in the ice-bath for half an hour for complete precipitation. The compound was filtered in a sintered crucible and washed with petroleum ether and dried in a desiccator containing KOH pellets. Yield 0.64g. (55%, based on staring material).

Anal. Calcd. (found): C, 41.24 (41.32); H, 6.23 (6.40); N, 7.21 (7.13); S, 11.00 (11.20).

2. Reaction with HCl, synthesis of $[Bu_4N]_2[Mo^V_2O_3(Cl)_2(mnt)_2]$:

Same procedure was adopted as above. Only difference was that in place of HBr, dry HCl gas was passed through the solution containing $[Bu_4N]_2[Mo_2O_4(mnt)_2]$ for a minute when a red violet microcrystalline compound was precipitated out. Yield 0.59g. (55% based on starting material).

Anal. Calcd.(found): C, 44.65 (44.52); H, 6.74 (6.81); N, 7.81 (7.74); S, 11.91 (11.83).

3. Reaction with PhSH , synthesis of $[Bu_4N]_2[Mo^V_2O_3(SPh)_2(mnt)_2]$:

0.78 mmol of $[Bu_4N]_2[Mo^V_2O_4(mnt)_2]$ (800mg) was dissolved in 10 ml dry deaerated CH_2Cl_2, 9.70 mmol of PhSH (1 ml) was added dropwise with constant stirring. The solution was then kept overnight at 30°C in a waterbath when the color changed to brown-red. Upon standing the solution at ~10°C, dark red cubic crystals were precipitated out which were filtered and washed with diethyl ether, dried under vacuum. Yield 0.72g. (75%, based on starting material).

Anal. Calcd. (found): C, 51.05 (51.21); H, 6.75 (6.82); N, 6.86 (6.91); S, 15.72 (15.78).

4. Reaction with *p*-chlorothiophenol (C_6H_4ClS) synthesis of $[Bu_4N]_2[Mo^V_2O_3(C_6H_4ClS)_2(mnt)_2]$:

0.800 g of $[Bu_4N]_2[Mo^V_2O_4(mnt)_2]$ (0.78 mmol) was dissolved in 3 ml of dry degassed CH_2Cl_2, to this 1.7 mmol *p*-chlorothiophenol (0.245 g) in 10 ml dry MeOH was added. The mixture was kept overnight at 30°C in a waterbath. During this time the starting yellow color changed to red-brown and finally brown microcrystalline compound was precipitated out which was filtered, washed with petroleum ether and dried under vacuum. Yield 0.6g. (60%, based on the starting complex).

Anal. Calcd. (found): C,48.32 (48.37); H, 6.24 (6.36); N, 6.50 (6.59); S, 14.88 (14.97).

3.1.6 REACTION OF $[Bu_4N]_2[Mo^{V}_2O_4(mnt)_2]$ WITH Na_2mnt ,AMMONIUM CITRATE, SODIUM BISULFITE AND BIPYRIDINE .

1. Using Na_2mnt and ammonium citrate :

0.25 mmol of $[Bu_4N]_2[Mo^{V}_2O_4(mnt)_2]$ (0.225 g) was dissolved in 6 ml of CH_3CN, 0.75 mmol of Na_2mnt (0.14 g) dissolved in 3 ml of water was added to it .Excess amount (1.0 g) of ammonium citrate was added and stirred for 15 min. with the addition of 2 drops glacial acetic acid. The mixture was allowed to stand for 24hrs. at room temperature. Addition of water precipitated a dirty-green microcrytalline compound which was filtered and washed with water, isopropanol and dried under vacuo. Yield 0.260g (60%, based on the starting compound). From spectral analysis it was confirmed that the compound was $[Bu_4N]_2[Mo^{IV}O(mnt)_2]$.

2. Using Na_2mnt and $NaHSO_3$:

0.25 mmol of $[Bu_4N]_2[Mo^{V}_2O_4(mnt)_2]$ (0.225 g) was dissolved in 6 ml of CH_3CN, to this solution 0.50 mmol of Na_2mnt and 0.50 mmol of $NaHSO_3$ dissolved in 2 ml of water was added and kept for overnight at room temperature. During this time the starting yellow color changed to brown-green, 20 ml of water was added and a dirty-green microcrystalline compound was isolated by filtration and washed with water ,isopropanol and dried under vacuo . Yield, 0.350 g (80 % , based on the starting complex). From analysis it was confirmed that the compound was $[Bu_4N]_2[Mo^{IV}O(mnt)_2]$.

3. Using only ammonium citrate :

0.25 mmol of $[Bu_4N]_2[Mo^{V}_2O_4(mnt)_2]$ (0.225 g) was dissolved in

6 ml of CH_3CN ,to this solution excess amount (0.5 g) of ammonium citrate dissolved in 3 ml of water was added and the mixture was kept for 2 days at 50°C in a waterbath . 20 ml of water was added to the solution, a dirty-green compound was precipitated which was filtered ,washed with water,isopropanol and dried under vacuo. Yield 0.22 g (50 % , based on the starting complex) From analysis the compound was confirmed as $[Bu_4N]_2[Mo^{IV}O(mnt)_2]$.

4. Using bipyridine : method A

0.25 mmol of $[Bu_4N]_2[Mo^{V}_2O_4(mnt)_2]$ (0.225 g) was dissolved in 10 ml of acetone . 0.50 mmol of bipyridine (0.080 g) and 3-4 drops of glacial acetic acid were added to the acetone solution and themixture was allowed to stand for 24 hrs. at room temperature . The starting yellow color changed to pink and finally blue-violet microcrystalline compound was separated out which was filtered and washed with methanol and dried under vacuo. Yield 0.125 g (60%, based on starting the compound).Anal. Calcd. (found): C, 40.39 (40.30); H, 1.94 (2.03); N, 13.46 (13.55); S, 15.40 (15.33).

Method B. 0.5 mmol of $[Mo^{V}_2O_3(Br)_2(mnt)_2]^{2-}$was dessolved in 5ml of dry CH_2Cl_2, 1.1 mmol of bipyridyl (.17g) was added to it and stirred for 1 hr. The starting deep blue violet color was changed to blue by this time and a blue microcrystalline compound was precipitated which was filtered, washed with CH_2Cl_2 and dried. Yield 90%, 0.4g., based on the starting complex. Analytical spectroscopic data were found to be the same as that of the compound $[Mo_2O_3(bipy)_2(mnt)_2]$, obtained from method A.

3.1.7 REACTION OF $[Bu_4N]_2[Mo^{IV}O(mnt)_2]$ WITH N,N DIETHYLDITHIOCARBAMATE (dtc) AND WITH DIETHOXYDITHIOPHOSPHATE (dtp):

1. Using (dtc):

0.4g. (0.45 mmol) of $[Bu_4N]_2[Mo^{IV}O(mnt)_2]$ and 0.11g. (0.49 mmol) of dtc were dessolved in 15 ml of CH_3CN. 5-6 drops of chlorosulfonic acid was added with constant stirring. The initial green-brown solution turned rosy-red. 100ml of distilled water was added to precipitate a red compound. The precipitate was filtered and washed with water and sucked dry. Yield 0.21g. (60% based on the starting compound).

Anal. Calcd. (found): C, 45.43 (45.50); H, 6.05 (6.12); N, 10.95 (10.87); S, 25.04 (25.13).

2. Using (dtp):

The same procedure was adopted as above, only instead of dtc, dtp was used. Yield 0.18g. 50% based on the starting complex.

Anal. Calcd. (found): C, 42.69 (42.60); H, 5.88 (5.96); N, 8.89 (8.95); S, 24.38 (24.30).

3.2 CHARACTERIZATION OF THE SYHTHESIZED COMPLEXES.

Characterization of the synthesized complexes has been made by infrared, electronic, and FAB mass spectroscopy, single crystal X-ray study and cyclic voltammetry.

3.2.1 IR SPECTROSCOPY:

Characterization of the presence of *cis* dioxo moiety in MoO_2(VI) complexes, Mo-O_t (monooxo) moiety in MoO(IV) complexes and Mo-O_t, Mo-O_b moieties in $Mo_2O_4^{2+}$ and $Mo_2O_3^{4+}$ complexes can be readily made from infrared spectroscopy. It is now well known[85] that ν(Mo-O_t) appears in the range ~ 900-1000 cm^{-1}. The detailed IR spectral analysis of dithiolene coordinated complexes are also known.[86] Based on these, assignment of vibrations of monooxo and dioxo dithiolene coordinated complexes are tabulated in Table 3.1. The spectra are reproduced in Figures 3.1 to 3.5. It is important to note that ν(Mo-S) vibration in monooxo complex (345 cm^{-1}) appeared at higher wave number compared to that (320 cm^{-1}) for dioxo complex. This is fully in agreement with the chemical properties of these complexes where it was found that chelation from dithiolene to monoxo species are stronger and hence these species are more stable compared to the corresponding dioxo species. Interestingly, the separation of molybdenum cofactor from its reduced state is reported to be quantitative compared to that in the oxidized state. This difference has been interpreted as to the linkage of the dithiolene ligand to Mo(IV) is stronger than that to Mo(VI).[87]

Resonance Raman Spectroscopy has been used to study DMSO reductase from *R. sphaeroids* and for the oxidized state of the enzyme the 350 cm^{-1} band has been assigned to a Mo-S vibration.[26] The ν(Mo-S) vibration (365 cm^{-1}) for $[Et_3NH]_2[MoO(mnt)_2]$ is higher than that (345 cm^{-1}) for the corresponding $[Et_4N]_2[MoO(mnt)_2]$. This is due the formation of stronger Mo-S bonds for the hydrogen bonded compound.

Table 3.1 IR (cm^{-1}) Spectral Data for Complexes[a]:

Complex	ν(Mo=O)	ν(Mo-S)	ν(CN)
$[(C_2H_5)_4N]_2[Mo^{IV}O(mnt)_2]$	938vs	345s	2204vs
$[(C_2H_5)_3NH]_2[Mo^{IV}O(mnt)_2]$	905vs	365vs	2215vs
$[BipyH]_2[Mo^{IV}O(mnt)_2]$	905vs	370s	2210vs
$[C_6H_{15}N_2O_2]_2[Mo^{IV}O(mnt)_2]$	890vs	b	2215vs
$[Bu_4N]_2[Mo^{VI}O_2(mnt)_2]$[c]	854s 889vs	320s	2200vs
$[Bu_4N][Mo^{IV}(dtc)(mnt)_2]$	----	360m	2210vs
$[Bu_4N][Mo^{IV}(dtc)(mnt)_2]$	----	365m	2210vs

[a] as CsI disk; vs = very strong, s = strong, m = medium, w = weak.
[b] not measured.
[c] ref. 97

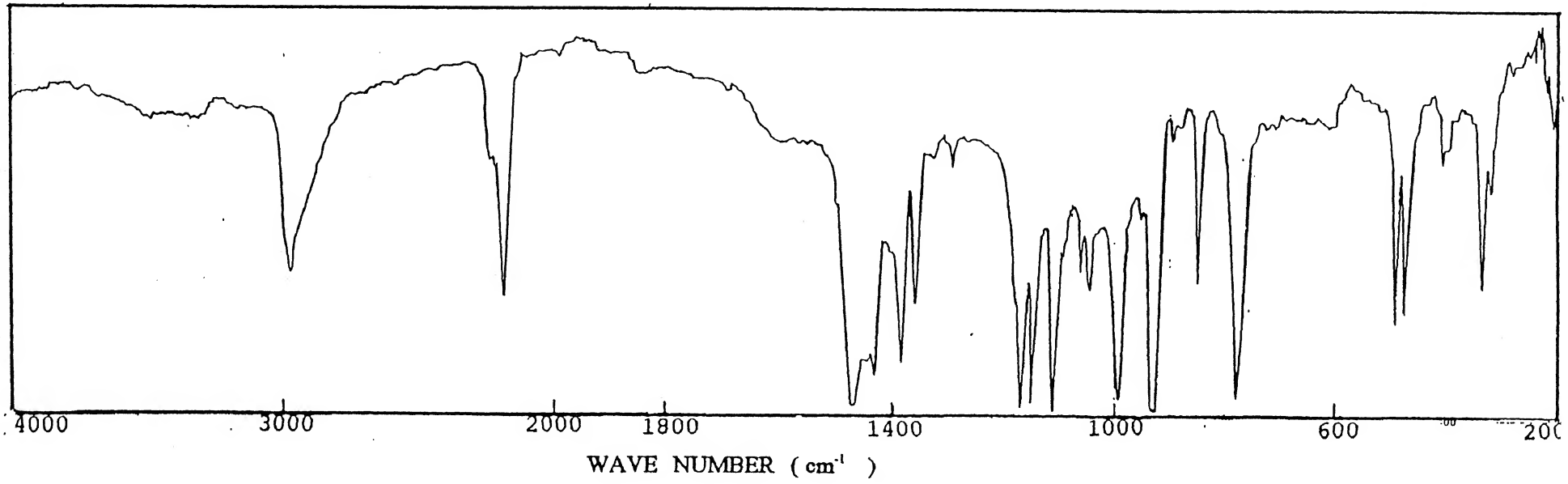

Fig.3.1 IR spectrum of $[Et_4N]_2[M\ddot{o}^{IV}O(mnt)_2]$

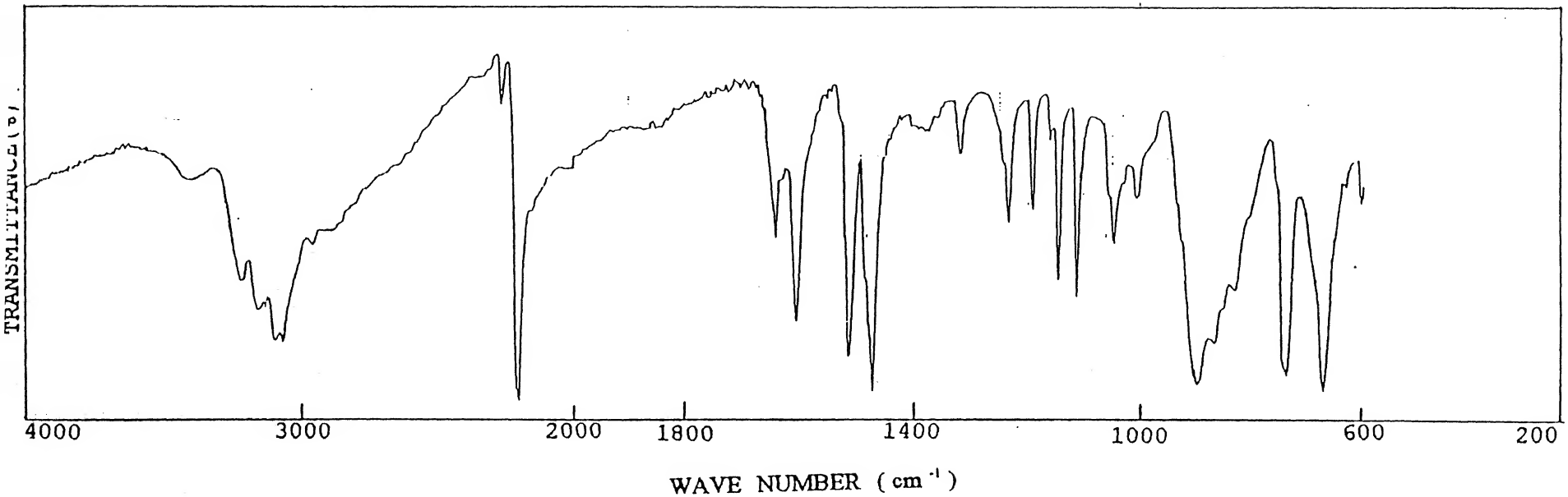

Fig.3.2 IR spectrum of $[PyH]_2[Mo^{IV}O(mnt)_2]$

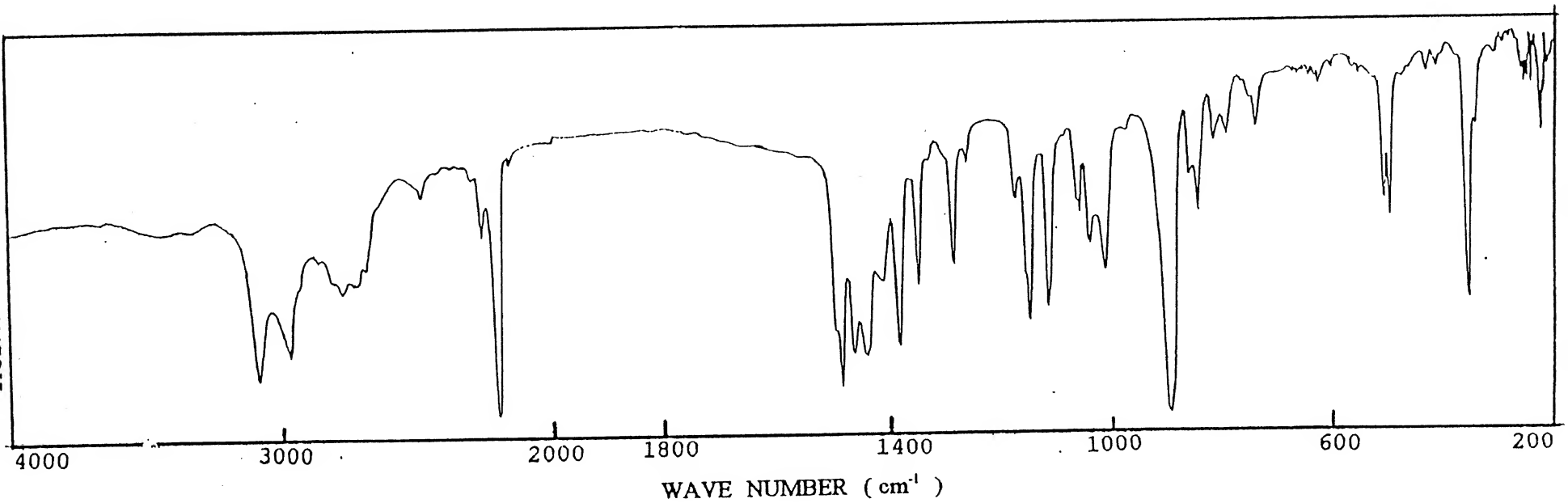

Fig.3.3 IR spectrum of $[Et_3NH]_2[Mo^{IV}O(mnt)_2]$

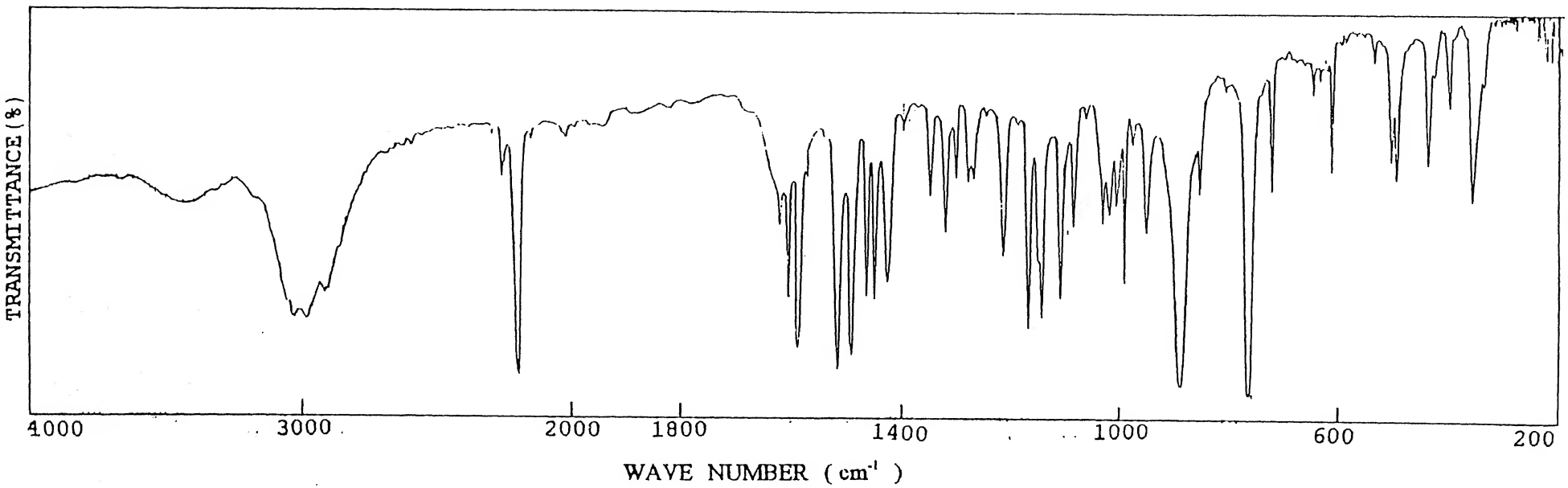

Fig.3.4 IR spectrum of $[BipyH]_2[M\overset{IV}{o}O(mnt)_2]$

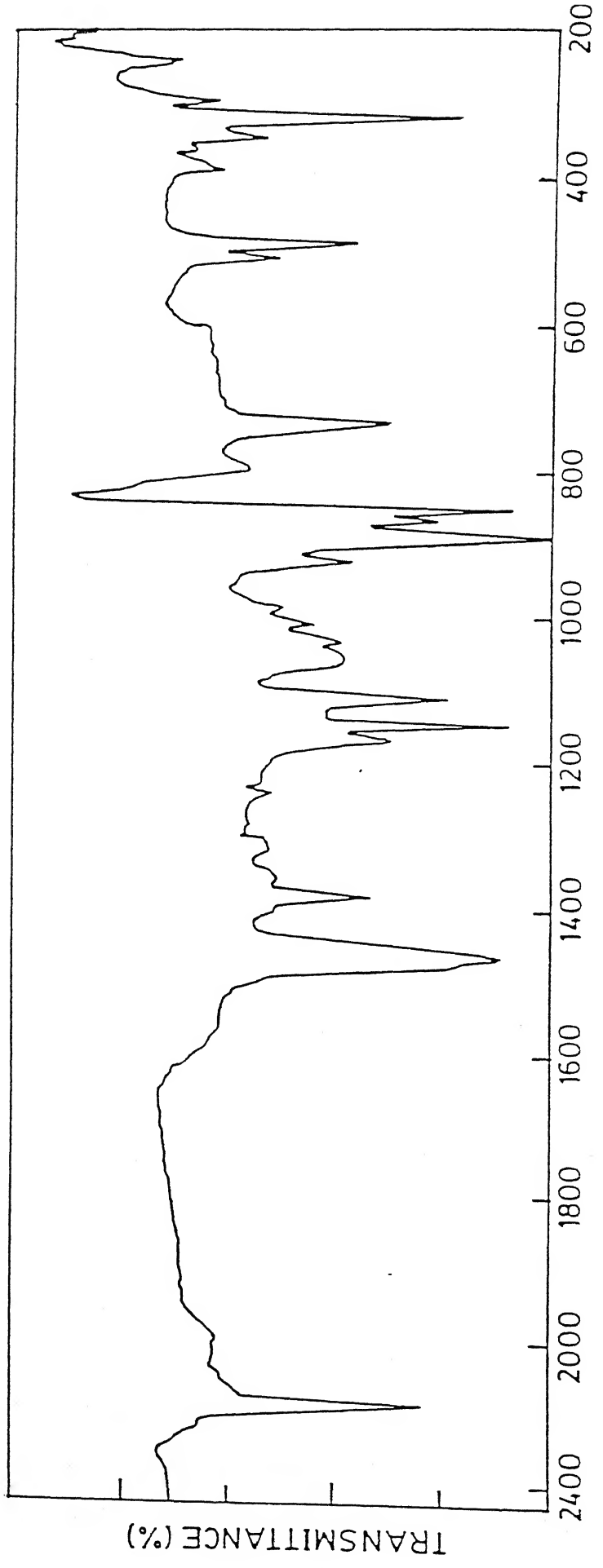

Fig.3.5 IR spectrum of $[Bu_4N]_2[Mo^{VI}O_2(mnt)_2]$

Similarly, identification of vibrations of the dimeric complexes having $Mo_2O_4^{2+}$ and $Mo_2O_3^{4+}$ core is also known.[88] Based on these assignments, the vibrations of the dinuclear complexes have been made which are tabulated in Table 3.2 and the corresponding IR spectra are reproduced in Figures 3.6 to 3.11.

3.2.2 ELECTRONIC SPECTROSCOPY:

Electronic spectra of the synthesized complexes are reproduced in Figures 3.14 to 3.21. Absorption maxima with molar extinction values are tabulated in Table 3.3.

The electronic spectra of the anion $[Mo^{IV}O(mnt)_2]^{2-}$ containing different counter cations like Et_4N^+, Et_3NH^+ and lysinium cation displayed interesting shift in the position of the absorption bands. The corresponding PyH^+ salt is not soluble in CH_2Cl_2, however, the electronic spectra of the salts containing Et_3NH^+ and Et_4N^+ cations in CH_2Cl_2 showed difference in the absorption spectra (Fig.3.15). However, these salts displayed identical electronic spectra in solvents like MeCN or Me_2CO. CH_2Cl_2 being a less polar solvent than these solvents may retain the hydrogen bonded interaction like Mo=O----H^+ which modified the electronic spectrum in this solvent. This hydrogen bond may possibly broken in more polar solvent like MeCN and Me_2CO. IR spectra in solid state already revealed the decrease in ν(Mo=O) in Et_3NH^+ (905 cm^{-1}) and PyH^+ (895 cm^{-1}) as compared to that of Et_4N^+ (938 cm^{-1}) salt. The corresponding lysinium salt which is soluble in water also showed similar shift of the absorption bands which may be due to the retention of the hydrogen bonded form. Menifestation of the existance of this hydrogen bonded form is also reflected in the

ble 3.2 IR (cm^{-1}) Spectral Data for Complexes[a]:

compound	ν(Mo=O)	ν(Mo-O_b)	ν(Mo-S)	ν(CN)	ν(Mo-X)[b]
$[MoO_2O_4(mnt)_2]^{2-}$	977vs 965w	730s 470m	360s	2210vs	----
$[MoO_2O_3(Br)_2(mnt)_2]^{2-}$	972vs	455w	366m	2210vs	335m
$[MoO_2O_3(Cl)_2(mnt)_2]^{2-}$	975vs	458m	366s	2215vs	355vs
$[MoO_2O_3(SPh)_2(mnt)_2]^{2-}$	955vs	462m	355s	2210vs	362s
$[MoO_2O_3(C_6H_4ClS)_2(mnt)_2]^{2-}$	955vs	460w	360w	2210vs	c
$[MoO_2O_3(bipy)_2(mnt)_2]$	962s 952vs	470w	358s	2210vs	c

as CsI pellet, vs = very strong, s = strong, m = medium, w = weak.

X = Cl, Br, S(Ph).

not measured.

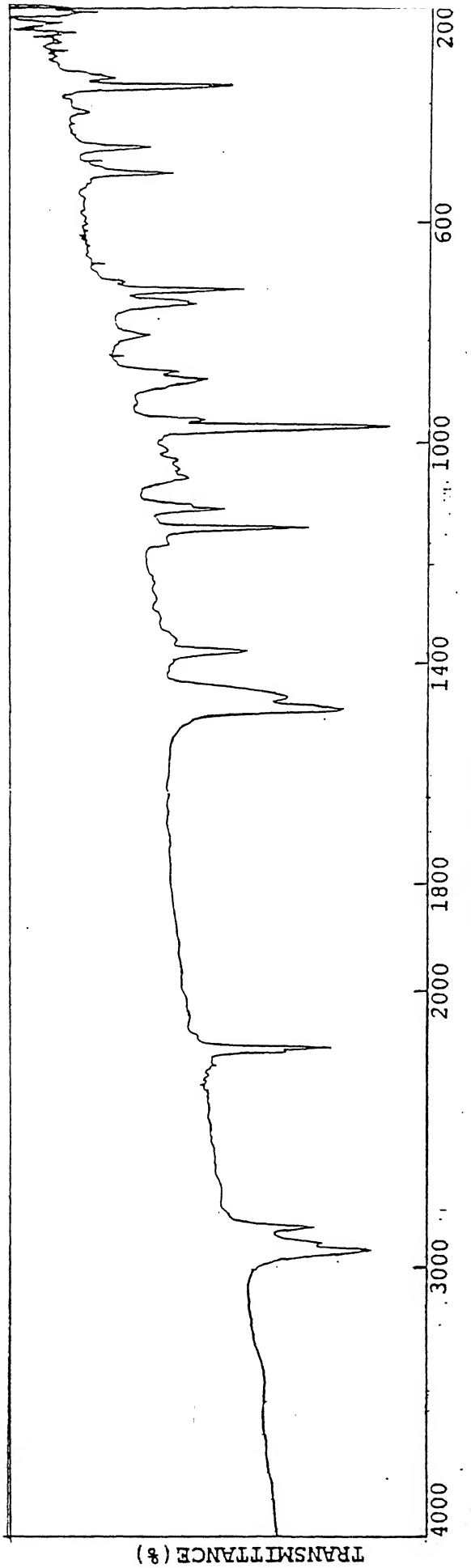

Fig.3.6 IR spectrum of $[Bu_4N]_2[MO_2^VO_4(mnt)_2]$

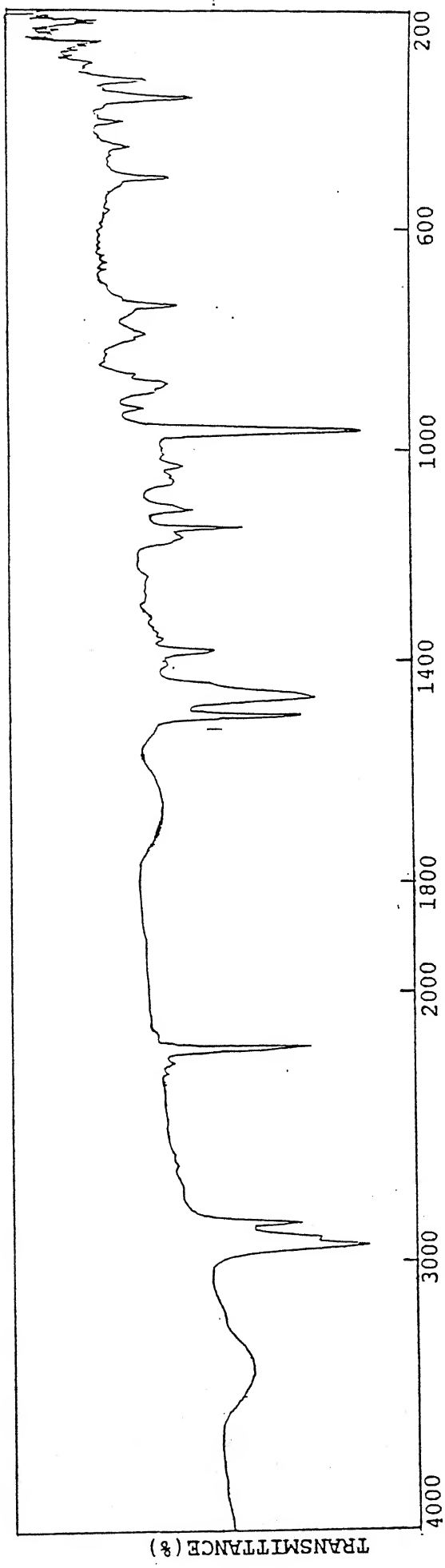

Fig.3.7 IR spectrum of $[Bu_4N]_2[Mo^{V}_2O_3(Br)_2(mnt)_2]$

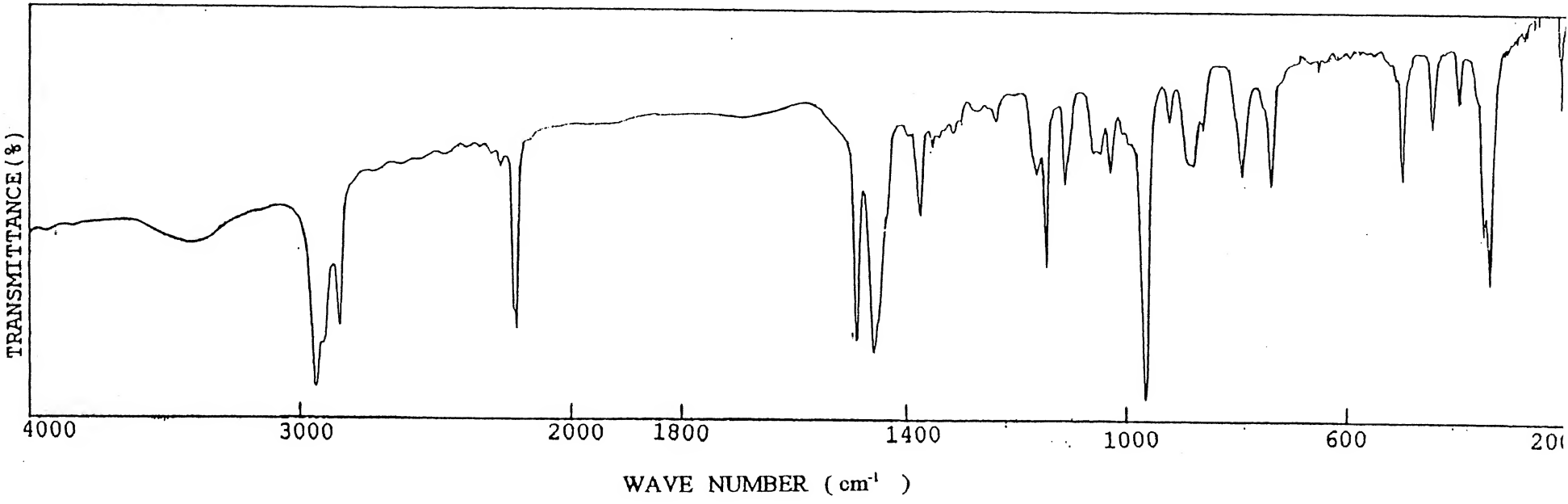

Fig.3.8 IR spectrum of $[Bu_4N]_2[Mo^{V}_2O_3(Cl)_2(mnt)_2]$

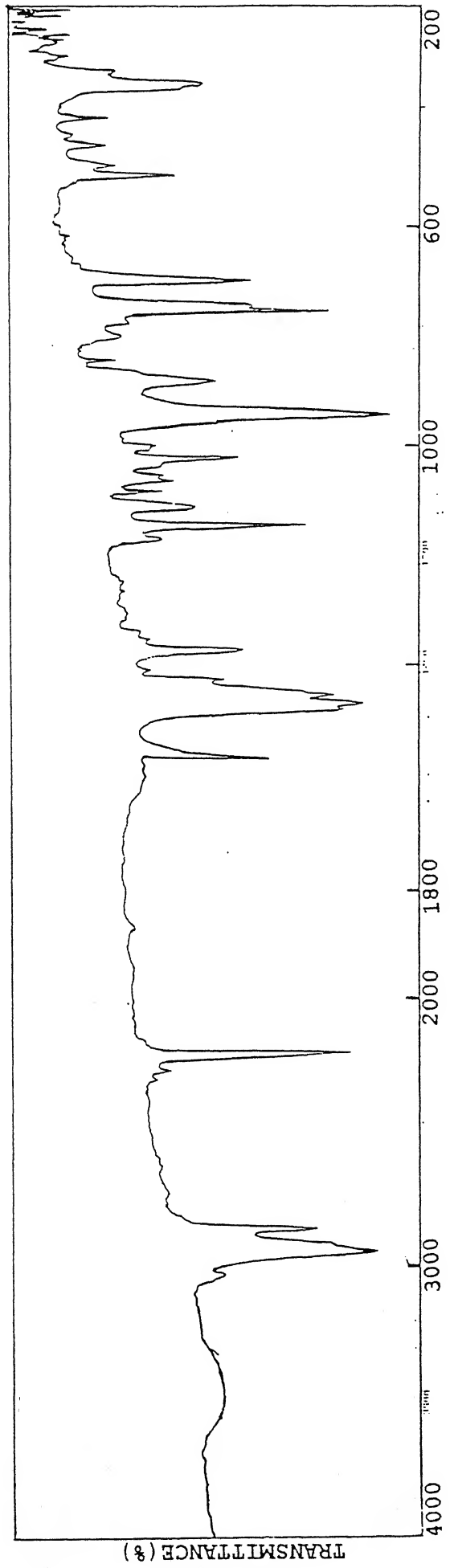

Fig.3.9 IR spectrum of $[Bu_4N]_2[\overset{V}{M}o_2O_3(SPh)_2(mnt)_2]$

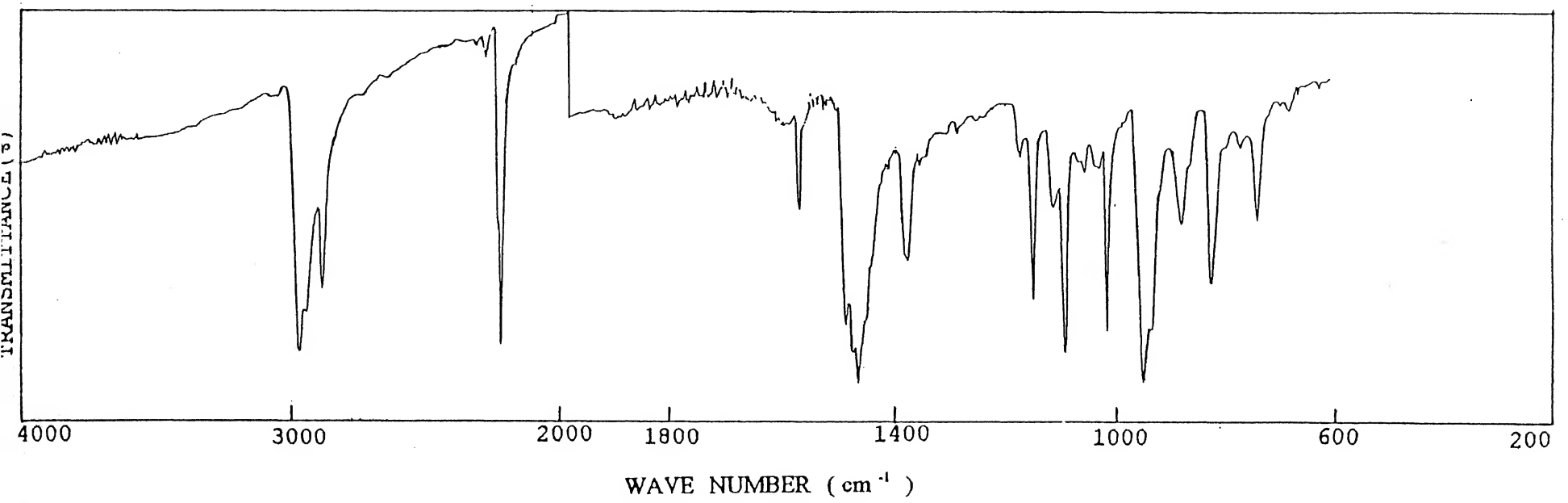

Fig.3.10 IR spectrum of $[Bu_4N]_2[Mo^{V}_2O_3(ClC_6H_4S)_2(mnt)_2]$

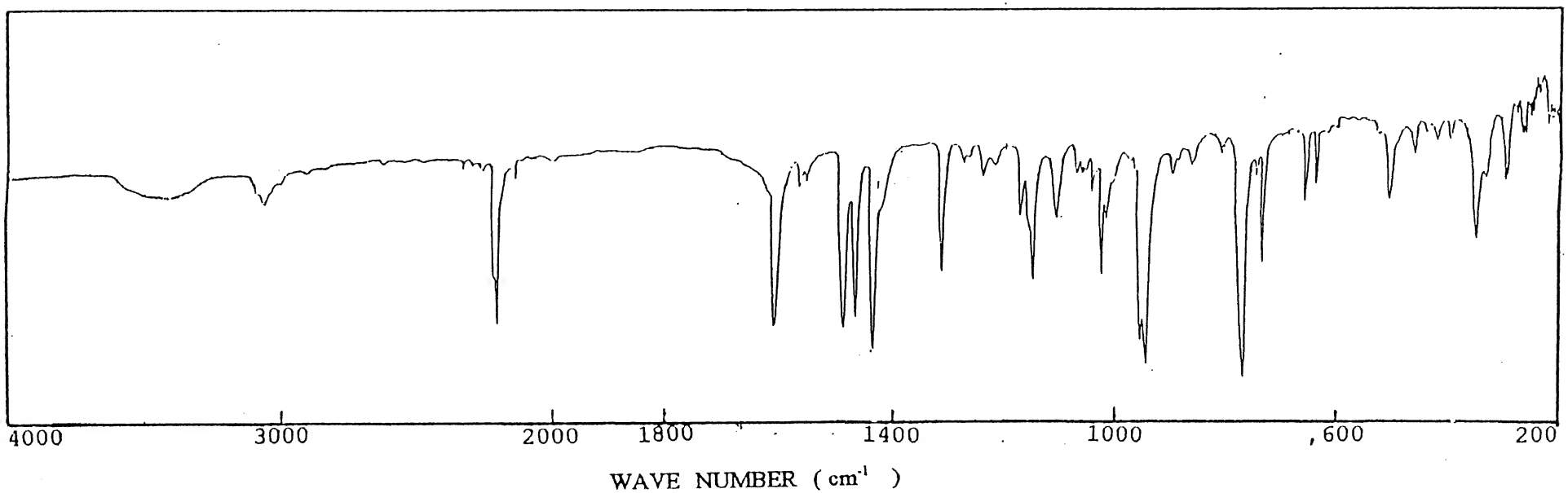

Fig.3.11 IR spectrum of $[Mo^{V}_{2}O_{3}(bipy)_{2}(mnt)_{2}]$

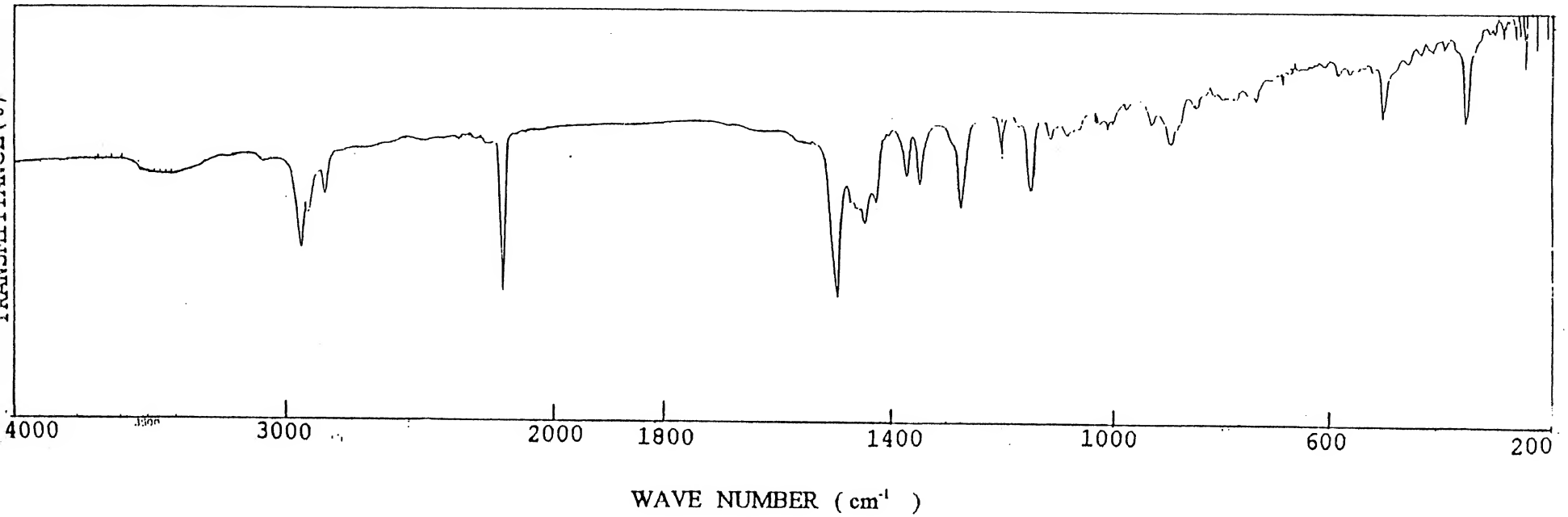

Fig.3.12 IR spectrum of $[Bu_4N][Mo^{IV}(dtc)(mnt)_2]$

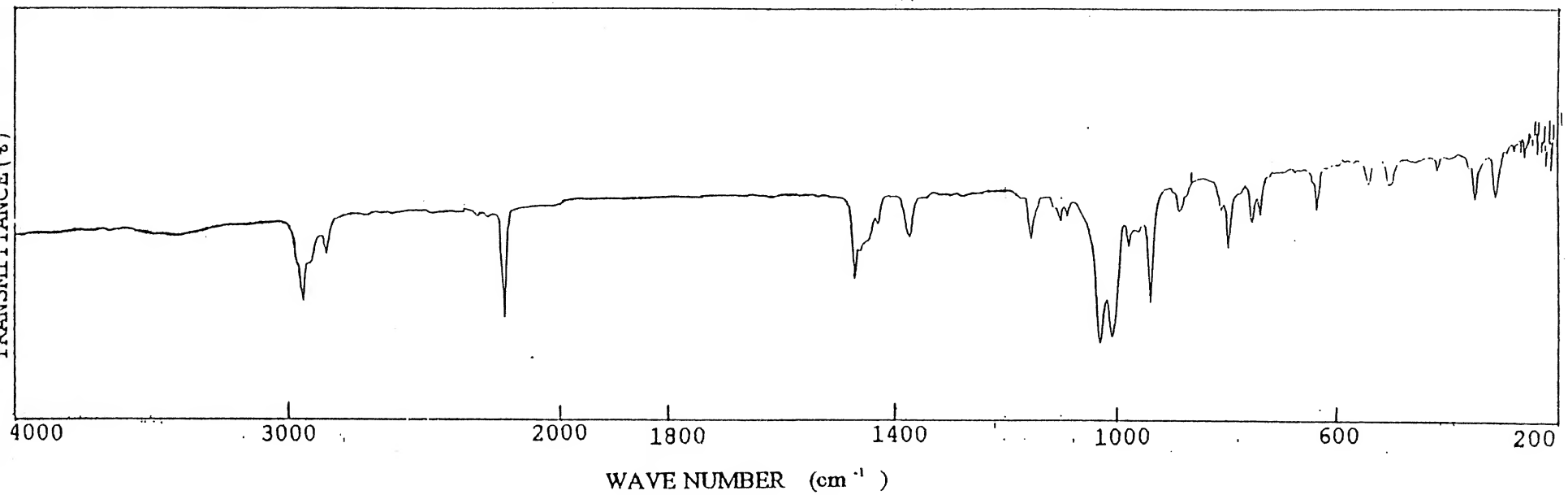

Fig.3.13 IR spectrum of $[Bu_4N][Mo^{IV}(dtp)(mnt)_2]$

ıble 3.3 UV-visible Spectroscopic Data for Complexes[a]

ɔmplexes	λ_{max}, (nm.) (ε, $M^{-1}cm^{-1}$)	Solvent Used
$fo_2O_4(mnt)_2]^{2-}$	357 (10660)	CH_2Cl_2
$fo_2O_3(Br)_2(mnt)_2]^{2-}$	587 (7910), 480 (16530), 377 (sh)	CH_2Cl_2
$fo_2O_3(Cl)_2(mnt)_2]^{2-}$	583 (7940), 477 (15950), 375 (sh)	CH_2Cl_2
$fo_2O_3(SPh)_2(mnt)]^{2-}$	590 (sh), 475 (sh), 400 (sh), 358 (7840)	CH_2Cl_2
$fo_2O_3(ClC_6H_4S)_2(mnt)_2]^{2-}$	580 (sh), 465 (sh), 396 (9450), 360 (9510)	CH_2Cl_2
$fo_2O_3(bipy)_2(mnt)_2]^{2-}$	580 (sh), 498 (9840), 380 (sh), 368 (7330)	DMF
$C_2H_5)_3NH]_2[MoO(mnt)_2]$	600 (170), 475 (sh), 397 (sh), 363 (7340)	CH_2Cl_2
$C_2H_5)_4N]_2[MoO(mnt)_2]$	610 (140), 496 (160), 395 (sh), 366 (8250)	CH_2Cl_2
$'_6H_{15}N_2O_2]_2[MoO(mnt)_2]$	589 (440), 470(sh), 359 (10920)	H_2O
$'h_4P]_2[MoO_2(mnt)_2]$	530 (1610), 423 (7620), 367 (6540)	CH_3CN
$fo(dtc)(mnt)_2]^-$	532 (4980), 487 (5590), 364 (6260)	CH_2Cl_2
$fo(dtp)(mnt)_2]^-$	550 (sh), 516 (5250), 365 (6520)	CH_2Cl_2

:oncentration taken 1 x 10^{-4}M.

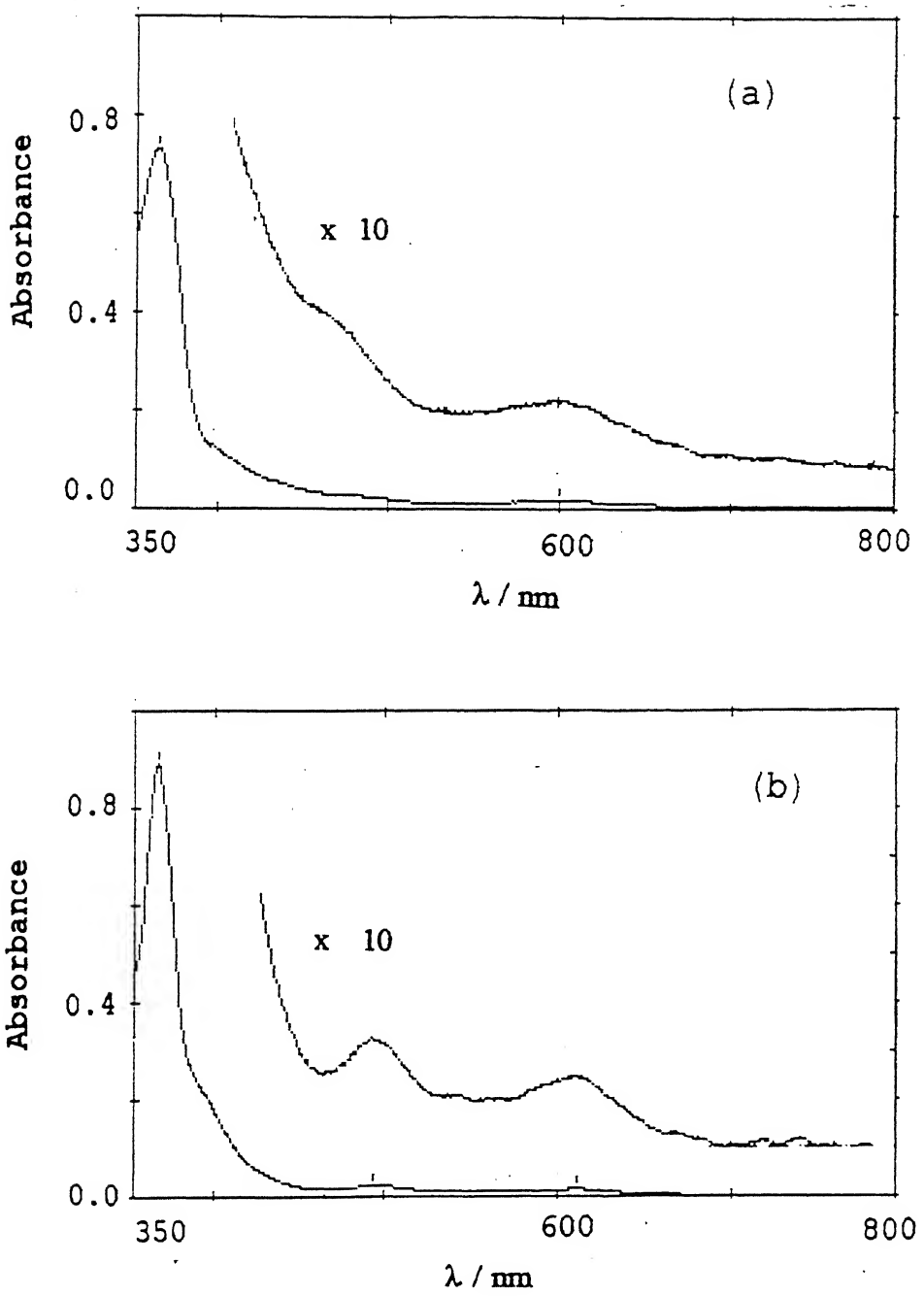

ig.3.14(a) UV-visible absorption spectra of $[Et_3NH]_2[Mo^{IV}O(mnt)_2]$ n CH_2Cl_2, Conc. $1x10^{-4}M$

(b) UV-visible absorption spectra of $[Et_4N]_2[Mo^{IV}O(mnt)_2]$ n CH_2Cl_2, Conc. $1x10^{-4}M$

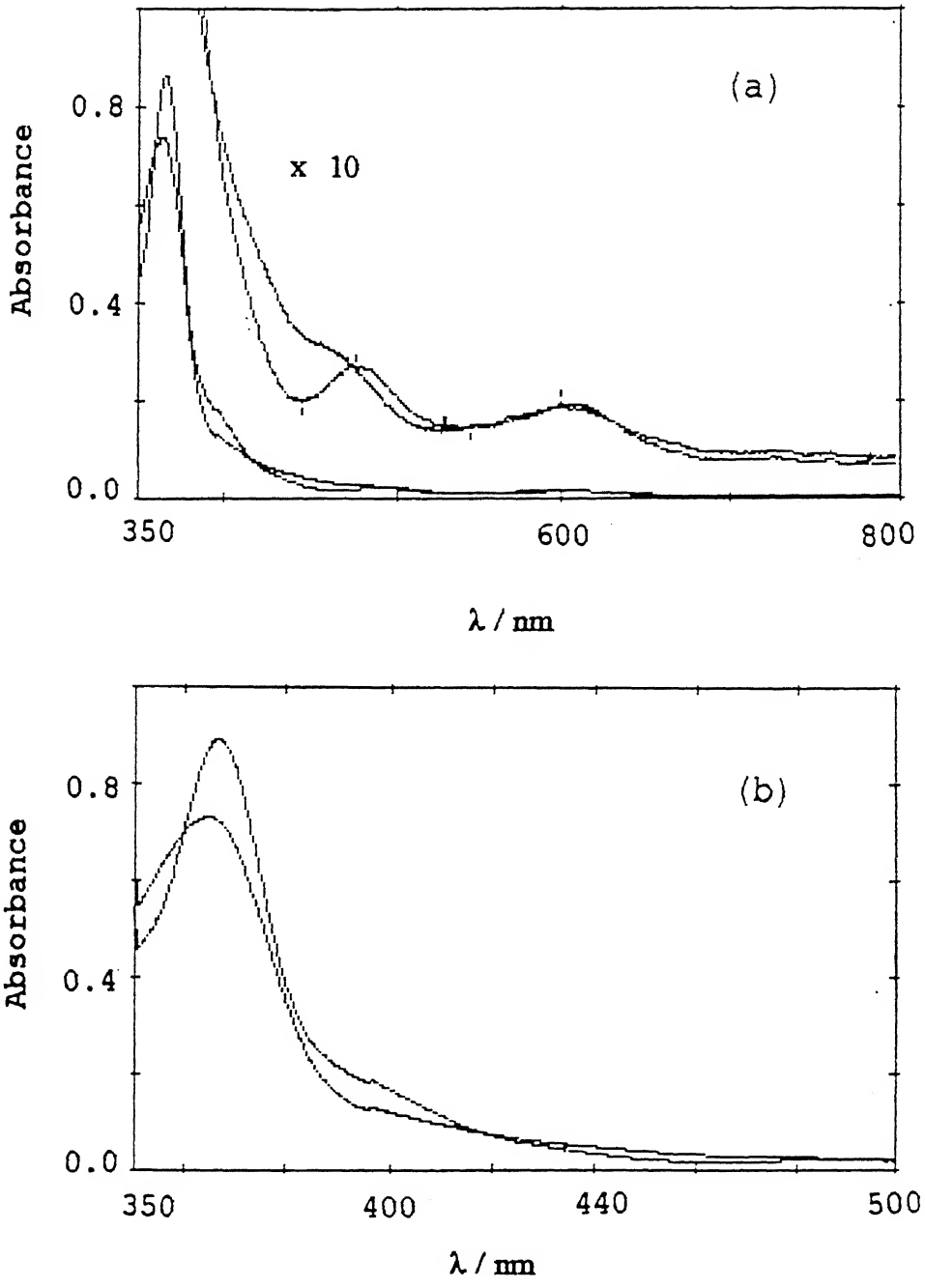

Fig.3.15 Superimposed UV-visible absorption spectra of $[Et_3NH]_2[Mo^{IV}O(mnt)_2]$ (1) and $[Et_4N]_2[Mo^{IV}O(mnt)_2]$ (2) in CH_2Cl_2, Conc. are $1x10^{-4}$M. **(a)** for d-d bands, **(b)** for charge transfer bands.

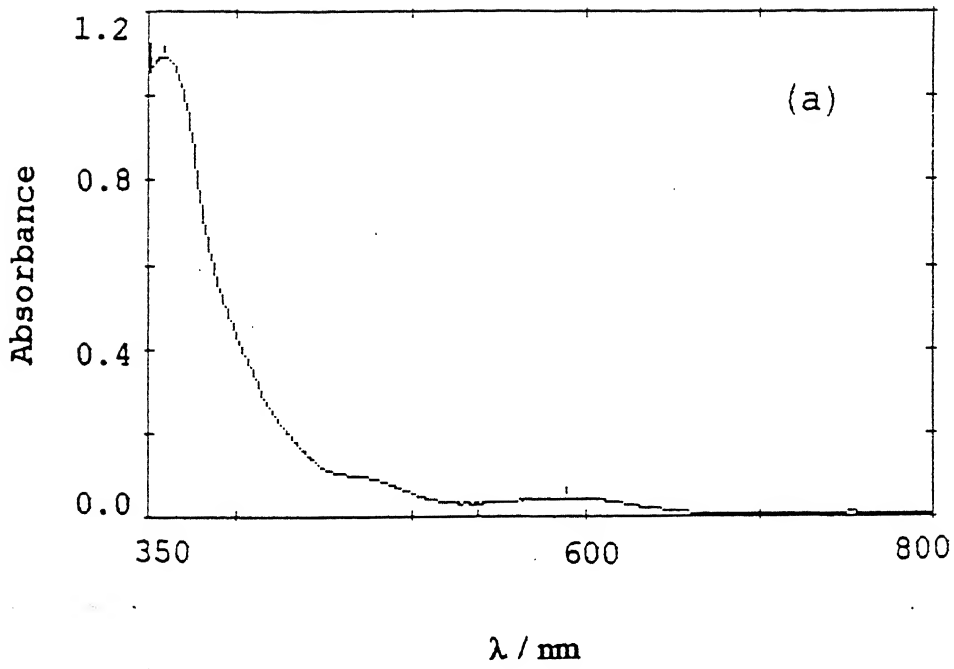

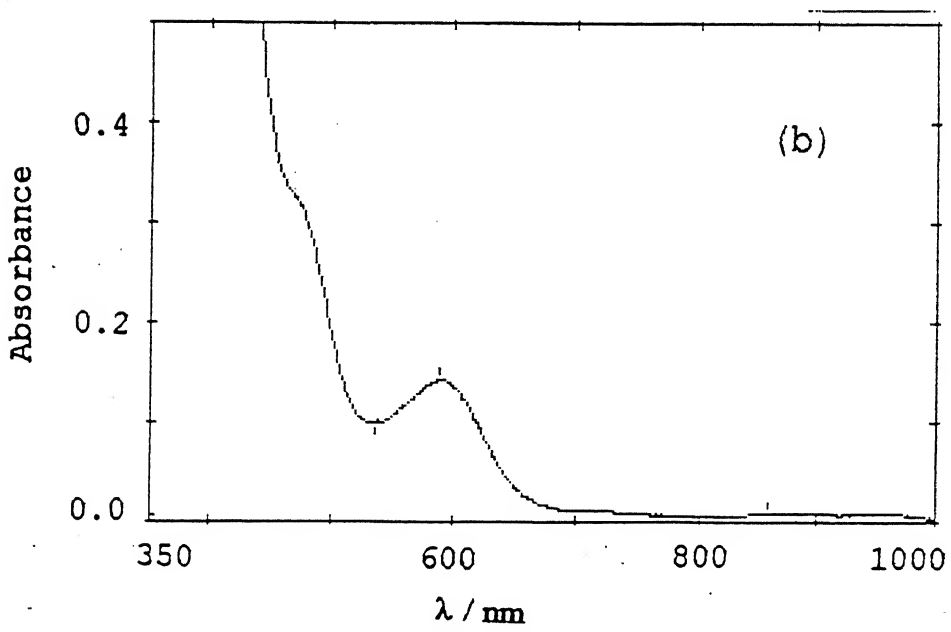

Fig.3.16(a) UV-visible absorption spectra of $[Lysinium]_2$-$[Mo^{IV}O(mnt)_2]$ in H_2O, Conc. $1x10^{-4}M$. **(b)** for d-d bands.

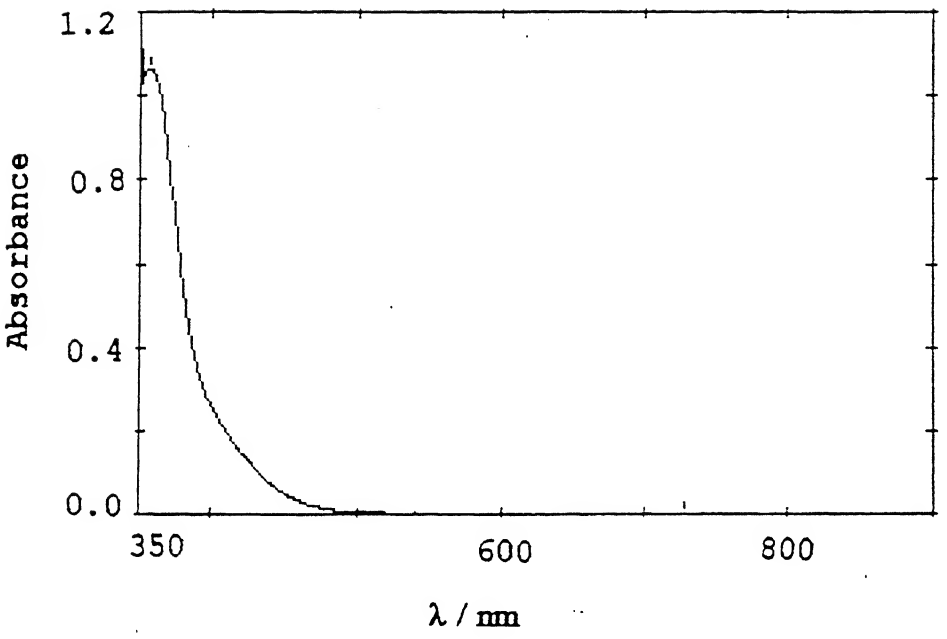

Fig.3.17 UV-visible absorption spectra of $[Bu_4N]_2[Mo^V_2O_4(mnt)_2]$ in CH_2Cl_2, Conc. $1x10^{-4}M$.

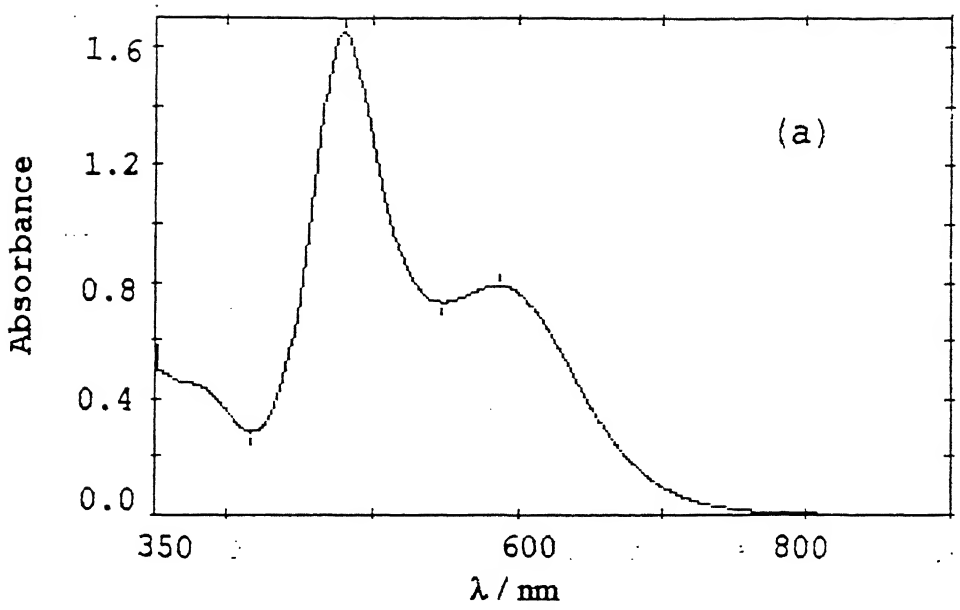

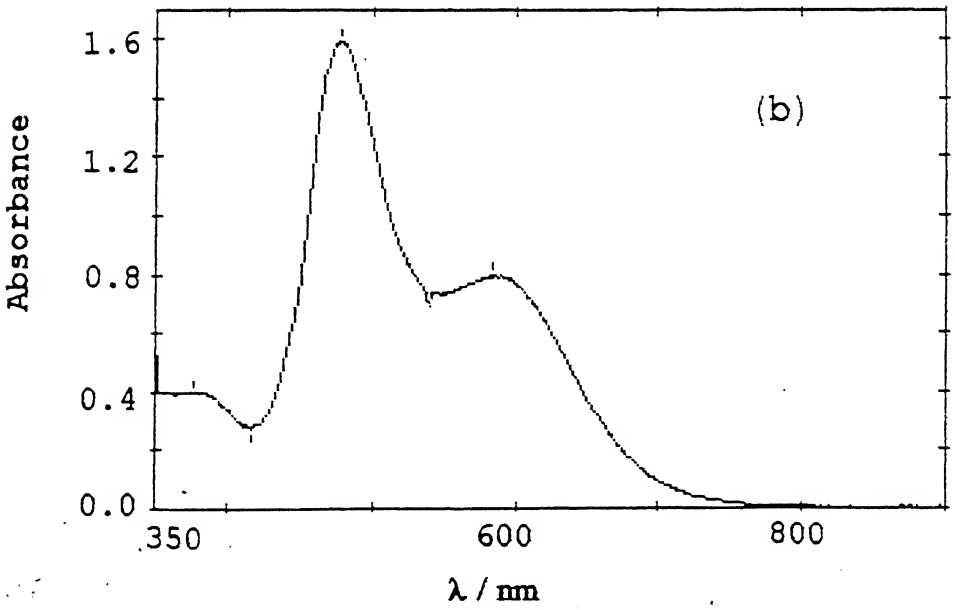

Fig.3.18 UV-visible absorption spectra of $[Bu_4N]_2[Mo^{V}_2O_3(Br)_2(mnt)_2]$ (a), and that of $[Bu_4N]_2[Mo^{V}_2O_3(Cl)_2(mnt)_2]$ (b), in CH_2Cl_2, Conc. $1x10^{-4}$M for both the compounds.

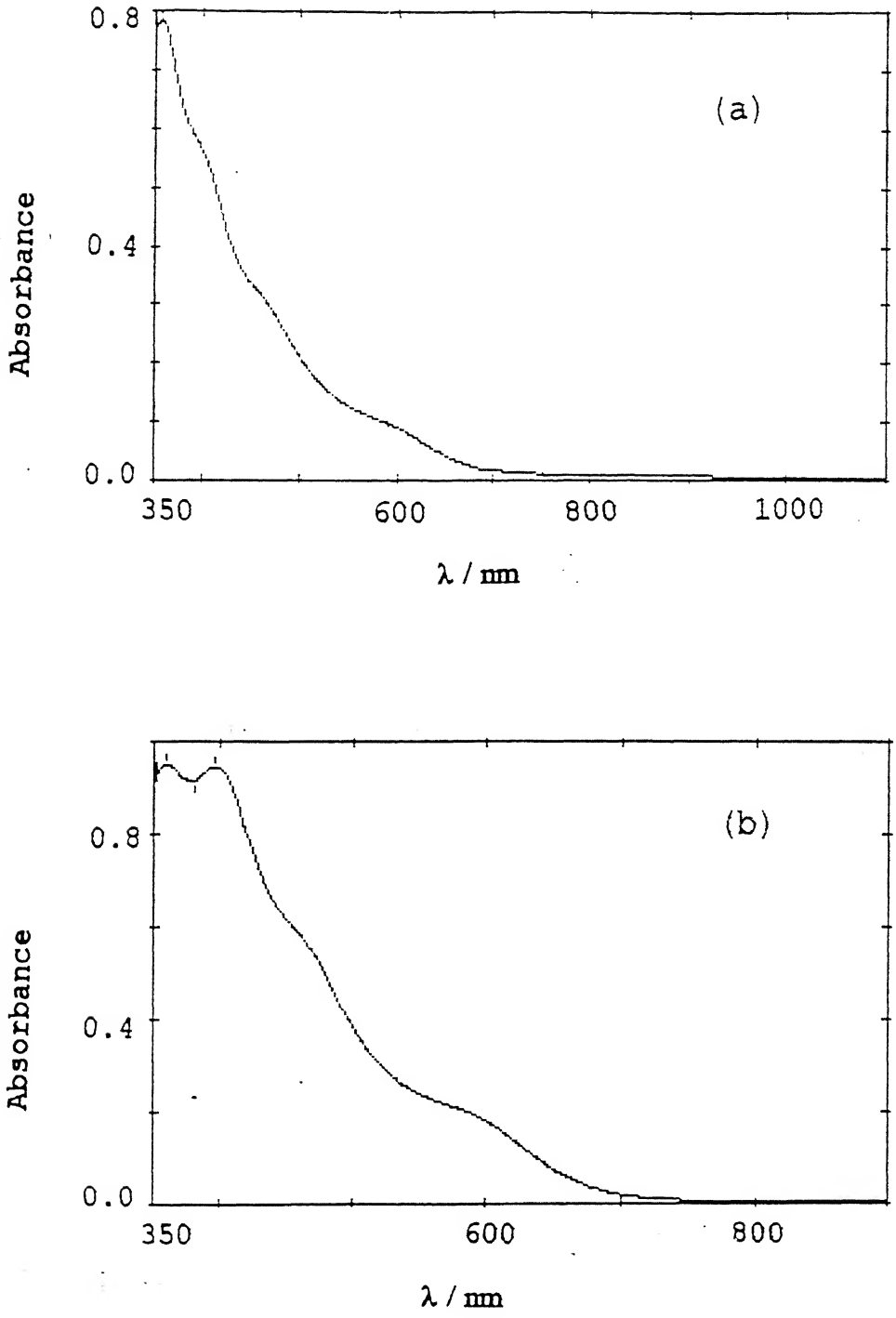

Fig.3.19 (a)UV-visible absorption spectra of $[Bu_4N]_2$-$[Mo^{V}_2O_3(SPh)_2(mnt)_2]$ in CH_2Cl_2, Conc. $1x10^{-4}$M, in presence of 10% PhSH, (b) that of $[Bu_4N]_2[Mo^{V}_2O_3(ClC_6H_4S)_2(mnt)_2]$ in CH_2Cl_2.

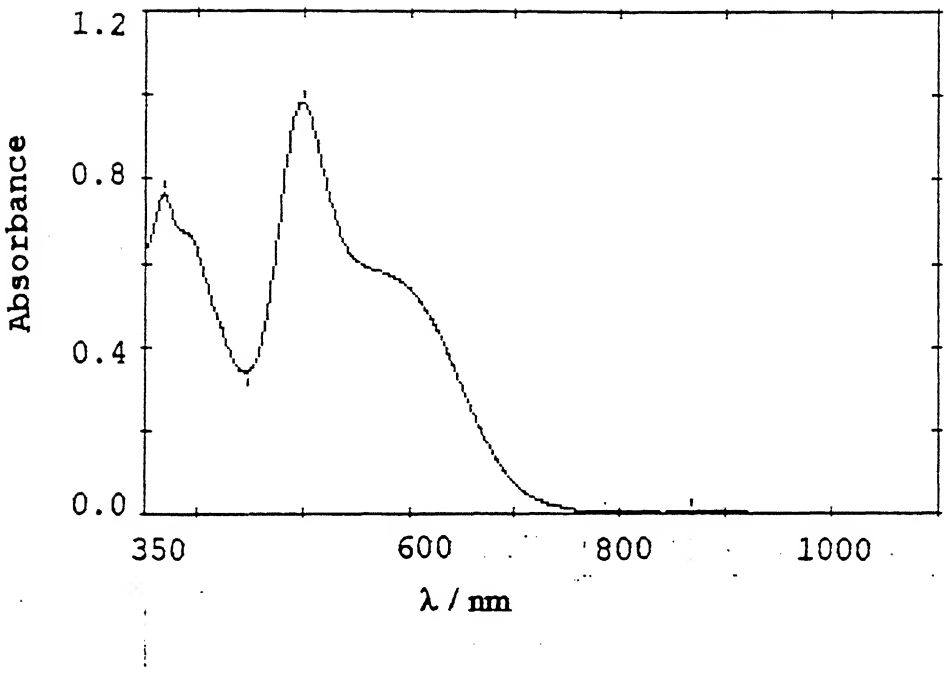

Fig.3.20 UV-visible absorption spectra of $[Mo^{V}_{2}O_{3}(bipy)_{2}(mnt)_{2}]$ in DMF, Conc. $1x10^{-4}$M.

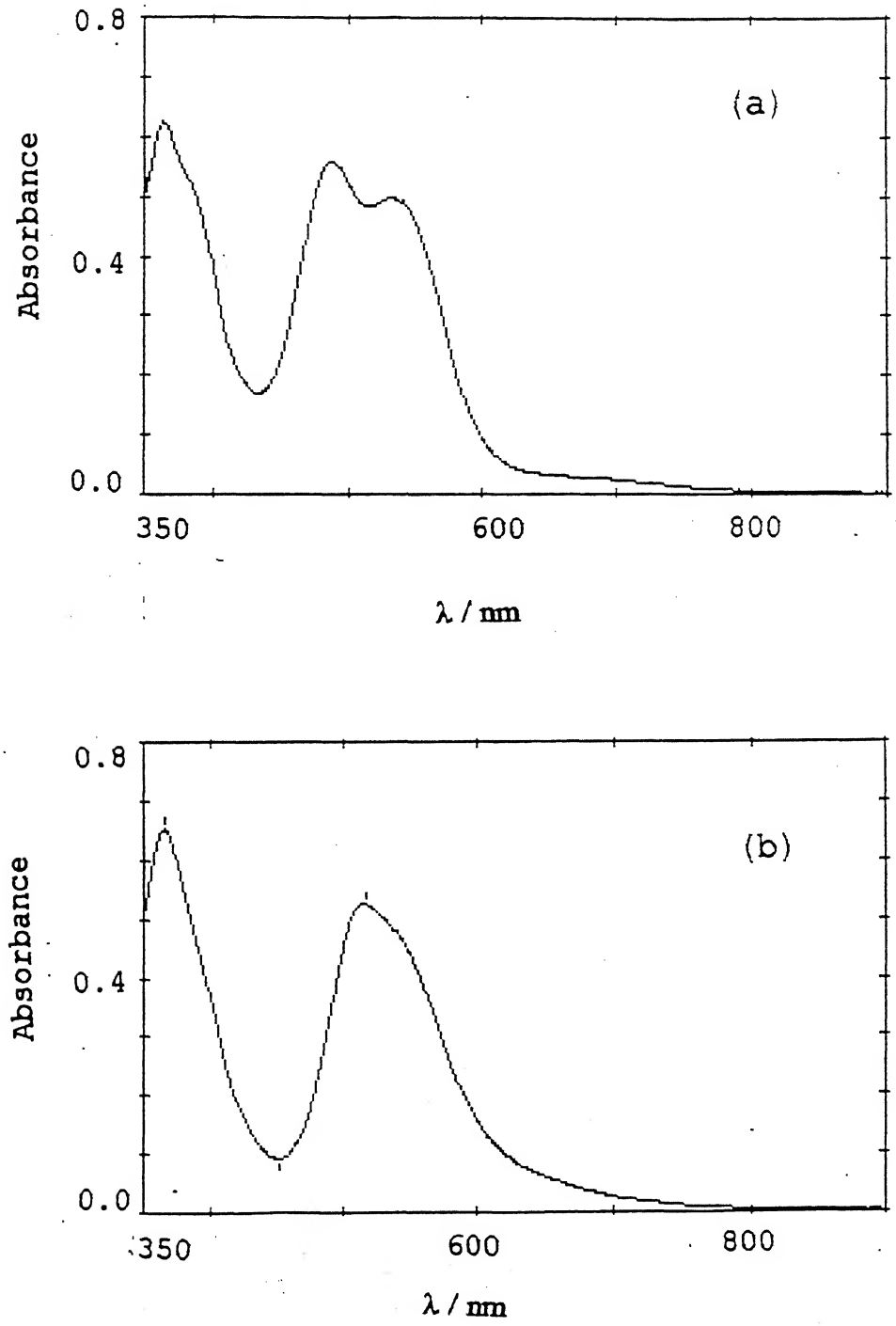

Fig.3.21 (a)UV-visible absorption spectra of $[Bu_4N][Mo^{IV}(dtc)(mnt)_2]$ and (b) that of $[Bu_4N][Mo^{IV}(dtp)(mnt)_2]$ in CH_2Cl_2, Conc. $1x10^{-4}$M.

corresponding electrochemical studies of these compounds (*vide infra*). Confirmation of the hydrogen bonded structure has been done by single crystal X-ray studies (*vide infra*).

3.2.3 FAB MASS SPECTROSCOPY:

Negative ion FAB mass spectra of the complexes can be divided into two parts: a "lower part" (M/Z < 350) where the matrix including their fragment ions, and some fragments of molecular anion can be observed and an "upper part" (M/Z > 350) with characteristic multiplet of mononuclear or dinuclear units. The negetive ion FAB mass spectra of the complexes are presented in Figures 3.22 to 3.29. In Figure 3.22 the complex $[Et_3NH]_2[M\overset{IV}{o}O(mnt)_2]$ appears as molecular anion $[MoO(mnt)_2]^{2-}$ (M/Z = 393). In Figure 3.23 the complex $[Bu_4N]_2[Mo_2O_4(mnt)_2]$ appears as molecular anion $[Mo_2O_4(mnt)_2]^{2-}$ (M/Z = 537) and as the ion pair $[Bu_4N][Mo_2O_4(mnt)_2]^-$ (M/Z = 778). There are also some peaks due to the fragmentation of the dinuclear molecular anion, these are assigned as $[Mo_2O_6(mnt)]^{4-}$ (M/Z = 429), and $[MoO(mnt)_2]^{2-}$ (M/Z = 394). In Figure 3.24 the complex, $[Bu_4N]_2[Mo_2O_3(Br)_2(mnt)_2]$, is not appeared as the molecular anion but the ion pair $[Bu_4N][Mo_2O_3(Br)_2(mnt)_2]^-$ (M/Z = 922) is observed. The abundance of this ion pair form is low which is due to its instability in FAB mass experimental condition. There are peaks for other fragmented anions which are assigned as $[MoOBr(mnt)_2]^-$ (M/Z = 470), $[Mo_2O_3Br(mnt)_2]^-$ (M/Z = 600), $[Mo_2O_4(mnt)_2]^{2-}$ (M/Z = 537), $[Bu_4N][Mo_2O_4(mnt)_2]^-$ (M/Z = 778) and $[MoO(mnt)_2]^{2-}$.The abundance of last three peaks showed the unstable nature of the compound and which can easily convert to stable dimeric $Mo_2O_4^{2+}$ or monomeric

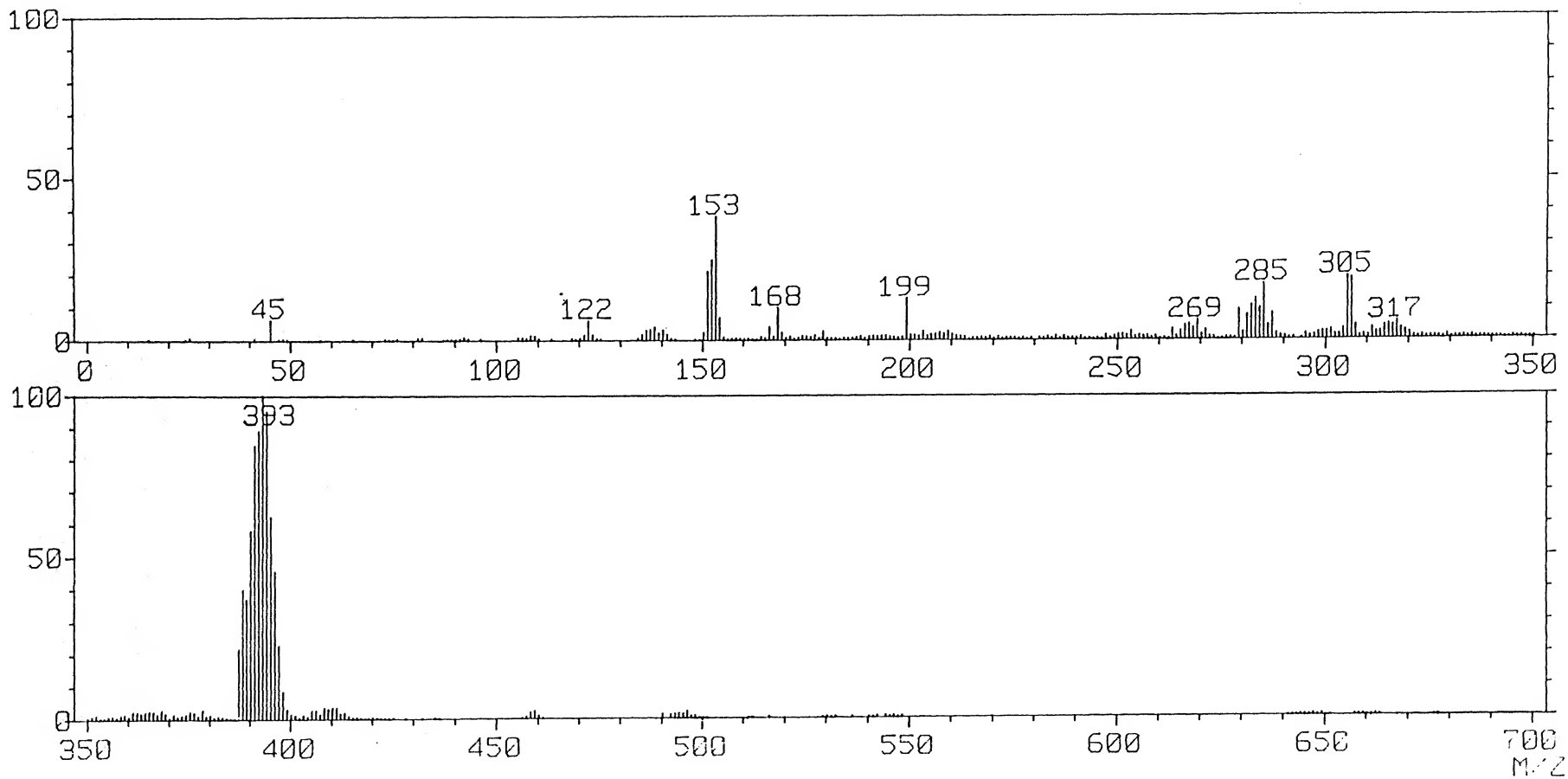

Fig.3.22 Negative ion FAB mass spectra of $[Et_3NH]_2[Mo^{IV}O(mnt)_2]$

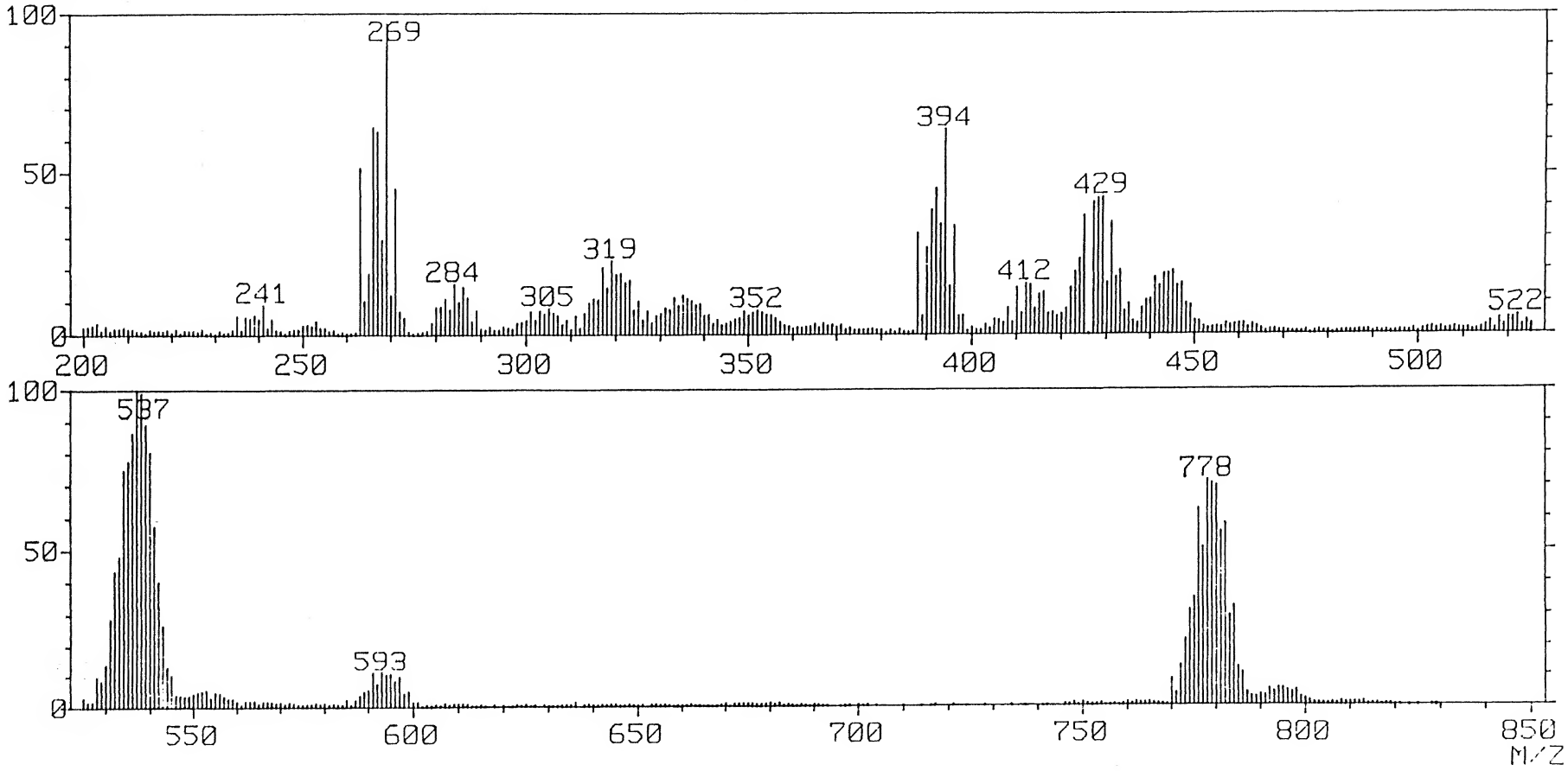

Fig.3.23 Negative ion FAB mass spectra of $[Bu_4N]_2[Mo^{V}_2O_4(mnt)_2]$

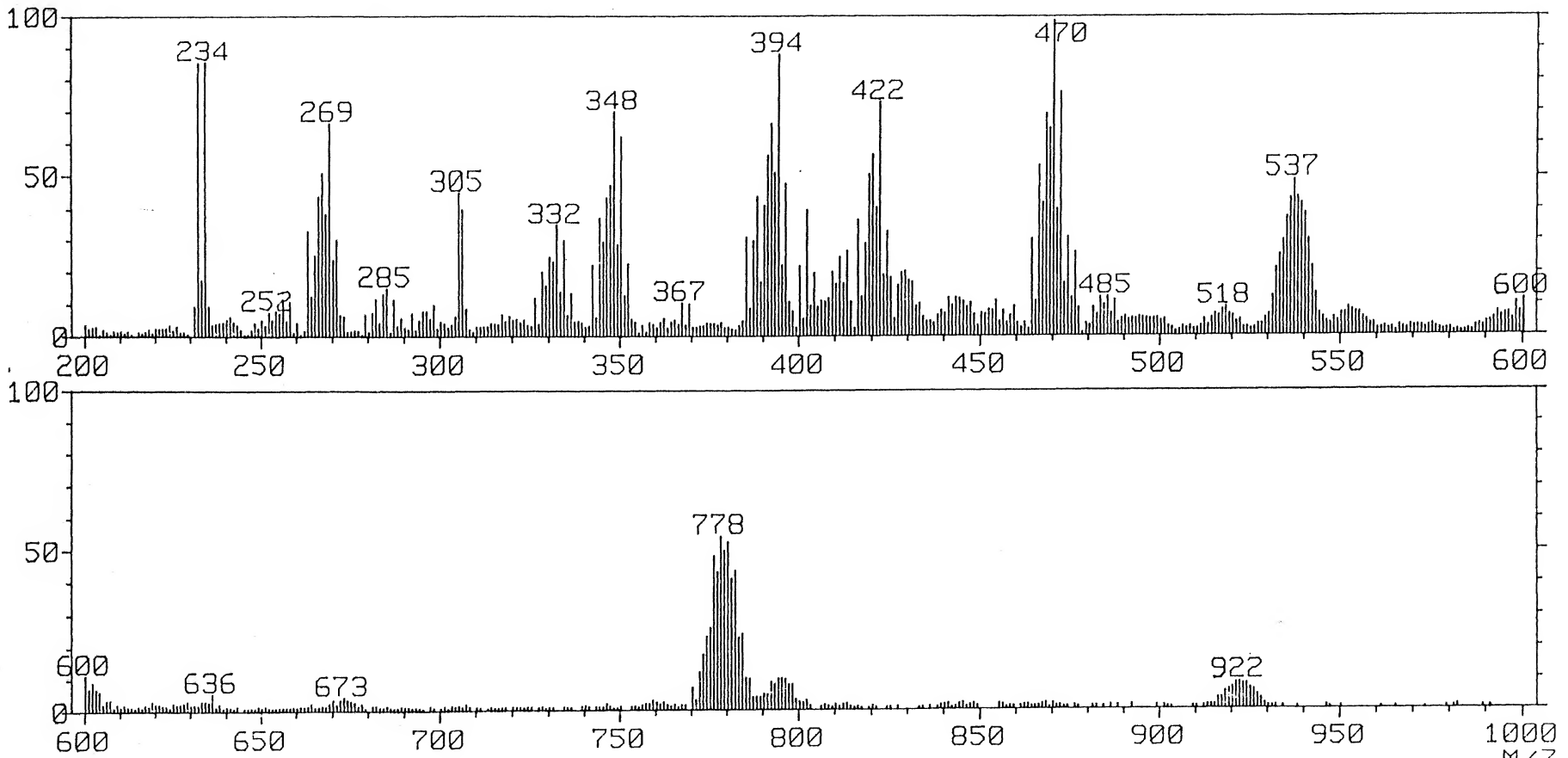

Fig.3.24 Negative ion FAB mass spectra of $[Bu_4N]_2$-$[Mo^{V}_2O_3(Br)_2(mnt)_2]$

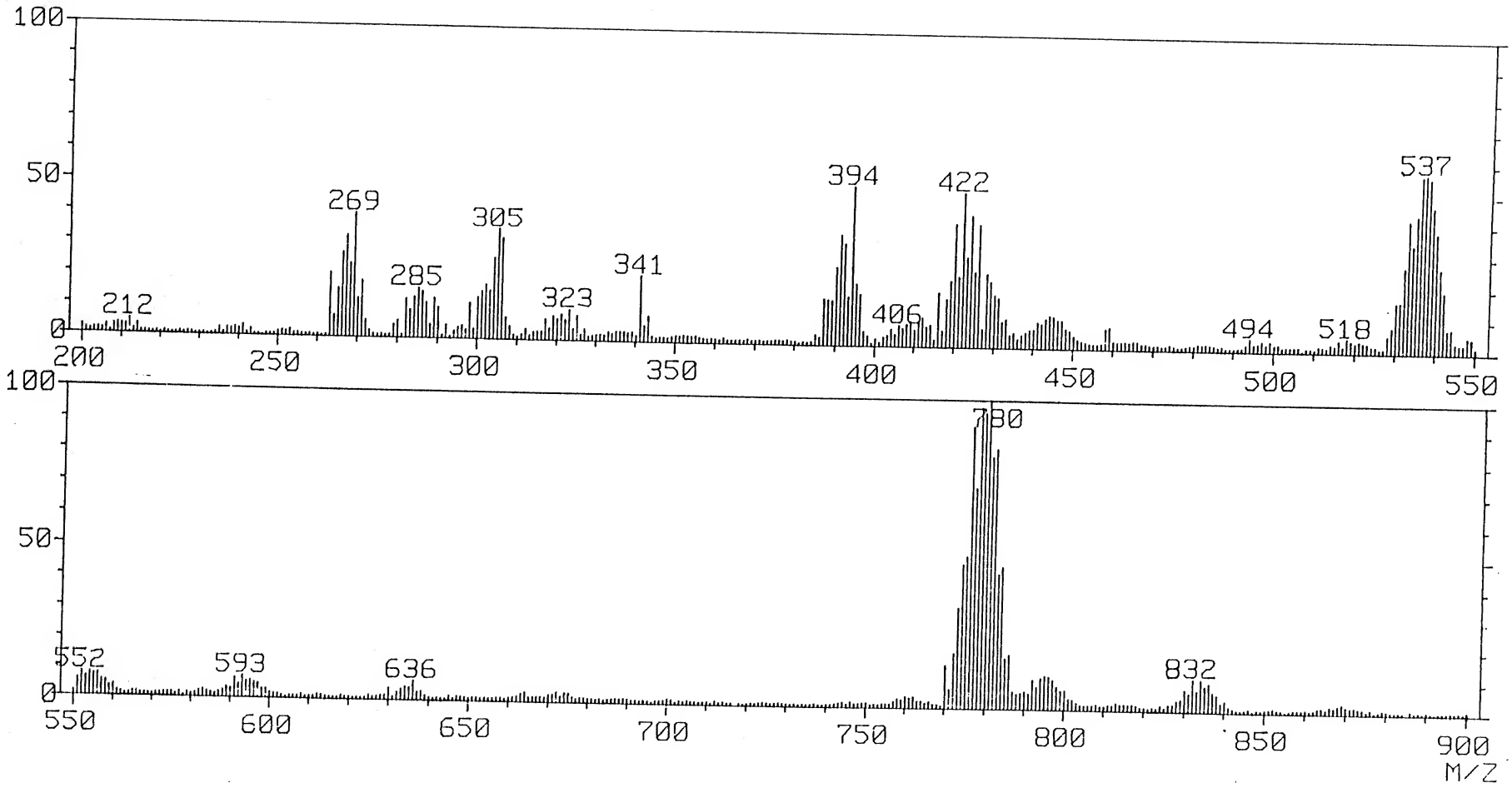

Fig.3.25 Negative ion FAB mass spectra of $[Bu_4N]_2$-$[Mo^{V}_2O_3(Cl)_2(mnt)_2]$

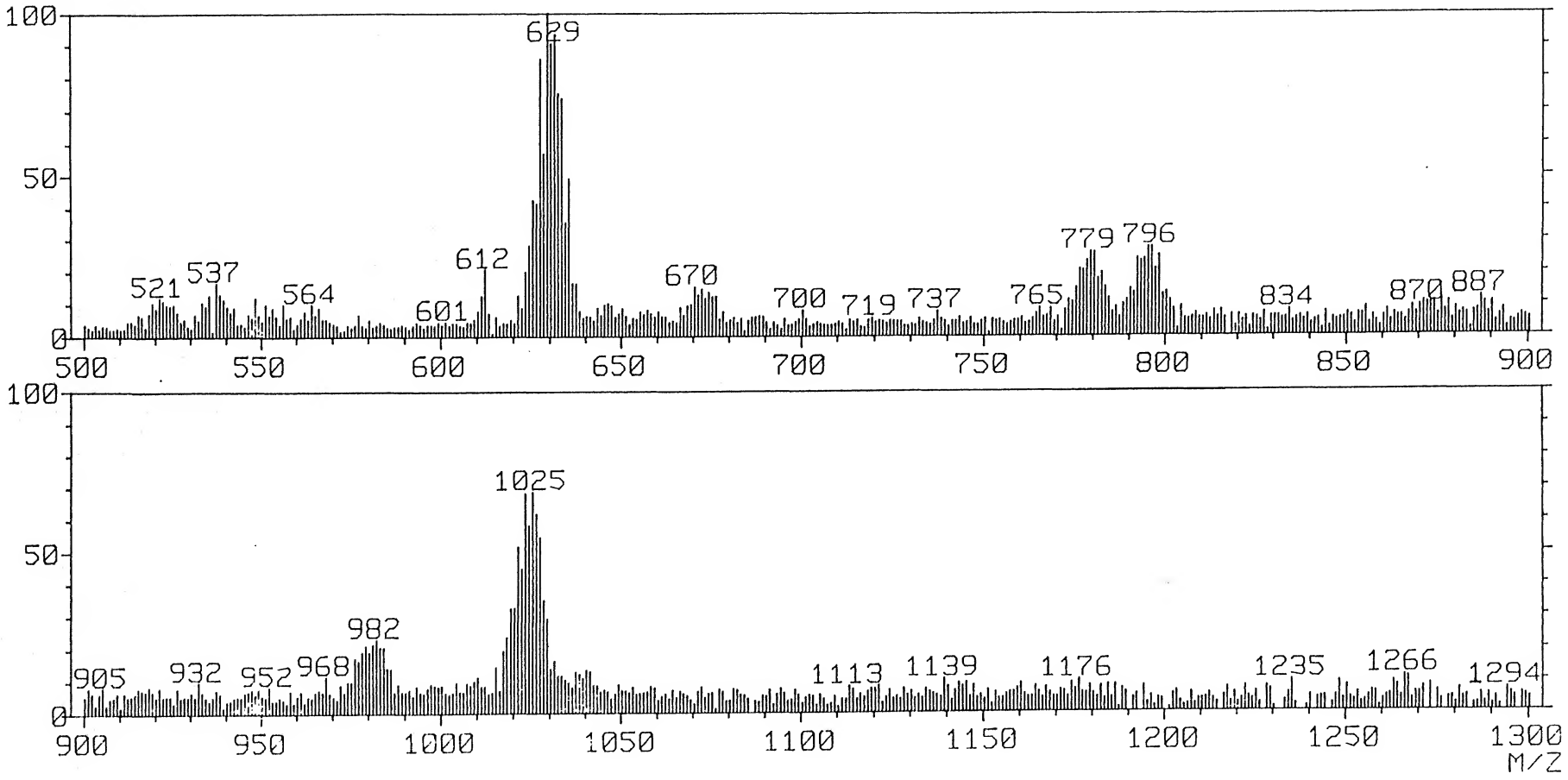

Fig.3.26 Negative ion FAB mass spectra of $[Bu_4N]_2$-$[Mo^{V}_2O_3(SPh)_2(mnt)_2]$

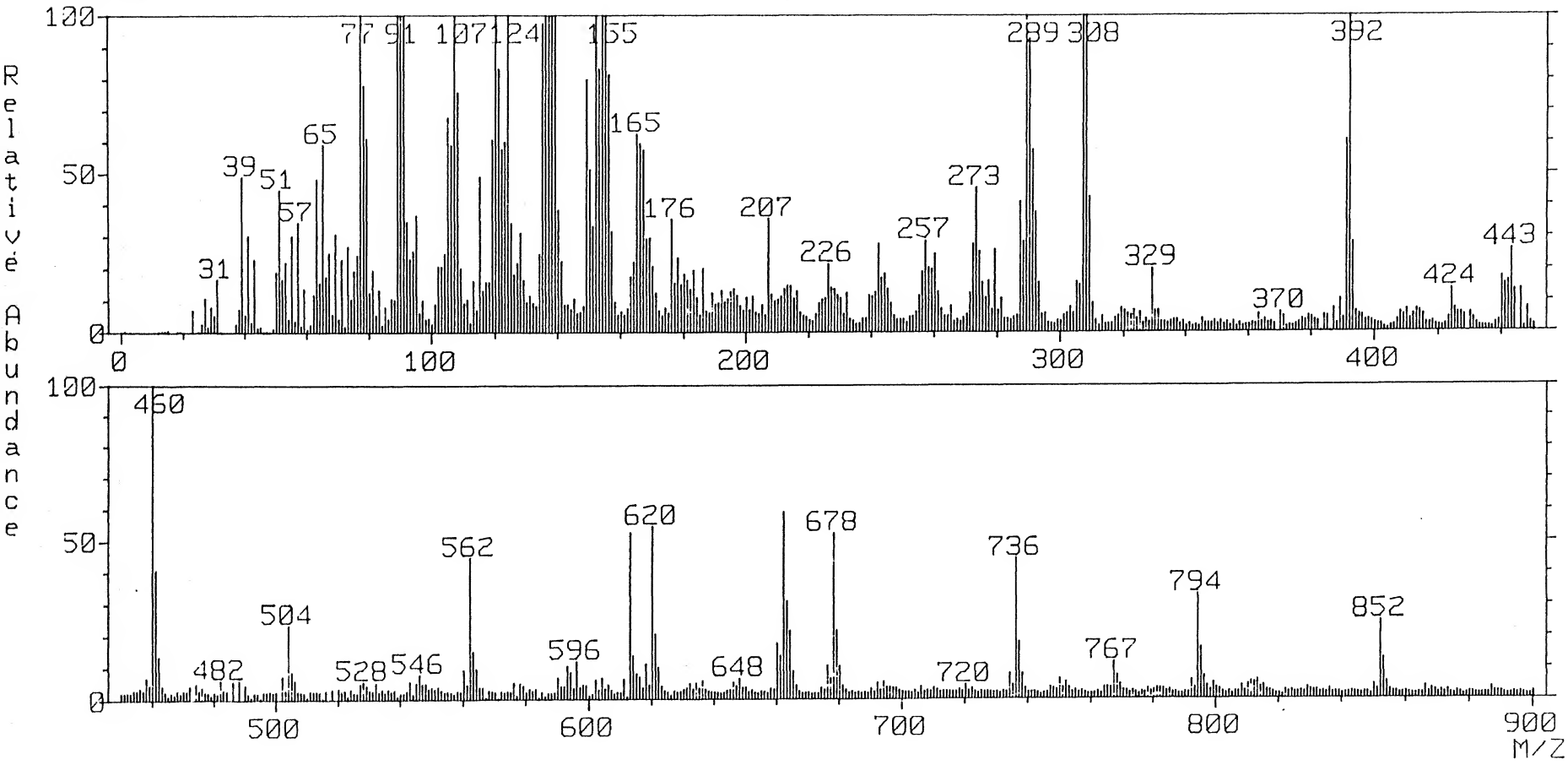

Fig.3.27 Negative ion FAB mass spectra of $[Mo^{V}_{2}O_{3}(bipy)_{2}(mnt)_{2}]$

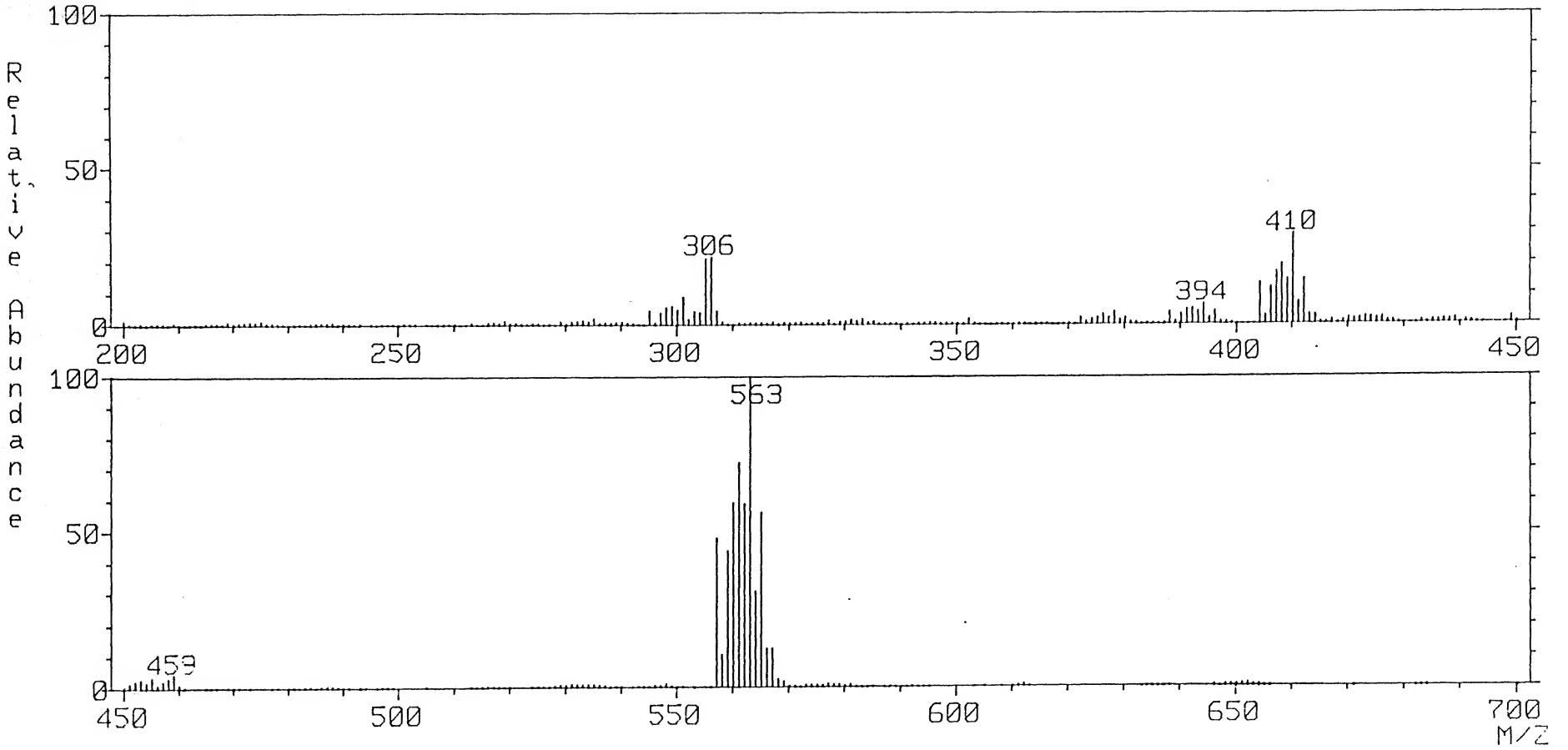

Fig.3.28 Negative ion FAB mass spectra of $[Bu_4N][Mo^{IV}(dtp)(mnt)_2]$

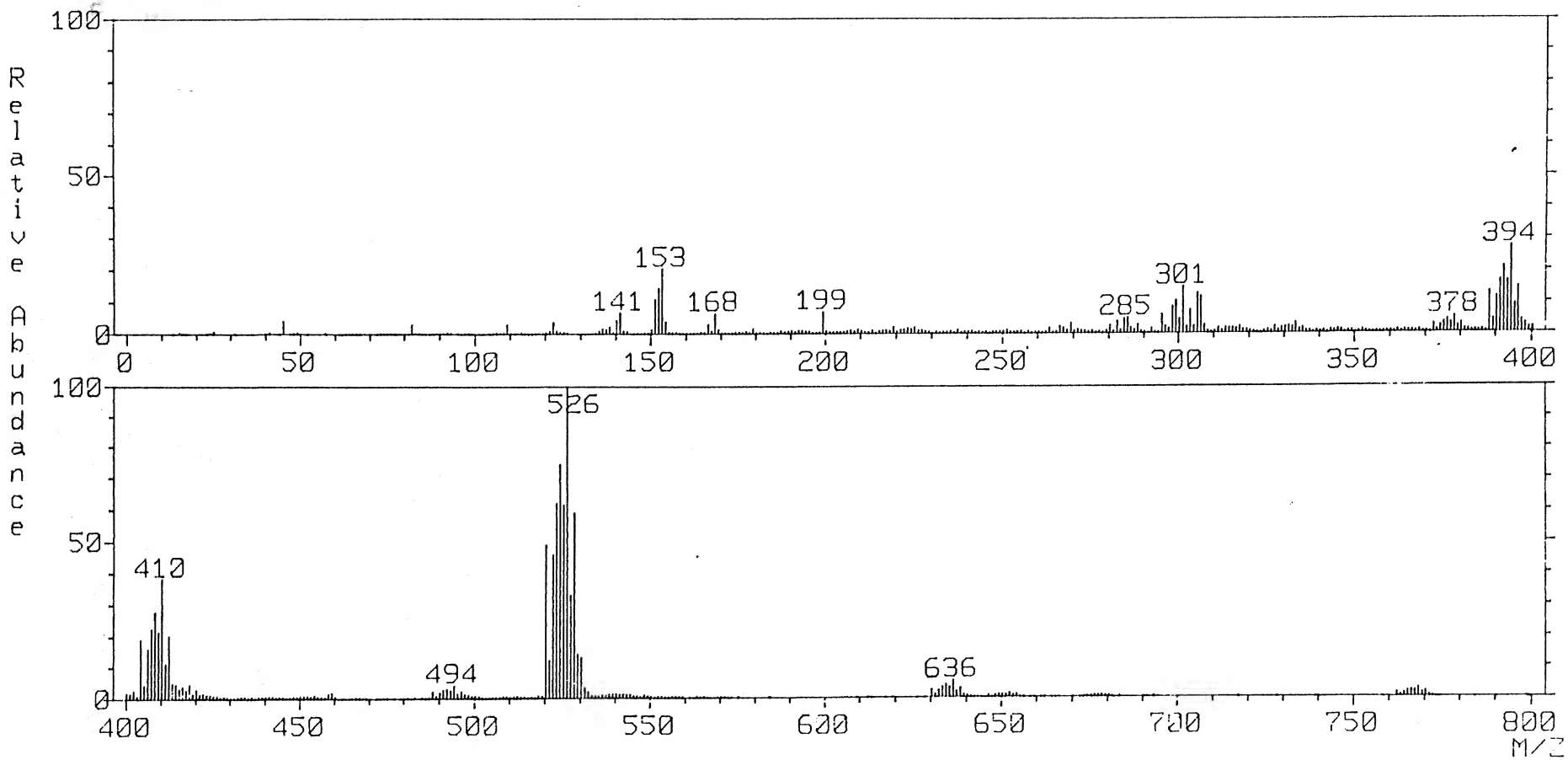

Fig.3.29 Negative ion FAB mass spectra of $[Bu_4N][Mo^{IV}(dtc)(mnt)_2]$

MoO^{2+} form. Figure 3.25 is for $[Bu_4N]_2[Mo_2O_3(Cl)_2(mnt)_2]$ complex which showed similar fragmentation pattern as the corresponding bromo species. Figure 3.26 is for the corresponding thiolato complex, $[Bu_4N]_2[Mo_2O_3(SPh)_2(mnt)_2]$, for which the molecular ion peak is not well defined for the ion pair form like $[Bu_4N][Mo_2O_3(SPh)_2(mnt)_2]^-$ (M/Z = 982) is present. A peak at (M/Z = 1025) may be due to the formamide coordinated species like $[Bu_4N][Mo_2O_3(SPh)_2(mnt)_2]^-.NH_2CHO$ as the spectra is recorded in DMF. The peak at M/Z = 629 is assigned for the species like $[Mo_2O_3(SPh)(mnt)_2]^-$. Figure 3.27 is a positive ion mass spectra for the complex, $[Mo_2O_3(bipy)_2(mnt)_2]$, where molecular ion peak is not observed but the species like, $[Mo_2O_3(bipy)(mnt)_2]$ (M/Z = 678), $[MoO_2(bipy)(mnt)]$ (M/Z = 424) are identified.Figure 3.28 is the negative ion mass spectra for $[Bu_4N][Mo(dtp)(mnt)_2]$ which show the appearance of molecular ion $[Mo(dtp)(mnt)_2]^-$ (M/Z = 563) and in Figure 3.29 the compound $[Bu_4N][Mo(dtc)(mnt)_2]$ showed the presence of molecular ion $[Mo(dtc)(mnt)_2]^-$ (M/Z = 526).

3.3.4 CYCLIC VOLTAMMETRY:

Electrochemical study on the reported complexes resulted some important observations. Thus $[Mo^{VI}O_2(mnt)_2]^{2-}$ has been shown to display a quasireversible reduction at -1.15V *vs* Ag/AgCl in MeCN. In the presence of 0.13M acetic acid and 3.5M water this reduction peak potential is shifted to a less negative irreversible reduction with E_{pc} at -0.77V *vs* Ag/AgCl which has been shown to be due to proton coupled electron transfer reaction.[33a] However, gradual addition of water into acetonitrile solution of

$[Mo^{VI}O_2(mnt)_2]^{2-}$ displayed gradual shift of the reduction process to a less negative value. Figure 3.30(i) showed the behavior of the reduction of $[Mo^{VI}O_2(mnt)_2]^{2-}$ in pure MeCN followed by the medium containing 6.3% and 10% water respectively. Final addition of trace quantity of glacial acetic acid into this mixed solvent media lead to the appearance of the voltammogram as reported earlier.[102] Figure 3.30(i) showed that in water containing MeCN media the quasireversible process became irreversible which is quite expected because of the formation of $[Mo^{V}O_2(mnt)_2]^{-}$ containing $\{Mo^{V}O_2^{+}\}$ moiety which is very susceptible to react with proton and thus became unstable. Replacing H_2O in this experiment by D_2O we could not observe any change in the profile of the voltammogram compared to those containing H_2O. Furthermore, addition of slight excess of 10% water did not result any shift in the appearance of the cathodic peak potential (-1.09V *vs* Ag/AgCl) further. This shift in cathodic peak potential may be understood by outer sphere hydrogen bonded interaction between the terminal cyano groups of the ligated mnt with water. This hydrogen bonding may be responsible to drift electron density from molybdenum center to nitrogen end of cyano group ***via*** molybdenum dithiolene ligation causing depletion of electron density on molybdenum center resulting easier reduction Optimum concentration of water in the reaction medium is required to complete this outer sphere complexation. Similar outer sphere hydrogen bonded complexation in complexes with cyano groups are reported.[89] Cyclic voltammogram of $[Mo^{IV}O(mnt)_2]^{2-}$ anion containing counter cation like Et_4N^{+} and $[Et_3NH]^{+}$ in CH_2Cl_2 is shown in Figure 3.30(ii). The C.V. of $[Et_4N]_2[Mo^{IV}O(mnt)_2]$ is identical to that reported earlier.[33a]

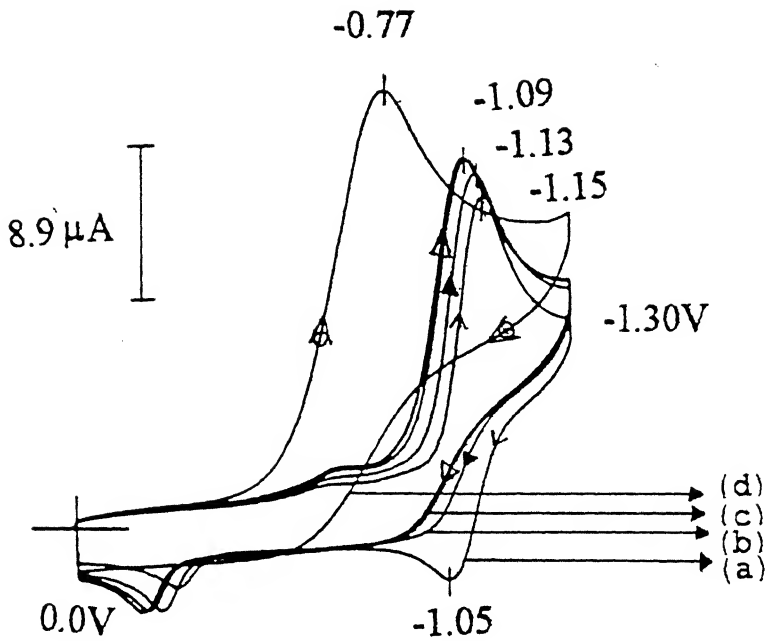

Fig.3.30(i) Cyclic voltammograms of $[Bu_4N]_2[Mo^{VI}O_2(mnt)_2]$ (a) in pure MeCN, (b) with 6.3% H_2O, (c) with 10% H_2O and (d) with 0.13M acetic acid.

However, for $[Et_3NH]_2[Mo^{IV}O(mnt)_2]$ though similar voltammogram is obtained but the following features are important to take note:

The ΔE, separation of anodic and cathodic peak potential, is 90mV compared to 70mV for the corresponding Et_4N^+ salt. We have already observed that in CH_2Cl_2 the hydrogen bonded structure is retained. If this be the case then it is expected that the molybdenum center should have developed more positive character resulting its oxidation more difficult. Contrary to this the appearance of E_{pa} at +0.46V compared to that at +0.48V for $[Et_4N]^+$ salt suggest the involvement of other interactions. A possible answer to this effect may be obtained from far-infrared data for the ν(Mo-S) vibrations for the two salts as presented in Table 3.1. The appearance of ν(Mo-S) at 365 cm^{-1} for $[Et_3NH]^+$ salt compared to that at 345 cm^{-1} for $[Et_4N]^+$ salt directly suggest the stronger Mo-S (dithiolene) interaction in the protonated salt. This increase in electron density by stronger Mo-S(dithiolene) bonding overweight the decrease in electron density due to the hydrogen bonding like Mo=O----H^+, resulting the accumulation of more electron density on the Mo center and easier oxidation. Another important consequence in this study is the deviation from reversibility of the protonated hydrogen bonded species compared to $[Et_4N]^+$ salt containing pure Mo=O moiety. Thus it may be inferred that protonation of the terminal Mo=O moiety tends to irreversibility. This phenomenan is further elaborated in the C.V. of the corresponding lysinium salt of the $[Mo^{IV}O(mnt)_2]^{2-}$ in water (Figure 3.30(ii)(c)) which demonstrated complete irreversible nature of this oxidation process. This finding can be correlated with the reported EPR spectroscopy of the molybdenum cofactor.[30c]

Hawkes and Bray have demonstrated that to generate any EPR active Mo-co the solvent should be organic (non-protic) in nature. They have failed to observe any EPR signal related to Mo-co in aqueous medium. We conclude that the isolated protein free Mo-co may respond similarly with the formation of very unstable pentavalent species. In the catalytic cycle of natural enzymes, the transient phase of EPR active species mostly at the regeneration stage may be due to the hydrophobic involvement imposed by the apoprotein near the active site which also might be responsible for displaying proton coupled EPR spectra which has not been observed in isolated Mo-co.[30c]

The cyclic voltammogram of $[Bu_4N]_2[Mo_2O_4(mnt)_2]$ is shown in Figure 3.31. The oxidation of this species occured with the appearance of an irreversible oxidation peak potential, E_{pa}, at +1.26V *vs* Ag/AgCl in CH_2Cl_2. In the reductive scan, a irreversible reduction appeared with E_{pc} at -1.62V *vs* Ag/AgCl. The reduction may be due to one electron reduction and the current height of the oxidation suggests that it is due to two electron oxidation process. The complexes $[Bu_4N]_2[Mo_2O_3X_2(mnt)_2]$ (X = Cl, Br) showed cyclic voltammetric responce as shown in Figures 3.32 and 3.33. Interestingly in both the cases the appearance of an irreversible reduction with E_{pc} at -0.72V for chloro and E_{pc} at -0.78V for bromo appeared. However, both the complexes showed another quasireversible reduction peak at identical potential of $E_{1/2}$ = -1.57V (+10mV, which is within the experimental error limits). Curiously enough, a similar reduction appeared in the dioxo bridged $Mo_2O_4^{2+}$ species (see Fig.3.31). The halo complexes are sensitive to traces of moisture and whether the second reduction

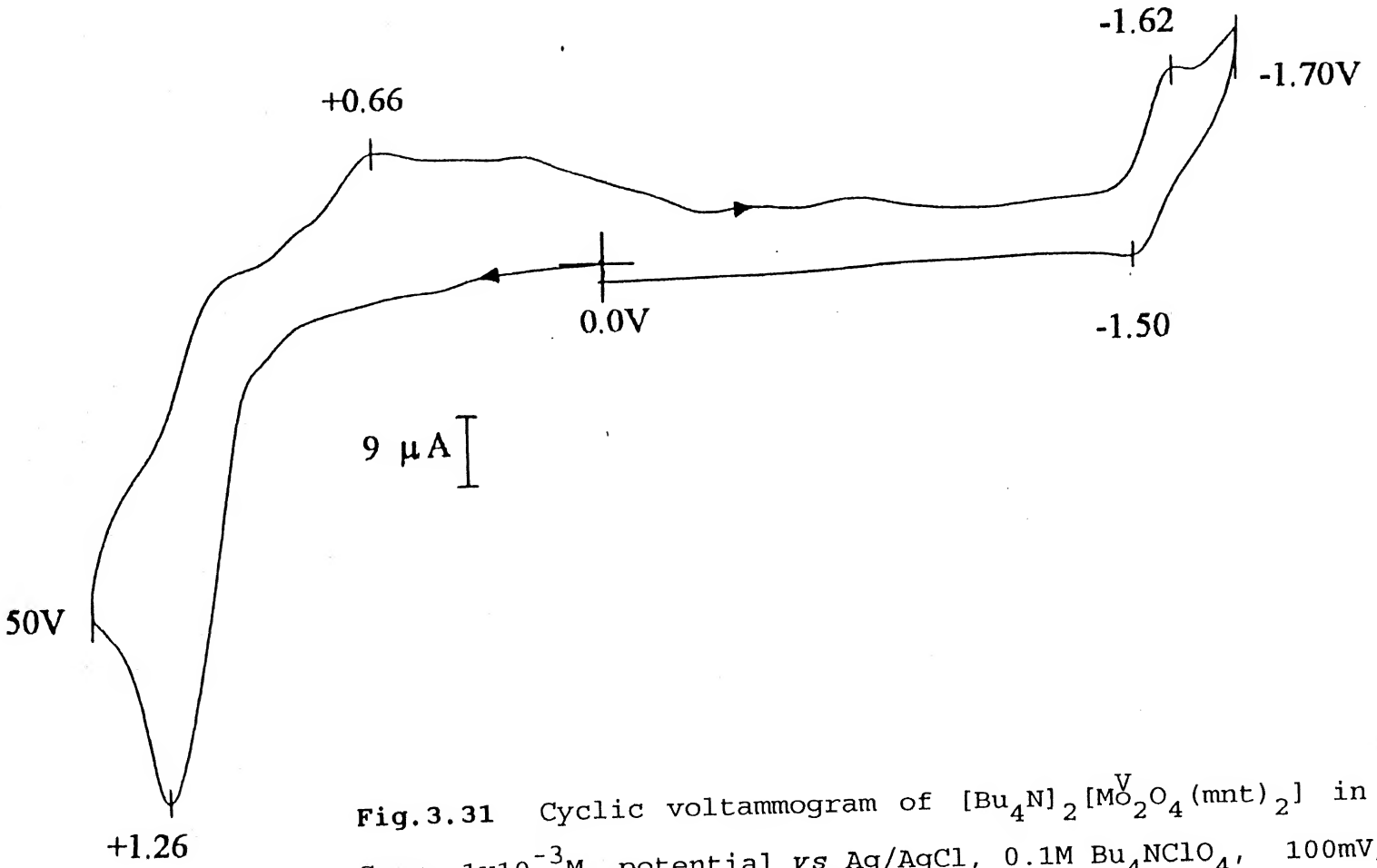

Fig.3.31 Cyclic voltammogram of $[Bu_4N]_2[Mo^V_2O_4(mnt)_2]$ in CH_2Cl_2, Conc. $1x10^{-3}$M, potential *vs* Ag/AgCl, 0.1M Bu_4NClO_4, 100mV/s.

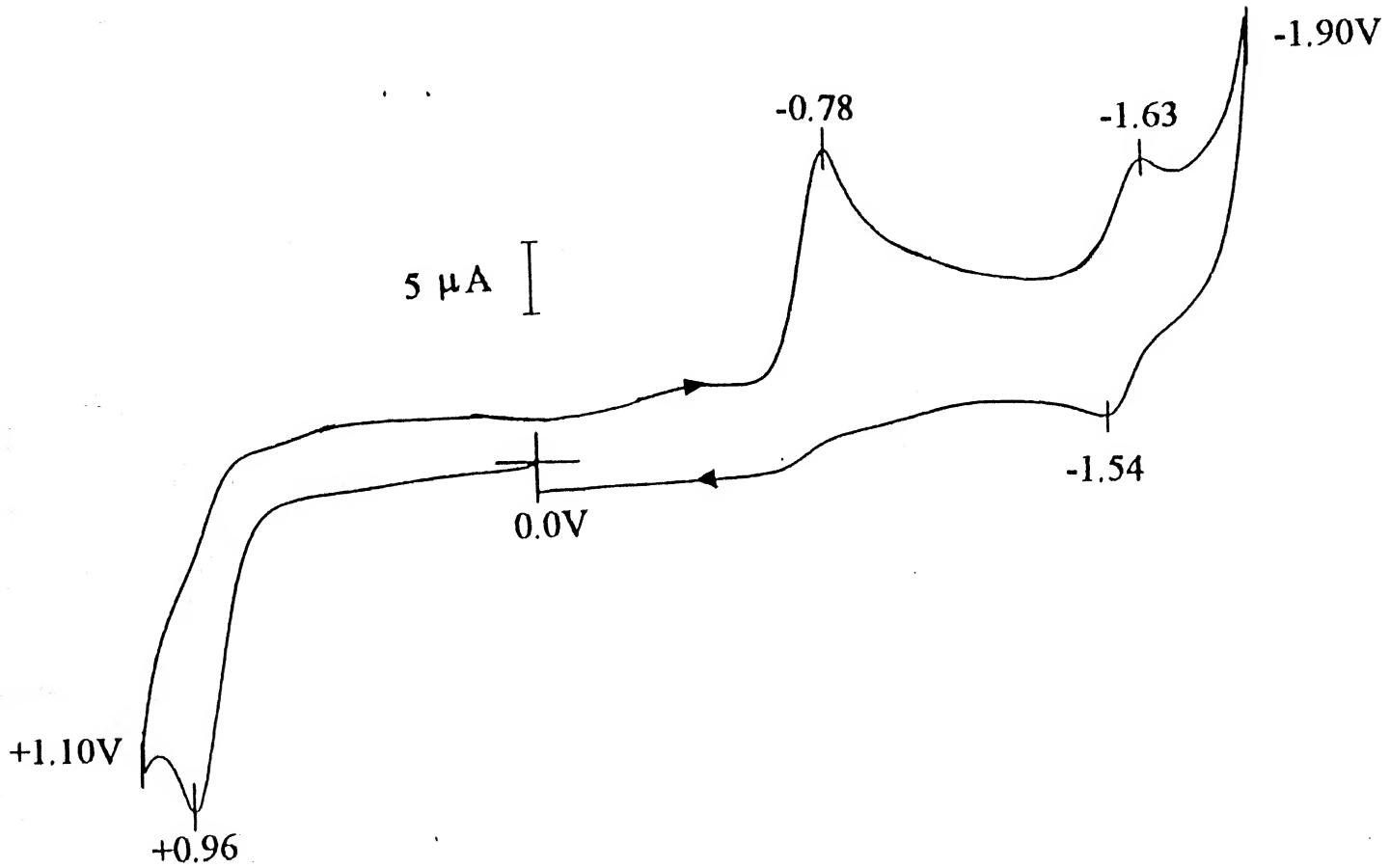

Fig.3.32 Cyclic voltammogram of $[Bu_4N]_2[Mo^{V}_2O_3(Br)_2(mnt)_2]$ in CH_2Cl_2, Conc. $1x10^{-3}$M, potential *vs* Ag/AgCl, 0.1M Bu_4NClO_4, 100mV/s.

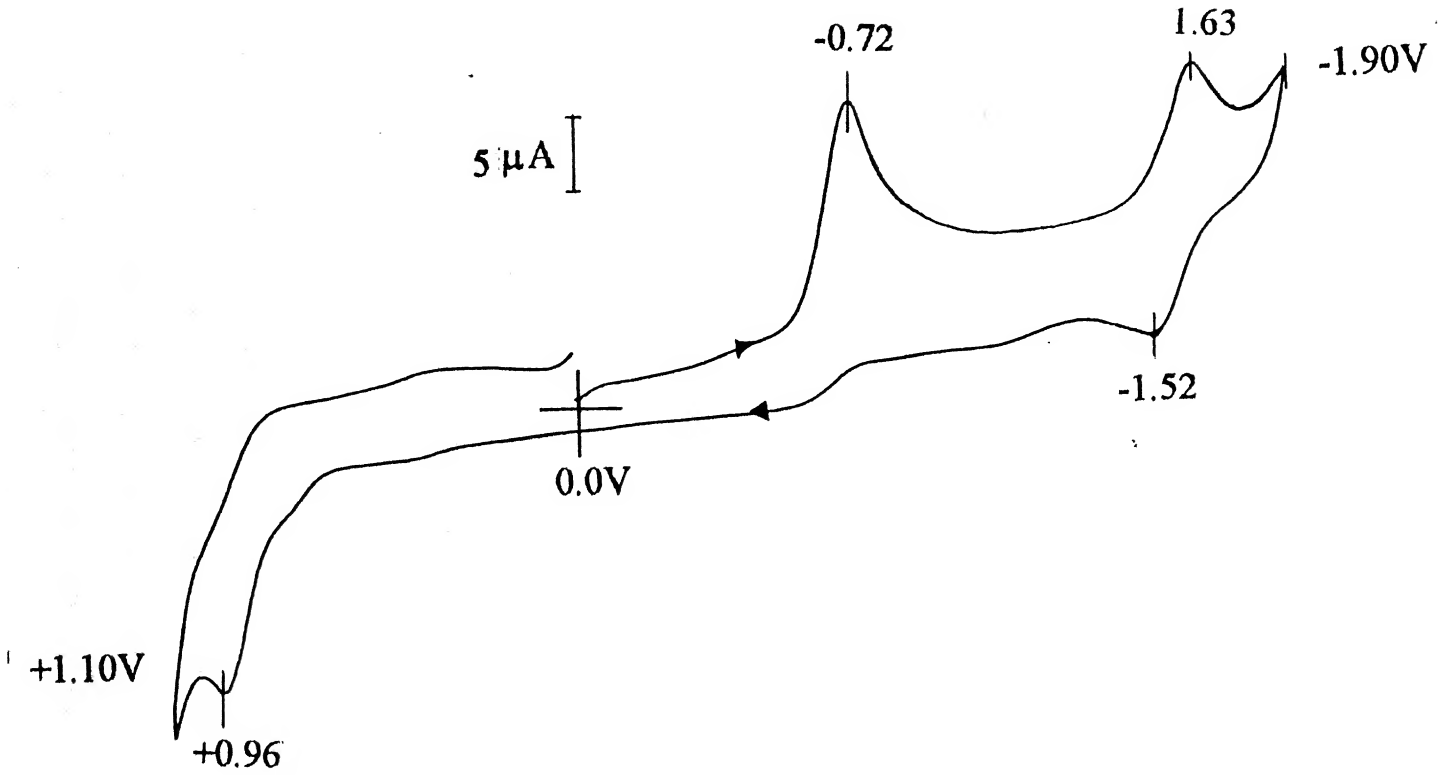

Fig.3.33 Cyclic voltammogram of $[Bu_4N]_2[Mo^{V}_2O_3(Cl)_2(mnt)_2]$ in CH_2Cl_2, Conc. $1x10^{-3}$M, potential *vs* Ag/AgCl, 0.1M Bu_4NClO_4, 100mV/s.

is associated with the formation of dioxo dimer is difficult to assess. However both the halo complexes display an irreversible oxidation process with E_{pa} at +0.96V *vs* Ag/AgCl. The absence of any irreversible oxidation at +1.26V justified that the second reduction process for both the halo complexes may not be due the formation of dioxo dimer in appreciable quantity to respond to electrochemical reduction within the short span of time involved. The time dependent hydrolysis process of these halo complexes are discussed latter (*vide infra*). The corresponding thiolato complexes are not soluble in CH_2Cl_2 and hence their C.V. are scaned in DMF medium. Both the voltammograms are reproduced in the Figure 3.34. In the oxidation scan both the complexes showed a broad strong anodic wave started to appear arround +0.60V and continued upto the limit of the scan (before switching potential) which may be due to the oxidative decomposition of the complexes. However in the reductive scan both showed a reversible reduction. The details of these reduction processes were difficult to assign. The corresponding bipyridine complex, $[Mo_2O_3(bipy)_2(mnt)_2]$ showed electrochemical response as shown in Figure 3.35. It displayed a very weak anodic peak potential in its oxidative scan at +0.54V *vs* Ag/AgCl. The appearance of borderline quasireversible-irreversible reduction process at E_{pa}= -0.36V Ag/AgCl followed by another reduction peak potential at +0.92V due to two stepwise one electron metal centered reductions. The third reduction peak at -1.40V may be due to the reduction of the coordinated bipy. The corresponding tris complexes like $[Bu_4N][Mo(dtc)(mnt)_2]$ and $[Bu_4N][Mo(dtp)(mnt)_2]$ showed C.V. responce as shown in the Figures 3.36 and 3.37 respectively. Both these tris systems showed a

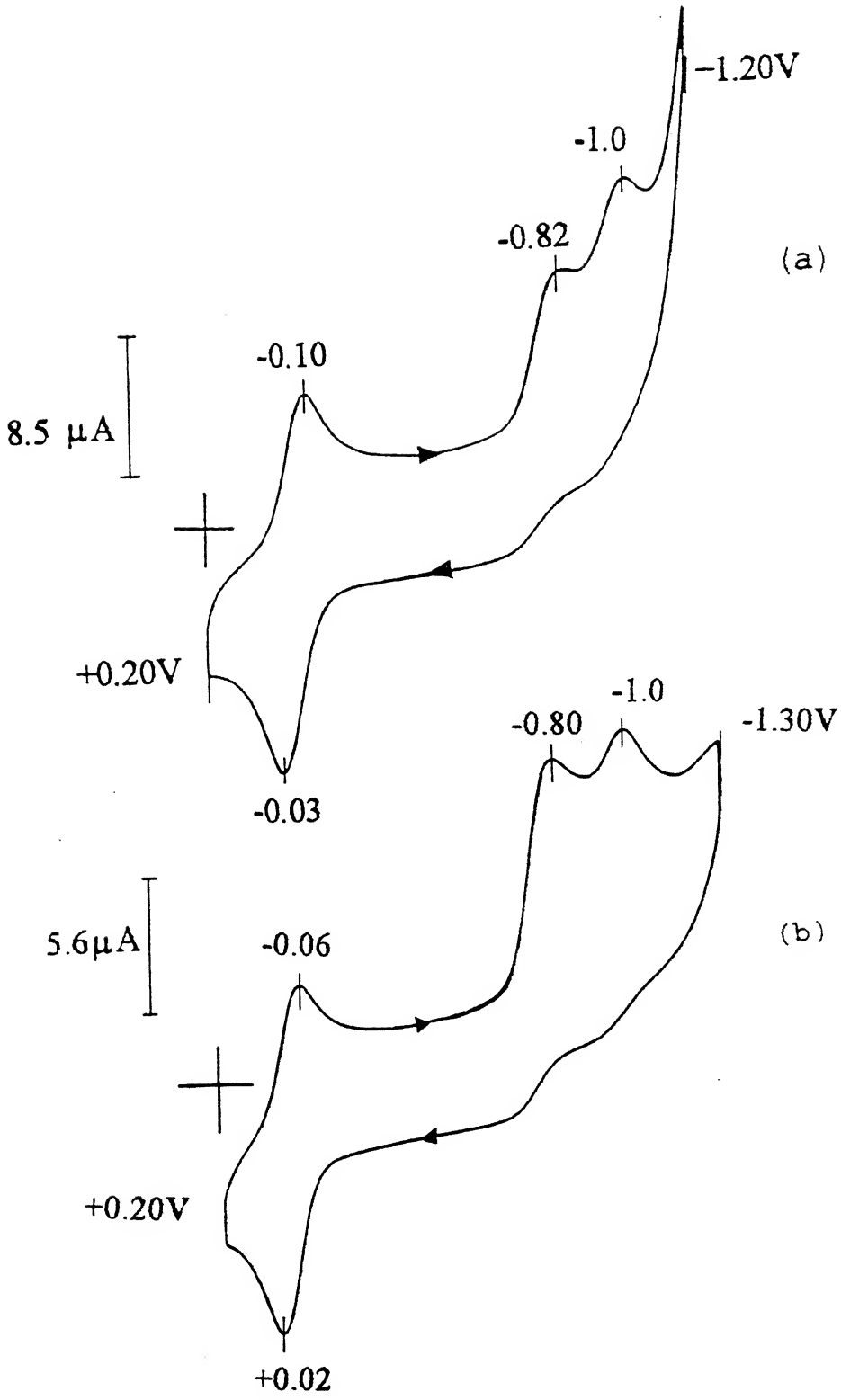

Fig.3.34 (a) Cyclic voltammogram of $[Bu_4N]_2[Mo^V_2O_3(SPh)_2(mnt)_2]$ and (b) is that of $[Bu_4N]_2[Mo^V_2O_3(ClC_6H_4S)_2(mnt)_2]$ in DMF Conc.

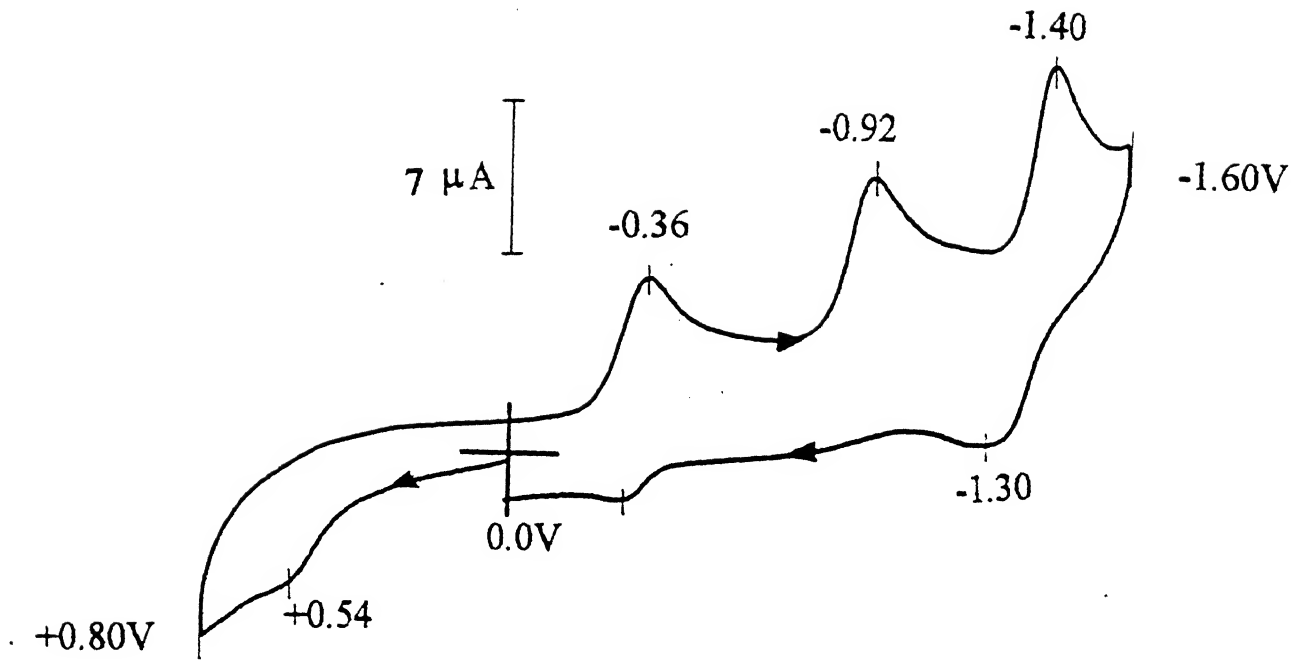

Fig.3.35 Cyclic voltammogram of $[Mo^{V}_{2}O_{3}(bipy)_{2}(mnt)_{2}]$ in DMF, Conc. $1x10^{-3}$M, potential *vs* Ag/AgCl, 0.1M Bu_4NClO_4, 100mV/s.

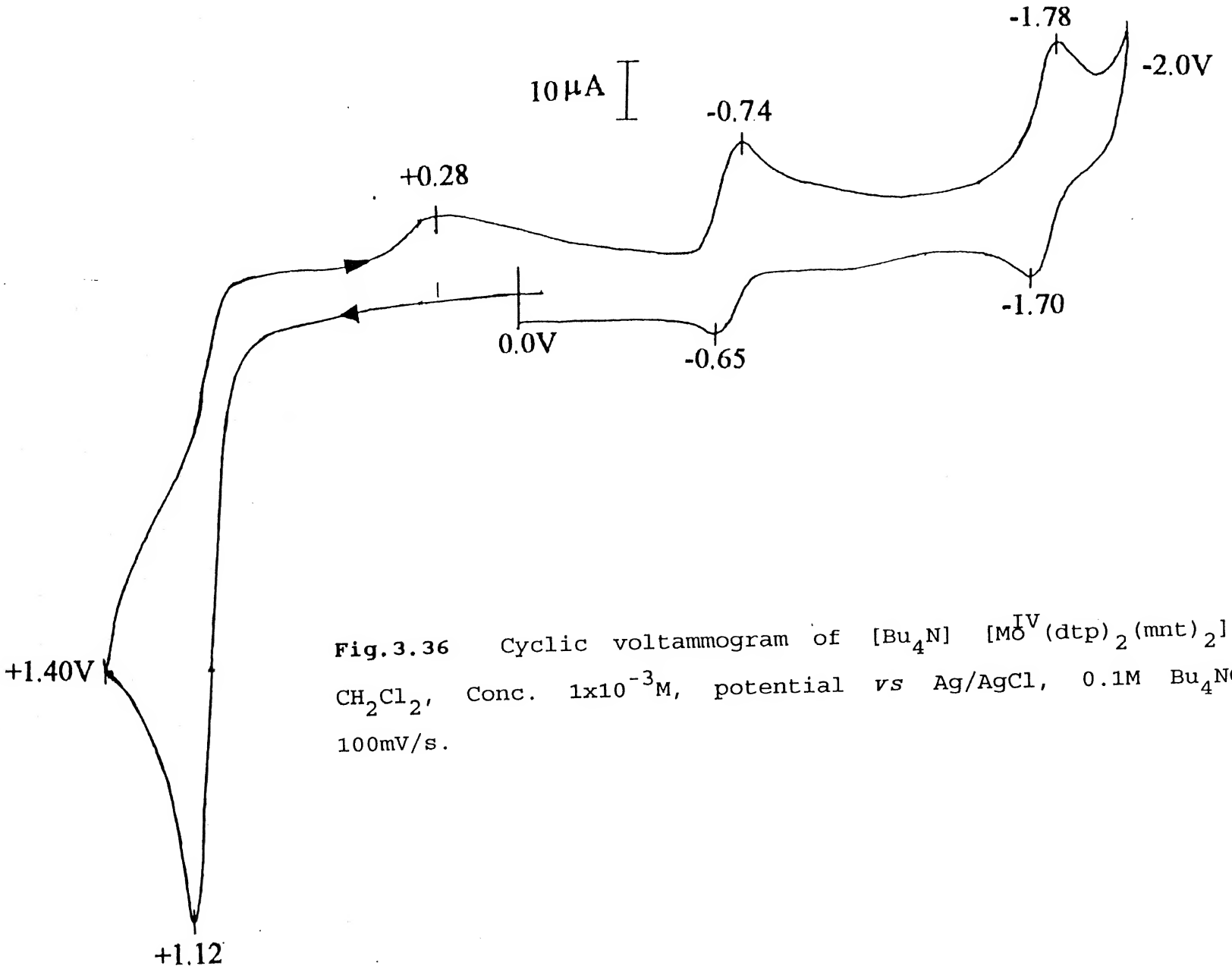

Fig.3.36 Cyclic voltammogram of $[Bu_4N]$ $[Mo^{IV}(dtp)_2(mnt)_2]$ in CH_2Cl_2, Conc. $1x10^{-3}M$, potential *vs* Ag/AgCl, 0.1M Bu_4NClO_4, 100mV/s.

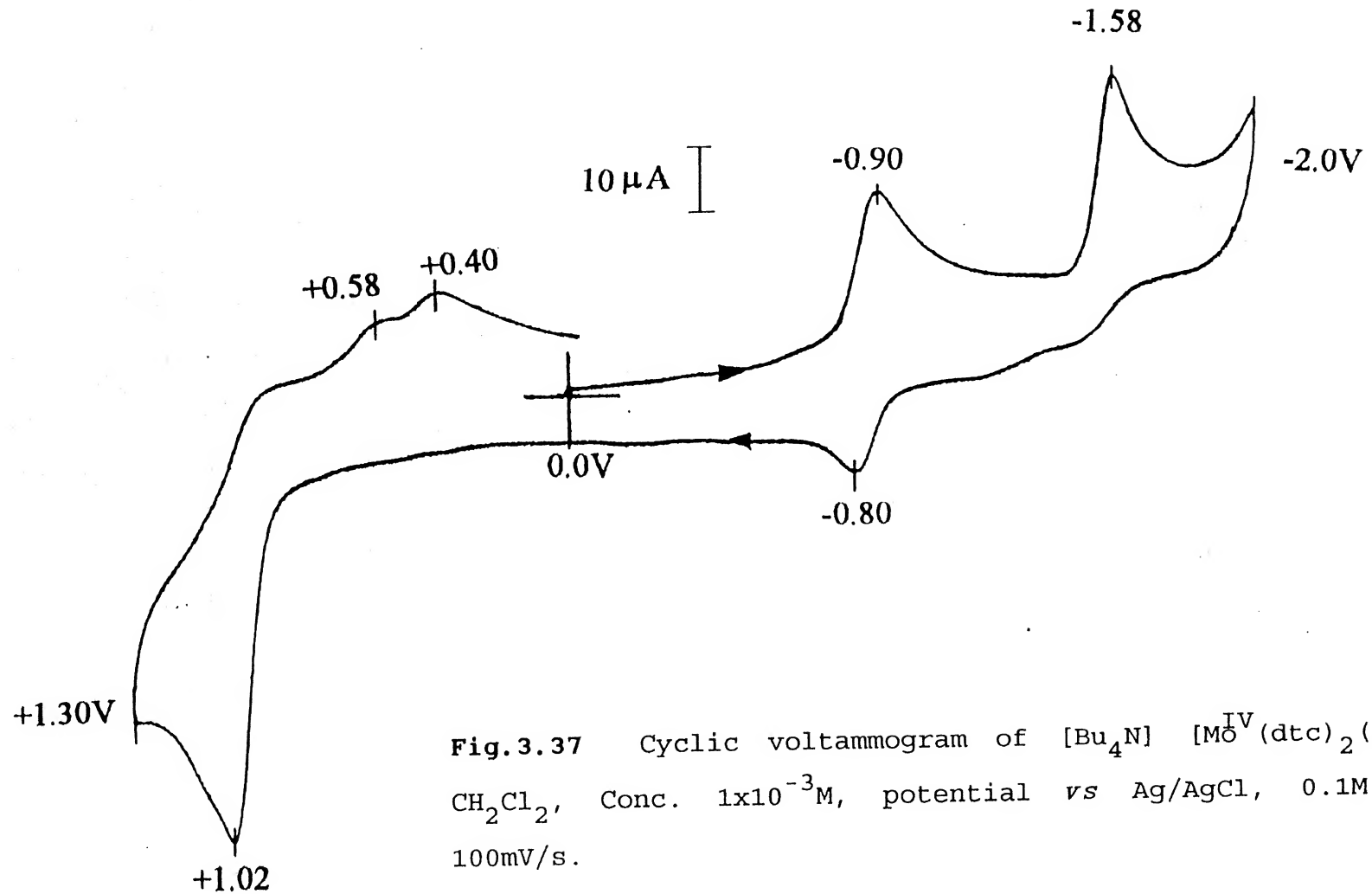

Fig.3.37 Cyclic voltammogram of $[Bu_4N]$ $[Mo^{IV}(dtc)_2(mnt)_2]$ in CH_2Cl_2, Conc. $1x10^{-3}M$, potential *vs* Ag/AgCl, 0.1M Bu_4NClO_4, 100mV/s.

Table 3.4 Cyclic voltammetric Data for Complexes: [a]

Complexes	E_{pc}(Volt)	E_{pa}(Volt)	Solvent Used
$[Mo^{V}_2O_4(mnt)_2]^{2-}$	-1.62 +0.66	---- +1.26	CH_2Cl_2
$[Mo^{V}_2O_3(Cl)_2(mnt)_2]^{2-}$	-1.63 -0.72 ----	-1.52 ---- +0.96	CH_2Cl_2
$[Mo^{V}_2O_3(Br)_2(mnt)_2]^{2-}$	-1.63 -0.78 ----	-1.54 ---- +0.96	CH_2Cl_2
$[Mo^{V}_2O_3(SPh)_2(mnt)_2]^{2-}$	-1.0 -0.82 -0.10	---- ---- -0.03	DMF
$[Mo^{V}_2O_3(ClC_6H_4S)_2(mnt)_2]^{2-}$	-1.0 -0.80 -0.60	---- ---- +0.02	DMF
$[Mo^{V}_2O_3(bipy)_2(mnt)_2]$	-1.40 -0.92 -0.36 ----	-1.30 ---- ---- +0.54	DMF
$[(C_2H_5)_4N]_2[Mo^{IV}O(mnt)_2]$	+0.41	+0.48	CH_2Cl_2
$[(C_2H_5)_3NH]_2[Mo^{IV}O(mnt)_2]$	+0.37	+0.46	CH_2Cl_2
$[C_6H_{15}N_2O_2]_2[Mo^{IV}O(mnt)_2]$	----	+0.48	H_2O [b]
$[Ph_4P]_2[Mo^{VI}O_2(mnt)_2]$	-1.15	-1.05	CH_3CN
$[Bu_4N][Mo^{IV}(dtc)(mnt)_2]$	-1.58 -0.90 +0.58	---- -0.80 +1.02	CH_3CN
$[Bu_4N][Mo^{IV}(dtp)(mnt)_2]$	-1.78 -0.74 +0.28	-1.70 -0.65 +1.12	CH_3CN

[a] concentration taken for all cases is 1 x 10^{-3} M, scan rate 100 mV/s, room temperature, electrolyte Bu_4NClO_4.

[b] Electrolyte KCl.

reversible reduction at $E_{1/2}$ = -0.85V, ΔE = 100mV for $[Bu_4N][Mo(dtc)(mnt)_2]$ and at $E_{1/2}$= -0.70V, ΔE= 90mV for $[Bu_4N][Mo(dtp)(mnt)_2]$. The dithophos- phate complex showed another reversible reduction at $E_{1/2}$= -1.74V, whereas the corresponding dtc complex displayed only an irreversible reduction with E_{pc} at -1.58V. In the oxidative scan both the complexes displayed apparently multielectron irreversible oxidation processes leading to partial decomposition with the appearance of some weak cathodic peak potentials after the onset of the switching potential (see Fig.3.36 and Fig.3.37). The appearance of the low current intensity peak potentials are associated with the oxidation process. This has been varified by scanning the respective voltammograms only upto +0.80V where in both the cases these small cathodic peak potentials did not appear. Cyclic voltammetric parameters are tabulated in Table 3.4.

3.3.5 SINGLE CRYSTAL X-RAY DIFFRACTION STUDY:

X-ray structure of some of the synthesized complexes are performed on a Enraf-Nonius CAD-4 diffractometer equipped with a Mo X-ray source and a graphite monochromator at 25 ^{o}C.

(a) For $[Et_4N]_2[MoO(mnt)_2]$ **(1)**; the diffraction quality single crystals are crystallized by making a layer of diethylether over the acetonitrile / 2-propanol solution of the compound at 15-20 ^{o}C. The summary of the crystal data is given in Table 3.5. Positional and isotropic thermal parameters for the nonhydrogen atoms are listed in Table 3.6. Selected bond lengths and bond angles are described in Table 3.7. The structure of the anion is

Table 3.5

Summary of X-ray crystallographic data for complexes 1 and 2 :

	$[Et_4N]_2[Mo^{IV}O(mnt)_2]$ (1)	$[C_5H_6N]_2[Mo^{IV}O(mnt)_2]$ (2)
1. Chemical formula	$C_{24}H_{40}MoN_6OS_4$	$C_{18}H_{12}MoN_6OS_4$
2. Formula weight	652.80	552.51
3. Crystal dimension, mm	0.6 x 0.4 x 0.2	0.5 x 0.3 x 0.2
4. Space group	$P2_12_12$	$P2/n$
5. Z	4	4
6. a, Å	29.948(6)	7.460(7)
7. b, Å	14.779(4)	11.449(1)
8. c, Å	7.373(2)	26.657(3)
9. β, deg	-----	93.89(3)
10. V, $Å^3$	3263.30(1.4)	2271.52(2.1)
11. ρ_{calcd}, g cm^{-3}	1.329	1.686
12. μ, cm^{-1}	6.8	9.7
13. Mo-K_α radiation	λ = 0.71073 Å	λ = 0.71073 Å
14. T, ^oC	25	25
15. Diffractometer	Enraf-Nonius CAD4	Enraf-Nonius CAD4
16. Monochromator	Graphite	Graphite
17. Scan Type	θ - 2θ	θ - 2θ
18. Scan Range	0.80 + 0.35tanθ	0.80 + 0.35tanθ
19. 2θ range, deg	2 - 50	2 - 50
20. Variation in std. intensity(%)	< 1	< 1
21. Corrections	L_p, Decay, Absorption	L_p, Decay, Absorption
22. Independent reflection	6418	3510
23. No. of reflection used ($Fo>3\sigma(Fo)$)	4575	3150
24. Data: Parameter ratio	~ 13	~ 10
25. Weighing scheme	Counting Statistics	Counting Statistics
26. Final GOF	4.203	3.302
27. R_f	0.064	0.045
28. R_{wf}	0.062	0.041
29. Largest shift / esd	0.002	0.002
30. Highest residual peak in diff. map e/ $Å^3$	0.45	0.45

Table 3.6 Non-Hydrogen Positional and Isotropic Displacement Parameters for Compound (1).

	x/a	y/b	z/c	U
Mo	0.65618(4)	0.52210(7)	0.2746(2)	* 0.0503(3)
S(2)	0.6549(1)	0.3816(2)	0.1197(5)	* 0.067(1)
S(1)	0.6236(1)	0.4385(2)	0.5189(6)	* 0.066(1)
S(3)	0.6463(1)	0.5894(2)	-0.0215(5)	* 0.057(1)
S(4)	0.6055(1)	0.6365(2)	0.3701(5)	* 0.062(1)
O	0.7085(3)	0.5489(6)	0.334(1)	* 0.067(4)
N(21)	0.6500(5)	0.1328(8)	0.210(2)	* 0.120(7)
N(11)	0.6079(6)	0.208(1)	0.706(3)	* 0.153(9)
N(31)	0.6109(5)	0.8016(9)	-0.246(2)	* 0.103(7)
N(41)	0.5538(5)	0.8513(9)	0.237(2)	* 0.117(7)
C(21)	0.6410(4)	0.2995(8)	0.285(2)	* 0.070(6)
C(22)	0.6453(5)	0.2069(9)	0.238(2)	* 0.078(6)
C(11)	0.6278(5)	0.3282(9)	0.463(2)	* 0.065(6)
C(12)	0.6172(5)	0.260(1)	0.608(3)	* 0.088(8)
C(31)	0.6172(5)	0.6907(9)	0.022(2)	* 0.054(5)
C(32)	0.6131(6)	0.7511(9)	-0.127(2)	* 0.081(7)
C(41)	0.6001(5)	0.7090(8)	0.191(2)	* 0.061(5)
C(42)	0.5753(5)	0.790(1)	0.217(2)	* 0.075(6)
N(5)	0.7739(4)	0.3542(8)	0.654(2)	* 0.063(5)
C(51)	0.8178(6)	0.388(1)	0.592(3)	* 0.108(8)
C(52)	0.8137(7)	0.469(1)	0.456(3)	* 0.128(9)
C(53)	0.7462(6)	0.428(1)	0.745(3)	* 0.112(8)
C(54)	0.7658(6)	0.469(1)	0.917(2)	* 0.107(8)
C(55)	0.7828(7)	0.276(1)	0.791(3)	* 0.110(9)
C(56)	0.7383(7)	0.227(1)	0.839(2)	* 0.116(9)
C(57)	0.7452(6)	0.327(1)	0.492(3)	* 0.113(8)
C(58)	0.7285(7)	0.745(1)	0.631(3)	* 0.13(1)
N(6)	1/2	0	0.731(3)	* 0.066(6)
C(61)	0.514(1)	0.084(2)	0.607(4)	* 0.19(2)
C(62)	0.5474(8)	0.073(2)	0.474(3)	* 0.20(2)
C(63)	0.537(1)	-0.034(2)	0.82(1)	* 0.58(7)
C(64)	0.555(1)	0.037(2)	0.928(5)	* 0.32(3)
N(7)	1/2	1/2	-0.110(2)	* 0.067(7)
C(71)	0.5260(5)	0.567(1)	-0.223(2)	* 0.086(7)
C(72)	0.4947(8)	0.625(2)	-0.352(3)	* 0.14(1)
C(73)	0.5349(5)	0.458(1)	0.006(2)	* 0.105(8)
C(74)	0.5162(7)	0.375(2)	0.131(3)	* 0.16(1)

Table 3.7

Bond Distances and Bond Angles of Compound (1).

Bond Distances	(Angstroms)	Bond Angles	(Degree)
Mo-O	1.673(8)	O-Mo-S1	108.0(3)
Mo-S1	2.393(4)	O-Mo-S2	110.4(3)
Mo-S2	2.371(4)	O-Mo-S3	104.6(3)
Mo-S3	2.417(4)	O-Mo-S4	110.6(3)
Mo-S4	2.379(4)	S1-Mo-S2	84.4(1)
S1-C11	1.69(1)	S2-Mo-S3	85.6(1)
S2-C21	1.77(2)	S3-Mo-S4	84.1(1)
S3-C31	1.76(1)	S4-Mo-S1	83.3(1)
S4-C41	1.71(1)	Mo-S1-C11	106.6(6)
C11-C12	1.50(2)	Mo-S2-C21	105.8(5)
C21-C22	1.42(2)	Mo-S3-C31	104.2(5)
C31-C32	1.42(2)	Mo-S4-C41	106.1(5)
C41-C42	1.42(2)	S1-C11-C12	120.0(1)
C11-C21	1.43(2)	S2-C21-C22	118.0(1)
C31-C41	1.38(2)	S3-C31-C32	116.0(1)
C12-N11	1.09(3)	S1-C11-C21	122.0(1)
C22-N21	1.12(2)	S2-C21-C11	119.5(9)
C32-N31	1.15(2)	S3-C31-C41	121.0(1)
C42-N41	1.12(2)	S4-C41-C31	123.0(1)

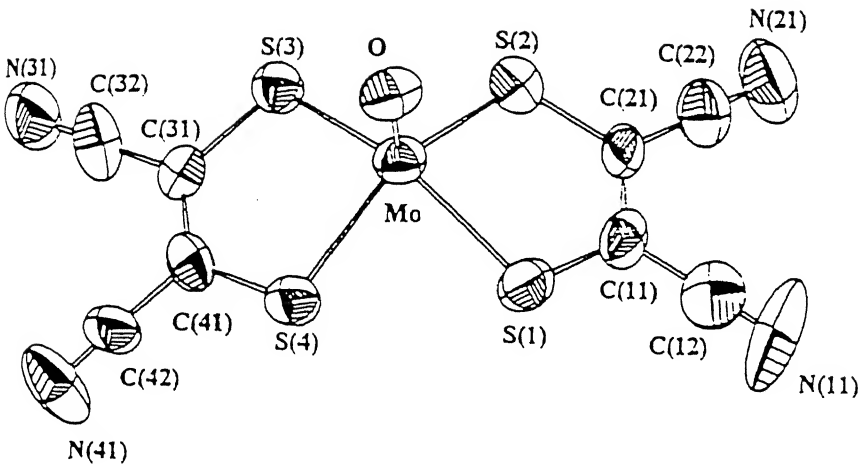

Fig.3.38 Crystal structure of $[Et_4N]_2[M\bar{o}^{IV}O(mnt)_2]$

shown in Figure 3.38. The complex crystallizes in the $P2_12_12$ space group (acentric). Anomalous dispersion corrections are applied and the coordinates of the atoms given belong to the correct enantiomer. The $[MoOS_4]$ core has a distorted square-pyramidal structure with an axial Mo=O bond and two mnt ligands have occupied the equatorial position of the square-pyramid. In the molecule one Et_4N^+ cation is in the general position and second one is situated in two special coordinate positions. The terminal oxo ligand with a Mo=O bond (1.673(8)Å) is shorter than the corresponding tungsten complex and the unequal Mo-S bonds have a mean value (2.390(4)Å) is longer than that for the corresponding tungsten complex.[34b] The Mo atom is situated at 0.752 Å above the plane formed by the four sulfur atoms of the dithiolene ligand.

(b) For $[PyH]_2[MoO(mnt)_2]$ **(2)**; the diffraction quality single crystals are crystallized by slow evaporation of acetone solution of the compound at room temperature. The summary of the crystal data is given in Table 3.5. Positional and isotropic thermal parameters for the nonhydrogen atoms are listed in Table 3.8. Selecled bond lengths and bond angles are described in Table 3.9. The structure of the anion is shown in Figure 3.39. The complex crystallizes in the *P*2/n space group. The $[MoOS_4]$ core has a distorted square-pyramidal structure with an axial Mo=O bond and the two mnt ligands have occupied the equatorial position of the square-pyramid. One of the PyH^+ cation is hydrogen bonded with the terminal oxo group and the length of the $MoO\text{----}H_{50}$ is (2.24(7)Å). The Mo=O bond (1.714(3)Å) is much longer than that (1.673(8)Å) for the corresponding Et_4N^+ salt of the anion. Due to this elongation

Table 3.8 Non-Hydrogen Positional and Isotropic Displacement Parameters for Compound (2).

	x/a	y/b	z/c		U
Mo	0.53748(5)	0.48226(4)	0.36984(1)	*	0.0369(1)
S(1)	0.5126(2)	0.2760(1)	0.37488(4)	*	0.0432(4)
S(2)	0.5375(2)	0.4490(1)	0.28187(5)	*	0.0488(5)
S(3)	0.3862(2)	0.6589(1)	0.34739(4)	*	0.0488(5)
S(4)	0.3523(2)	0.4847(1)	0.43896(4)	*	0.0496(5)
O	0.7518(4)	0.5188(3)	0.3914(1)	*	0.049(1)
N(11)	0.5720(8)	0.0022(4)	0.3055(2)	*	0.087(2)
N(21)	0.6152(6)	0.2247(4)	0.1861(2)	*	0.069(2)
N(31)	0.1739(7)	0.9136(5)	0.4056(2)	*	0.081(2)
N(41)	0.1220(7)	0.6896(6)	0.5210(2)	*	0.100(3)
C(11)	0.5511(6)	0.2246(4)	0.3146(2)	*	0.041(2)
C(12)	0.5630(7)	0.1014(5)	0.3084(2)	*	0.053(2)
C(21)	0.5622(6)	0.2986(4)	0.2753(2)	*	0.041(2)
C(22)	0.5918(6)	0.2556(4)	0.2255(2)	*	0.049(2)
C(31)	0.2821(6)	0.7014(4)	0.4018(2)	*	0.046(2)
C(32)	0.2194(7)	0.8187(5)	0.4036(2)	*	0.054(2)
C(41)	0.2682(6)	0.6273(5)	0.4404(2)	*	0.047(2)
C(42)	0.1846(7)	0.6619(6)	0.4856(2)	*	0.065(2)
N(50)	0.7498(5)	0.7682(4)	0.4186(2)	*	0.056(2)
N(60)	-0.0110(6)	0.3300(7)	0.3647(3)	*	0.092(3)
C(51)	0.7278(7)	0.7335(5)	0.4646(2)	*	0.066(2)
C(52)	0.7035(8)	0.8139(8)	0.5005(2)	*	0.082(3)
C(53)	0.7034(9)	0.9293(7)	0.4887(3)	*	0.092(3)
C(54)	0.7215(9)	0.9616(5)	0.4396(3)	*	0.088(3)
C(55)	0.7459(8)	0.8785(6)	0.4051(2)	*	0.069(2)
C(61)	0.0154(8)	0.2181(8)	0.3707(2)	*	0.079(3)
C(62)	0.0712(8)	0.1535(5)	0.3328(3)	*	0.073(3)
C(63)	0.0999(7)	0.2060(6)	0.2892(2)	*	0.065(2)
C(64)	0.0727(8)	0.3216(7)	0.2830(2)	*	0.076(3)
C(65)	0.0148(9)	0.3864(6)	0.3224(4)	*	0.091(3)

Table 3.9

Bond Distances and Bond Angles for Compound (2)

Distances	(Angstroms)	Angles	(Degree)
Mo-O	1.714(3)	O-Mo-S1	107.4(1)
Mo-S1	2.373(1)	O-Mo-S2	107.9(1)
Mo-S2	2.376(1)	O-Mo-S3	107.1(1)
Mo-S3	2.373(1)	O-Mo-S4	108.4(1)
Mo-S4	2.377(2)	S1-Mo-S2	84.35(4)
S1-C11	1.753(5)	S2-Mo-S3	85.40(4)
S2-C21	1.741(5)	S3-Mo-S4	83.91(5)
S3-C31	1.759(5)	S4-Mo-S1	85.19(5)
S4-C41	1.750(5)	Mo-S1-C11	105.3(2)
C11-C12	1.423(7)	Mo-S2-C21	105.4(2)
C21-C22	1.446(7)	Mo-S3-C31	104.9(2)
C31-C32	1.424(8)	Mo-S4-C41	104.8(2)
C41-C42	1.449(7)	S1-C11-C12	117.0(4)
C11-C21	1.355(6)	S2-C21-C22	116.9(3)
C31-C41	1.343(7)	S3-C31-C32	116.9(4)
C12-N11	1.141(8)	S1-C11-C21	121.4(4)
C22-N21	1.132(7)	S2-C21-C11	121.9(4)
C32-N31	1.141(8)	S3-C31-C41	121.2(4)
C42-N41	1.127(7)	S4-C41-C31	121.7(4)

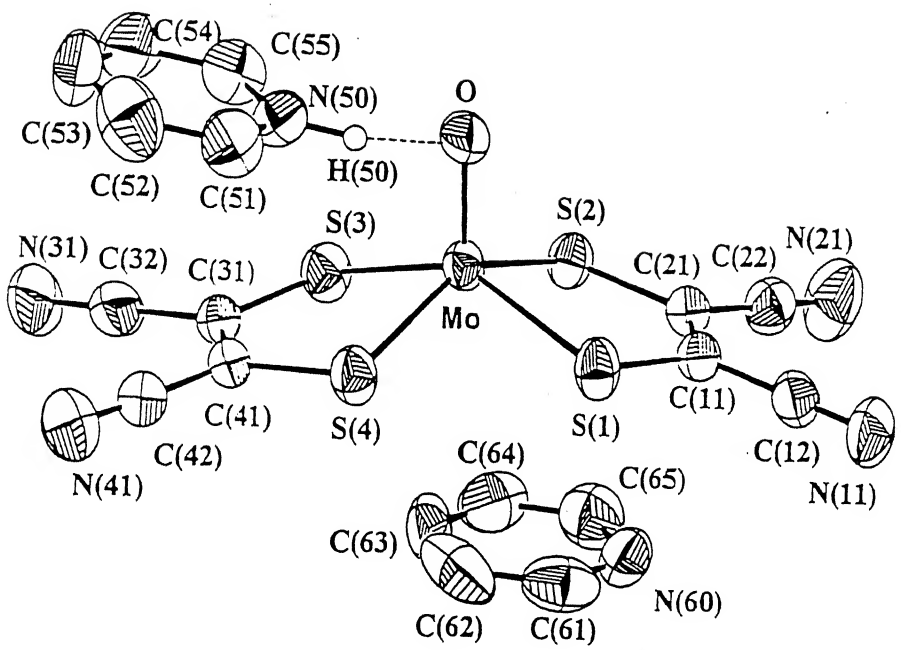

Fig.3.39 Crystal structure of $[PyH]_2[Mo^{IV}O(mnt)_2]$

of the bond the electron density from the mnt ligand is drifted over Mo atom and this is menifested by shorter mean Mo-S bond length (2.374(1)Å than that for the corresponding Et_4N^+ salt.

(c) For $[Ph_4P]_2[MoO_2(mnt)_2].2H_2O$ **(3)**; the diffraction quality crystals are crystallized by slow diffusion of diethylether into the acetonitrile / 2-propanol solution of the compound at 10°C. The summary of the crystal data is given in Table 3.10. Positional and isotropic thermal parameters for the nonhydrogen atoms are listed in Table 3.11. Selecled bond lengths and bond angles are described in Table 3.12. The structure of the anion is shown in Fig. 3.40. The complex crystallizes in the *Pbcn* space group. The molecule has a two fold symmetry and the molybdenum atom lies on the crystallographic 2-fold axis and only half of the molecule is present in the assymetric unit. Oxygen atom of one of the water molecule is also situated on the 2-fold axis. The structure of the complex having a $[MoO_2S_4]$ core is distorted octahedron with the oxo groups *cis* to each other and trans to the corresponding sulfur atoms. The Mo=O distance (1.694(7)Å) is shorter than that (1.701(6)Å) of the corresponding tungsten complex.[34b] The Mo-S bond distance (2.63(3)Å) *trans* to Mo=O group are longer than that for the other Mo-S bonds.

(d) For $[Ph_4P]_2[Mo_2O_4(mnt)_2]$ **(4)**; the diffraction quality crystals are crystallized by slow evaporation of the acetonitrile-water (9:1) solution of the compound at room temperature. The summary of the crystal data is given in Table 3.10. Positional and isotropic thermal parameters for the non-hydrogen atoms are described in

Table 3.10
Summary of X-ray crystallographic data for complexes 3 and 4 :

	$[Ph_4P]_2[Mo^{VI}O_2(mnt)_2]2H_2O$(3)	$[Ph_4P]_2[Mo_2O_4(mnt)_2]$(4)
1. Chemical formula	$C_{56}H_{44}MoN_4O_4P_2S_4$	$C_{56}H_{40}Mo_2N_4O_4P_2S_4$
2. Formula weight	1123.15	1215.06
3. Crystal dimension, mm	0.5 x 0.4 x 0.2	0.4 x 0.4 x 0.1
4. Space group	*Pbcn*	$P\bar{1}$
5. Z	4	2
6. a, Å	20.502(5)	11.335(2)
7. b, Å	15.775(8)	12.943(2)
8. c, Å	17.638(1)	18.886(3)
9. α, deg	90.00	79.33(1)
10. β, deg	90.00	80.20(1)
11. γ, deg	90.00	84.97(1)
12. V, $A^{\circ 3}$	5704.98(5.04)	2683.83(0.80)
13. ρ_{calcd}, g cm^{-3}	1.266	1.437
14. μ, cm^{-1}	4.9	10.3
15. Mo-K_α radiation	λ = 0.71073 Å	λ = 0.7103 Å
16. T, ^{o}C	25	25
17. Diffractometer	Enraf-Nonius CAD4	Enraf-Nonius CAD4
18. Monochromator	Graphite	Graphite
19. Scan Type	θ - 2θ	θ - 2θ
20. Scan Range	0.80 + 0.35tanθ	0.80 + 0.35tanθ
21. 2θ range, deg	2 - 50	2 - 50
22. Variation in std. intensity	(%) < 1	(%) < 1
23. Corrections	L_p, Decay, Absorption	L_p, Decay, Absorption
24. Reflections collected	5781	10297
25. Independent reflections	5007	9431
26. Parameters	335	649
27. Weighing scheme	Counting Statistics	Counting Statistics
28. Final GOF	3.156	3.074
29. R_f	0.069	0.038
30. R_{wf}	0.055	0.038
31. Largest shift / esd	0.002	0.002
32. Highest residual peak in diff. map e/ $Å^3$	0.45	0.45

Table 3.11 Non-Hydrogen Positional and Isotropic Displacement Parameters for Compound (3).

	x/a	y/b	z/c	U
Mo	1/2	0.32717(9)	3/4	* 0.0615(5)
S(1)	0.4495(1)	0.3001(2)	0.8734(2)	* 0.072(1)
S(2)	0.4208(1)	0.2024(2)	0.7138(2)	* 0.065(1)
O	0.4505(3)	0.3946(4)	0.7022(4)	* 0.079(3)
N(11)	0.3216(5)	0.1919(7)	0.9796(5)	* 0.094(5)
N(21)	0.2875(5)	0.0710(7)	0.7906(6)	* 0.092(5)
C(11)	0.3914(5)	0.2238(7)	0.8617(6)	* 0.059(5)
C(12)	0.3528(5)	0.2054(7)	0.9272(7)	* 0.065(5)
C(21)	0.3780(5)	0.1828(7)	0.7948(6)	* 0.057(4)
C(22)	0.3281(6)	0.1213(8)	0.7930(7)	* 0.065(5)
P	0.1426(1)	0.3276(2)	0.9146(1)	* 0.057(1)
C(31)	0.0668(5)	0.3830(7)	0.9020(6)	* 0.055(5)
C(32)	0.0653(6)	0.4557(8)	0.8593(8)	* 0.089(6)
C(33)	0.0092(8)	0.5052(8)	0.8529(8)	* 0.101(6)
C(34)	-0.0441(7)	0.4827(9)	0.8864(9)	* 0.093(7)
C(35)	-0.0444(6)	0.410(1)	0.9251(9)	* 0.125(8)
C(36)	0.0102(7)	0.3599(7)	0.9345(7)	* 0.097(6)
C(41)	0.1291(5)	0.2179(7)	0.9322(6)	* 0.057(4)
C(42)	0.1507(6)	0.1570(8)	0.8842(6)	* 0.075(5)
C(43)	0.1408(7)	0.0729(8)	0.8972(7)	* 0.094(7)
C(44)	0.1097(7)	0.0464(8)	0.9606(9)	* 0.102(7)
C(45)	0.0896(6)	0.1052(9)	1.0127(7)	* 0.086(6)
C(46)	0.0994(5)	0.1901(7)	0.9994(6)	* 0.074(5)
C(51)	0.1859(5)	0.3769(8)	0.9910(6)	* 0.056(5)
C(52)	0.2154(6)	0.3309(8)	1.0493(7)	* 0.084(6)
C(53)	0.2502(8)	0.3700(9)	1.1039(7)	* 0.103(7)
C(54)	0.2581(7)	0.4547(9)	1.1041(7)	* 0.088(6)
C(55)	0.2305(7)	0.5011(8)	1.0470(8)	* 0.087(6)
C(56)	0.1942(6)	0.4629(8)	0.9914(7)	* 0.076(6)
C(61)	0.1903(5)	0.3384(7)	0.8286(6)	* 0.055(5)
C(62)	0.2552(6)	0.3577(6)	0.8322(5)	* 0.055(5)
C(63)	0.2922(6)	0.3627(7)	0.7660(8)	* 0.076(6)
C(64)	0.2622(8)	0.3472(8)	0.6995(7)	* 0.081(6)
C(65)	0.1975(7)	0.329(1)	0.6958(7)	* 0.093(7)
C(66)	0.1601(5)	0.3232(8)	0.7573(7)	* 0.081(5)
O(2)	1/2	0.333(2)	5/4	* 0.28(2)
C(57)	0.470(2)	0.392(2)	1.211(2)	* 0.35(3)
C(58)	0.444(1)	0.363(2)	1.148(1)	* 0.21(1)

Table 3.12

Bond Distances and Bond Angles For Compound (3)

Distances	Angstroms	Angles	Degree
Mo-O1	1.694(7)	S1-Mo-O1	85.4(2)
Mo-S1	2.449(3)	S2-Mo-O1	107.4(2)
Mo-S2	2.630(3)	Mo-S1-C11	108.1(4)
S1-C11	1.71(1)	S1-C11-C12	115.6(8)
S2-C21	1.71(1)	S2-C21-C22	118.6(9)
C11-C12	1.43(2)	S1-C11-C21	125.2(8)
C21-C22	1.41(2)	S2-C21-C11	122.1(8)
C12-N11	1.14(2)	C11-C12-N11	179.0(1)
C22-N21	1.15(2)	C21-C22-N21	179.0(1)

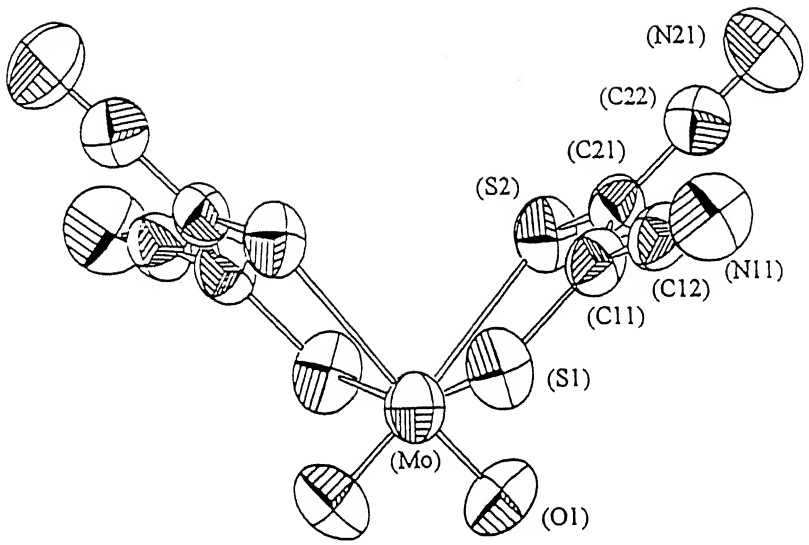

Fig.3.40 Crystal structure of $[Ph_4P]_2[Mo^{VI}O_2(mnt)_2].2H_2O$

Table 3.13. Bond distances and bond angles are listed in Table 3.14. The structure of the anion is shown in Fig.3.41. The complex crystallizes in $P\bar{1}$space group. There is a strong Mo-Mo bonding of bond length 2.582(6)Å which is similar to other reported complexes having $[Mo_2O_4]^{2+}$ core.[66] Each molybdenum atom possess aproximately square-pyramidal coordination with a terminal oxygen atom (O_t) at the apex. Two bridging oxygen (O_b) atoms and two sulfur atoms from mnt have formed the square base of the pyramid. The anion $[Mo_2O_4(mnt)_2]^{2-}$ is comprized of two such square-pyramids sharing a common oxo-bridging edge. Molybdenum atoms are 0.73Å above from their respective basal planes. Interestingly, the molybdenum atoms in this compound are penta coordinated. Related complexes having $[Mo_2O_4]^{2+}$ cores in which the chelating ligand contains donor atoms other than thiolate sulfur frequently but not invariably contains hexa-coordinated Mo(V).[59,66,75] The two Mo-O_t bond lenghts are 1.678(3)Å and 1.680(3)Å, the two mnt ligands are approximately symmetrically bonded to different Mo atoms having mean Mo-S distance 2.433(1)Å.

(e) For $[Bu_4N]_2[Mo_2O_3(Br)_2(mnt)_2]$ **(5)**; the diffraction quality crystals are obtained from the slow diffusion of petroleum ether into a saturated dichloromethane solution of the compound. And for $[Bu_4N]_2[Mo_2O_3(SPh)_2(mnt)_2]$ **(6)**; the diffraction quality crystals are obtained from the undisturbed reaction mixture of the dimeric $[Bu_4N]_2[Mo_2O_4(mnt)_2]$ and thiophenol in CH_2Cl_2 at room temperature. The summary of the crystal data for **(5)** and **(6)** are given in Table 3.15. Positional and isotropic thermal parameters for the non-hydrogen atoms are listed in Table 3.16 and Table 3.18

Table 3.13 Non-Hydrogen Positional and Isotropic Displacement Parameters for Compound (4).

	x/a	y/b	z/c	U
Mo(1)	0.89498(3)	0.86685(3)	0.33618(2)	0.0387(1)
Mo(2)	0.94425(3)	0.74103(3)	0.24247(2)	0.0377(1)
S(1)	0.6956(1)	0.9382(1)	0.37999(7)	0.0503(4)
S(2)	0.9459(1)	1.0485(1)	0.32095(7)	0.0540(5)
S(3)	1.0477(1)	0.78311(9)	0.11771(6)	0.0469(4)
S(4)	0.8033(1)	0.66567(9)	0.18480(6)	0.0464(4)
O(1)	0.9530(3)	0.8047(2)	0.4098(2)	0.057(1)
O(2)	1.0207(3)	0.6369(2)	0.2843(2)	0.058(1)
O(3)	1.0093(2)	0.8735(2)	0.2468(1)	0.043(1)
O(4)	0.7964(2)	0.7744(2)	0.3039(1)	0.042(1)
C(1)	0.7190(4)	1.0617(3)	0.3953(2)	0.047(2)
C(11)	0.6197(5)	1.1188(4)	0.4330(3)	0.060(2)
N(1)	0.5429(4)	1.1665(4)	0.4609(3)	0.086(2)
C(2)	0.8251(4)	1.1079(4)	0.3720(2)	0.051(2)
C(21)	0.8443(5)	1.2076(4)	0.3888(3)	0.072(2)
N(2)	0.8624(5)	1.2857(4)	0.4031(3)	0.117(3)
C(3)	0.9803(4)	0.7115(3)	0.0682(2)	0.041(2)
C(31)	1.0342(4)	0.7117(4)	-0.0057(3)	0.050(2)
N(3)	1.0788(4)	0.7152(4)	-0.0651(2)	0.076(2)
C(4)	0.8770(4)	0.6623(3)	0.0967(2)	0.043(2)
C(41)	0.8198(4)	0.6074(4)	0.0535(3)	0.054(2)
N(4)	0.7717(4)	0.5632(4)	0.0212(2)	0.081(2)
P(1)	0.4575(1)	0.88211(9)	0.15955(6)	0.0393(4)
P(2)	0.7039(1)	0.67386(9)	0.65982(6)	0.0417(4)
C(28)	0.8303(4)	1.0055(4)	0.0996(3)	0.070(2)
C(17)	0.3658(4)	0.8213(4)	0.0469(2)	0.049(2)
C(34)	0.6743(7)	0.9927(4)	0.6241(4)	0.099(3)
C(6)	0.5096(4)	0.7885(4)	0.2967(2)	0.048(2)
C(13)	0.4835(5)	0.6895(4)	0.1158(3)	0.065(2)
C(36)	0.8446(5)	0.9413(4)	0.5467(3)	0.061(2)
C(38)	0.7487(4)	0.6058(3)	0.5849(2)	0.042(2)
C(18)	0.3629(4)	1.0006(3)	0.1430(2)	0.039(2)
C(54)	0.8401(6)	0.5090(4)	0.8348(3)	0.071(2)
C(5)	0.4245(4)	0.8142(3)	0.2509(2)	0.043(2)
C(53)	0.7697(5)	0.5417(4)	0.7814(3)	0.060(2)
C(16)	0.3452(4)	0.7478(5)	0.0069(3)	0.064(2)
C(9)	0.2785(5)	0.7321(4)	0.3474(3)	0.077(2)
C(43)	0.8638(4)	0.4678(3)	0.5306(3)	0.056(2)
C(26)	0.6482(4)	0.9839(4)	0.1830(3)	0.052(2)
C(25)	0.6096(4)	0.9225(3)	0.1391(2)	0.041(2)
C(56)	0.9641(5)	0.6501(5)	0.7852(3)	0.072(2)
C(30)	0.6817(4)	0.9025(4)	0.0757(2)	0.050(2)
C(52)	0.7957(4)	0.6291(3)	0.7300(2)	0.045(2)
C(20)	0.1703(4)	1.0933(4)	0.1472(3)	0.074(2)
C(12)	0.4346(4)	0.7925(3)	0.1022(2)	0.042(2)
C(32)	0.7247(4)	0.8098(3)	0.6251(2)	0.042(2)
C(24)	0.4126(4)	1.0943(4)	0.1098(3)	0.054(2)
C(37)	0.8219(4)	0.8369(4)	0.5721(2)	0.052(2)
C(44)	0.8286(4)	0.5169(3)	0.5901(2)	0.049(2)
C(39)	0.7080(4)	0.6443(4)	0.5194(3)	0.055(2)
C(29)	0.7928(4)	0.9452(4)	0.0564(3)	0.063(2)
C(40)	0.7458(5)	0.5954(4)	0.4600(3)	0.063(2)
C(23)	0.3418(5)	1.1862(4)	0.0950(3)	0.060(2)
C(22)	0.2211(5)	1.1856(4)	0.1142(3)	0.065(2)
C(27)	0.7598(5)	1.0250(4)	0.1628(3)	0.065(2)

Table 3.14

Bond Distances and Bond Angles for Compound (4)

Distances	Angstroms	Angle	Degree
Mo1-Mo2	2.582(6)	S1-Mo1-S2	83.04(4)
Mo1-O1	1.678(3)	S1-Mo1-O1	107.0(1)
Mo1-S1	2.434(1)	S1-Mo1-O3	139.74(9)
Mo1-S2	2.423(1)	S1-Mo1-O4	79.63(8)
Mo1-O3	1.938(3)	S2-Mo1-O1	105.2(1)
Mo1-O4	1.946(3)	S2-Mo1-O3	80.97(9)
Mo2-O2	1.680(3)	S2-Mo1-O4	143.25(8)
Mo2-S3	2.433(1)	O1-Mo1-O3	112.8(1)
Mo2-S4	2.439(1)	O1-Mo1-O4	110.8(2)
Mo2-O3	1.945(3)	O3-Mo1-O4	91.8(1)
Mo2-O4	1.934(3)	S3-Mo2-S4	82.99(4)
S1-C1	1.726(5)	S3-Mo2-O2	107.0(1)
S2-C2	1.742(5)	S2-Mo2-O3	80.30(8)
S3-C3	1.734(5)	S3-Mo2-O4	141.21(8)
S4-C4	1.736(4)	S4-Mo2-O2	105.0(1)
C1-C11	1.448(7)	S4-Mo2-O4	80.6(1)
C11-N1	1.134(7)	O2-Mo2-O3	111.9(1)
C2-C21	1.427(8)	O2-Mo2-O4	111.1(1)
C21-N2	1.138(9)	O3-Mo2-O4	91.9(1)
C3-C31	1.423(6)	Mo1-S1-C1	104.4(2)
C31-N3	1.144(6)	Mo1-S2-C2	104.2(2)
C4-C41	1.439(7)	Mo2-S3-C3	105.1(1)
C41-N4	1.137(8)	Mo2-S4-C4	104.5(2)
C1-C2	1.359(6)		
C3-C4	1.362(6)		

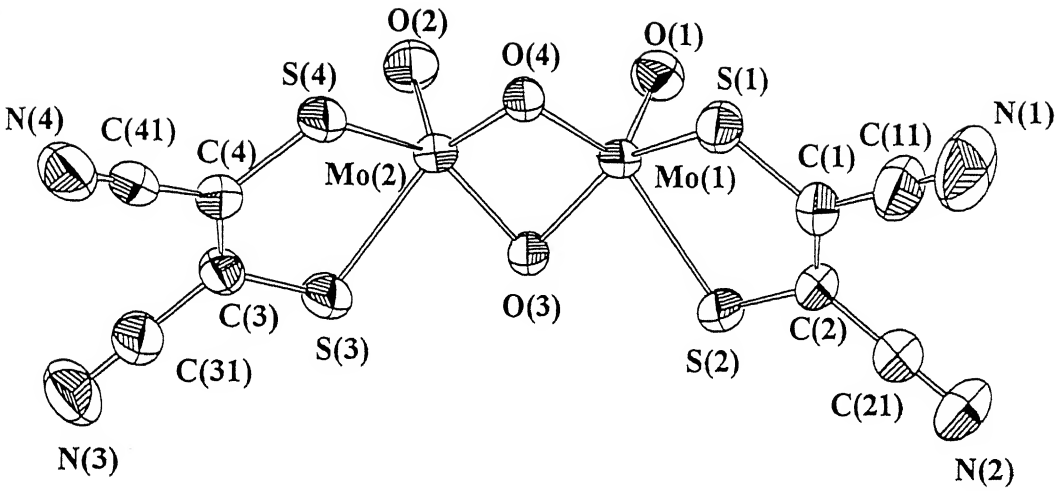

Fig.3.41 Crystal structure of $[Ph_4P]_2[Mo^{V}_2O_4(mnt)_2]$

Table 3.15

Summary of X-ray crystallographic data for complexes 5 and 6 :

	$[Bu_4N]_2[Mo_2O_3(SPh)_2(mnt)_2]$(5)	$[Bu_4N]_2[Mo_2O_3(Br)_2(mnt)_2]$(6)
1. Chemical formula	$C_{52}H_{82}Mo_2N_6O_3S_6$	$C_{40}H_{72}Br_2Mo_2N_6O_3S_4$
2. Formula weight	1223.55	1165.01
3. Crystal dimension, mm	0.6 x 0.5 x 0.3	0.45 x 0.3 x 0.18
4. Space group	$P2_1/n$	$P2_1/c$
5. Z	2	2
6. a, Å	9.416(2)	11.868(2)
7. b, Å	24.294(6)	8.505(5)
8. c, Å	13.738(5)	27.416(5)
9. β, deg	98.56(2)	91.34(1)
10. V, $Å^3$	3108(2)	2766.5(1.01)
11. ρ_{calcd}, g cm^{-3}	1.308	1.398
12. μ, cm^{-1}	6.47	20.8
13. Mo-K_α radiation	λ = 0.71073 Å	λ = 0.71073 Å
14. T, °C	25	25
15. Diffractometer	Enraf-Nonius CAD4	Enraf-Nonius CAD4
16. Monochromator	Graphite	Graphite
17. Scan Type	Θ - 2Θ	Θ - 2Θ
18. Scan Range	0.80 + 0.35tanΘ	0.80 + 0.35tanΘ
19. 2Θ range, deg	2 - 50	2 - 50
20. Variation in std. intensity(%)	< 1	< 1
21. Corrections	L_p, Decay, Absorption	L_p, Decay, Absorption
22. Reflections collected	3109	3550
23. Independent reflections	2857	3458
24. Final GOF	1.105	0.966
25. R_f	0.0538	0.058
26. R_{wf}	0.156	0.185
27. Largest shift / esd	0.002	0.002
28. Highest residual peak in diff. map e/ $Å^3$	0.45	0.45
29. Data parameter ratio	8	20
30. Parameters	296	213

Table 3.16

Atomic Coordinates (x 10^4) and Equivalent Isotropic Displacement Parameters (A^2x 10^3) for Compound (5)

	X	Y	Z	U(EQ)
Mo	-1089(1)	1440(1)	181(1)	86(1)
Br1	-2131(1)	935(2)	-615(1)	108(1)
S1	-735(2)	525(4)	987(1)	90(1)
S2	-2978(3)	1690(5)	455(1)	115(1)
O1	-569(8)	3269(11)	144(3)	138(3)
O2	0	0	0	109(3)
N1	-1799(10)	601(15)	2227(4)	145(4)
N2	-4662(14)	2038(28)	1551(5)	248(10)
C1	-1915(10)	986(12)	1307(3)	85(3)
C2	-2871(10)	1442(14)	1082(4)	101(3)
C3	-1877(11)	789(17)	1810(4)	117(4)
C4	-3860(5)	1756(9)	1342(2)	164(7)
N3	-2303(5)	5756(9)	-1328(2)	85(2)
C5	-3353(5)	5295(9)	-1612(2)	142(5)
C6	-3840(5)	3706(9)	-1525(2)	171(7)
C7	-4897(5)	3432(9)	-1817(2)	223(10)
C8	-5321(5)	1773(9)	-1818(2)	283(14)
C9	-2414(11)	5599(16)	-784(5)	125(4)
C10	-3383(11)	6421(17)	-559(5)	125(4)
C11	-3194(14)	6516(25)	-11(5)	183(8)
C12	-4145(17)	7245(25)	256(8)	195(7)
C13	-1365(11)	4636(15)	-1461(5)	117(4)
C14	-232(12)	4960(17)	-1275(5)	131(5)
C15	604(12)	3718(24)	-1401(7)	189(8)
C16	1769(15)	4045(23)	-1216(7)	181(6)
C17	-2027(13)	7452(18)	-1450(5)	136(5)
C18	-1709(13)	7765(20)	-1949(5)	186(7)
C19a	-2135(13)	9141(20)	-2239(5)	2581(6)
C20a	-1475(13)	10554(20)	-2065(5)	258(16)
C19b	-1301(13)	9357(20)	-2130(5)	251(14)
C20b	-2253(13)	10392(20)	-1996(5)	251(14)

Table 3.17

Bond Distances and Bond Angles for Compound (5)

Distances	Angstroms	Angles	Degree
Mo-O1	1.677(9)	O1-Mo-O2	109.7(4)
Mo-O2	1.8562(10)	O1-Mo-S1	107.6(3)
Mo-S1	2.371(3)	O1-Mo-S2	106.6(4)
Mo-S2	2.391(3)	O1-Mo-Br1	106.3(3)
Mo-Br1	2.519(14)	Br1-Mo-O2	89.27(5)
S1-C1	1.717(11)	Br1-Mo-S1	145.46(9)
S2-C2	1.734(12)	Br1-Mo-S2	80.93(9)
C1-C2	1.336(14)	Mo-S1-C1	105.9(4)
C1-C3	1.387(12)	Mo-S2-C2	104.7(4)
C3-N1	1.156(13)	S1-C1-C3	118.2(9)
C2-C4	1.414(11)	S2-C2-C4	115.8(9)
C4-N2	1.15(2)	C1-C3-N1	177.1(14)
C1-C2	1.336(14)	C2-C4-N2	178.7(14)
		Mo-O2-Mo1	180.0

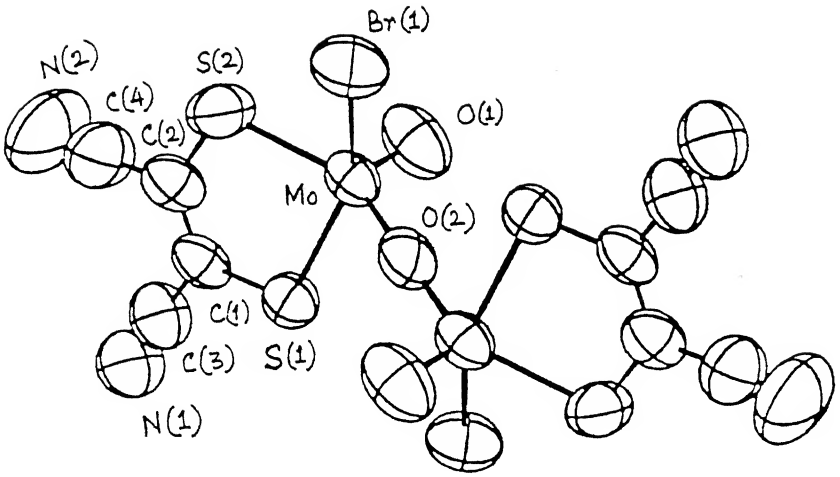

Fig.3.42 Crystal structure of $[Bu_4N]_2[Mo^V_2O_3(Br)_2(mnt)_2]$

Table 3.18

Atomic Coordinates (x 10^4) and Equivalent Isotropic Displacement Parameters (A^2x 10^3) for Compound (6)

	X	Y	Z	U(EQ)
Mo	468(1)	696(1)	-432(1)	51(1)
S1	1741(3)	1188(1)	-1565(1)	60(1)
S2	-1117(3)	458(1)	-1916(1)	68(1)
S3	2790(3)	511(1)	455(1)	65(1)
O1	-295(8)	1174(3)	182(4)	76(2)
O2	0	0	0	64(3)
N1	1357(11)	1754(3)	-4088(5)	91(3)
N2	-2174(12)	833(4)	-4517(5)	111(4)
C1	594(12)	1175(3)	-2684(5)	63(4)
C2	-605(13)	865(3)	-2828(5)	61(4)
C3	1037(12)	1496(3)	-3461(5)	72(4)
C4	-1489(13)	850(3)	-3775(5)	80(4)
C5	3923(13)	1060(3)	260(5)	46(3)
C6	3640(11)	1587(4)	609(5)	67(3)
C7	4565(15)	2016(4)	451(6)	66(4)
C8	5802(16)	1926(5)	37(7)	70(3)
C9	6043(13)	1410(5)	-288(6)	77(3)
C10	5150(15)	963(4)	-139(7)	64(3)
N3	1391(8)	-1528(2)	-2858(4)	56(3)
C11	2229(11)	-1062(3)	-2297(5)	65(3)
C12	2646(13)	-590(3)	-2935(6)	82(4)
C13	3610(14)	-199(4)	-2336(7)	102(4)
C14	4125(17)	266(5)	-2914(9)	126(5)
C15	1049(11)	-1927(3)	-2079(5)	59(3)
C16	275(13)	-2445(4)	-2449(6)	82(4)
C17	-15(12)	-2777(4)	-1596(6)	108(5)
C18	-814(12)	-3310(4)	-1813(6)	164(7)
C19	2308(12)	-1808(3)	-3554(5)	60(3)
C20	3676(12)	-2047(3)	-3097(6)	66(4)
C21	4466(15)	-2299(4)	-3888(8)	90(5)
C22	5851(17)	-2550(5)	-3514(11)	127(6)
C23	15(11)	-1315(4)	-3472(6)	67(4)
C24	-1125(15)	-1077(4)	-2921(8)	117(5)
C25A	-2541(15)	-883(4)	-3527(8)	225(14)
C26A	-2077(15)	-668(4)	-4502(8)	225(14)
C25B	-2017(38)	-724(14)	-3592(26)	204(12)
C26B	-3400(39)	-1018(21)	-4000(39)	204(12)

Table 3.19

Bond Distances and Bond Angles for Compound (6)

Distances	Angstroms	Angles	Degree
Mo-O1	1.661(6)	O1-Mo-O2	109.4(2)
Mo-O2	1.866(7)	O1-Mo-S3	107.8(2)
Mo-S1	2.418(2)	O2-Mo-S3	84.75(6)
Mo-S2	2.411(2)	O1-Mo-S2	109.8(2)
Mo-S3	2.382(3)	O2-Mo-S2	84.60(6)
S1-C1	1.743(8)	S3-Mo-S2	142.44(10)
S2-C2	1.722(8)	O1-Mo-S1	105.9(2)
S3-C5	1.747(10)	S3-Mo-S1	85.25(9)
C1-C2	1.346(13)	S2-Mo-S1	83.01(8)
C1-C3	1.434(11)	Mo-S3-C5	108.6(3)
C2-C4	1.437(11)	Mo-S1-C1	104.9(3)
C3-N1	1.141(9)	Mo-S2-C2	105.8(3)
C4-N2	1.123(11)	Mo-O2-Mo1	180.0

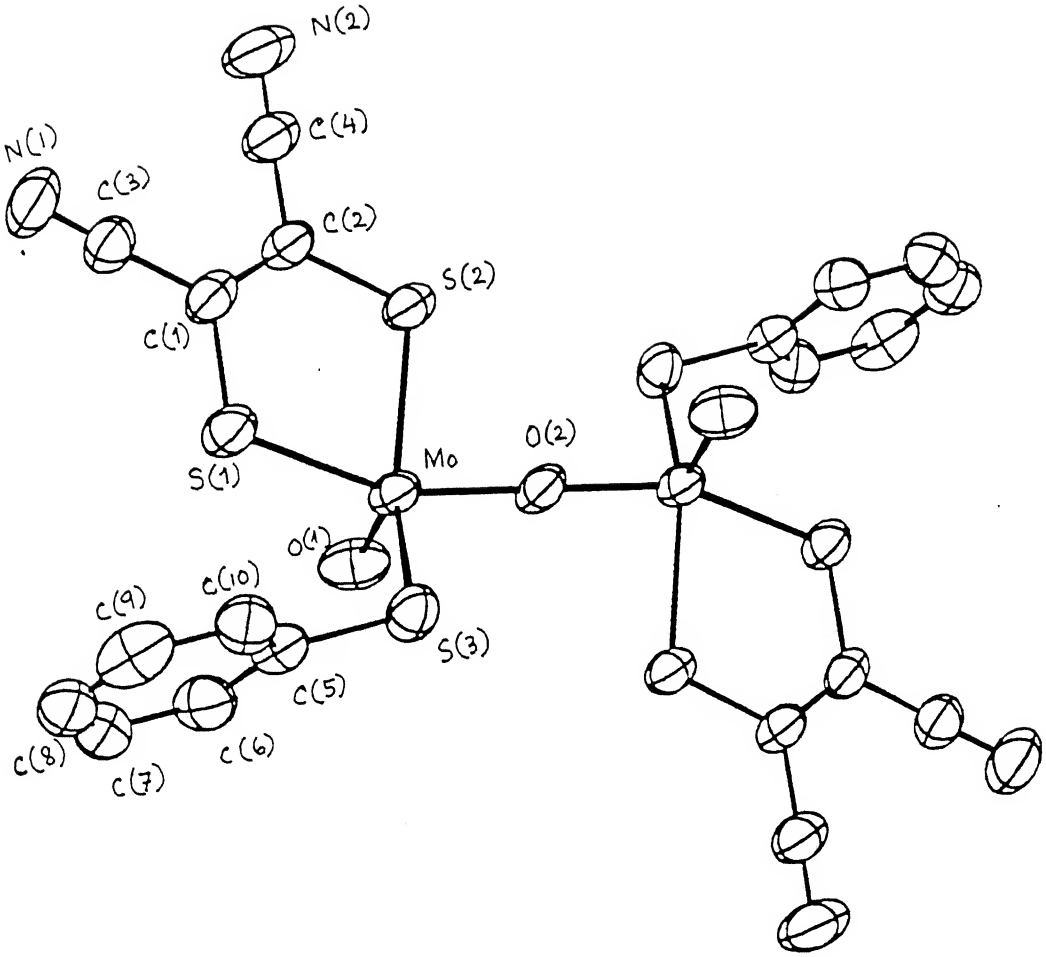

Fig.3.43 Crystal structure of $[Bu_4N]_2[Mo^V_2O_3(SPh)_2(mnt)_2]$

respectively. Bond distances and bond angles are given in Table 3.17 and Table 3.19 respectively. The structures of the anions are shown in Figure 3.42 and Figure 3.43 respectively. Both these structures contain a linear Mo-O-Mo bridging unit, have crystallographically imposed center of symmetry and the oxo groups are trans to each other. The bridging oxygen atom of the anions located at the inversion center, the assymetric units of the complexes (5) and (6) comprize with half of the anion and one Bu_4N^+ cation. Each crystallographically independent Mo atom in both the complexes is pentacoordinated in a distorted square-pyramidal arrangement. The distortion of the coordination sphere are reflected in the wide range of angles formed by the donor atoms at the metal center[83.01(8)^o to 144.69(6)^o in (5) and 80.93(9)^o to 145.46(9)^o in (6)]. The Mo atoms are situated at 0.705 Å and 0.680(2) Å above the basal plane of (5) and (6) respectively. One of the cations in (5) and (6) is orientationally disordered about the CH_3CH_2 positions.

CHAPTER 4

RESULTS AND DISCUSSION

SYNTHETIC DISCUSSION:

The synthesis of $[Bu_4N]_2[Mo^{VI}O_2(mnt)_2]$ used in the present study was made as reported earlier.[33a] The role of phosphate buffer in achieving the desired product was suggested due to the stabilization of MoO_2^{2+} moiety present in equilibrium with other polymolybdate species around pH~ 6.[2] Oxalate is known to form anionic binuclear oxo complexes having *cis* MoO_2^{2+} moiety with one Mo-O-Mo group.[90] So addition of oxalic acid in aqueous molybdate solution may lead to the stabilization of *cis* MoO_2^{2+} moiety over other existing species. The isolation of $[Et_4N]_2[Mo^{VI}O_2(mnt)_2]$ using oxalic acid instead of phosphate buffer strongly support the view that incorporation of molybdenum has occured as *cis* MoO_2^{2+} moiety in desired dithiolene ligated complex which may suggest the mechanism of biological incorporation of this metal into free molybdopterin. In the reconstitution assay using Moco and *nit-1* mutant of *N.crassa* to yield active nitrate reductase, the stability of the isolated cofactor was reported to be low and it has been observed that the isolated cofactor became inactive due to the loss of molybdenum coordinated to molybdopterin. The activity of the cofactor is enhanced by the addition of exogenous molybdate presumably due to the enhanced rate of the back reaction of the hydrolytic cleavage of Mo-co.[30b] However it has been suggested that when the Mo-co dissociate into the molybdate and free molybdopterin (MPT) the resulting molybdate instantaneously acquire low activity to reconstitute the Moco similar to the low

activity of exogenous MoO_4^{2-} used. This suggest that the incorporation or released of molybdenum into molybdopterin or from Moco is not in the form of tetrahedral molybdate[12a], it is suggested,therefore, that the incorporation of molybdenum into Moco is possibly happen in the form of polymolybdate or in the form of some loosely complexed form of Mo(VI) containing the active *cis* MoO_2^{2+} moiety.

The high yield synthesis of $[Mo^{VI}O_2(mnt)_2]^{2-}$ from $[Mo^{IV}O(mnt)_2]^{2-}$ using trimethylamine N-oxide(TMANO) is a good example of oxotransfer reaction of the native enzyme, trimethylamine N-oxide TMANO reductase. The detailed pH dependent kinetics of this reaction is discussed latter(*vide infra*). Interestingly for this oxotransfer reaction the solvent used play an important role. Thus in DMF solvent the oxotransfer from TMANO to $[MoO(mnt)_2]^{2-}$ complex is extremely slow. This reaction does not proceed appreciably even using acetic acid in other polar solvents like CH_3CN or aqueous CH_3CN . However, a CH_2Cl_2 solution of $[MoO_2(mnt)_2]^{2-}$ when mixed with an aqueous solution of TMANO the reaction does not proceed but on the addition of trace amount of acetic or benzoic acid or even dilute H_2SO_4 lead to completion of the oxotransfer reaction in the CH_2Cl_2 phase. These observations suggest that the oxotransfer reagent is probably the protonated form of TMANO which may readily transfer to CH_2Cl_2 phase by forming ion-pair resulting the said oxotransfer reaction. The failure of reaction in DMF even under protic condition may be due to the formation of DMF solvated protonated TMANO.[91] Proton translocation coupled to TMANO reduction is reported in *E.coli* which when grown in the presence of TMANO to induce the function

reduced inside the cell or on the outer surface of the cell membrane, yet the role of membrane bound TMANO reductase strongly suggest the involvement of hydrophobic phospholipid membrane in this redox coupled phosphorylation reaction. The facile oxotransfer reaction in the CH_2Cl_2 layer with the synthesized complex, presented here, is a good example to demonstrate the involvement of hydrophobic site (CH_2Cl_2 phase) of the said reaction.

Membrane bound TMANO reductase of *E.coli* , accepts electrons from NADH/ formate/ lactate through the b-type and c-type cytochromes.[92] This suggest that once TMANO reductase gets oxidized at the molybdenum center by TMANO, the oxidized molybdenum center gets reduced by some physiological reductants as stated above. These reductants do not directly involve in reducing the oxidized center for its regeneration but act via hemeproteins. However thiols are known to be good physiological reducing agent in several biochemical reactions. The reduction of $[MoO_2(mnt)_2]^{2-}$ using thiophenol to $[MoO(mnt)_2]^{2-}$ in 90% yield is a good model reaction where regeneration of the reduced form is achieved (for detail kinetics *vide infra*). The synthesis of $[MoO(mnt)_2]^{2-}$ using protonated cation like PyH^+, $bipyH^+$, Et_3NH^+ or even with lysinium ion$(C_6H_{15}N_2O_2)^+$ is interesting in the sense that the Moco is an anionic species. Considering the presence of only one molybdopterin ligation the suggested involvement of a thiolate bonding from protein[12a] leaves out negative charge which must be discipitated through hydrogen bonding. Furthermore the chemistry of denaturation experiments to isolate Moco from molybdoenzymes invariably involve denaturants like guanidinium$^+$ or SDS (sodium dodecyl sulfate) like cationic species. It may be presumed that

these cationic species effectively stabilize the counter anionic Moco thus facilitating its release from the apoprotein. The involvement of DMSO as denaturant in some of these enzymes does not fall exactly on these arguments just stated above. However the extensive use of buffer in these experiments may readily supply alkali metal ions and solvated cationic species like $[Na(DMSO)_2]^+$ has been demonstrated to form salt with anionic molybdenum complex.[93]

In the alkylation reactions it has been clearly shown that such reaction does not require the hydrolytic release of reactive sulfhydryl groups. It is also important to note that this alkylation reaction is of general nature which is not dependent only on the iodoacetamide but can be extended to methyliodide where the characterization of the methylated organic part became easier. However, iodoacetamide has the advantage of its solubility in polar solvents including water, which is the most relevant solvent for biochemical work. The isolation of $[Bu_4N]_2[Mo_6O_{19}]$ from these reactions is important in the context that in the reconstitution assay it has been shown that the incorporation of exogenous molybdate used required time. From the chemistry point of view it is well known that polymetalate ions are better source of metal than the rigid MoO_4^{2-} ion in a particular reaction. Polymetalate ions are generaly formed by protonation of MoO_4^{2-} ion in the reaction conditions used herein. The solvent CH_3CN containing roughly 5% water may account for the generation of some HI when excess of alkylating agent was used and this acidity may be sufficient to trigger the condensation reaction. Interestingly, when MoO(IV) complex was used the products obtained were hexavalent polymolybdate, pentavalent dimer, $[Bu_4N]_2[Mo_2O_4(mnt)_2]$

, and tetravalent, $[Bu_4N]_2[Mo(mnt)_3]$. These reactions were carried out under argon and the formation of Mo(VI) and Mo(V) complexes from Mo(IV) complex may be due to the presence of iodine which may form under photodissociation of the alkylating agent even under diffused laboratory light. Once this iodine is formed this can oxidise Mo(IV) to Mo(V) readily.[33a] The intermediate monomeric MoO(V) species is known to disproportionate to produce Mo(VI) and Mo(VI). At this stage, a part of the released ligand is alkylated in the presence of excess of alkylating agent. The pentavalent species with monodithiolene coordination attain stability by dimerization. The longer time involvement in the alkylation reaction of reduced MoO(IV) species may be due to the slow release of photodissociated free iodine. For the corresponding WO(IV) complex the need for the oxidation of this species to the corresponding pentavalent complex to participate similar reactions like its molybdenum analogue does not arise because WO(IV) species even in anaerobic condition was not stable in solution in the presence of water and rapidly destabilized in the presence of acid.[84] Interestingly, our search for the isolation of dimeric WO(V) species similar to the molybdenum one failed. This is due to the greater tendency of W(V) species responding disproportionation specially under polar environment and particularly in the presence of water.[84]

The isolation of $[Mo_2O_4(mnt)_2]^{2-}$ as a product in the above stated alkylation reactions in low yield restricts its detail chemical ractivity studies. Therefore a high yield direct synthesis of this species from molybdate is achieved.

Its reaction with HX (X= Cl, Br) and with thiophenols is highly interesting yielding complexes having the general

formulation $[Mo_2O_3X_2(mnt)_2]^{2-}$ (X= Cl, Br, SPh, *p*-chlorothiophenol). The dithiolene thiolato complex is important in the sense that it contains one dithiolene and one thiophenolate ligation attached per molybdenum (X-ray structure *vide infra*). These complexes show interesting hydrolytic properties which in the presence of trace amounts of moisture (or water) converted back into the starting di-μ-oxo bridged $[Mo_2O_4(mnt)_2]^{2-}$ involving interesting monomeric EPR active species(*vide infra*). The thiol derivative in the presence of excess thiophenol also converted to monomeric EPR active species (*vide infra*).

The conversion of the dimeric $[Mo_2O_4(mnt)_2]^{2-}$ into monomeric $[MoO(mnt)_2]^{2-}$ is interesting. Mo(V) dimer generally respond to disproportionation reactions yielding Mo(IV) and Mo(VI) species. The present complex, $[Mo_2O_4(mnt)_2]^{2-}$, is shown to yield pentavalent monoxo dimer containing $Mo_2O_3^{4+}$ core even under high acidic conditions. This suggest that at least in acidic to neutral solutions this is not susceptible to disproportionation reaction. The isolation of $[MoO(mnt)_2]^{2-}$ from this complex in the presence of ammonium citrate in 50% yield thus suggest the involvement of ammonium citrate as the reducing agent in this reaction. The yield of $[MoO(mnt)_2]^{2-}$ is increased when one equivalent of mnt^{2-} is used in this reaction. It is known that mnt^{2-} is a mild reducing agent so when three equivalents of mnt^{2-} alone is used similar higher yield of the MoO(IV) complex is obtained. With one equivalent of mnt^{2-} in the presence of $NaHSO_3$ lead to 80% isolation of the $[MoO(mnt)_2]^{2-}$ species. All these reactions suggest that $[Mo_2O_4(mnt)_2]^{2-}$ is susceptible to reduction even under mild reducing condition to produce monomeric $[MoO(mnt)_2]^{2-}$ species. These reactions implicate a possible chemistry in relation to the

isolation of Moco using ascorbic acid or other reducing agents. The reported stability of the reduced Moco under anaerobic condition using dithionite in aqueous medium[30], once more strongly suggest that MoO(IV) species with dithiolene coordination may remain as such is most likely as bis molybdopterin coordinated species. The intact activity of the reduced Moco even after 24 hrs. standing[30] also suggest the stability of the possible bis coordinated species similar to the synthesized $[MoO(mnt)_2]^{2-}$ complex.

The retention of the Mo(V) species is observed using strong chelating ligands like bipy to isolate $[Mo_2O_3(bipy)_2(mnt)_2]$ from $[Mo_2O_4(mnt)_2]^{2-}$. The conversion of $Mo_2O_4^{2+}$ core to $Mo_2O_3^{4+}$ core probably took place by protonation from acetic acid used in the reaction . This is found to be true when the reaction is carried out with $[Mo_2O_3Br_2(mnt)_2]^{2-}$ instead of $[Mo_2O_4(mnt)_2]^{2-}$ in the absence of any acid. These conversions yielding the same product do suggest protonation in the earlier reaction. When the $[Mo_2O_3(Br)_2(mnt)_2]^{2-}$ compound is treated with excess of thiophenol in CH_2Cl_2 solution , the red-brown microcrtstalline compound $[Mo_2O_3(SPh)_2(mnt)_2]^{2-}$ was obtained. This reaction suggest the greater tendency to form the latter complex with sulfur ligation.

SECTION 4.1

FUNCTIONAL ANALOGUE REACTION OF TRIMETHYLAMINE N-OXIDE REDUCTASE :

Trimethylamine N-oxide (TMANO) reductase, an inducible terminal enzyme for anaerobic respiration of bacteria like *Escherichia coli*[92a,94], *Salmonella tiphimurium*[95] and *Proteus spp*[96], contains molybdenum cofactor common to all oxomolybdo-enzymes.[12c,79b] The molybdenum cofactor is proposed to be a complex of molybdopterin and molybdenum, with the metal linked to dithiolene moiety of molybdopterin.[12c] This TMANO reductase generally shows activity with ClO_3^- but no activity with NO_3^- and no or a little (pH dependent) activity with dimethylsulfoxide (DMSO).[79b] It has been shown earlier that the model complex $[MoO(mnt)_2]^{2-}$ mimics the activity of trimethylamine N-oxide reductase.[97] It has also been reported that Cl^- ion competitively inhibits the oxotransfer reaction[97] as shown in figure 4.1.1 and Figure 4.1.2. The kinetic evidence of *cis* binding has been supported by the EPR and cyclic voltammetric studies on the one electron oxidized species $[MoO(mnt)_2]^-$ and with Mo(V)/Mo(IV) redox couple involved in the absence and the presence of Cl^- ion.[33a]

However TMANO is a unique substrate among all the known physiological oxotransfer agents which may exist in the following form in aqueous medium :

$$(CH_3)_3NO + H_2O \rightleftharpoons (CH_3)_3NOH^+ + OH^- \qquad \text{---------(4.1)}$$

The involvement of this substrate in membrane bound enzyme coupled with phosphorelation reaction is interesting. It has been shown that when TMANO was to anaerobic suspension of *E.coli* rapid acidification of the medium was observed.[79c] The apperant H^+/TMANO

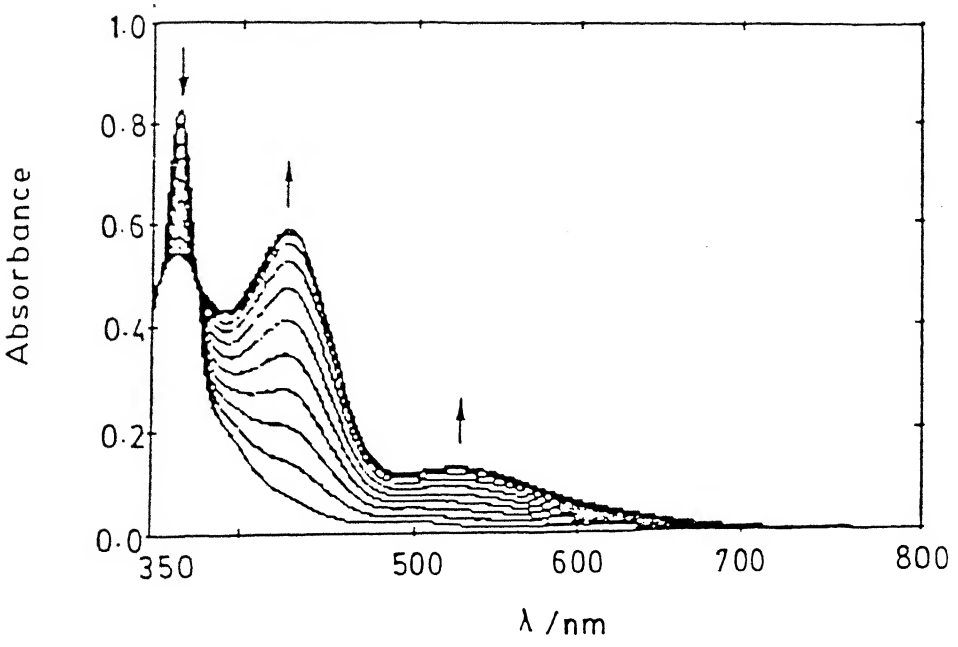

Fig.4.1.1 (a) Spectral changes for the reaction between $[Bu_4N]_2$-$[Mo^{IV}O(mnt)_2]$ (0.9 x 10^{-4} M) and $(CH_3)_3NO.2H_2O$ (1.8 x 10^{-3} M) in acetone-acetic Acid (effective pH = 6) at 20 ± 0.1°C.

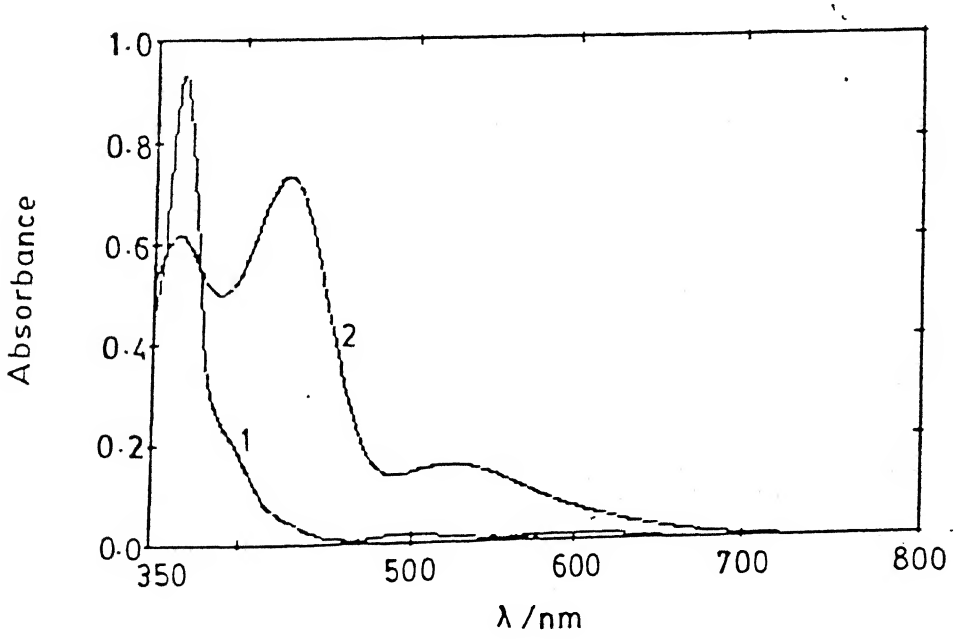

Fig.4.1.1 (b) UV-visible absorption spectra of $[Bu_4N]_2[Mo^{IV}O(mnt)_2]$ 1 and $[Bu_4N]_2[Mo^{VI}O_2(mnt)_2]$ 2 in acetone-acetic Acid (effective pH 6).

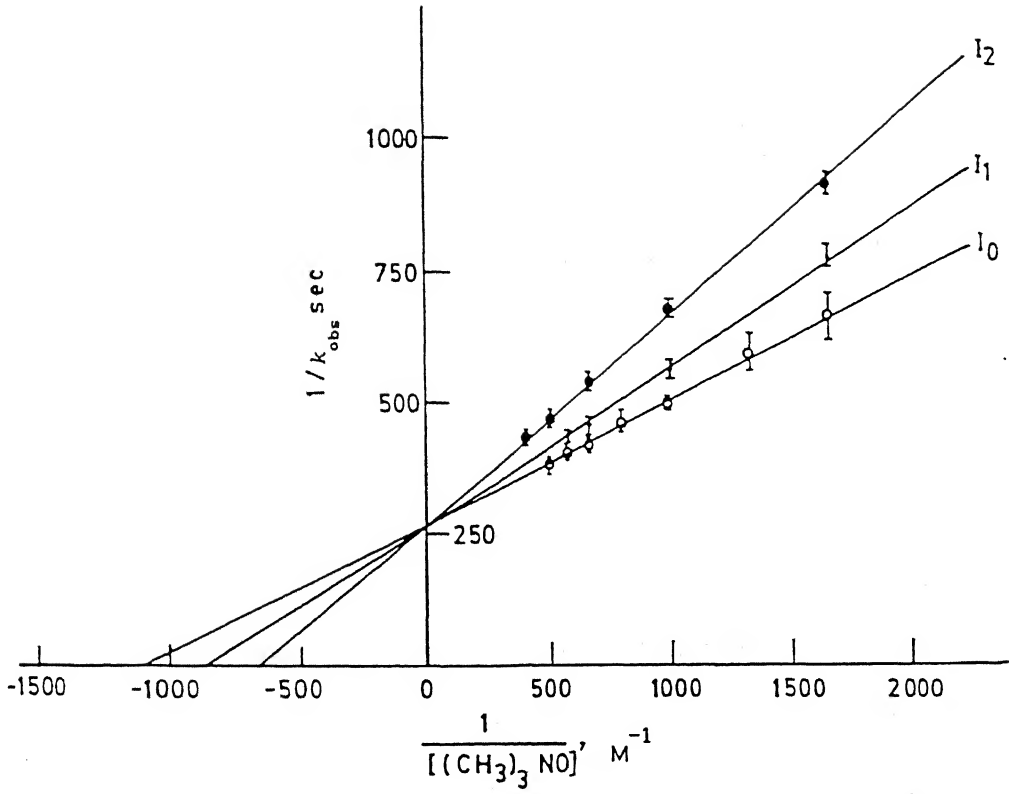

Fig. 4.1.2 Double reciprocal plots, each containing 1 x 10^{-4}M of $[Bu_4N]_2[Mo^{IV}O(mnt)_2]$ with varying concentrations of $(CH_3)_3NO.2H_2O$; I_o represents reaction without Cl^- as inhibitor. I_1 and I_2 represent reactions carried out in the presence of Bu_4NCl as inhibitor with fixed concentrations of 8 x 10^{-4}M and 15 x 10^{-4}M respectively (reaction medium: acetone-acetic acid with effective pH 6)

ratio in cells oxidizing endogenous substrates was found to be 3 to 4 gram-ions of H^+ translocated per mole of TMANO. These findings raise the question whether the actual substrate is TMANO or its protonated form. It is also to be noted that the reduced product of TMANO gets protonated with the consumption of one proton per trimethylamine form as :

$$(CH_3)_3NO + 2[H] + H^+ \longrightarrow (CH_3)_3NH^+ + H_2O \quad \text{-------(4.2)}$$

To understand the pH effect of the model reaction the pH dependent kinetics of the oxotransfer reaction

$$\underset{\textbf{(E)}}{[MoO(mnt)_2]^{2-}} + \underset{\textbf{(S)}}{(CH_3)_3NO} \xrightarrow{H^+} \underset{\textbf{(E')}}{[MoO_2(mnt)_2]^{2-}} + \underset{\textbf{(P)}}{(CH_3)_3NH^+}$$

----------(4.3)

was performed and the dependence of k_{obs} *vs* pH at a fixed nonsaturation concentration of TMANO has been shown in Table 4.1. Each of the oxotransfer reactions at a particular pH in the range used followed substrate saturation behavior. The dependence of k_{obs} against substrate concentrations and the corresponding double reciprocal plots of these reactions are reproduced in Figures 4.1.3(a,b,c,d,e&f). The observed rate k_{obs} for the reaction (3) was found to be in agreement with the reaction scheme as shown in Scheme 4.1.1.

DERIVATION OF THE RATE EXPRESSION :

Rate expressions were derived for different model schemes and experimental data fitting was tried with those expressions . The scheme **4.1.1** under quasi equilibrium conditions was found to explain the data satisfactorily.

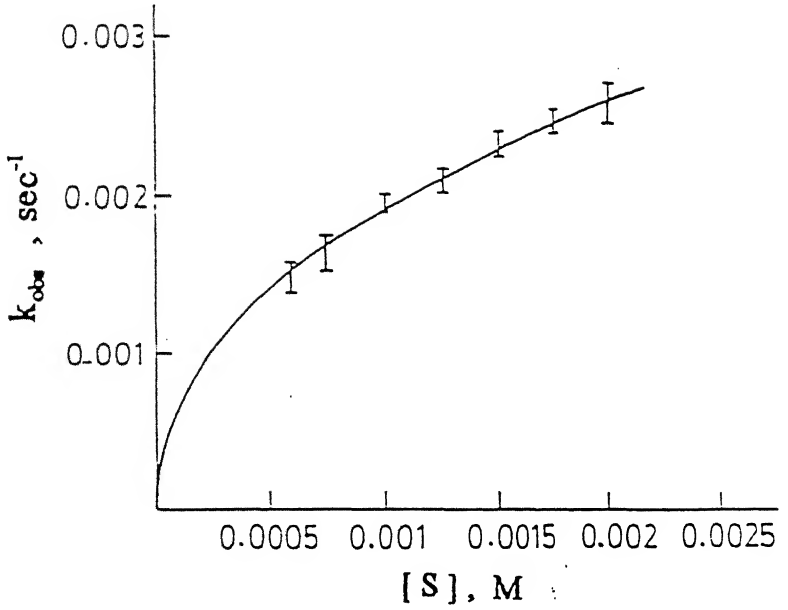
0.003
0.002
0.001
k_{obs} , sec^{-1}
0.0005
0.001
0.0015
0.002
0.0025
[S], M

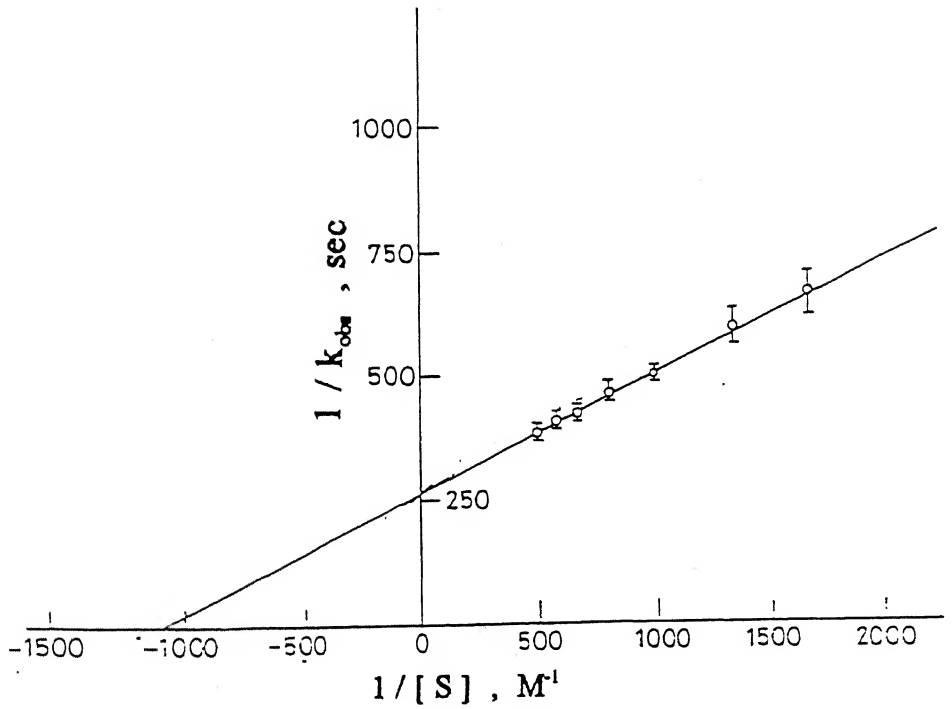
1000
750
500
250
1 / k_{obs} , sec
-1500
-1000
-500
0
500
1000
1500
2000
1/[S] , M^{-1}

Fig. 4.1.3 (a)

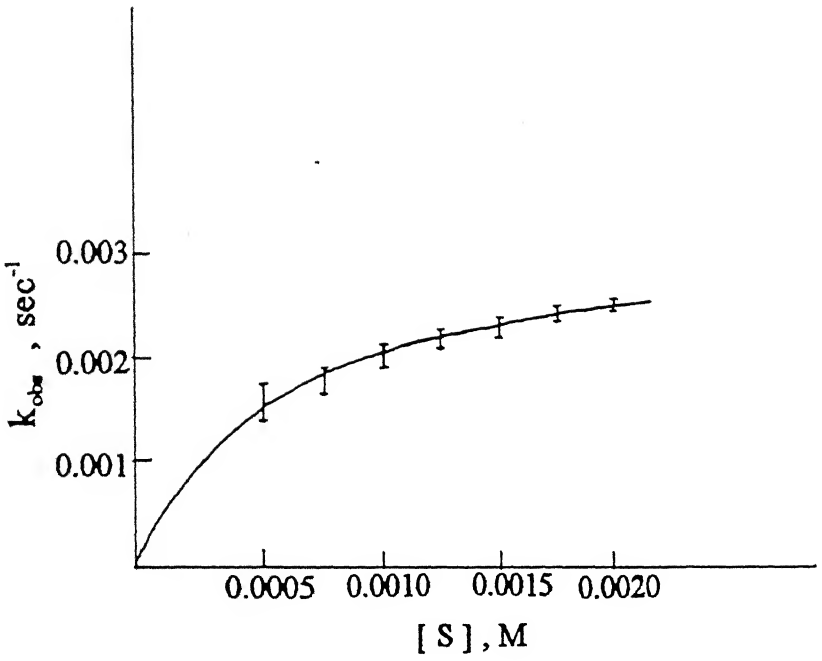
0.003
0.002
0.001
k_{obs} , sec^{-1}
0.0005
0.0010
0.0015
0.0020
[S], M

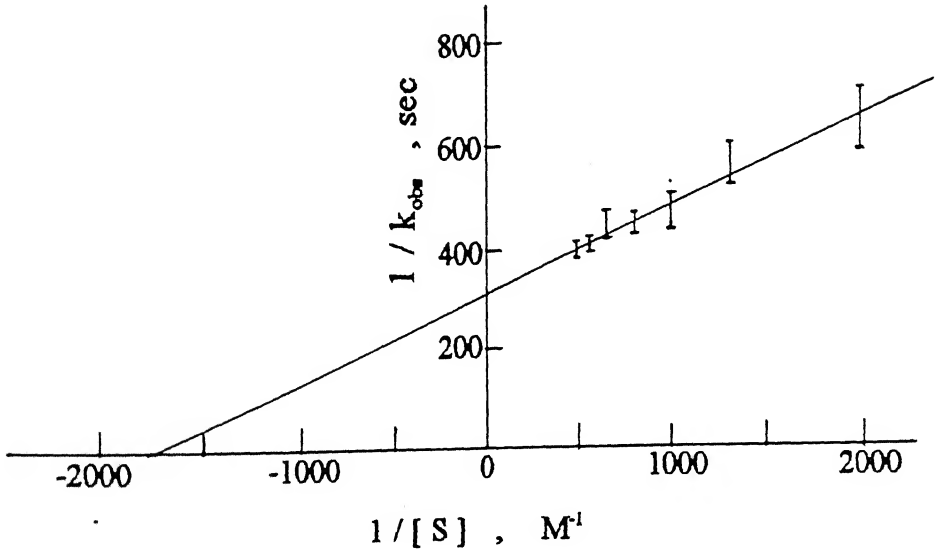
800
600
400
200
1 / k_{obs} , sec
-2000
-1000
0
1000
2000
1/[S] , M^{-1}

Fig. 4.1.3 (b)

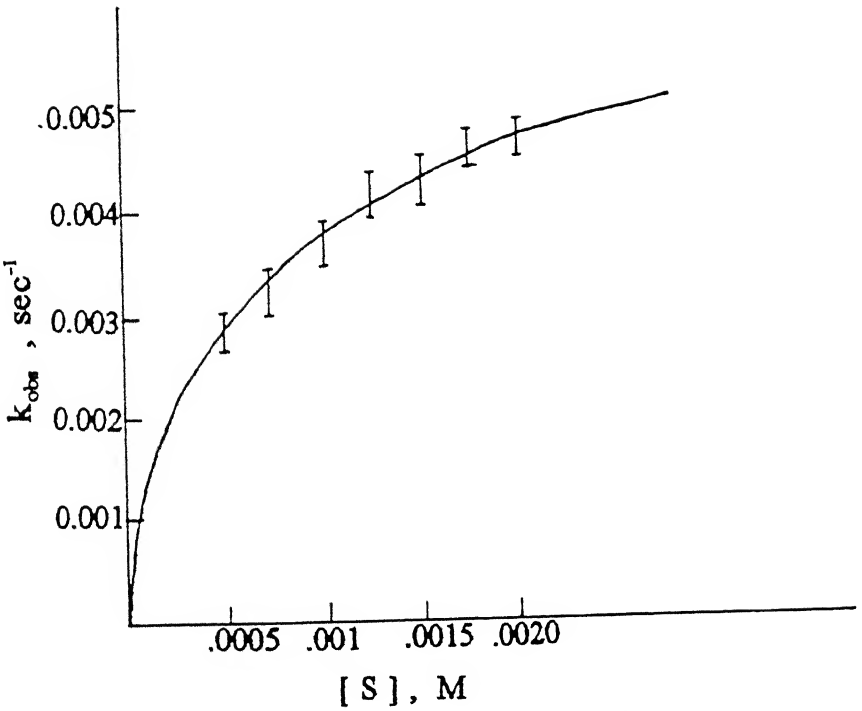
0.005
0.004
0.003
0.002
0.001
k_{obs} , sec^{-1}
.0005 .001 .0015 .0020
[S], M

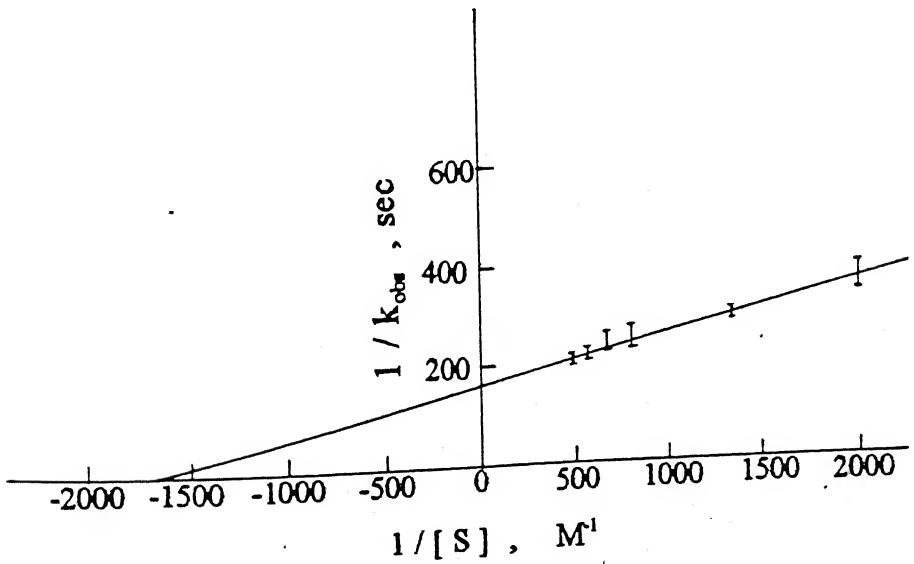
600
400
200
1 / k_{obs} , sec
-2000 -1500 -1000 -500 0 500 1000 1500 2000
1 / [S], M^{-1}

Fig.4.1.3 (c)

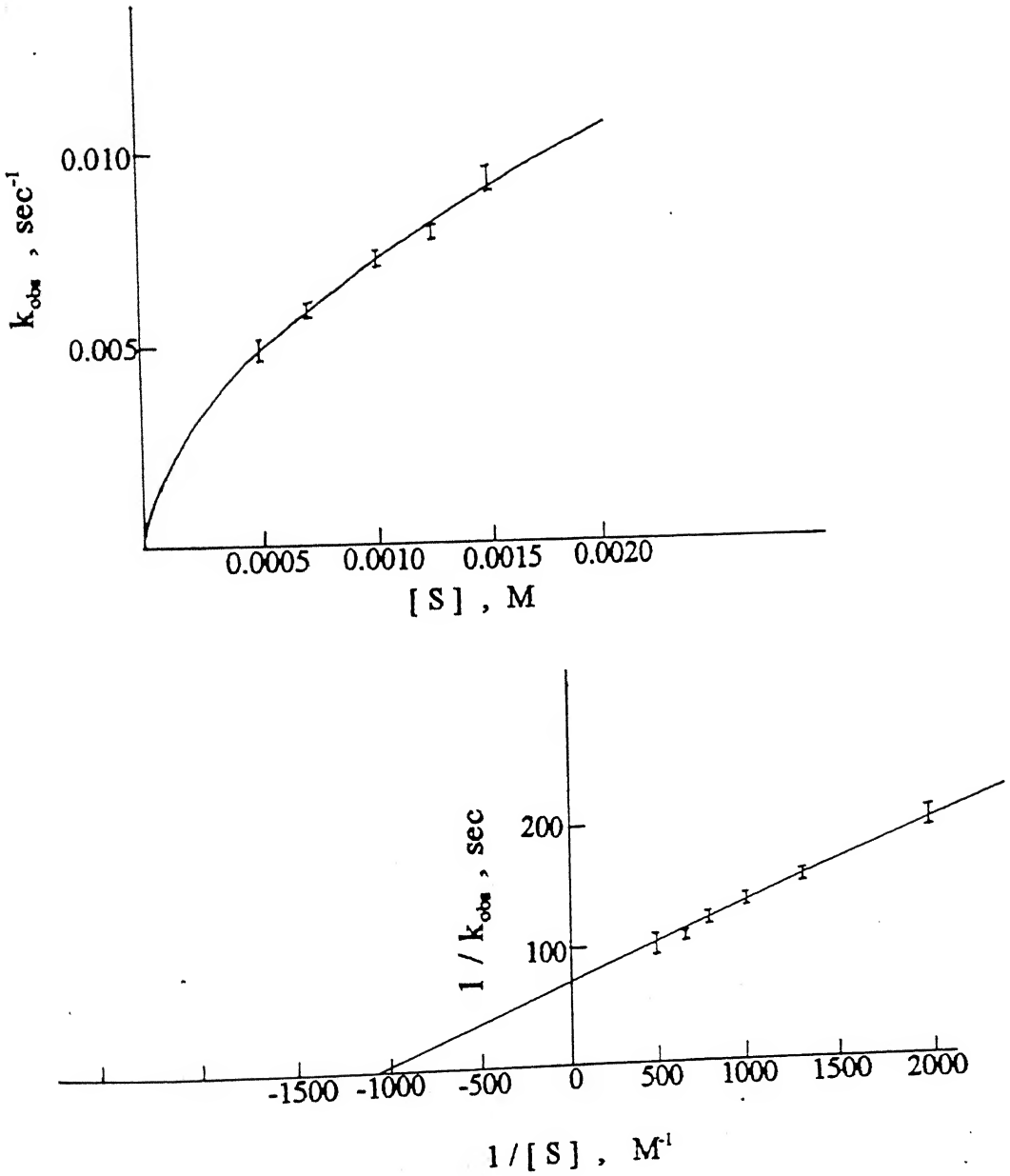
0.010
0.005
k_{obs} , sec^{-1}
0.0005
0.0010
0.0015
0.0020
[S] , M
200
100
1 / k_{obs} , sec
-1500
-1000
-500
0
500
1000
1500
2000
1/[S] , M^{-1}

Fig. 4.1.3(d)

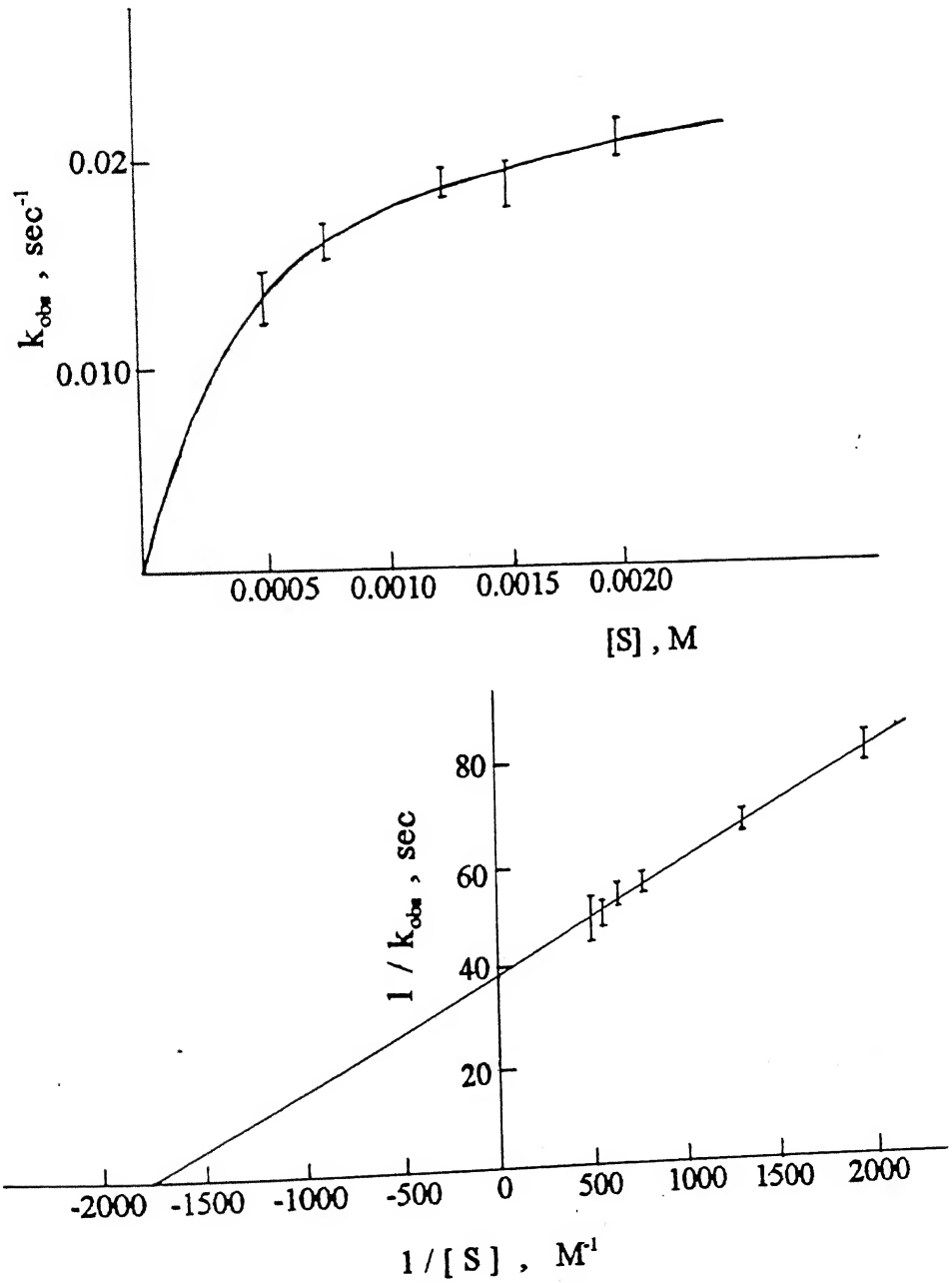
0.02
0.010
k_{obs} , sec^{-1}
0.0005
0.0010
0.0015
0.0020
[S] , M
80
60
40
20
1 / k_{obs} , sec
-2000
-1500
-1000
-500
0
500
1000
1500
2000
1 / [S] , M^{-1}

Fig. 4.1.3 (e)

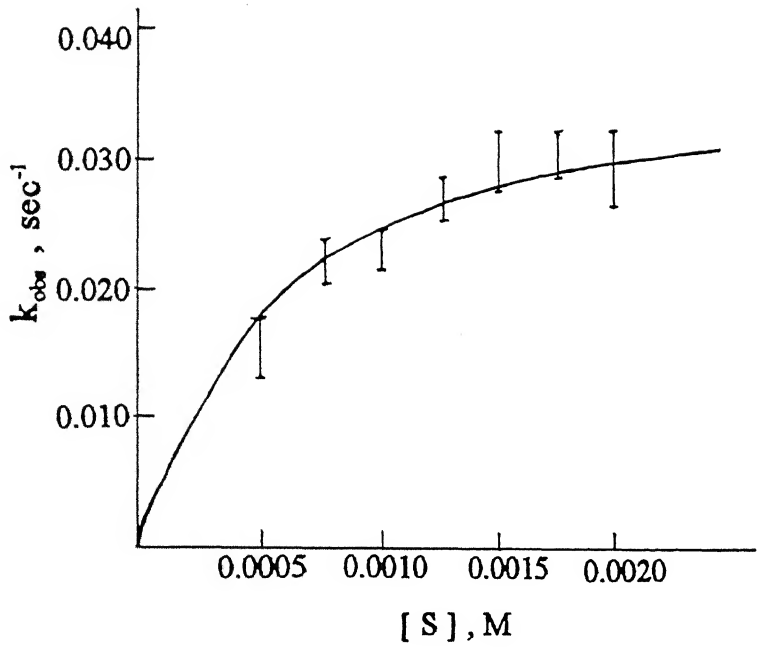

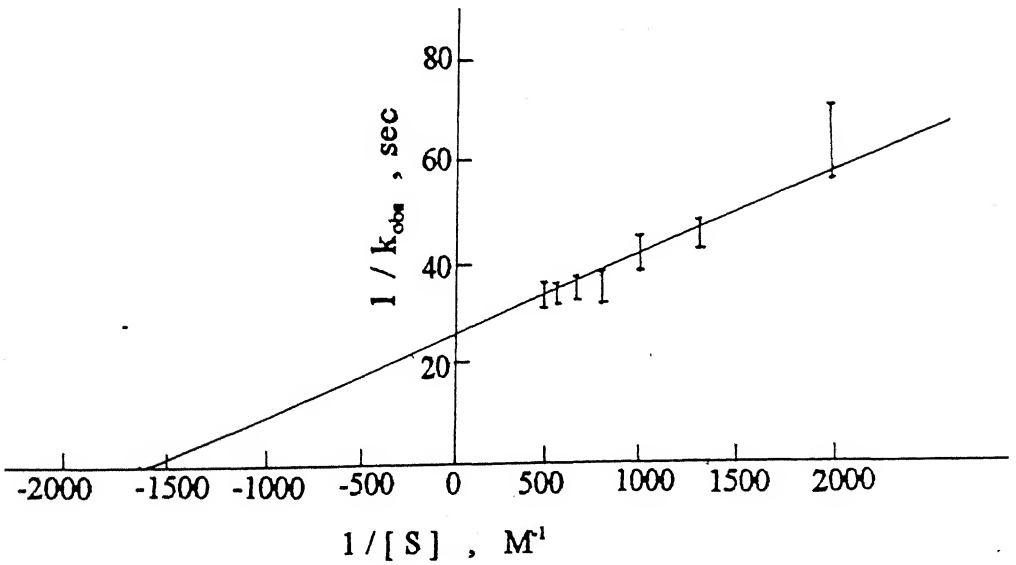

Fig.4.1.3(f)

Fig.4.1.3 Substrate saturation and corresponding double reciprocal plots for the reaction between $[Et_4N]_2[Mo^{IV}O(mnt)_2]$ ($1x10^{-4}$M) and TMANO in acetone-acetic acid medium at $\lambda_{effective}$ (a) pH = 6.0, (b) pH = 5.5, (c) pH = 5.14, (d) pH = 4.8, (e) pH = 4.2 and (f) pH = 4.0.

Table 4.1 Results of the pH dependent kinetic experiment for the reaction of $[MoO(mnt)_2]^{2-}$ and Me_3NO in acetone.

pH	$V_{max}(s^{-1})$	K_M (M)
4.0	38.2×10^{-3}	6.11×10^{-4}
4.2	26.0×10^{-3}	5.53×10^{-4}
4.8	13.9×10^{-3}	5.90×10^{-4}
5.14	6.19×10^{-3}	5.80×10^{-4}
5.5	3.35×10^{-3}	5.78×10^{-4}
6.0	3.05×10^{-3}	6.23×10^{-4}

$$k_{obs} = \frac{[S_o]\left[k_2 + \frac{k_2''}{k'}[H^+] + \frac{k_2}{K'K''}[H^+]^2 \right]}{\left[\frac{K_s(K + [H^+]}{K} + [S_o]\left(1 + \frac{1}{K'}[H^+] + \frac{1}{K'K''}[H^+]^2\right)\right]}$$

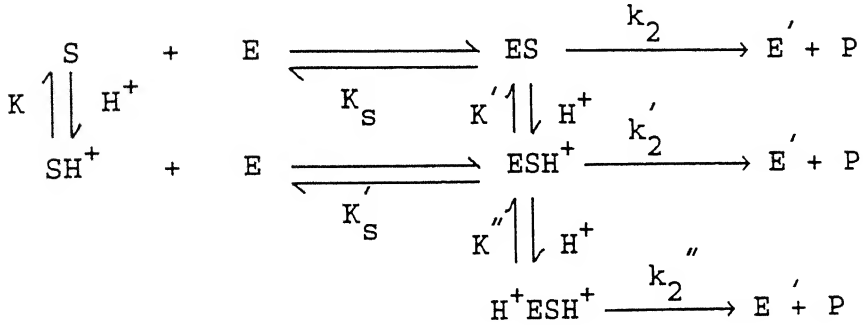

Scheme 4.1.1

In the above Scheme, E represents the model enzyme. S and SH^+ are the deprotonated and protonated form of the substrate and P is the product. Now introducing the following definitions:

$$\frac{[S][H^+]}{[SH^+]} = K \qquad \text{--------(i)}$$

if the total concentration of the substrate is $[S_o]$,

$$[S] = \frac{K[S_o]}{(K + [H^+])} \quad \text{and} \quad [SH^+] = \frac{[S_o][H^+]}{(K + [H^+])}$$

Also, $K_s = \frac{[I][S]}{[ES]}$ hence, $[ES] = \frac{[E]\ K[S_o]}{K_s(K + [H^+])}$ -----(ii)

Similarly, $K' = \frac{[ES][H^+]}{[ESH^+]}$, hence, $[ESH^+] = \frac{[E]\ K[S_o][H^+]}{K_s(K + [H^+])K'}$ ------(iii)

and $K'' = \frac{[ESH^+][H^+]}{[H^+ESH^+]}$,

therefore, $[H^+ESH^+] = \frac{[E][S_o]\ K[H^+]^2}{K'\ K''\ K_s(K + [H^+]}$ ----------(iv)

The total concentration of the enzyme $[E_t]$,

$[E_t] = [E] + [ES] + [ESH^+] + [H^+ESH^+]$

$$= [E]\left[1 + \frac{K[S_o]}{K_s(K + [H^+])} + \frac{K[S_o][H^+]}{K_s(K+[H^+])K'} + \frac{K[S_o][H^+]^2}{K'K''\ K_s(K+[H^+])}\right]$$

Therefore,

$$[E] = \frac{[E_t]K_s(K+[H^+])}{K\left[\frac{K_s(K+[H^+])}{K} + [S_o]\{1 + \alpha[H^+] + \beta[H^+]^2\}\right]} \quad \text{------(v)}$$

where $\alpha = \frac{1}{K'}$ and $\beta = \frac{1}{K'\ K''}$

Therefore the rate of the reaction is:

Rate $= k_2[ES] + k_2'[ESH^+] + k_2''[H^+ESH^+]$ ----------(vi)

Substituting equations (ii), (iii) and (iv) in equation (vi) and simplifying we get,

$$\text{Rate} = \frac{[E_t]\ [S_o]\ (K_2 + a[H^+] + b[H^+]^2)}{\left[\frac{K_s(K+[H^+]}{K} + [S_o](1 + \alpha[H^+] + \beta[H^+]^2)\right]}$$

Therefore, $k_{obs} = \frac{[E_t]\ [S_o]\ (K_2 + a[H^+] + b[H^+]^2)}{\left[\frac{K_s(K+[H^+]}{K} + [S_o](1 + \alpha[H^+] + \beta[H^+]^2)\right]}$ -----(vii)

This equation can be rewritten as,

$$K_{obs} = \frac{\dfrac{[S_o](K_2 + a[H^+] + b[H^+]^2)}{1 + \alpha[H^+] + \beta[H^+]^2}}{\left[\dfrac{K_s(K + [H^+])}{K(1 + \alpha[H^+] + \beta[H^+]^2)} + [S_o]\right]} \qquad \text{where } a = K_2'/K' \text{ and } b = K_2''/K'K'' \qquad \text{-------(viii)}$$

Hence the expression for the apparent Michaelis constant

$$K_M = \frac{K\,K_s + K_s[H^+]}{K + \alpha K[H^+] + \beta\,K[H^+]^2} \qquad \text{----------(ix)}$$

and the expression for the maximum velocity,

$$V_m = k_{max} = \frac{K_2 + a[H^+] + b[H^+]^2}{1 + \alpha[H^+] + \beta[H^+]^2} \qquad \text{----------(x)}$$

The dissociation constant (M) and rate constants (s^{-1}) values obtained are: $K_s = 5.00 \times 10^{-3}$; $K_s' = 1.63 \times 10^{-3}$; $K = 3.04 \times 10^{-7}$; $K' = 9.93 \times 10^{-6}$; $K'' = 1.00 \times 10^{-4}$ and $k_2 = 5.43 \times 10^{-4}$; $k_2' = 1.20 \times 10^{-2}$; $k_2'' = 9.99 \times 10^{-2}$. $[S_o]$ = total concentration of TMANO. This kinetic data reveal the participation of $[MoO(mnt)_2]^{2-}$ and its hydrogen bonded form $[PyH]_2[MoO(mnt)_2]$ **(EH^+)** to utilize $(CH_3)_3NOH^+$ as substrate in this reaction. The formation of essential precursor complex is controlled by the loan pairs on sulfurs perpendicular to the Mo-S-C planes (Figs.3.39 and 3.40) in **E** or **EH^+**.

Reaction (3) is very slow in higher polar solvents like DMF, CH_3CN and virtually no reaction occured in aqueous-organic mixed solvents. Noticeably, this reaction smoothly occured in CH_2Cl_2 phase in contact with an acidified aqueous solution of $(CH_3)_3NO$ which is similar to membrane bound (hydrophobic site) enzymatic

reaction of *E.coli*.[79c] The formation of Me_3NOH^+ is known which on phase transfer leads to faster reaction in CH_2Cl_2. The existence of hydrogen bonded form of $[MoO(mnt)_2]^{2-}$ **(EH^+)** in CH_2Cl_2 is shown in the following way: the electronic spectra of $[MoO(mnt)_2]^{2-}$ are identical in solvents like CH_3CN, $(CH_3)_2CO$ and CH_2Cl_2 whereas that of $[Et_3NH]_2[MoO(mnt)_2]$ is different in CH_2Cl_2 solvent(Fig.3.15). Infra red spectroscopy revealed the decrease in (Mo=O) stretching frequency in $[PyH]_2[MoO(mnt)_2]$ (906 cm^{-1}) and $[Et_3NH]_2[MoO(mnt)_2]$ (895 cm^{-1}) compounds as compared to that of the $[Et_4N]_2[MoO(mnt)_2]$ (928 cm^{-1}) compound. The weakening of Mo=O bond in protonated cationic salts is due to the formation of Mo=O----H^+ type hydrogen bonding.This is confirmed by the crystal structure determination of the $[PyH]_2[MoO(mnt)_2]$ compound (Fig. 3.40). Unlike the existence of hydrogen bonded form as such in CH_2Cl_2, the participation of this form in the reaction scheme is envisaged in the formation H^+ES .

Alike TMANO reductase, $[Et_4N]_2[MoO(mnt)_2]$ responds to oxotransfer reaction with ClO_3^- (finally bleached) but not with NO_3^- or DMSO. In contrast to other model complexes[9], the inactivity of $[Et_4N]_2[MoO(mnt)_2]$ to reduce NO_3^- or DMSO is related to its intrinsic stereoelectronic control with credible dithiolene coordination unit which is similar to structurally characterized related tungsten coofactor of the aldehyde ferredoxin oxidoreductase.[14] In both of the $[PyH]_2[MoO(mnt)_2]$ and $[Et_4N]_2$-$[MoO(mnt)_2]$ compounds, the lone pairs on sulfur atoms ($p\pi$) perpendicular to Mo-S-C planes impose electron density congestion towards oxo donor substrates (O-X) in their approach *cis* to Mo=O group. The approach of O-X faces stereoelectronic repulsion from the lone pairs of sulfurs of the dithiolenes. This restriction is

not faced by $(CH_3)_3NO$ and ClO_3^- due to longer O-N(Cl) bond distance(s). However, relatively shorter O-N(S) distance(s) in NO_3^- and DMSO could be the reason for the failure to form Michaelis type complex in TMANO reductase. The formation of Michaelis type complex with $(CH_3)_3NOH^+$ takes place by further elongation of the O-N bond in $(CH_3)_3NOH^+$ with possible stabilization of the sulfur pπ orbital by N-OH----S type hydrogen bond.[98] Thus the substrate specificity is mainly controlled by the dihedral angle between O-Mo-S and Mo-S-C planes which are dictated by Mo=O and Mo-S bonds. In native enzymes, these bonds may be appropriately tuned by polypeptide interactions directly with the Mo=O bond or indirectly *via* pterin part of the molybdopterin containing dithiolenes of the cofactor[23] to control Mo-S bonds for the selective approach of a substrate.

SECTION 4.2

Mo(VI) TO Mo(IV) REDUCTION WITH THIOPHENOLS:

It is long known that Mo(VI) complexes can be reduced to corresponding Mo(IV) complexes using thiophenol (PhSH).The synthesis of $MoO(dtc)_2$ from $MoO_2(dtc)_2$ is known by this method.[59b] Similar reaction like

$$MoO_2(L\text{-}NS_2) + 2RSH \longrightarrow MoO(L\text{-}NS_2)(DMF) + H_2O \quad ----(4.4)$$

where $L\text{-}NS_2$ = 2,6-bis(2,2-diphenyl-2-sulfidoethyl)pyridine(2-), has been demonstrated.[59a] The present complex $[MoO_2(mnt)_2]^{2-}$ has also been shown to react with PhSH to yield $[MoO(mnt)_2]^{2-}$ and PhSSPh. And in this reaction for the first time this reduction has been followed to some extent in detail to understand the formation of the reaction intermediates. This work suggest[97] the reaction as

shown in scheme 4.2.1:

$$[MoO_2(mnt)_2]^{2-} + 2PhSH \longrightarrow \{Mo^{VI}O(mnt)_2(SPh)_2\} + H_2O$$

$$\{Mo^{VI}O(mnt)_2(SPh)_2\} \xrightarrow{\text{intramolecular redox reaction}} [Mo^{IV}O(mnt)_2]^{2-} + PhSSPh$$

Scheme 4.2.1

Thiols are physiologically potent electron donor[99] by the reaction

$$2Cys.SH \rightleftharpoons Cys.SS.Cys + 2H^+ + 2e^- \text{ ------- } (4.5)$$

and the reduction of Mo(VI) to Mo(IV) by thiol is an appropriate simulation of biological reduction. However, the reported redox potential of PHSH is not sufficiently negative to cause reduction of $[Mo^{VI}O_2(mnt)_2]^{2-}$ (*vide infra*). Even then the reduction of Mo(VI) proceeds smoothly as shown in Figure (4.2.1). To understand more about the steps involved in this slow reduction a repetitive scan of the progress of the reaction at the initial stage has been recorded as shown in Figure 4.2.2. This figure clearly demonstrates that $[MoO_2(mnt)_2]^{2-}$ in the presence of excess thiol changed to a species (B) which finally changed to another species (C) with an isosbestic point for the conversion of B to C at 570 nm. The entire course of this reaction was completed within 10 min. and within this time period virtully no reduction of these species to $[MoO(mnt)_2]^{2-}$ took place. Thus the entire sequence of reaction may presumably followed as A $\longrightarrow$ B $\longrightarrow$ C $\longrightarrow$ P

(P = product)

Under reaction condition the species formed may be speculated as

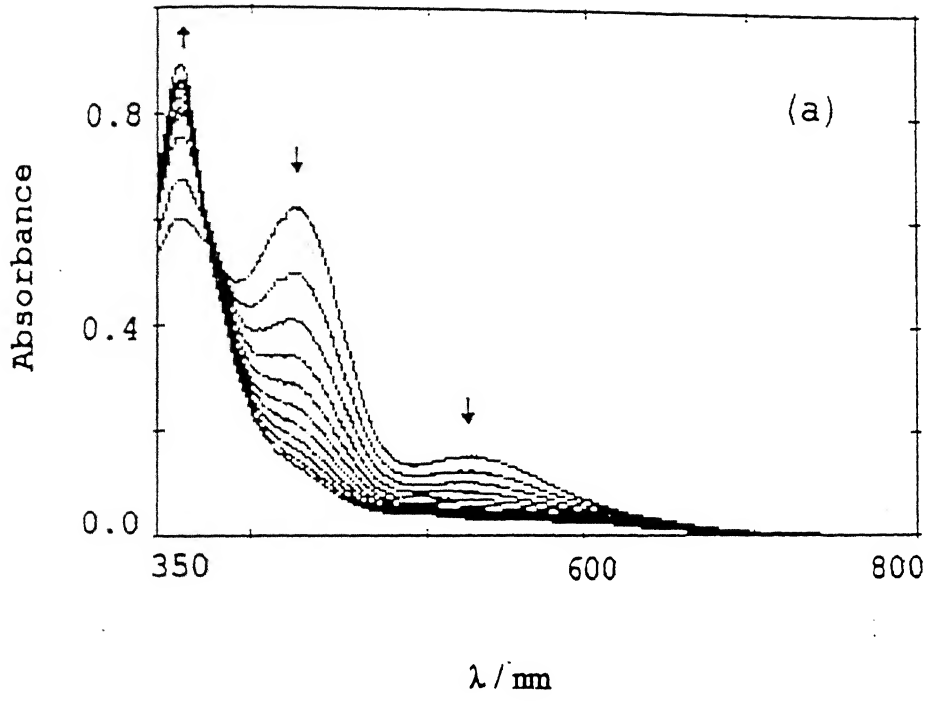

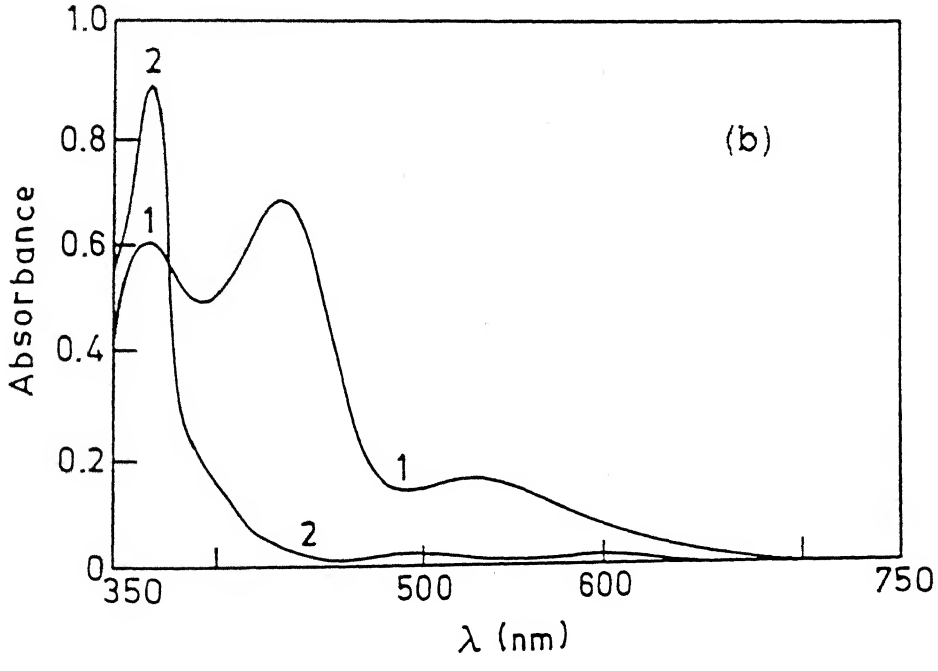

Fig.4.2.1 (a) Spectral changes for the reaction between $[Bu_4N]_2[Mo^{VI}O_2(mnt)_2]$ ($1x10^{-4}M$) and PhSH ($5x10^{-2}M$) in MeCN, scan time gap 30 min.

(b) Superimposed UV-visible spectrum of $[Bu_4N]_2[Mo^{VI}O_2(mnt)_2]$ (1) and $[Bu_4N]_2[Mo^{IV}O(mnt)_2]$ (2) in MeCN, Conc. $1x10^{-4}M$.

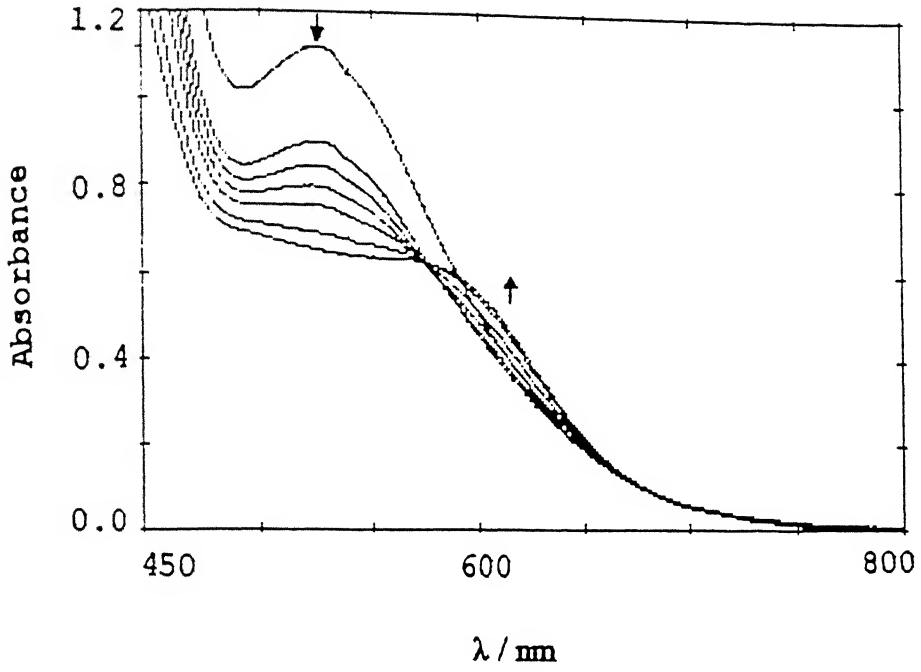

Fig.4.2.2 Spectral changes for the reaction between $[Bu_4N]_2[Mo^{VI}O_2(mnt)_2]$ ($1x10^{-3}$M) and PhSH ($5x10^{-1}$M) in MeCN(expanded form), scan time gap 2 min.

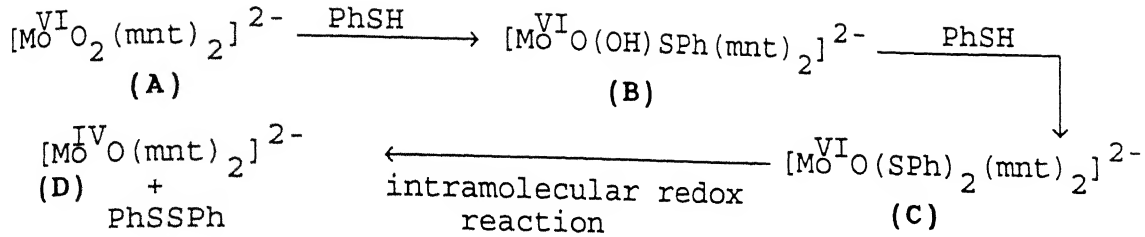

Scheme 4.2.2

From Fig.4.2.2 the penultimate product before electron transfer reaction may be identified as $[MoO(SPh)_2(mnt)_2]^{2-}$, the shift of the lowest energy band of $[MoO_2(mnt)_2]^{2-}$ from 525 to 610 nm in the low energy region justifies all sulfur ligation. The identification of the species B that is $[MoO(OH)(SPh)(mnt)_2]^{2-}$ was difficult as the excess quantity of PhSH used to record the spectrum. When small amount of PhSH was used the electronic spectrum in the range of 450 to 800 nm remain virtually unchanged with very slow reduction of the intensity of the band at 525 nm. Identification of this species was tried by cyclic voltammetry on the assumption that all these species should display different cathodic peak potentials. To facilitate the stability of $[MoO(OH)(SPh)(mnt)_2]^{2-}$ electrochemical experiments were performed with varied amounts of water in the range of 0-10% in acetonitrile medium. Interestingly, the cyclic voltammetric experiments were performed with similar water-CH_3CN concentration without thiophenol to check whether aquation may influence the reported reduction potential of $[MoO_2(mnt)_2]^{2-}$. It has been already shown that the quasireversible reduction peak potential of $[MoO_2(mnt)_2]^{2-}$ centered at - 1.10 volt *vs* Ag/ AgCl with cathodic peak potential at - 1.15 volt in the presence of 0.13 M CH_3COOH and 3.5 M H_2O the reduction became irreversible with the appearance of a cathodic peak potential at -0.77 V *vs* Ag/ AgCl.[33a]

Surprisingly, the influence of small amount of water in the electrochemistry of $[Mo^{VI}O_2(mnt)_2]^{2-}$ is dramatic as shown in Figure 3.30(i). With the increase of water concentration the quasireversible nature of the reduction process is replaced by irreversible process of reduction with gradual shift of the cathodic peak potential to less negative value. This shift in potential ceased when the concentration of added water is 6.3 % in CH_3CN. The change from quasi reversible to irreversible process in the reduction can readily be explained due to the instability of the reduced $MoO_2(V)$ species in the presence of water. The gradual shift in the potential may be explained due to aquation of the cyano groups of the ligated mnt by hydrogen bonding. The electron accepting property of water from the nitrogen atom of the terminal cyano groups in the coordinated mnt by hydrogen bond makes outer sphere complex formation,[100] this phenomenon forces a drift of electron density from the molybdenum center causing it slightly but distinctly more positively charged which facilitates easier reduction. In other words this study implies that the delocalization of the valence electrons extends onto the terminal cyano groups of the ligated mnt ligand. A similar conclusion has been made from combined resonance Raman and electronic spectral work on mnt ligated other complexes.[101] We have characterized this shift in reduction potential due to hydrogen bonding and the experiments with thiophenol (PhSH) has been done using the concentration of water the same as done earlier. The dramatic shift of the cathodic peak potential on addition of acetic acid is similar to what we observed earlier.[102] The electrochemical response of $[Mo^{VI}O_2(mnt)_2]^{2-}$ in CH_3CN containing limited amount of water in the presence of PhSH is shown in Figure 4.2.3(a). When

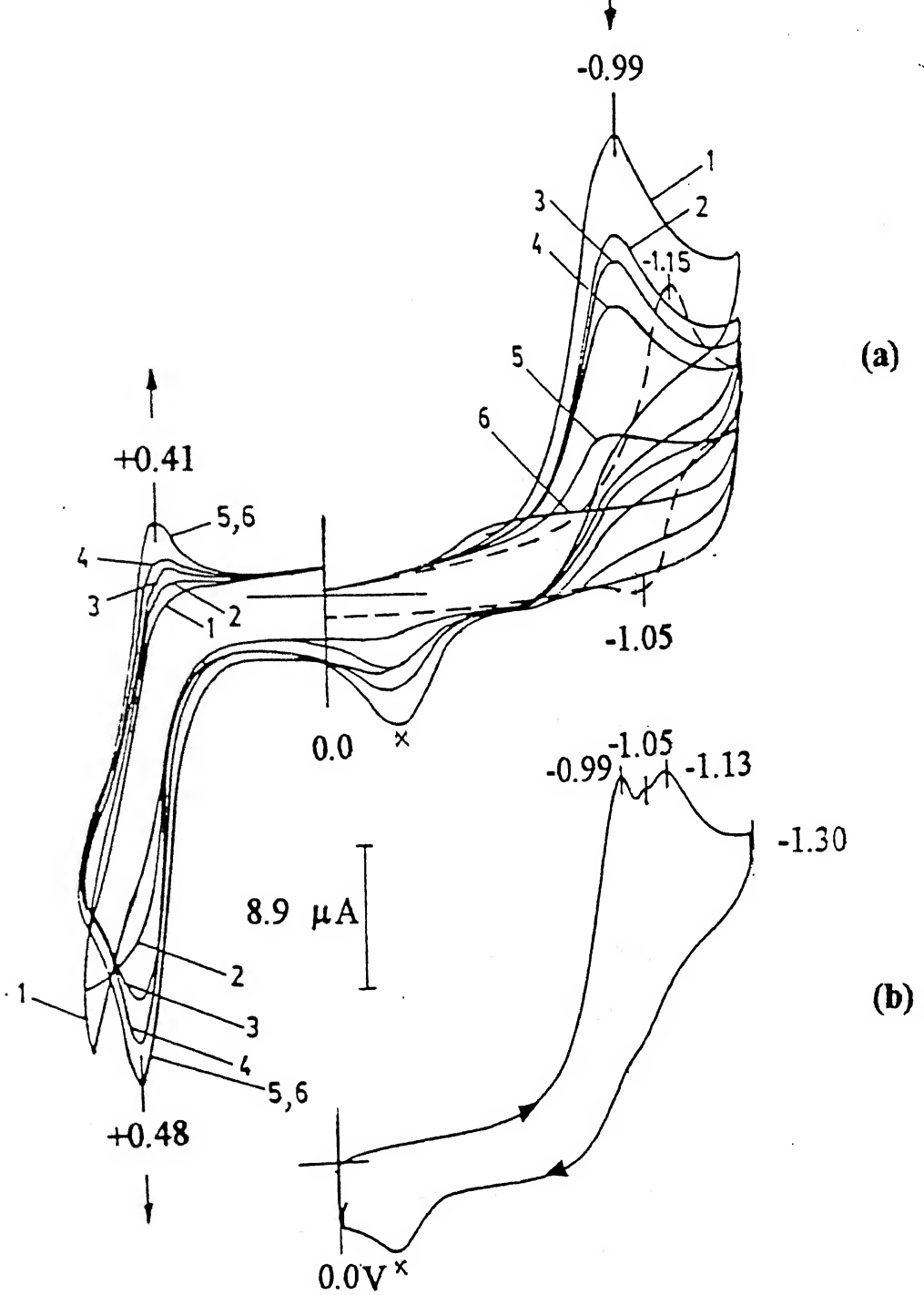

Fig.4.2.3 (a) Cyclic voltammograms for the progress of reaction between $[Bu_4N]_2[Mo^{VI}O_2(mnt)_2]$ ($1x10^{-3}$M) and PhSH ($5x10^{-1}$M) in MeCN, 0.1M Et_4NClO_4, scan rate 100mV/s. Broken line is for the pure complex. Each scan(1-6) in 5min. interval, x marked peaks are unidentified.

excess amount of PhSH was added the cyclic voltammetric scan demonstrated the existence of a species which is irreversibly reduced with appearance of the cathodic peak potential at -0.99V *vs* Ag /AgCl. Interestingly, within about 5 min. no oxidation peak is observed due to the oxidation of $[Mo^{IV}O(mnt)_2]^{2-}$ to $[Mo^{V}O(mnt)_2]^{-}$ which is known to appear at +0.45 volt. After the lapse of 5 min. this oxidative process slowly started and the current intensity of this process progressively increased with defined oxidative potential (in the positive side) concomitant to the decrease of the current hight of the cathodic peak potential at -0.99V. This suggest that the species which showed cathodic peak potential at -0.99V slowly produces the reduced $[Mo^{IV}O(mnt)_2]^{2-}$. It has been shown in Figure 4.2.3(a). that with excess of PhSH the $[Mo^{VI}O_2(mnt)_2]^{2-}$ complex within 5 min. changed to a species designated as **C** which should be $[Mo^{VI}O(SPh)_2(mnt)_2]^{2-}$.

However, in this cyclic voltammogram the appearance of quasireversible reduction potential of $[Mo^{VI}O_2(mnt)_2]^{2-}$ is clearly observed with the appearance of the cathodic peak potential at -1.15 volt *vs* Ag/ AgCl as reported earlier.[33a] It is expected now that the addition of trace amount water will shift the cathodic peak potential of $[MoO_2(mnt)_2]^{2-}$ from -1.15V to -1.13V. The existence of any species like $[MoO(OH)(SPh)(mnt)_2]^{2-}$ may be recognized if a new cathodic peak potential is observed with intermediate value of those for $[MoO_2(mnt)_2]^{2-}$ and $[MoO(SPh)_2(mnt)_2]^{2-}$. Variation of concentration of PhSH with water finally allowed to identify the appearance of this intermediate reduction peak potential (-0.105V) as shown in Figure 4.2.3(b) Thus by electrochemical means the existence of all the three intermediate species could be identified.

The kinetics of this reaction has been carried out in both CH_3CN and aqueous- CH_3CN medium following the change of absorption at 610 nm. The rate of change of the absorption at 610 nm. was recorded spectrophotometrically taking a fixed concenctation of $[Mo^{VI}O_2(mnt)_2]^{2-}$ and thiophenol with a fixed time interval. The absorbance *vs* time curve obtained is reproduced in Figure 4.2.4.

DERIVATION OF THE KINETIC EXPRESSIONS :

Rate expressions were derived for model scheme and experimental data fitting was tried with those expressions. The scheme 3 under consecutive reaction condition was found to explain the data satisfactorily and it can be written in simple form as:

$$A \xrightarrow{k_1} B \xrightarrow{k_2} C \xrightarrow{k_3} D \qquad (D = \text{product})$$

which consists of three consecutive irreversible first order (or pseudo first order) reactions. The differential rate equations are[103]:

$$dC_A/dt = -k_1C_A \text{ ------- (i)} \qquad dC_B/dt = k_1C_A - k_2C_B \text{ ------ (ii)}$$

$$dC_C/dt = k_2C_B - k_3C_B \text{ ----- (iii)} \qquad dC_D/dt = k_3C_C \text{ ------ (iv)}$$

To find the dependence of C_A, C_B, C_C and C_D with time the equations (i) to (iv) have been solved, which resulted as :

$$C_A = C_A^{\,o}\, e^{-k_1t} \text{-------- (v)}$$

$$C_B = C_A^{\,o}\, k_1 \left(e^{-k_1t} - e^{-k_2t} \right) / (k_2-k_1) \text{ ------- (vi)}$$

$$C_C = C_A^{\,o} k_1k_2 \left[\{e^{-k_1t} / (k_2-k_1)(k_3-k_1)\} - \{e^{-k_2t} / (k_2-k_1)(k_3-k_2)\} + \{e^{-k_3t} / (k_3-k_1)(k_3-k_2)\} \right] \text{ ------ (vii)}$$

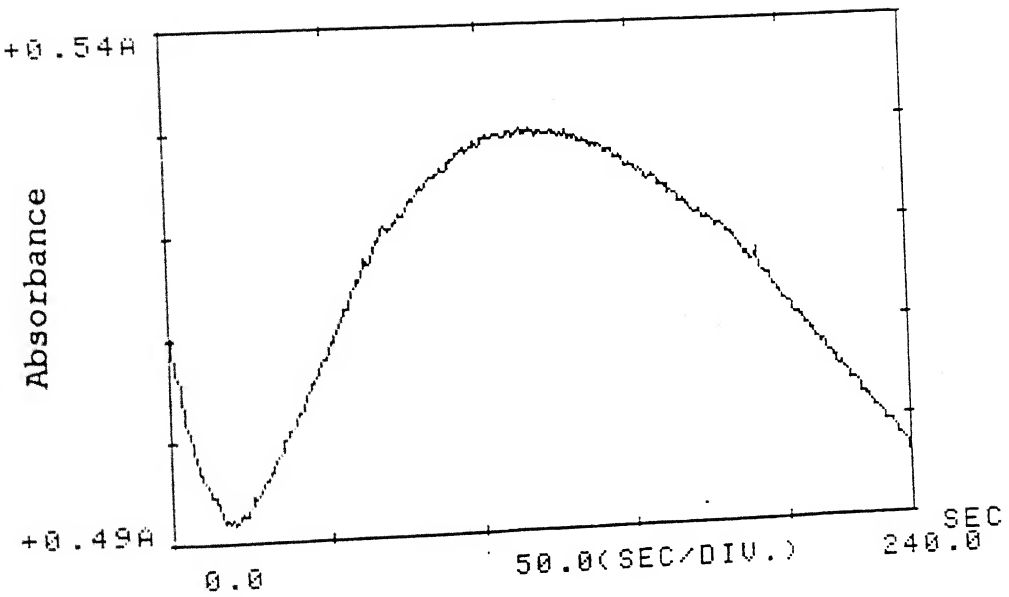

Fig.4.2.4 Change of absorption at 610 nm. for the reaction of $[Bu_4N]_2[Mo^{VI}O_2(mnt)_2]$ ($1x10^{-3}M$) and PhSH ($5x10^{-1}M$) in MeCN, at $25\pm1^{o}C$.

$$C_D = C_A^{o} \left[1 - \{k_2k_3e^{-k_1t} / (k_2-k_1)(k_3-k_1)\} + \{k_1k_3e^{-k_2t} / (k_2-k_1)(k_3-k_2)\} - \{k_1k_2e^{-k_3t} / (k_3-k_1)(k_3-k_2)\} \right] \text{------(viii)}$$

As the reaction has been carried out by following the absorption at 610 nm with time hence, at any time t, the optical density (OD) is the sum of the optical densities of all the species thus ,

$$OD = \varepsilon_1 C_A + \varepsilon_2 C_B + \varepsilon_3 C_C + \varepsilon_4 C_D \quad \text{--------- (ix)}$$

where, ε denotes the molar extinction coefficients of the respective species (ε_1 = 642 and ε_4= 120 ; ε_2 and ε_3 are unknown).

Substituting equations (v), (vi), (vii) & (viii) in equation (ix) we get,

$$OD = \varepsilon_1 C_A^{o} e^{-k_1t} + \varepsilon_2 C_A^{o} k_1 (e^{-k_1t} - e^{-k_2t}) / (k_2-k_1) + \varepsilon_3 C_A^{o} k_1k_2 \left[\{e^{-k_1t} / (k_2-k_1)(k_3-k_1)\} - \{e^{-k_2t} / (k_2-k_1)(k_3-k_2)\} + \{e^{-k_3t} / (k_3-k_1)(k_3-k_2)\} \right] + \varepsilon_4 C_A^{o} \left[1 - \{k_2k_3e^{-k_1t} / (k_2-k_1)(k_3-k_1)\} + \{k_1k_3e^{-k_2t} / (k_2-k_1)(k_3-k_2)\} - \{k_1k_2e^{-k_3t} / (k_3-k_1)(k_3-k_2)\} \right] \text{------ (x)}$$

solving the equation (x) by nonlinear least-square regression analysis using E04FDF NAG Fortran Library routine document[104] the values for the k_1, k_2, k_3, ε_2 and ε_3 obtained are tabulated in Table 4.2.

Table 4.2 Results of the kinetic experiment for the reaction of $[Mo^{VI}O_2(mnt)_2]^{2-}$ and PhSH.

	In CH_3CN	In CH_3CN with 6.3% H_2O
Compound conc.	1×10^{-3} M	1×10^{-3} M
PhSH conc.	3.25×10^{-1} M	4.86×10^{-1} M
Temperature	25(± 0.1) °C	25(± 0.1) °C
k_1	$2.82(6) \times 10^{-1} s^{-1}$	$2.91(4) \times 10^{-1} s^{-1}$
k_2	$6.09(5) \times 10^{-2} s^{-1}$	$6.15(3) \times 10^{-2} s^{-1}$
k_3	$1.66(8) \times 10^{-3} s^{-1}$	$3.41(6) \times 10^{-3} s^{-1}$
ε_1	$580\ M^{-1}$	$642\ M^{-1}$
ε_2	$498.8\ M^{-1}$	$514.9\ M^{-1}$
ε_3	$809.8\ M^{-1}$	$749.5\ M^{-1}$
ε_4	$120\ M^{-1}$	$120\ M^{-1}$
Sum of square	3.64×10^{-2}	5.84×10^{-3}
Correlation coeff.	0.9674	0.9981

SECTION 4.3

ALKYLATION REACTION :

The characterization of the organic component present in molybdenum cofactor(Moco) was rigorously persued by Rajagopalan and coworkers.[29] Due to extreme unstable nature of the Mo-co it was extremely difficult to characterize it. However, derivatization of the organic component present in Moco has been achieved by alkylation, wherein the readily dessociable sulfhydryl groups get alkylated and relatively stable dicarboxamidomethyl derivative of molybdopterin (camMPT) could be isolated in pure form involving iodoacetamide as the alkylating agent. Mass and other spectral characterization established the nature of camMPT. From this it was proposed that the Moco contains a reduced pterin derivative (***vide supra***) that can bind to molybdenum through the sulfur atoms of a dithiolene side chain. Interestingly, fairly good yield of camMPT obtained from sulfite oxidase which is proportionate to the composition of one MPT per molybdenum of Mo-co as has been directly quantitated by phosphate assay.[11]Significantly lower yield of camMPT obtained from oxotungstoenzyme like aldehydeferredoxinoxidoreductase(AOR) using similar alkylation conditions[25,35] is not proportionate to its composition. Fortunately the structure of the AOR by X-ray crystallography is known[14] from that the following salient points in relevance to our discussion are :

(i) the presence of two molybdopterin ligands per tungsten, (ii) the absence of any covalent linkage between tungsten cofactor and apoprotein and (iii) the unexceptional protein structure for water soluble globular proteins. In contrast to AOR enzyme the proposed structure of molybdoenzyme like sulfite oxidase contains

authenticated one MPT per molybdenum ligation with the proposed protein thiol ligation[12a]. The structure of sulfite oxidase has been heavily relied upon the proposed Mo-EXAFS analysis(*vide supra*). Even for AOR enzyme W-EXAFS results proposed its structure very similar to that of sulfite oxidase.[16] The recent X-ray structure of AOR enzyme refutes the proposed structure of the enzyme based on EXAFS results. Thus the dependence on the EXAFS results for the structure of sulfite oxidase became questionable. In view of the foregoing arguments it is extremely important to understand the composition Moco in a unbiased manner. The strongest evidence for the composition of Moco is the quantitative phosphate assay per subunit activity of sulfite oxidase as reported by Rajagopalan and coworkers.[11] The important analytical data furnished in this publication (in Table. V) are retabulated in Table 4.3.1.

Interestingly, it has been demonstrated that in trichloro-acetic acid the native enzyme (sulfite oxidase) is quantitatively precipitated and the trichloroacetic acid (TCA) pellet of the native enzyme showed phosphate / subunit activity ratio as one, as has been observed from the untreated native enzyme. It was further documented that the TCA pellet of the native enzyme after the fractional release of 'Form A' showed the presence of 18.25 nmol subunit activity from which 10.05 nmol phosphate was assayed thus showing phosphate / subunit activity ratio as 0.55. This last data amply demonstrate that the experimental conditions used in this phosphate assay did not respond properly to quantify the phosphate assay as described by Ames.[105] Furthermore, the degradative product of MPT as 'Form A' has never been obtained in more than 50% yield assuming the presence of one molybdopterin per

4.3.1 Quantitation of molybdopterin in sulfite oxidase by phosphate analysis

	nmol subunits[a]	nmol phosphate	P/subunit
Native enzyme	25.58	25.66	1.003
	21.67	23.13	1.07
Trichloroacetic acid pellet of native enzyme	25.58	25.27	0.99
Trichloroacetic acid supernatant of native enzyme	25.58[b]	0.40	0.02
Guanidine denatured enzyme (dialyzed)	8.77	1.05	0.12
	9.70	1.17	0.12
Trichloroacetic acid supernatant after release of Form A	12.95[b]	6.60	0.51
	11.32[b]	5.21	0.46
Trichloroacetic acid pellet after release of Form A	18.25	10.05	0.55

[a] Concentration of sulfite oxidase subunits was determined using an ε_{mM} of 113 at 414 nm.

[b] Nanomoles of subunits in trichloroacetic acid precipitate.

molybdenum. To account for the remaining portion, the authors state that, "The remaining portion of the phosphate (and presumably of the pterin) is now tightly, perhaps covalently, associated with the denatured protein fraction. The chemical nature of the residual phosphate has not been established but may provide important clues as to the mechanism whereby molybdopterin is converted to Form A." If one considers the Moco as a complex of oxomolybdenum moiety with dithiolene coordination then the chemistry of oxomolybdenum dithiolene complexes can provide some answers to these reactions if carried out similarly using model complexes. Interestingly, these reactions with Mo-co never addressed to the fate of the essential element molybdenum. Presumably because of the assumption that hydrolytic cleavage of the Moco will release all the available molybdenum in the form of oxomolybdate ion. Interestingly, it has been demonstrated that by Hawkes and Bray that the isolated Moco in the reduced form is extremely stable to retain its activity in aqueous medium under dithionite to prevent aerial oxidation.[30] The extra stability of this active reduced Moco is not compatible to the existing chemistry of oxomolybdenum(IV) in aqueous medium. If one assume that this reduced cofactor has only one dithiolene coordination then the Mo-co will be coordinately unsaturated and the available ligand in aqueous medium will be only water. The well known MoO(IV) chemistry in aqueous medium is the formation of very stable trinuclear cluster, $[Mo^{IV}_3O_4]$ core containing peripheral aqua or other ligands.[90] Thus prolonged activity of the reduced Moco is not compatible with the common chemistry of MoO(IV) in aqueous medium.

Based on these facts, the experiments carried out with

oxomolybdenum-dithiolene complexes produced interesting results. These experiments were also carried out with similar oxotungsten-dithiolene complexes which were recently been shown structurally as well as functionally similar to native AOR enzyme.[34b] The alkylation reactions using these complexes involving iodoacetamide and methyliodide were already described earlier (*vide supra*). However, the different products obtained in these alkylation reactions are summarized in Table 4.3.2. Irrespective of the alkylating agent used and the redox state of the molybdenum complex used, the yield of the alkylated mnt (R_2mnt, R = cam or Me) was proportionate to one per molybdenum complex used. Contrary to this, the yield of R_2mnt were invariably lower for the respective tungsten complexes.[84] This yield pattern is strikingly similar to that obtained from the alkylation reaction of the native enzyme.[11,35] The apparent difference in reactivity of model molybdenum- and tungsten-dithiolene complexes can be understood by the difference in product formation and their isolated yields which can best be represented as shown in equation(4.6) and (4.7).

$$24\ [MoO(mnt)_2]^{2-} \xrightarrow{RI/\ H_2O} 2\ [Mo_6O_{19}]^{2-} + 3\ [Mo_2O_4(mnt)_2]^{2-} + 6\ [Mo(mnt)_3]^{2-} + 24\ R_2mnt + 26\ R_4NI + \text{-------}. \qquad \text{-------(4.6)}$$

$$12\ [WO_2(mnt)_2]^{2-} \xrightarrow{RI/\ H_2O} [W_6O_{19}]^{2-} + 6\ [W(mnt)_3]^{2-} + 6\ R_2mnt + 10\ R_4NI + \text{-------}. \qquad \text{-------(4.7)}$$

Equations (4.6) and (4.7) which closely represent the reaction pattern as observed by the isolated yields of the products demonstrated nicely the striking similarity of the yields

ALKYLATION REACTION OF $[Bu_4N]_2[MO_n(mnt)_2]$, (n = 1,2 ; M = Mo,W).[a]

Compound used	Reagent used	Products isolated (%)[b]				Released mnt	
		A	B	C	D	mnt (%)[c]	mnt/ compd.
MoO_2^{2+}	X	47.0	30.0	---	21.5	52.7	1.05
MoO_2^{2+}	Y	51.5	22.8	6.0	18.5	54.8	1.09
MoO^{2+}	X	49.5	24.0	---	25.0	50.5	1.01
MoO^{2+}[d]	Y	53.0	23.0	---	23.0	53.9	1.08
WO_2^{2+}	X	48.0	---	---	51.0	23.5	0.470
WO_2^{2+}	Y	48.4	---	---	51.2	23.2	0.464
WO^{2+}	X	49.0	---	---	50.0	24.9	0.499
WO^{2+}	Y	48.5	---	---	51.0	23.5	0.469

[a] X = Methyliodide , Y = Iodoacetamide .

$MoO_2^{2+} = [Mo^{VI}O_2(mnt)_2]^{2-}$,

$MoO^{2+} = [Mo^{IV}O(mnt)_2]^{2-}$,

$WO_2^{2+} = [W^{VI}O_2(mnt)_2]^{2-}$,

$WO^{2+} = [W^{IV}O(mnt)_2]^{2-}$.

[b] A = $[M_6O_{19}]^{2-}$ (M = Mo/W),

B = $[Mo^{V}_2O_4(mnt)_2]^{2-}$,

C = $[Mo^{IV}O(mnt)_2]^{2-}$,

D = $[M^{IV}(mnt)_3]^{2-}$.

[b] Based on the amount of Mo/W obtained as products from the starting compound at ambient conditions for 24 hrs. Products were separated by fractional crystallization in CH_3CN / 2-propanol / water.

[c] Based on the amount of ligated mnt present in starting compound .

[d] Reaction time 60 hrs.

obtained from the alkylation reactions of sulfite oxidase and AOR enzymes. From Table 4.3.2 as well as equation (4.6) it is evident that, the released alkylated mnt is stoichemetrically one with respect to the starting oxomolybdo-dithiolene complex used. Interestingly in both these reactions unligated metal released were not in the form of simple tetrahedral oxo-metalate ions rather than polymetalate ions. For molybdenum the analytical and IR spectral data closely suggest the formation of a polymolybdate like $[Bu_4N]_2[Mo_6O_{19}]$ and the polytungstate closely resembles to the formulation of $[Bu_4N]_2[W_6O_{19}]$.

The distribution of dithiolene predominantly as $[M(mnt)_3]^{2-}$ in these reactions is consistent to earlier findings of the stability of the starting oxodithiolene complexes.[33a,34b] In the presence of acid or iodine these complexes finally transform predominantly to the most stable trisdithiolene complexes. The new species formed in alkylation reactions of oxomolybdo-dithiolene compounds is characterized by spectrally and by X-ray structure determination (*vide supra*) as the di-μ-oxo bridged dimer of molybdenum, $[Mo^{V}_2O_4(mnt)_2]^{2-}$. These results strongly suspect the nature of reaction involved in the release of the "Form A" from these cofactors. Iodine oxidation in the presence of strong acid may lead to the formation of these cofactors to stable trisdithiolene coordinated species as observed with the model compounds. All these results strongly suggest that Moco in sulfite oxidase may be stabilized by two MPT ligation similar to W-co in AOR. This proposal requires X-ray structural confirmation either from Moco or from sulfite oxidase.

SECTION 4.4

REACTIVITY OF MONODITHIOLENE LIGATED DIMERIC Mo(V) COMPLEXES :

In our attempts to synthesize monodithiolene ligated monomeric oxomolybdenum compounds, we failed to achieve success in this regard. The compound which we could isolate and characterize is the $[Mo^{V}_{2}O_{4}(mnt)_{2}]^{2-}$ anion. The possibility of the existence of such type of dimeric species in the isolation of Moco from native enzymes may exist. This may also account for the deactivation of the released cofactor. However, it has already been described (*vide supra*) that this dimeric di-μ-oxo species is not even stable in the presence of citrate, wherein reduction took place with the formation of the more stable $[Mo^{IV}O(mnt)_{2}]^{2-}$ species. The extensive use of ascorbic acid in the isolation procedure of molybdenumcofactor from native enzyme thus may prevent the dimerization of the isolated Moco. However, our model reactions once more strongly implicate that of a monomeric oxomolybdenum-dithiolene complex can achieve stability preferentially when ligated with two dithiolene groups.

To understand if there is an equilibrium between the formation of monomeric and dimeric pentavalent molybdenum species under certain pH conditions the reactivity of $[Mo^{V}_{2}O_{4}(mnt)_{2}]^{2-}$ with different acids were undertaken. The dimer-monomer oxo molybdenum(V) chemistry in aqueous acidic medium is well recognised.[90] The isolation of complexes with the general formula $[Mo^{V}_{2}O_{3}X_{2}(mnt)_{2}]^{2-}$ (X = Cl, Br, SPh and C_6H_4ClS) were not novel in the sense that the transformation like,

$$[Mo_2O_4]^{2+} \xrightarrow{2\ HX} [Mo_2O_3X_2]^{2+} + H_2O \qquad \text{------(4.8)}$$

is a well known in oxomolybdenum(V) chemistry.[66] The reverse reaction like hydrolysis of $[Mo_2O_3]^{4+}$ core to produce $[Mo_2O_4]^{2+}$ moiety is also known. The diamagnetism of mono-μ-oxo bridged complexes reported here can be readily understood from their respective X-ray structure (*vide supra*) which is consistant with the analysis furnished by Cotton and coworkers.[106] Interestingly, we were interested to explore the solution behavior of these complexes.The electronic spectrum of $[Mo_2O_3Br_2(mnt)_2]^{2-}$ when recorded in CH_2Cl_2 showed interesting results. With time there is a progressive decay of the starting compound. The repeatitive time dependent electronic spectral scan is reproduced in Figure 4.4.1. Interestingly after the lapse of 6 hrs. the rate of gradual decrease of intensity of the spectral bands slowed down and on prolong keeping the solution for days the final spectrum appears to be the spectrum of $[Mo_2O_4(mnt)_2]^{2-}$. In CH_2Cl_2 saturated with water the electronic spectrum of $[Mo_2O_3Br_2(mnt)_2]^{2-}$ could not be recorded due to its fast conversion to $[Mo_2O_4(mnt)_2]^{2-}$ according to the reaction :

$$[Mo_2O_3Br_2(mnt)_2]^{2-} \underset{HBr}{\overset{H_2O}{\rightleftharpoons}} [Mo_2O_4(mnt)_2]^{2-} + 2\ HBr \qquad \text{---------(4.9)}$$

The reverse of this reaction (4.9) is the synthetic method utilized to get the mono-μ-oxo bridged complex. The corresponding chloro complex behaved similarly and representative time dependent electronic spectrum for this species is reproduced in Figure 4.4.2. Unfortunately, very low solubility of the corresponding thiophenol complex restricted to follow similar spectral observation in CH_2Cl_2. Interestingly the fall of the electronic spectrum of the $[Mo_2O_3Br_2(mnt)_2]^{2-}$ attained a steady state within

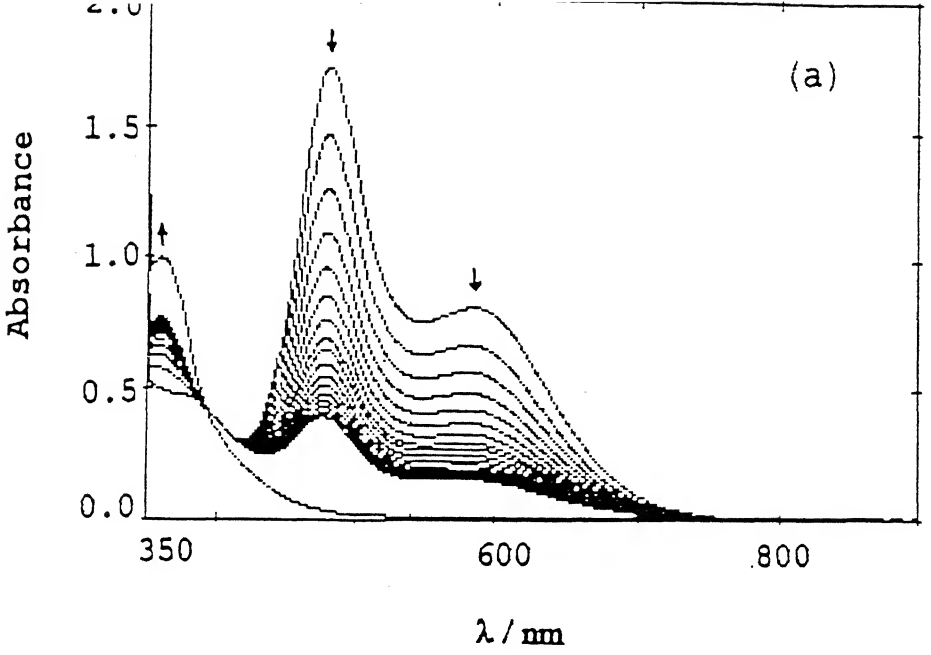

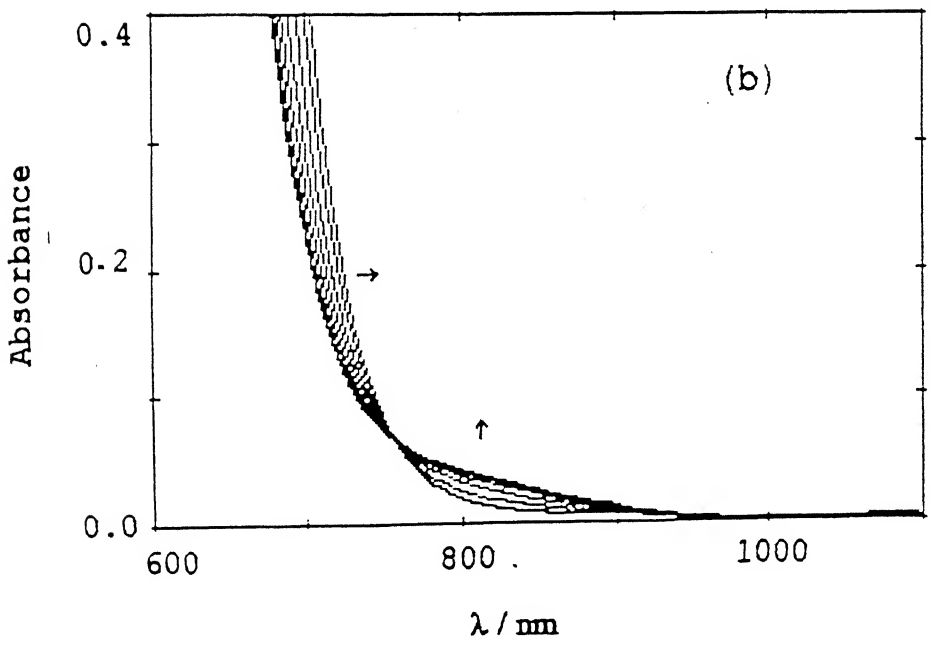

Fig.4.4.1 (a) Spectral changes for the hydrolysis reaction of $[Bu_4N]_2[Mo^{V}_2O_3(Br)_2(mnt)_2]$ ($1.1x10^{-4}$M) in CH_2Cl_2, scan time gap 20min., last scan after 48hrs.

(b) Spectral changes for the same reaction (expanded form), scan time gap 1hr.

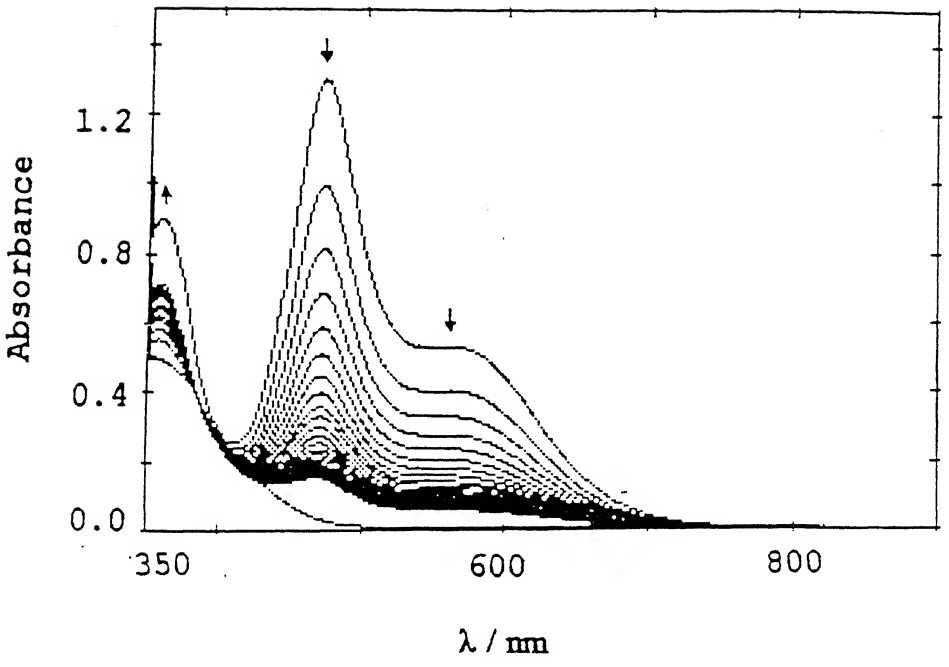

4.4.2 Spectral changes for the hydrolysis reaction of $_{4}N]_2[Mo^{V}_2O_3(Cl)_2(mnt)_2]$ ($1.1x10^{-4}M$) in CH_2Cl_2, scan time gap .n., last scan after 24hrs.

6 hrs. after which the spectrum remain virtually constant for several hours. To understand more about this hydrolysis event in CH_2Cl_2 (containing trace amount of water) the repeatitive electronic spectral scan was monitored in the visible to near IR region that is near the tail of the lowest energy band (585 nm.) of the starting complex. The result of such experiment is displayed in Figure 4.4.1b. It is interesting to note that during this initial slow hydrolysis process a new species is formed with an isosbestic point at 758 nm. The final product $[Mo_2O_4(mnt)_2]^{2-}$ did not have any absorption in this region. From the known chemistry of pentavalent oxomolybdenum species it is well known that monomeric MoO(V) complexes showed a weak electronic transition, $^2B_2 \longrightarrow {}^2E$, in this region.[107] Thus the hydrolysis of the $[Mo_2O_3Br_2(mnt)_2]^{2-}$ to $[Mo_2O_4(mnt)_2]^{2-}$ may involve some reactive monomeric MoO(V) species. To understand the nature of the species time dependent EPR studies of $[Mo_2O_3Br_2(mnt)_2]^{2-}$ in CH_2Cl_2 were undertaken. The result of such investigation is shown in Figure 4.4.3. The slow formation of a paramagnetic species was clearly observed in this EPR spectral study. Parallel to our earlier observation in electronic spectral studies shown in Figure 4.4.1, the gradual formation of MoO(V) was observed. After 6 hrs. the concentration of the EPR active species remain virtually constant for several hours suggesting that this species is slowly formed at the expense of the hydrolysis of $[Mo_2O_3Br_2(mnt)_2]^{2-}$. Interestingly, the line shape of this species right from the begining till the end of the experiment remained the same. This was a spectrum of seven lines. At the end of the measurement the EPR spectrum was recorded under high gain and high microwave power to observe the hyperfine splitting due to ^{95}Mo and ^{97}Mo. The

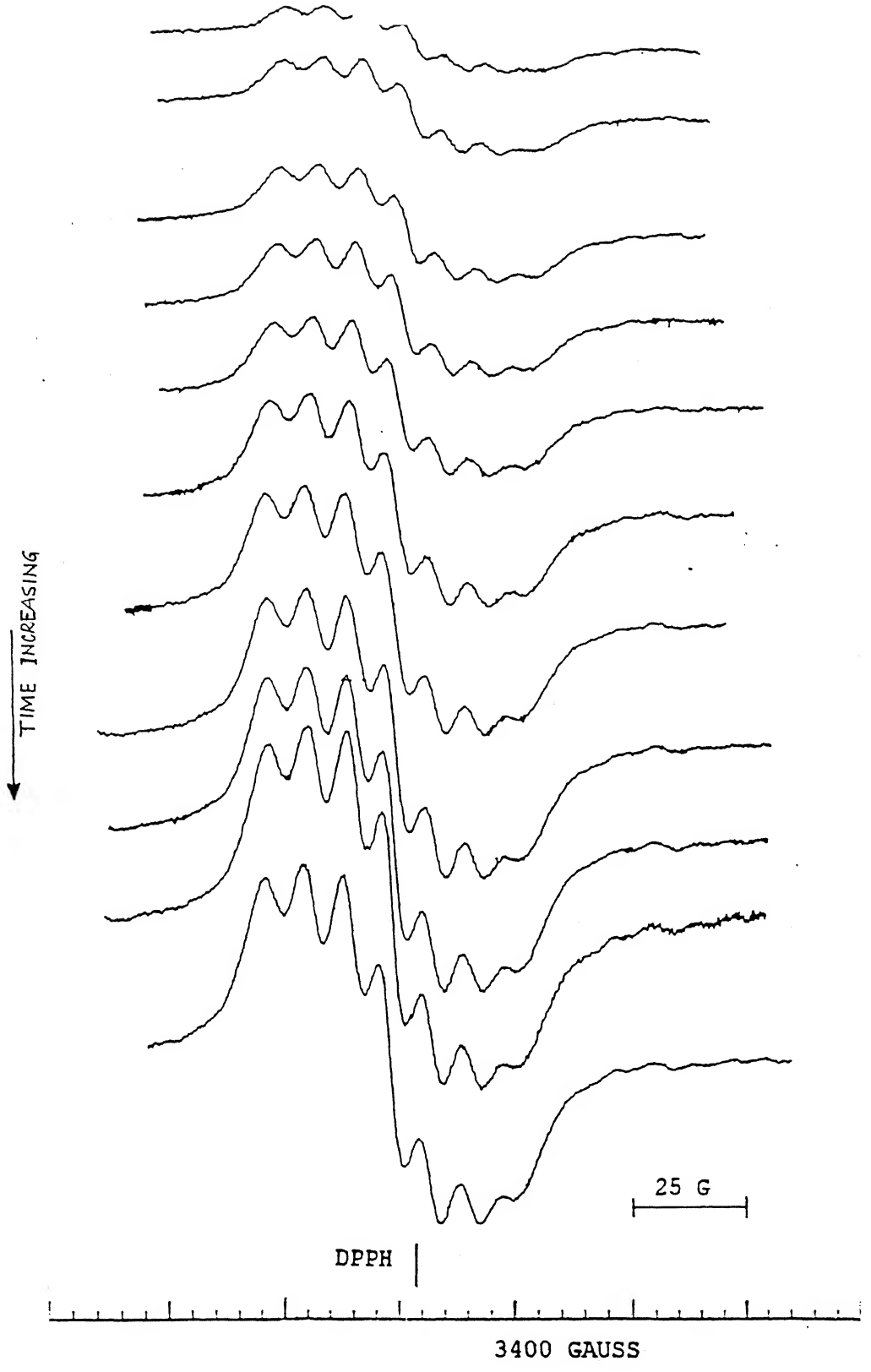

Fig.4.4.3 Time dependent EPR spectral changes for the hydrolysis reaction of $[Bu_4N]_2[Mo^{V}_2O_3(Br)_2(mnt)_2]$ ($1x10^{-3}M$) in CH_2Cl_2, scan time gap 30min.

spectrum is reproduced in Figure 4.4.4. This Figure showed a few of the hyperfine lines further splitted by superhyperfine interaction with two equivalent bromine atoms (S = 3/2) near midfield region. To overcome the complicacy arised due to superhyperfine splitting due to bromo coordination, we have recorded EPR spectrum of the corresponding chloro complex, $[Mo_2O_3Cl_2(mnt)_2]^{2-}$, under identical conditions. Chlorine also has two isotopes ^{35}Cl and ^{37}Cl (natural abundance 100 %) having nuclear spin 3/2 with low nuclear magnetic moment. Thus the superhyperfine interaction due to chlorine is expected to be not that profound as has been observed for the bromo complex where ^{79}Br and ^{81}Br (natural abundance 100%) with nuclear spin 3/2 have large nuclear magnetic moment. The EPR spectrum of the $[Mo_2O_3Cl_2(mnt)_2]^{2-}$ after the lapse of half an hour was recorded which is reproduced in Fig4.4.5a. The main signal was recorded with a slow scan to observe the superhyperfine interaction due to chlorine and the spectrum is reproduced in Fig4.4.5b. This distinctly displayed the superhyperfine interaction due to chlorine as expected. More importantly Figure 4.4.5a clearly demonstrated the origin of the signal is due to MoO(V) with hyperfine splitting with <A> = 14Gauss. Regarding the superhyperfine interaction in the bromo complex the seven line spectrum is deinitely due to the interaction of two equivalent bromine atoms with the molybdenum nucleus. Thus to understand the mechanism of this hydrolysis reaction (4.9) the combined electronic and EPR spectral observations lead to the following scheme 4.4.1. The initial aquation of the $[Mo_2O_3Br_2(mnt)_2]^{2-}$ compound should form two equivalent of monomeric pentavalent $\{OMo(Br)(OH)(mnt)\}^-$ species, the extreme instability of this

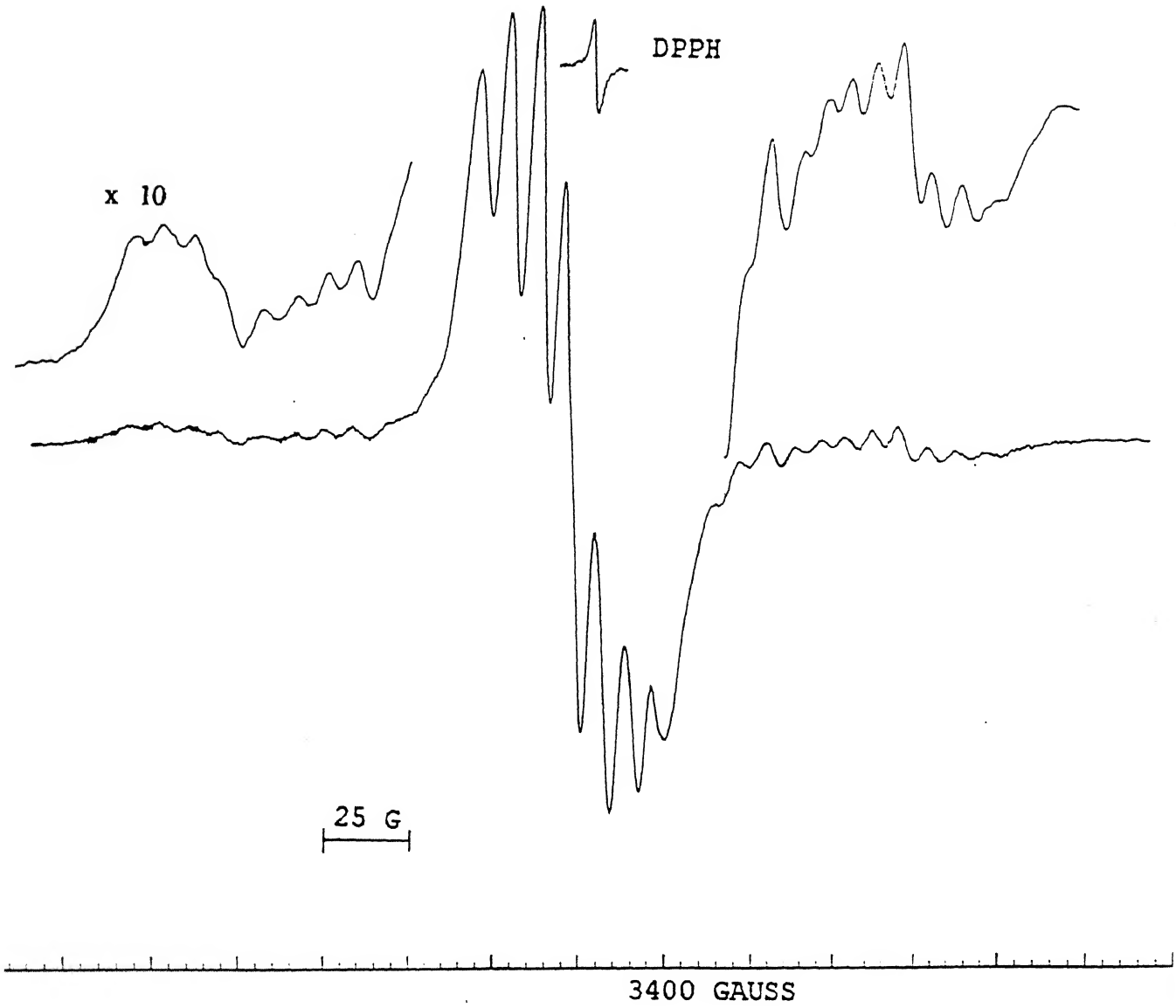

Fig. 4.4.4 EPR spectra of $[Bu_4N]_2[Mo^V_2O_3(Br)_2(mnt)_2]$ ($1x10^{-3}M$) in CH_2Cl_2 after 6hrs.

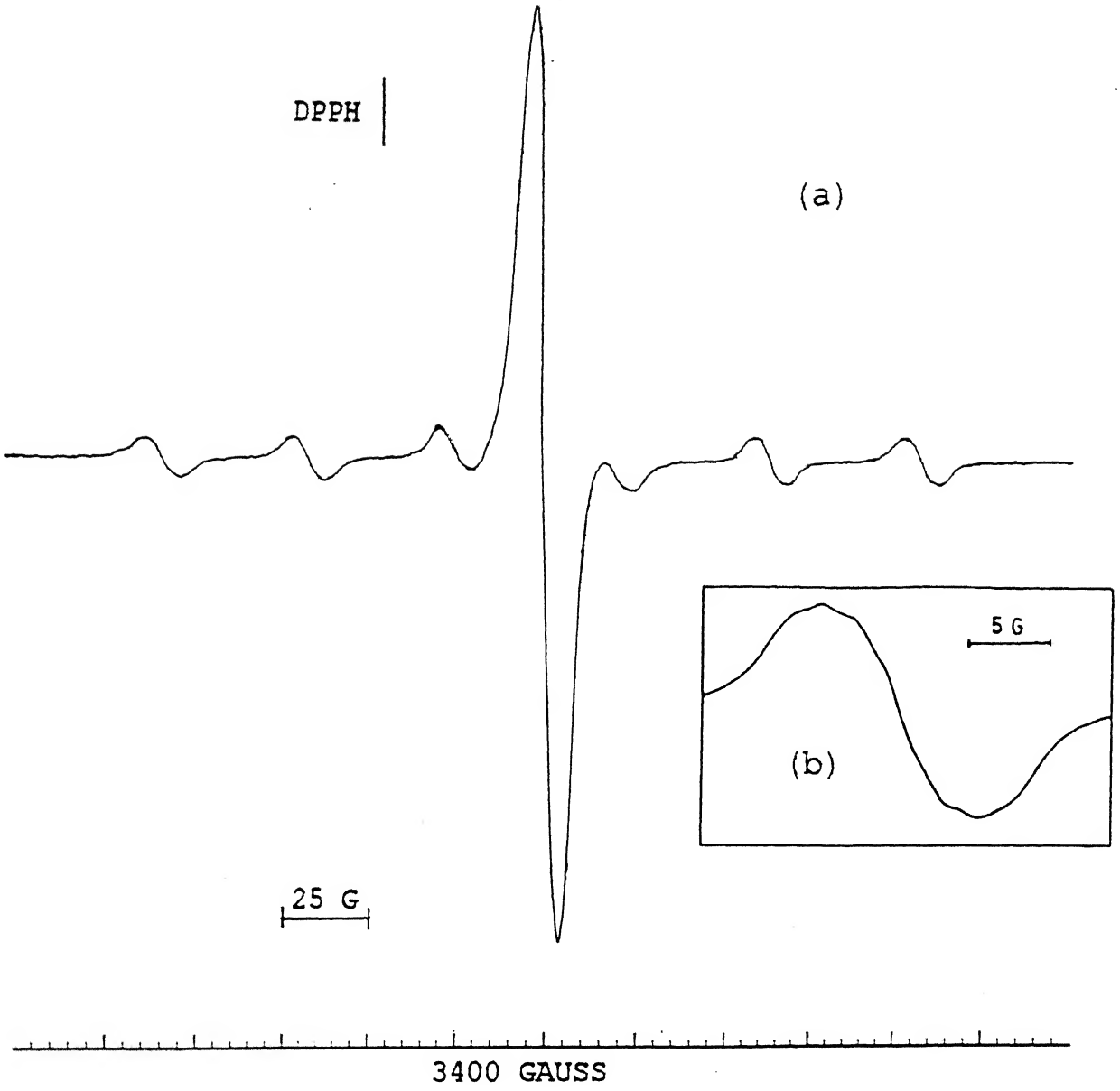

Fig. 4.4.5 (a) EPR spectra of $[Bu_4N]_2[Mo^{V}_2O_3(Cl)_2(mnt)_2]$ ($1x10^{-3}$M) in CH_2Cl_2 after 1hr. (b) Expanded form of the main signal of (a).

species is accounted for due to the absence of any other species in the time dependent EPR study. This species should have displayed four line spectrum due to one bromine atom which could have been further splitted by the proton of the adjacent OH^- ion.

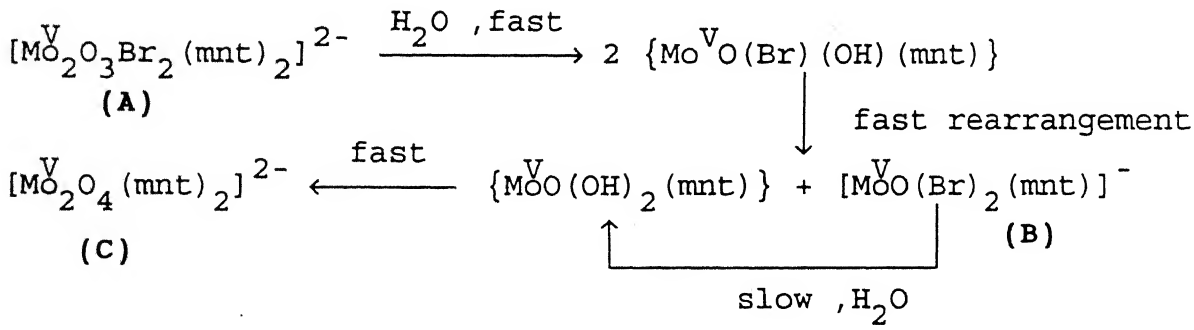

Scheme 4.4.1

The absence of any four or eight line spectrum in the EPR studies strongly suggest that this species which is initially formed rearranged very fast into other species as $[MoO(Br)_2(mnt)]^-$ and $[MoO(OH)_2(mnt)]^-$. The absence of any species where only the protons of the two hydroxo groups may interact with the molybdenum nucleus also suggest that the dihydro species is dimerized very fast to yield EPR inactive $[Mo_2O_4(mnt)_2]^{2-}$ complex. EPR study with D_2O treated CH_2Cl_2 did not altered the line shape of the spectrum as reported in Figure 4.4.4 suggesting no involvement of proton interaction in this hydrolysis system. The formation of the EPR active $[MoO(Br)_2(mnt)]^-$ species can thus be understood that this species slowly hydrolyzed to yield the reactive intermediate dihydroxo species which in turn very rapidly dimerized to yield the final product with the release of two equivalent of HBr. Thus excluding the fast reaction steps the hydrolysis of the complex $[Mo_2O_3Br_2(mnt)_2]^{2-}$ is now involved with the initial aquation to yield the dibromo species $[MoO(Br)_2(mnt)]^-$ which finally hydrolyse to yield the di-μ-oxo dimeric compound $[Mo_2O_4(mnt)_2]^{2-}$. Thus the

hydrolytic scheme as shown in Scheme 4.4.1 can be simplified as:

$$\mathbf{A} \xrightarrow{k_1} \mathbf{B} \xrightarrow{k_2} \mathbf{C} \qquad (\mathbf{C} = \text{product}) \text{ -----(4.10)}$$

DERIVATION OF THE KINETIC EXPRESSIONS:

The hydrolysis reaction of $[Mo_2O_3Br_2(mnt)_2]^{2-}$ in CH_2Cl_2 (containing trace amount of H_2O) representedin equation (4.10) consists of two consecutive irreversible first order reactions. The concentrations of the species **A** and **B**, (C_A and C_B), at any time t, can be derived same as the equations (v) & (vi) (*vide supra*). And the concentration of the species C is then found from the mass balance,

$$C_A^{\,o} = C_A + C_B + C_C \text{ ----------(xi)}$$

substituting the equations (v) & (vi) in equation (xi) we get,

$$C_C = C_A^{\,o} + \{C_A^{\,o}(k_2 e^{-k_1 t} - k_1 e^{-k_2 t})\} / (k_2 - k_1) \text{ ------(xii)}$$

The above reaction was monitored by following the change of absorption (Figure 4.4.6) at two different wave lengths (478 nm. and 585 nm.) with time. At any time t, the optical density (OD) is the sum of the optical densities of all the species, thus,

$$OD = \varepsilon_1 C_A + \varepsilon_2 C_B + \varepsilon_3 C_C \text{ --------(xiv)}$$

where ε(epsilons) are the molar extinction coefficients of the respective species. At wavelength 478 nm. the ε_1= 16530 and ε_3= 130 whereas at 585 nm. ε_1= 7910 and ε_3= 10. Substituting the equations (v), (vi) and (vii) in equation (xiv) we get,

$$OD = \varepsilon_1 C_A^{\,o} e^{-k_1 t} + \varepsilon_2 C_A^{\,o} k_1 (e^{-k_1 t} - e^{-k_2 t}) / (k_2 - k_1)$$

$$+ \varepsilon_3 C_A^{\,o} + \{\varepsilon_3 C_A^{\,o}(k_2 e^{-k_1 t} - k_1 e^{-k_2 t})\} / (k_2 - k_1) \text{ ------(xv)}$$

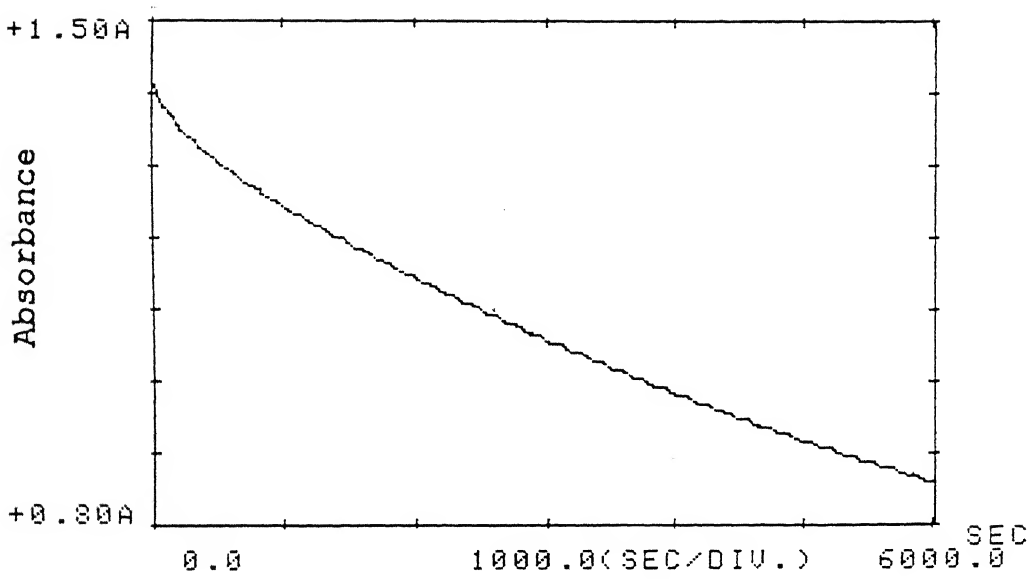

Fig. 4.4.6 Change of absorption at 480nm. for the hydrolysis reaction of $[Bu_4N]_2[Mo^{V}_2O_3(Br)_2(mnt)_2]$ ($1x10^{-4}$M) in CH_2Cl_2 at $25\pm1^{o}C$.

solving the equation (xv) by nonlinear-least square regression analyses using E04FDF NAG fortran library routine document[104], the k_1, k_2 and ε_2 values thus obtained are tabulated in Table 4.4.

The insolubility of the corresponding thiolato complex, $[Mo_2O_3(SPh)_2(mnt)_2]^{2-}$, did not permit to perform similar kinetic studies. However, the EPR studies of the corresponding hydrolysed product of the said complex will be of interest. This is due to the fact that Hawkes and Bray[30c] have shown that the isolated Moco in the presence of thiophenol under oxidation generating Mo(V) species showed an EPR signal in high value of <g> = 1.9948 which is identical to cofactor signal but deffers in $g_\perp$ and $g_\parallel$ values.[30c] Interestingly, they have also reported that, Moco signal also changed if bidentate ethanedithiol is used instead of thiophenol. However, when mercaptoethanol is used the EPR signal intensity did not increase drastically and the cofactor signal alongwith a modified signal under the influence of mercaptoethanol (HOC_2H_4SH) is observed. Among all the three thiols used the thiophenol treated cofactor has been shown to remain intact in its activity for reconstitution assay with *nit-1* mutants of *N. crassa*. They have suggested that the cofactor as isolated may contain some residual peptides from which two cysteine were originally ligated to Moco. Thus the g values of the EPR spectra suggest that in the Mo(V) state of the cofactor four thiolate groups are attached in addition to one terminal oxo group. The extra two thiolate groups have been assigned from the organic part of the cofactor which today we know is from MPT ligand. In our study with the corresponding halo complexes we have demonstrated that the EPR active species is a monomeric pentacoordinated dihalo monodithiolene OMo(V) species. However, we have observed that when

Table 4.4 Results of the kinetic experiment for the hydrolysis reaction of $[Mo_2O_3(Br)_2(mnt)_2]^{2-}$ in CH_2Cl_2 containing trace amount of moisture

	at 478 nm.	at 585 nm.
Compound conc.	1×10^{-4} M	1×10^{-4} M
Temperature	25(± 0.1) °C	25(± 0.1) °C
k_1	$3.043(4) \times 10^{-2}$ s^{-1}	$2.416(7) \times 10^{-2}$ s^{-1}
k_2	$7.798(5) \times 10^{-5}$ s^{-1}	$8.919(6) \times 10^{-5}$ s^{-1}
ε_1	16530 M^{-1}	7910 M^{-1}
ε_2	13450 M^{-1}	6902 M^{-1}
ε_3	130 M^{-1}	10^{-1}
Sum of squares	1.873×10^{-3}	6.325×10^{-4}
Correlation coeff.	0.9981	0.9980

$[Mo_2O_4(mnt)_2]^{2-}$ is taken in CH_2Cl_2 saturated with HBr gas the yellow color of the compound immediately changed to blue-violet color of $[Mo_2O_3(Br)_2(mnt)_2]^{2-}$, the EPR study of this solution displayed a spectrum as shown in Figure 4.4.7. This showed the presence of $[\overset{V}{M}OO(Br)_2(mnt)]^-$ along with another EPR signal with <g> = 1.992 which is very close to the value reported[108] for $[\overset{V}{M}OOBr_5]^{2-}$ is caused by the use of excess of strong acid like HBr, which is sufficient to break the coordinated dithiolene bond. However, thiophenol is not a strong acid and displacement of coordinated dithiolene ligand by thiolate would be difficult because of the chelating effect of dithiolene. Under these considerations the EPR study on $[Mo_2O_3(SPh)_2(mnt)_2]^{2-}$ in the presence of excess of thiophenol in CH_2Cl_2 was undertaken (this was observed that the said complex slowly went into the solution in presence of excess of thiophenol in CH_2Cl_2). The EPR spectra for the reacton between $[Mo_2O_4(mnt)_2]^{2-}$ and PhSH, recorded at different time interval are shown in Figures (4.4.8a, 4.4.8b & 4.4.8c). During the process of this slow reaction the profile of the spectra did not changed much. However, these spectra displayed the presence of a species with <g> = 1.992 along with characteristic six hyperfine lines due to ^{95}Mo, ^{97}Mo. Dissolution of the solid $[Mo_2O_3(SPh)_2(mnt)_2]^{2-}$ in CH_2Cl_2 containing PhSH showed EPR spectrum displayed in Figure 4.4.9, demonstrating the presence of two EPR active Mo(V) species with <g>=1.992 and 1.982. Interestingly, the former <g> value is identical to that observed in the earlier EPR experiment with the $[Mo_2O_4(mnt)_2]^{2-}$ and PhSH (showed in Figure 4.4.8). The relative intensity of the species with <g>=1.982 is weak compared to that of the species with <g>=1.992. It is now known for the dithiolene ligated complexes of

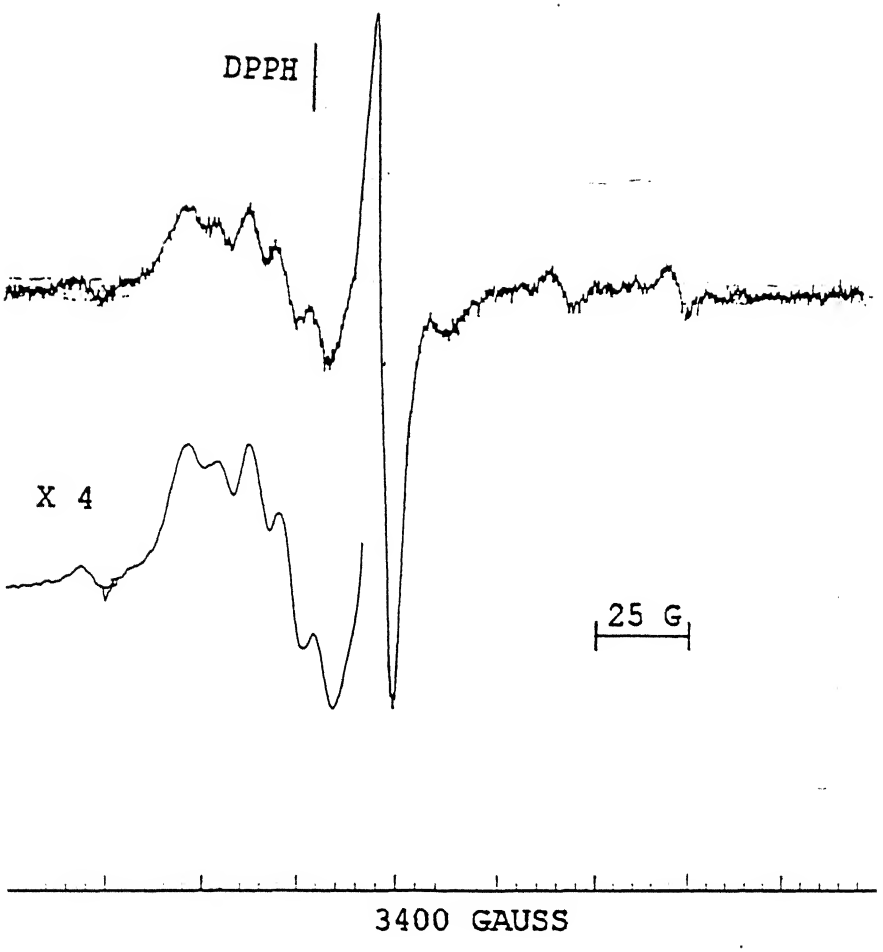

Fig.4.4.7 EPR spectra for the reaction of $[Bu_4N]_2[Mo^V_2O_4(mnt)_2]$ and HBr in CH_2Cl_2.

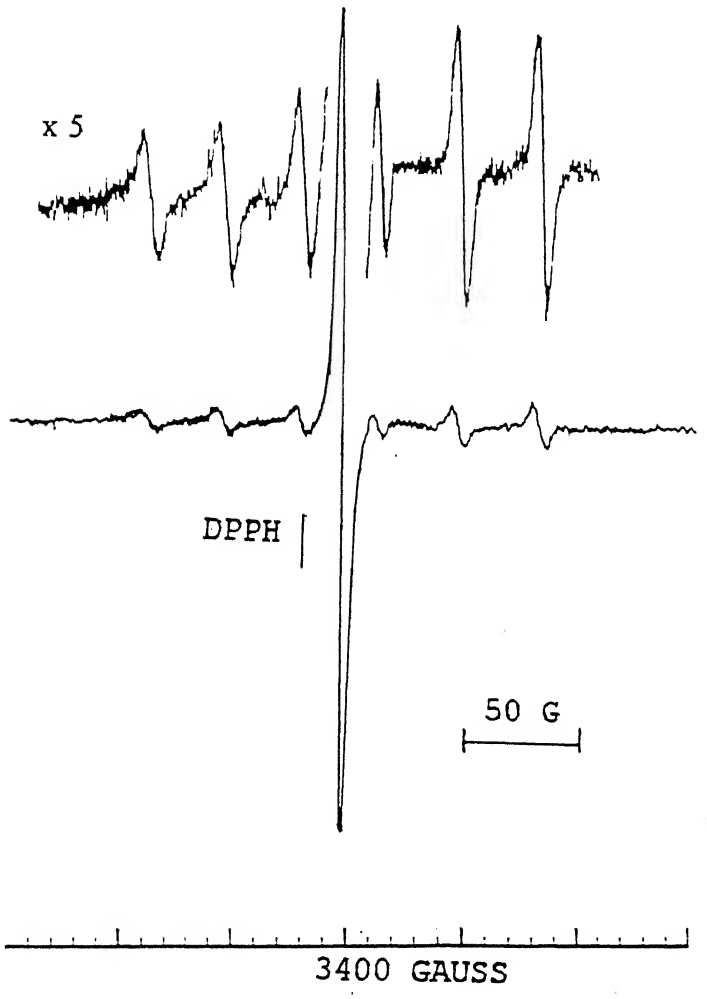

Fig.4.4.8 (a)

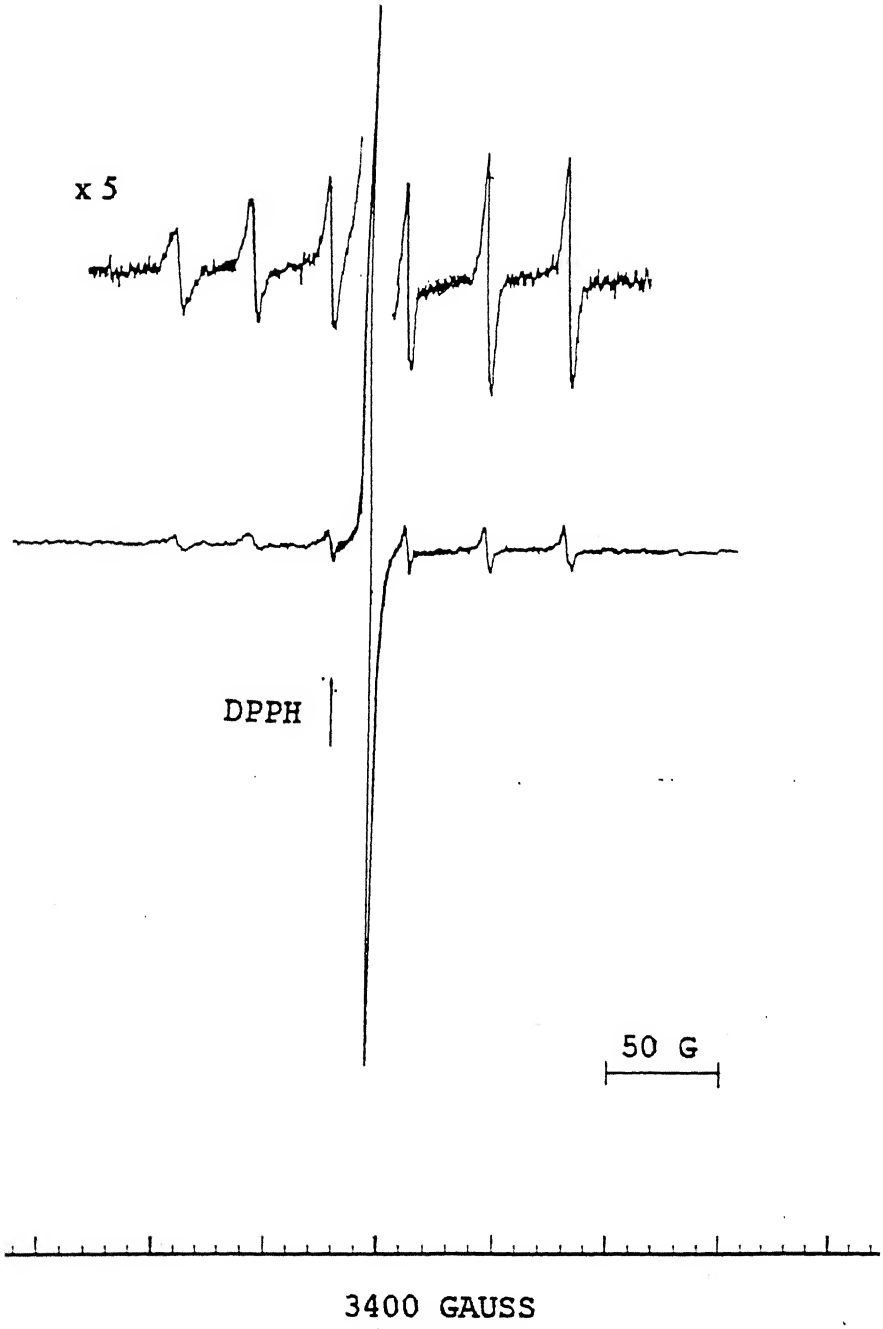

Fig.4.4.8 (b)

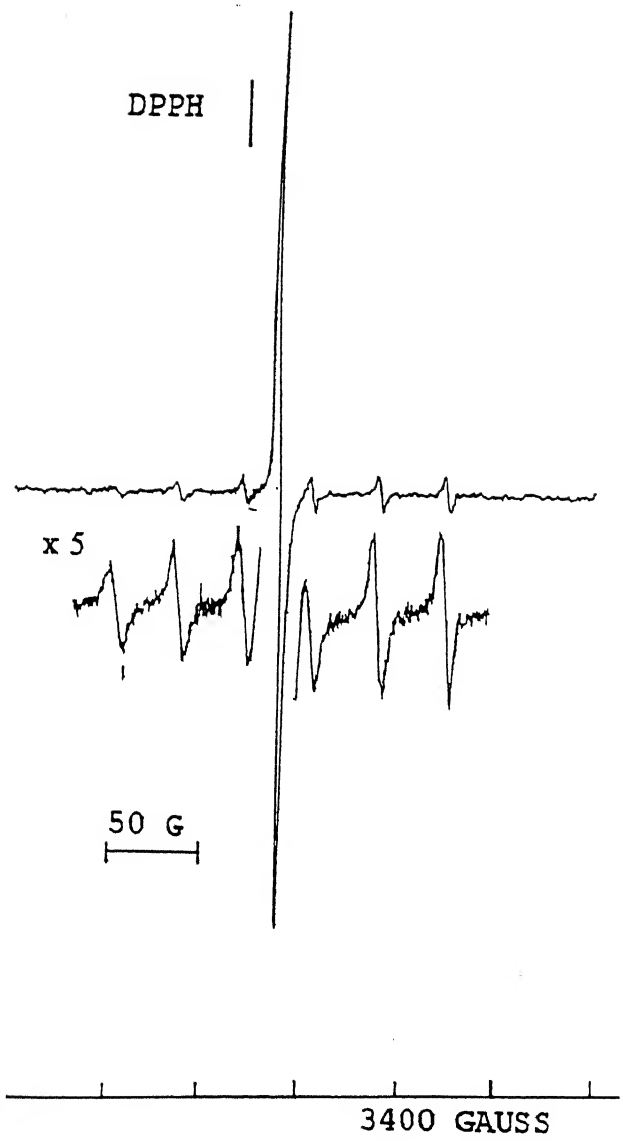

Fig.4.4.8 (c)

g.4.4.8 EPR spectra for the reaction of $[Bu_4N]_2[Mo^V_2O_4(mnt)_2]$ d PhSH, (a) after 3hrs., (b) after 6hrs. and (c) after 24hrs.

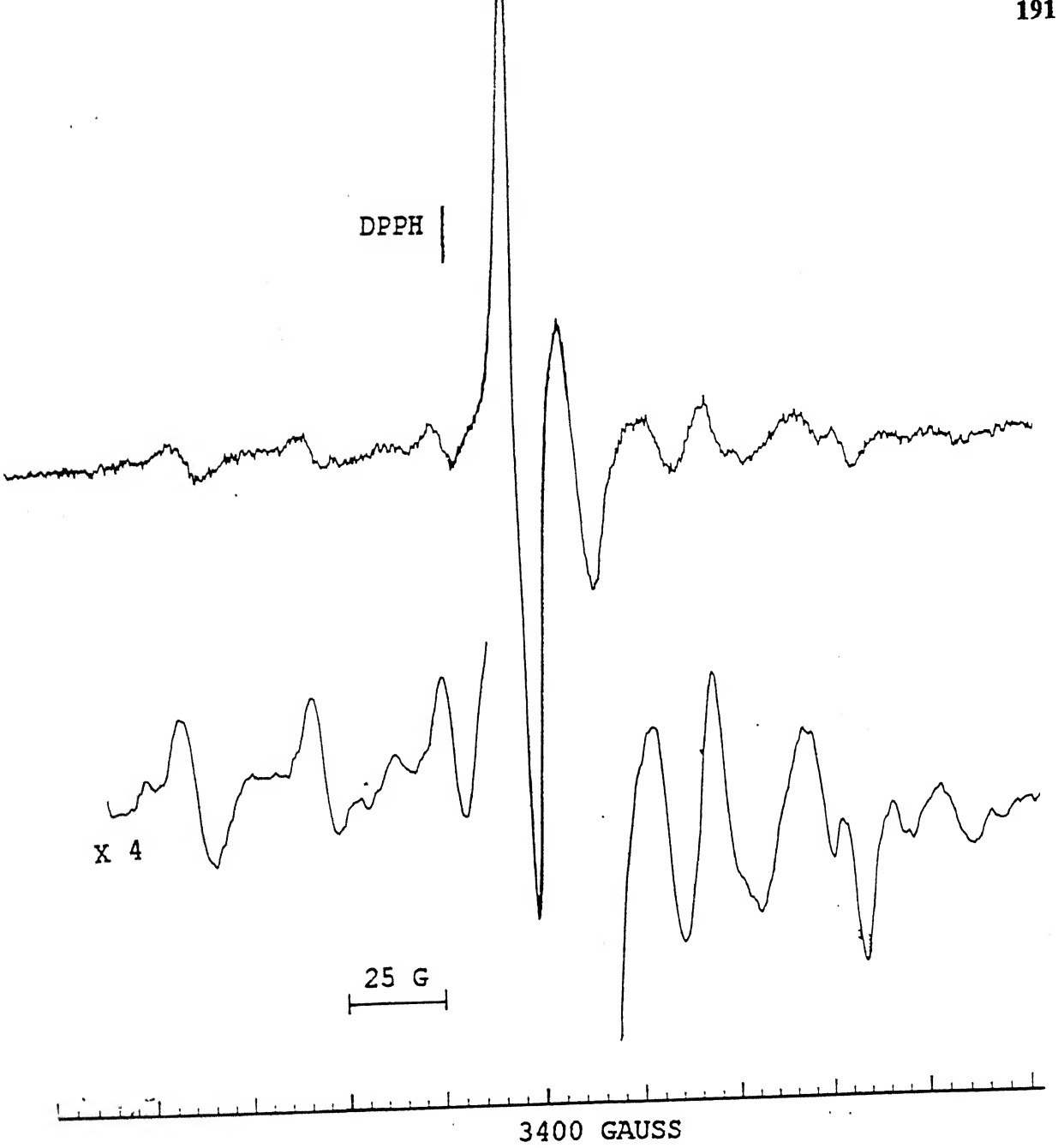

Fig. 4.4.9 EPR spectra of $[Bu_4N]_2[Mo^{V}_2O_3(SPh)_2(mnt)_2]$ in presence of excess PhSH in CH_2Cl_2.

molybdenum and tungsten that the <g> values are lower for hexacoordinated complexes than those of pentacoordinated complexes.[33a,34b] Hence the species with <g>=1.992 is suggested to be due to $[Mo^{V}O(SPh)_2(mnt)]^-$ and <g>=1.982 is due to the formation of $[Mo^{V}O(SPh)_3(mnt)]^{2-}$. It is proposed that in the latter case the extra thiolate is coordinated *cis* to the oxo group attached to molybdenum.[33a] It has been already shown that the dithiolene sulfur donors are comparable to thiolate sulfur donors in their effect on Mo(V) <g> values.[33a] Thus the <g> value reported for the cofactor signal at 1.9948 is similar to what was observed for the species $[Mo^{V}O(SPh)_2(mnt)]^-$ (our reported <g> value of 1.992 is based on the DPPH line assuming at 2.0023; however if this value is taken as 2.0037, as has taken by Hawkes and Bray[30b], then our reported <g> value for the complex is changed to 1.993).

Hawkes and Bray conjectured that thiophenol, mercaptoethanol or ethanedithiol replace two cysteine thiolate which were ligated to the crude cofactor extract. Interestingly, they have reported EPR spectra using crude extract and also with the protein free Mo-co. Comparison of both these spectra taken under identical conditions does not show any drastic change of the main signal centered at <g> = 1.9948. It is thought that the crude extract may be associated with residual protein part from which two cysteine thiol groups are ligated to Mo-co. However for the protein free cofactor does not have any possibility to get extra cysteine thiol linkages in the absence of any protein residue. Furthermore, they have proposed that thiophenol competes with this cysteine thiolate ligation and the proposed cystein thiolate ligation can only be replaced under very high concentration of thiophenol. The change in the line shape in the EPR spectra of Moco under excess of

thiophenol may be related to further coordination of PhS^-. This may be similar to what we have observed with model complexes discussed above. The restoration of the cofactor activity with modified cofactor may be simply by the dessociation of this extra thiolate group under the influence of apoprotein of the *nit-1* mutant of *N.crassa.* Partial and full inactivation of Moco under the treatment of mercaptoethanol and ethanedithiol respectively is due to the displacement of at least one MPT chelation of the cofactor under the influence of large excess of these chelating thiols. The relatively low yield of the mercaptoethanol derivative strongly suggest the difficulty to displace coordinated MPT ligands.

In conclusion, the EPR studies presented here along with the already reported EPR work on Moco[30c,109] complemented our earlier proposal based on alkylation reaction that Moco has the composition of four thiolate ligation from two MPT ligands with an oxo group in its reduced state.

EFFECTIVE POTENTIALS IN ATOM TRANSFER REACTIONS WITH BIOLOGICAL PERSPECTIVE:

While the potential of the molybdenum site is an important component of the molybdenum enzymes for catalyzing the oxotransfer reactions. It is difficult to reconcile the thermodynamic driving force for several oxotransfer reactions. The dillema to interprete these redox reactions will be apparent from the reported redox potentials of some molybdoenzymes and their physiological redox partners[110] as shown in Table 4.5.There is another aspect to deal with proton coupled electron transfer in the overall catalytic turn over reactions. The reported reaction,

$$DMSO + 2H^+ + 2e^- \longrightarrow DMS + H_2O \text{ ---------(4.11)}$$

is said to have E^o (pH~ 7) = +0.16V (*vs* NHE).[80] This potential has been measured by spectroscopy coupled to potentiometry using mediator dye for native DMSO reductase. Interestingly, for the Mo(VI)/Mo(V) and Mo(V)/Mo(IV) couples of DMSO reductase the measured midpoint potential values range between +0.065 and -0.15V (*vs* NHE) in the pH range 5-9. In the same report it was also measured that the potential for the reaction,

$$Me_3NO + 2H^+ + 2e^- \longrightarrow Me_3N + H_2O \text{ ------(4.12)}$$

is +0.13V. Interestingly, DMSO, the substrate for DMSO reductase is routinely used in electrochemical studies as a good solvent which has a fairly large range of potential window from far +ve to far -ve values. Thus the reported reduction potential of DMSO can not be a true measure of its real reduction potential value.

From Table 4.5 the reported midpoint potential of DMSO/DMS (+0.16V) and Me_3NO/ Me_3N (+0.13V) suggest that DMSO is better oxidant than TMANO. However electrochemically DMSO cannot be reduced at +0.16V. The complex, $[MoO(mnt)_2]^{2-}$ in this work displayed $E_{1/2}$ Mo(V)/Mo(IV) = +0.45V in CH_3CN and an irreversible oxidation at E_{pa} = 0.50V *Vs* Ag/AgCl in 1:1 CH_3CN:H_2O. This shift of anodic peac potential is due to the aquation of the terminal cyano groups of the coordinated mnt as was observed in reduction of $[MoO_2(mnt)_2]^{2-}$ in aqueous CH_3CN medium (*vide supra*). The oxotransfer reaction between Me_3NO and $[MoO(mnt)_2]^{2-}$ cannot be explained by individual measured potential values of the oxidant and reductant as apparently there is no +ve difference in the driving potential which is a basic thermodynamical necessity for a reaction to occur. This discrepancy can be resolved if we consider the following two reactions,

Table 4.5 Substrate and Enzyme Redox Potentials:[110]

Reduction Potential for Moco catalyzed Reaction		Mo redox Potentials for the Moco Enzymes
Reaction Enzyme	$E^{o'}$(pH 7)V	Mo(VI)/Mo(V) / Mo(V)/Mo(IV)
$DMSO + 2H^+ + 2e \longrightarrow DMS + H_2O$	+0.16 ref.(80)	
DMSO Reductase		-0.090 / -0.075
$Me_3NO + 2H^+ + 2e \longrightarrow Me_3N + H_2O$	+0.13 ref.(80)	
TMANO Reductase		------
$SO_4^{2-} + 2H^+ + 2e \longrightarrow SO_3^{2-} + H_2O$	-0.38	
Sulfite Oxidase		+0.038 / -0.239
$NO_3^- + 2H^+ + 2e \longrightarrow NO_2^- + H_2O$	+0.42	
Respiratory Nitrate Reductase		-0.034 / -0.054
Uric acid + $2H^+$ + 2e $\longrightarrow$ xanthine + H_2O	-0.36	
Xanthine Oxidase		-0.355 / -0.355

$$Me_3NO + 2H^+ + 2e^- \longrightarrow Me_3N + H_2O \quad \text{----------(4.13)}$$

$$Me_3NO + Mo^{IV}O_2^{2+} \{Mo^{VI}O + 2e^-\} \longrightarrow Me_3N + Mo^{VI}O_2^{2+} \text{----(4.14)}$$

The midpoint potential of reaction (4.13) is related to proton coupled electron transfer reaction whereas reaction (4.14) is related to molybdenum mediated reaction. And thus both the reactions are different in nature and cannot be equated in a straight forward manner. Interestingly, the midpoint potential of NO_3^-/NO_2^- (+0.42V)[80] justifies that $[MoO(mnt)_2]^{2-}$ cannot be oxidised by nitrate and which was found to be true for this system. The midpoint potential of ClO_3^-/ClO_2^- (> +0.60V) does suggest that it has the power to oxidize $[MoO(mnt)_2]^{2-}$, it has been observed that such reaction did occur however the dioxo molybdenum species thus formed is immediately bleached presumably due to the formation of ClO_2^- which is a strong oxidant.Similarly for the reaction, $S + 2H^+ + 2e^- \longrightarrow H_2S$, E^o = -0.29V (pH=7) and it is obvious that this cannot reduce $[Mo^{VI}O_2(mnt)_2]^{2-}$ which has reduction potential value $E_{1/2}$= -1.10V *vs* Ag/AgCl. But H_2S can effectively reduce $[MoO_2(mnt)_2]^{2-}$ to $[MoO(mnt)_2]^{2-}$ (Figure 4.4.10). Similarly with reduction potential (+0.60V) for PhSH *vs* $Ag/AgNO_3$[61] reduces $[MoO_2(mnt)_2]^{2-}$ to $[MoO(mnt)_2]^{2-}$ (***vide supra***). This important reaction we have shown to take place ***via*** the intermediate species $[Mo^{VI}O(SPh)_2(mnt)_2]^{2-}$ (***vide supra***) which explains these atom (electron) transfer reactions. It is therefore evident that an enzymatic oxotransfer reaction primarily demands the formation of a substrate bound new molybdenum species (Michaelis complex) by inner-sphere mechanism.[112] The intrinsic instability of the species $[MoO(SPh)_2(mnt)_2]^{2-}$, by reductive elimination produced $[MoO(mnt)_2]^{2-}$ and PhSSPh.

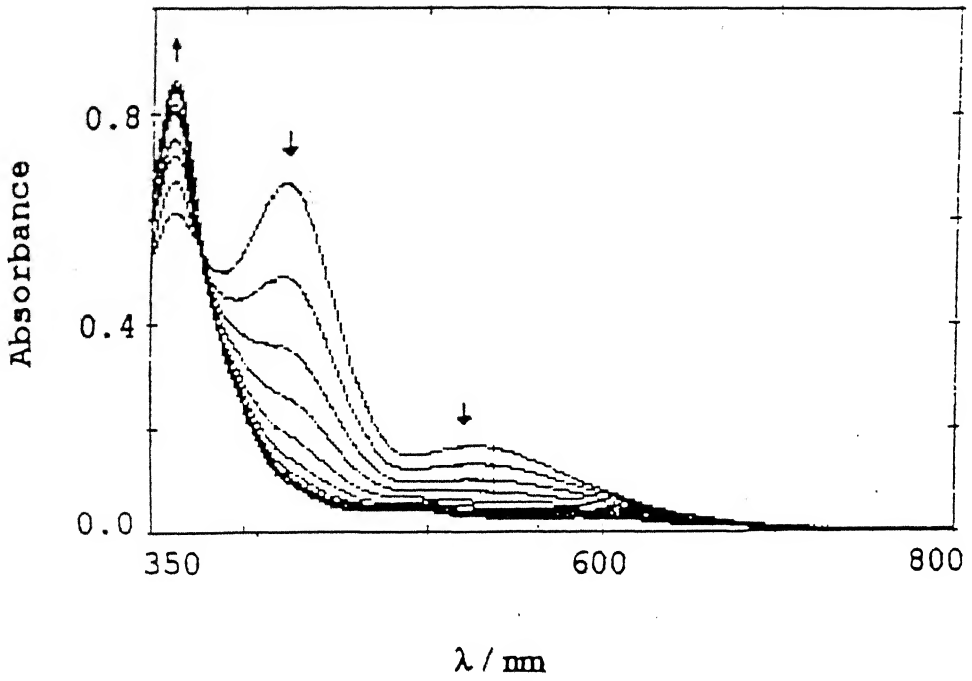

Fig. 4.4.10 Spectral changes for the reaction between $[Bu_4N]_2[Mo^{VI}O_2(mnt)_2]$ ($1x10^{-4}$M) and H_2S in H_2S saturated CH_2Cl_2, scan time gap 5 min.

CHAPTER 5

FUTURE SCOPE

The reaction of oxomolybdenum enzymes are poorly understood.[9,19a,110,113] Model chemistry of these enzymes developed an oxygen atom transfer concept as shown in equation 5.1:

$$XO + (Mo^{IV}O)^{2+} = \{(Mo^{VI}O)^{4+} + 2e^-\} \rightleftharpoons X + (Mo^{VI}O_2)^{2+} \quad ----(5.1)$$

This reaction is not conceptually identical to the proton mediated (coupled electron-proton) reaction 5.2:

$$XO + 2H^+ + 2e^- \rightleftharpoons X + H_2O \quad -----(5.2)$$

The formation of a precursor (Michaelis) complex prior to the redox reaction in any direction of equation (5.1) makes the predictibility of these inner sphere reaction impossible by measuring the driving potential difference of XO/X and MoO_2/MoO couples involving outer sphere concept.[34b]

The present investigation with respect to the slow reaction between PhSH and $[Mo^{VI}O_2(mnt)_2]^{2-}$ as shown in Scheme (5.1) is important.

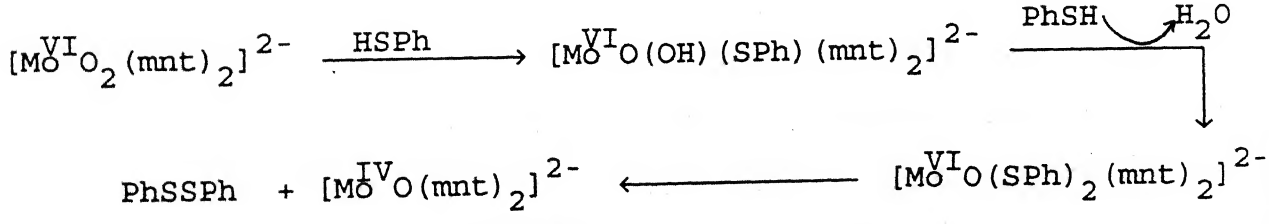

Scheme 5.1

This reaction in MeCN did not show any EPR active Mo(V) or PhS· species for the entire duration of the reduction suggesting no involvement of stepwise one electron reaction. The detail study of this reaction described earlier is now viewed as the reaction in Scheme 5.1 is actually an addition reaction followed by simple substitution of M-OH to M-SPh. The resulting heptacoordinated Mo(VI) species then respond to reductive elimination reaction with the release of PhSSPh forming pentacoordinated Mo(IV) species. Similarly the reported reaction[33a] between $[Mo^{VI}O_2(mnt)_2]^{2-}$ and HSO_3^- may be viewed as the addition of HSO_3^- across Mo=O bond which is similar to that of the classical reaction of carbonyl compound with HSO_3^-. This adduct finally respond to similar reductive elimination as shown in Scheme 5.2:

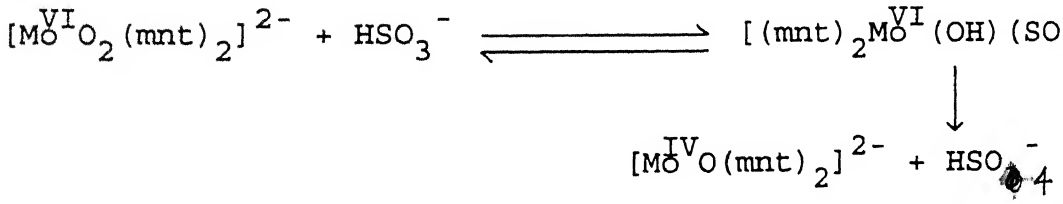

Scheme 5.2

Addition of C-H bond of xanthine across Mo=S bond of xanthine oxidase has recently been reported by Bray and coworkers.[114] The oxotransfer reaction of DMSO reductase virtually does not show any dependency on the measured redox potential data[34b] and therefore a similar addition of OMo(IV) moiety across $O{=}SMe_2$ bond may yield $\{OMo^{IV}(\eta^2\text{-}OSMe_2)\}$ in which the reductive elimination at the S-center may yield $Mo^{VI}O_2$ species with the release of Me_2S.

Thus most of the enzymatic reactions of oxomolybdoenzymes may be viewed in a simple and general way as addition of the substrate

with the enzyme at the active site to form an enzyme-substrate complex. This precursor complex then respond to reductive elimination at the molybdenum center of an oxidase type of reaction or the reductive elimination at the central atom of the bound substrate for reductase class of enzymatic reaction. Further model studies with different substrates should be developed in support of this generalization.

REFERENCES

1. H. J. M. Bowen, *Trace Elements in Biochemistry*, Academic Press, New York, 19-20 (1966).
2. R. J. P. Williams, in *Molybdenum and Molybdenum-Containing Enzymes*, (M.P. Coughlan, Ed.), Pergramon Press, New York, (1980).
3. K. V. Rajagopalan, in *Molybdenum and Molybdenum-Containing Enzymes*, (M.P. Coughlan, Ed.), Pergramon Press, New York, (1980).
4. R. H. Holm, *Coord. Chem. Rev*, 1990, **100**, 183.
5. B. E. Schultz, Russ Hille, R. H. Holm, *J. Am. Chem. Soc.*, 1995, **117**, 827.
6. (a) A. G. McEwan, S. J. Ferguson, J. B. Jackson, *Biochem. J.* 1991,**274,** 305; (b) T. Satoh, F. N. Kurihara, *J. Biochem.(Tokyo)*, 1987, **102,**191; (c) N. R. Bastian, C. J. Kay, J. M. Barber, K.V. Rajagopalan, *J. Biol. Chem.*, 1991, **266**,45.
7. R. C. Bray, in *The Enzymes* (P. D. Boyer, ed.), 3rd ed, Vol. 12, Part B, p.299.
8. S. P. Kramer, R. Wahl, K. V. Rajagopalan, *J. Am. Chem. Soc.*, 1981, **103**, 7721.
9. J. H. Enemark, C. G. Young, in *Advances in Inorganic Chemistry*, 1993, **40**, 1.
10. J. A. Pateman, D. J. Cove, B. M. Rever, D. B. Roberts, *Nature*, 1964, **201**, 58.
11. J. L. Johnson, B. E. Hainline, K. V. Ragagopalan, B. H.

Arison, *J. Biol. Chem.*, 1984, **259**, 5414.

12. (a) R. C. Wahl, R. V. Hageman, K. V. Rajagopalan, *Arch. Biochem. Biophys.*, 1984, **230**, 264; (b) S. Kramer, R. V. Hageman,K. V. Rajagopalan, *Arch. Biochem. Biophys.*, 1984, **233**, 821; (c) S. P. Kramer, J. L. Johnson, A. A. Riberio, D. S. Millington, K.V.Rajagopalan, *J. Biol. Chem.* 1987, **262**, 16357.

13. (a) P. A. Ketchum, R. J. Downey, *Biochem. Biophys. Acta,* 1975, **385**, 354; (b) A. Nason, K. Y. Lee, S. S. Pan, R. H. Erickson, *J. Less Common Metals*, 1974, **1**, 449.

14. M. K. Chan, S. Mukund, A. Kletzin, M. W. W. Adams, D. C. Rees, *Science*, 1995, **267**, 1463.

15. S. P. Kramer, in '*Advances in Inorganic and Bioinorganic Mechanisms*' (A. G. Sykes, ed.), Academic Press, London, 1983, **2**, 529.

16. G. N. George, R. C. Prince, S. Mukund, M. W. W. Adams, *J. Am. Chem. Soc.*, 1992, **114**, 3521.

17. (a) M. M. Georgiadis, H. Komiya, P. Charkrabarti, D. Woo, J. J. Kornuc, D. C. Rees, *Science*, 1992, **257**, 1653; (b) J. Kim, D. C. Rees, *Science*, 1992, **257**, 1677.

18. G. Palmer, J. S. Olson, in *Molybdenum and Molybdenum-Containing Enzymes*, (M.P. Coughlan, Ed.), Pergramon Press, New York, (1980).

19. (a) R. C. Bray, *Q. Rev. Biophys.*, 1988, **21**, 299; (b) R. C. Bray, *Biol. Magn. Reson.*, 1980, **2**, 45.

20. L. S. Meriwether, W. F. Murzluff, W. G. Hodgson, *Nature*, 1966, **212**, 465.

21. (a) C. D. Garner, J. M. Charnock, *Compre. Coord. Chem.*, 1987,

3, 1329; (b) C. D. Garner, S. Bristow, in *Molybdenum Enzymes*, (T. G. Spiro, ed.), p. 343, Wiley, New York, 1985; (c) J. R. Bradbury, M. F. Mackay, A. G. Wedd, *Aust. J. Chem.*, 1978, **31**, 2423.

22. (a) D. L. Kessler, K. V. Rajagopalan, *J. Biol. Chem.*, 1972, **247**, 6566; (b) D. L. Kessler, K. V. Rajagopalan, *Biochim. Biophys. Acta*, 1974, **370**, 389.

23. *Molybdenum and Molybdenum-Containing Enzymes*, (M.P. Coughlan, Ed.), Pergramon Press, New York, (1980).

24. (a)G. N. George, C. A. Kipke, R. C. Prince, R.A. Sunde, J. H. Enemark, S. P. Kramer, *Biochemistry*, 1989, **28**, 5075; (b) J. T. Spence, C. A. Kipke, J. H. Enemark, R. A. Sunde, *Inorg. Chem.*, 1991,**30**, 3011.

25. J. L. Johnson, N. R. Bastian, K. V. Rajagopalan, *Proc. Natl. Acad. Sci. U. S. A.*, 1990, **87**, 3190.

26. S. Gruber, L. Kilpatrick, N. R. Bastian, K. V.Rajagopalan, T. G. Spiro, *J. Am. Chem. Soc.*, 1990, **112**, 8179.

27. R. S. Pilato, K. A. Eriksen, M. A. Greaney, E. I. Stiefel, S. Goswami, L Kilpatrick, T. G. Spiro, E. C. Taylor, A. L. Rheingold, *J. Am. Chem. Soc.*, 1991, **113**, 9372.

28. (a) A. Nason, A. D. Antoine, P. A. Ketchum, W. A. Frazier III, D. K. Lee, *Proc. Natl. Acad. Sci. U.S.A.*, 1970, **65**, 137; (b) P. A. Ketchum, H. Y. Cambier, W. A. Frazier III, C. H. Madansky, A. Nason, *Proc. Natl. Acad. Sci. U.S.A.*, 1970, **66**, 1016; (c) A. Nason, K. Y. Lee, S. S. Pan, P. A. Ketchum, A. Lamberti, J. DeVries, *Proc. Natl. Acad. Sci. U.S.A.*, 1971, **68**, 3242.

29. (a) K. V. Rajagopalan, *Adv. Enzymol. Relat. Areas Mol. Biol.*,

1991, **64**, 215; (b) J L Johnson, B. E. Hainline, K. V. Rajagopalan, *J. Biol. Chem.*,1980, **255**, 1783; (c) J. L. Johnson, K. V. Rajagopalan, *Proc. Natl. Acad. Sci. U.S.A.*, 1982, **79**, 6856.

30. (a) J. Deistung, R. C. Bray, *Biochem. J.*, 1989, **263**, 477; (b) T. R. Hawkes, R. C. Bray, *Biochem. J.*, 1984, **219**, 481; (c) T. R. Hawkes, R. C. Bray, *Biochem J.*, **222**, 587,

31. B. Krûger, O. Meyer, *Eur. J. Biochem.*, 1986, **157**, 121.

32. (a)M. Karrasch, G. Börner, M. Enssle, R. K. Thauer, *Eur. J. Biochem.*, 1990, **194**, 367; (b) J. L. Johnson, K. V. Rajagopalan, O. Meyer, *Arch. Biochem. Biophys.*, 1990, **283**, 542; (c) G. Börner, M.Karrasch, R. K. Thauer, *FEBS Lett.*, 1991, **290**, 31.

33. (a) S. K. Das, P. K. Chaudhury, D. Biswas, S. Sarkar, *J. Am. Chem. Soc.*, 1994, **116**, 9061; (b) N. Ueyama, H. Oku, M. Kondo, T. Okamura, N. Yoshinaga, A. Nakamura, *Inorg. Chem.* 1996, **35**, 643; (c) H. Oku, N. Ueyama, M. Kondo, A. Nakamura, *Inorg. Chem.*, 1994, **33**, 209.

34. (a) N. Ueyama, H. Oku, A. Nakamura, *J. Am. Chem. Soc.*, 1992, **114**,7310; (b) S. K. Das, D. Biswas, R. Maiti, S. Sarkar, *J. Am. Chem. Soc.*, 1996, **118**, 1387.

35. J. L. Johnson, K. V. Rajagopalan, S. Mukund, M. W. W. Adams, *J. Biol. Chem.*, 1993, **268**, 4848.

36. (a) M. L. Larson, F. W. Moore, *Inorg. Chem.*, 1966, **5**, 801; (b) H. L. Krauss, W. Huber, *Chem. Ber.*, 1961, **94**, 2864.

37. (a) E. Wendling, *Bull. Soc. Chim. France*, 1965, 427; (b) W. P. Griffith, T. d. Wickins, *J. Chem. Soc. (A)*, 1967, 675.

38. (a) B. Kojic-Prodic, Z. Ruzic-Toros, D. Grdenic, L. Golic,

531.

49. (a) O. A. Rajan, A. Chakraborty, *Inorg. Chim. Acta*, 1979, **37**, L503; (b) O. A. Rajan, A. Chakraborty, *Inorg.Chem.*, 1981, **20**, 660.

50. (a) I. W. Boyd, J. T. Spence, *Inorg. Chem.*, 1982, **21**, 1602; (b) J. Topich, J. T. Lion III, *Polyhedron*, 1984, **3**, 55, 61.

51. J. M. Berg, R. H. Holm, *Inorg. Chem.*, 1983, **22**, 1768.

52. (a) S. Bhattacharjee, R. G. Bhattacharya, *J. Chem. Soc. Dalton Trans.*, 1992, 1357; (b) S. Bhattacharjee, R. G. Bhattacharya, *J. Chem. Soc. Dalton Trans.*, 1993, 1151.

53. C. D. Garner, S. Bristow, in *Molybdenum Enzymes*, ed. T. G. Spiro, Wiley-Interscience, New York, 1985, p.360.

54. S. A. Roberts, C. G. Young, W. E. Cleland Jr, R. B. Ortega, J. H. Enemark, *Inorg. Chem.*, 1988, **27**, 3044.

55. J. M. Berg, R. H. Holm, *J. Am. Chem. Soc.*, 1985, **107**, 917.

56. J. M. Hawkins, J. C. Dewan, K. B. Sharpless, *Inorg. Chem.*, 1986, **25**, 1501.

57. (a) A. Bruce, J. L. Corbin, P. L. Dahlstrom, J. R. Hide, M. Minelli, E. I. Stiefel, J. T. Spence, J. Zubieta, *Inorg. Chem.*, 1982, **21**, 917; (b) P. L. Dahlstrom, J. R. Hyde, P. A. Vella, J. Zubieta, *Inorg. Chem.*, 1982, **21**, 927; (c) P. Subramanian, J. T. Spence, R. Ortega, J. H. Enemark, *Inorg. Chem.*, 1984, **23**, 2564; (d) B. B. Kaul, J. H. Enemark, S. L. Merbs, J. T. Spence, *J. Am. Chem. Soc.*, 1885, **107**, 2885.

58. R. N. Jowitt, P. C. H. Mitchell, *J. Chem. Soc. (A)*, 1969, 1476.

59. (a) E. W. Harlan, J. M. Berg, R. H. Holm, *J. Am. Chem. Soc.*, 1986, **108**, 6992; (b) J. W. McDonald, J. L. Corbin, W. E.

Newton, *Inorg. Chem.*, 1976, **15**, 2056; (c) C. Pickett, S. Kumar, P. A. Vella, J. Zubieta, *Inorg. Chem.*, 1982, **21**, 908.

60. J. A. McCleverty, J. Locke, B. Ratcliff, E. J. Wharton, *Inorg.Chim. Acta*, 1969, **3**, 283.

61. (a)M. A. Ansari, J. Chandrasekaran, S. Sarkar, *Inorg. Chim. Acta*, 1987, **133**, 133; (b) D. Coucouvanis, A. Hajikyriacou, M. Draganjac, M. G. Kanatzidis, O. Ileperuma, *Polyhedron*, 1986, **5**, 349.

62. (a) R. A. Walton, P. C. Crouch, B. J. Brisdon, *Spectrochim. Acta Part A*, 1968, **24**, 601; (b) E. B. Fleischer, T. S. Srivastava, *Inorg. Chim. Acta*, 1971, **5**, 151; (c) T. Imamura, T. Numatatsu, M. Terni, M. Fujimoto, *Bull. Chem. Soc. Jpn.*, 1981, **54**, 170.

63. (a) P. Subramanian, B. B. Kaul, J. T. Spence, *J. Mol.Catal.*, 1984 **23**, 163; (b) F. Farchione, G. R. Hanson, C. G. Rodrigues, T. D. Bailey, R. N. Bagchi, A. M. Bond, J. R. Pilbrow, A. G. Wedd, *J. Am. Chem. Soc.*, 1986, **108**, 831; (c) G. L. Wilson, R. J. Greenwood, J. P. Pilbrow, J. T. Spence, A. G. Wedd, *J. Am. Chem. Soc.*, 1991, **113**, 6803.

64. E. I. Stiefel, *Prog. Inorg. Chem.*, 1977, **22**, 1.

65. D. M. Baird, S. D. Croll, A. T. DiCenso A. L. Rheingold, *Inorg. Chem.*, 1986, **25**, 3458.

66. S. Lincoln, S. A. Koch, *Inorg. Chem.*, 1986, **25**, 1594.

67. Z. Xiao, J. H. Enemark, A. G. Wedd, C. G. Young, *Inorg. Chem.*, 1994, **33**, 3438.

68. A. Cervilla, E. Llopis, J. A. Ramirez, A. Domenech, P. Palanca, M. T. Picher, C. A. Ghilardi, A. Orlandini, *J. Chem. Soc. Dalton Trans.*, 1994, 175.

69. L. Ricard, J. Estienne, P. Karagiannidis, P. Toledano, J. Fischer, A.Mitschler, R.Weiss, *J. Coord. Chem.*, 1974, **3**, 227.

70. M. Tatsumisago, G. Matsubayashi, T. Tanaka, S. Nishigaki, K. Nakatsu, *J. Chem. Soc. Dalton Trans.*, 1982, 121.

71. J. J. Johnson, W. R. Scheidt, *J. Am. Chem. Soc.*, 1977, **99**, 294.

72. J. A. Craig, E. W. Harlan, B. S. Snyder, M. A. Whitener, R. H. Holm, *Inorg. Chem.*, 1989, **28**, 2082.

73. F. A. Cotton, P. E. Fanwick, J. W. Fitch III, *Inorg. Chem.*, 1978, **17**, 3254.

74. M. R. DuBois, *Inorg. Chem.*, 1978, **17**, 2405.

75. K. Weighardt, M. Guttmann, P. Chaudhuri, W. Gebert, M. Minelli, C. G. Young, J. H. Enemark, *Inorg. Chem.*, 1985, **25**, 3151.

76. V. S. Joshi, M. Nandi, H. Zhang, B. S. Haggerty, A. Sarkar, *Inorg. Chem.*, 1993, **32**, 1301.

77. I. G. Dance, A. G. Wedd, I. W. Boyd, *Aust. J. Chem.*, 1978, **31**, 519.

78. (a) S. P. Kramer, K. V. Rajagopalan, T. N. Sorrell, *Biochem. Biophys. Res. Commun.*, 1979, **91**, 434,; (b) R. C. Bray, *Polyhedron*, 1986, **5**, 591.

79. (a) O. Shimokawa, M. Ishimoto, *J. Biochem.*, 1979, **86**, 1709; (b) I. Yamamoto, N. Okubo, M. Ishimoto, *J. Biochem.*, 1986, **99**, 1773; (c) M. Tagaki, T. Tsuchiya, M. Ishimoto, *J. Bact.*, 1981, **148**, 762.

80. J. H. Weiner, R. Cammack, *Biochemistry*, 1990, **29**, 8410.

81. A. I. Vogel, in *A Text Book of Quantitative Inorganic Analysis*, 4th. edn., Longman, London, 1978.

82. E. I. Stiefel, L. E. Bennette, Z. Dori, T. H. Crawford, C. Simo, H. B. Gray, *Inorg. Chem.*, 1970, **9**, 281.

83. J. A. McCleverty, J. Locke, E. J. Wharton, *J. Chem. Soc.*, 1968, 816.

84. S.Sarkar *et.al.*, unpublished work.

85. K. Nakamoto, *Infrared and Raman Spectra of Inorganic and Coordination Compounds*, 4th. edn., John-Wiley & Sons, New York, 1986.

86. C. W. Schlapfer, K. Nakamoto, *Inorg. Chem.*, 1975, **14**, 1338.

87. K. V. Rajagopalan, J. L. Johnson, *J. Biol. Chem.*, 1992, **267**, 10199.

88. (a) S. Linclon, T. M. Loehr, *Inorg. Chem.*, 1990, **29**, 1908; (b) W. E. Newton, J W. McDonald, in *Chemistry & Uses of Molybdenum*, Climax Molybdenum Co. Ltd., London, 1976.

89. (a) P. K. Mascharak, *Inorg. Chem.*, **25**, 245; (b) S. Sarkar, R. Sah, P. K. Chaudhury, R. Maiti, S. K. Das, *Proc. Indian Acad. Sci.(Chem. Sci.)*, 1995, **107**, 355.

90. F. A. Cotton, G. Wilkinson, *Advanced Inorganic Chemistry*, (5th.edition), Wiley-Interscience, New York, 1988, p.829.

91. L. P. Hammett, *Physical Organic Chemistry*, McGraw-Hill, New York, 1970.

92.(a) M. Ishimoto, O. Shimokawa, Z. *Allg. Mikrobiol.*, 1978, **18**, 173; (b) M. Sakaguchi, A. Kawai, *Bull. Jpn. Soc. Sci. Fish.*, 1978, **44**, 511; (c) I. Yamamoto, M. Ishimoto, Z. *Allg. Mikrobiol.*, 1977, **17**, 235.

93. N. J. S. Burgmayer, E. I. Stiefel, *J. Am. Chem. Soc.*, 1986, **108**, 8310.

94. M. Ishimoto, O. Shimokawa, Z. *Allg.Mikrobiol.*, 1978, **18**, 173.

95. (a)K. E. Kim, G. W. Chang, *Can. J. Microbiol.*, 1974, **20**, 1745., (b) H. S. Kawn, E. L. Barrett, *J. Bacteriol.*, 1983, **155**, 1455.

96. (a)E. Stenberg, O. B. Styrvold, A. R. Strom, *J. Bacteriol.*, 1982, **149**, 22; (b) A. R. Strom, J. A. Olafsen, H. Larsen, *J. Gen. Mikrobiol.*, 1979, **112**, 315.

97. S. K. Das, *Ph.D. Thesis*, I.I.T. Kanpur, 1993.

98. N. Ueyama, T-aki. Okamura, A. Nakamura, *J. Am. Chem. Soc.*, 1992, **114**, 8129.

99. (a) N. E. Engstrom, A. Holmgren, A. Larson, S. Söderhall, *J. Biol. Chem.*, 1974, **249**, 205; (b) A. Holmgren, B.O. Söderberg, H. Eklund, C. I. Bräden, *Prog. Natl. Acad. Sci. U.S.A.*, 1975, **72**, 2305; (c) A. Holmgren, *Trends Biochem. Sci.*, 1981, **6**, 26.

100. S. Sarkar, R. Sah, P. K.Chaudhury, R. Maiti, S. K. Das, *Proc. Indian Acad. Sci. (Chem. Sci.)*, 1995, **107**, 355.

101. R. J. H. Clark, P. C. Turtle, *J. Chem. Soc., Dalton Trans.*, 1977, 2142.

102. S. K. Das, S. Sarkar, *Proc. Indian Acad. Sci. (Chem. Sci.)*, 1992, **104**, 437.

103. K. A. Connors, *Chemical Kinetics*, VCH, New York, 1990.

104. G. E. P. Box, W. G. Hunter, J. S. Hunter, in *Statistics for Experiments*, John Wiley & Sons, New york, 1978.

105. B. E. Ames, *Methods Enzymol.*,1966, **8**, 115.

106. A. B. Blake, F. A. Cotton, J. S. Wood, *J. Am. Chem. Soc.*, 1964, **86**, 3024.

107. C.R. Hare, I. Bernal, H. B. Gray, *Inorg. Chem.*, 1962, **1**, 831.

108. B. A. Goodman, J. B. Raynor, in *Adv. Inorg. Chem. Radiochem.*, 1970, **13**, 136.

109. I. K. Dhawan, A. Pacheco, J. H. Enemark, *J. Am. Chem. Soc.*, 1994, **116**, 7911.

110. R. S. Pilato, E. I. Stiefel, in *Bioinorganic Catalysis* (ed. J. Reedijk), Marcel Dekker, New York, 1993.

111. J. R. Bradbury, A. F. Masters, A. C. McDonell, A. A. Brunette, A. M. Bond, A. G. Wedd, *J. Am. Chem. Soc.*, 1981, **103**, 1959.

112. L. E. Bennett, *Prog. Inorg. Chem.*, 1973, **18**, 1.

113. (a) R. C. Bray, *Adv. Enzymol. Relat. Areas Mol. Biol.*, 1980, **51**, 107; (b) R. Hille, *Biochim. Biophys. Acta*, 1994, **1184**, 143; S. J. Lippard, J. M. Berg, in *Principles of Bioinorganic Chemistry*, University Science Books, Mill Vale, CA, 1994, 318.

114. B. D. Howes, R. C. Bray, R. L. Richards, N. A. Turner, B. Bennett, D. J. Lowe, *Biochemistry*, 1996, **35**, 1432.